Exploration and validation of novel liquid biomarkers in ovarian cancer of diagnostic or prognostic value

A thesis submitted for the degree of

Doctor of Philosophy

by

Juhi Kumar

College of Health, Medicine and Life Sciences (CHMLS)

BRUNEL UNIVERSITY LONDON

December 2020

Dedicated to my mother, Sujata

Thank you for inspiring me to dream big…

Abstract

Ovarian cancer (OC) is a lethal malignancy that severely impacts female health within the UK and across the world. It is the 6th most common cause of gynaecological cancer affecting women in the UK and affects approximately 7,500 per annum. Majority of women receive a confirmed diagnosis after they have progressed to an advanced stage (stage III/IV) of the disease, usually due to presentation of vague abdominal or gastrointestinal symptoms which is often mistaken for more benign conditions, like Irritable Bowel Syndrome (IBS). Serum CA125 is considered to be the current gold standard for diagnosing ovarian cancer in patients, however, it is found to be elevated in other malignancies as well as in non-cancerous conditions such as liver cirrhosis and pregnancy. CA125 levels are also not elevated in a significant amount of early-stage OC cases, which may lead to further delay in referral and treatment. Once diagnosed, patients respond well to treatment initially, but soon develop chemoresistance, leaving patients with limited treatment options.

Liquid biopsies have been gaining significant attention within the scientific community as a promising alternative to tissue samples, providing non-invasive diagnostic approaches or serial monitoring of disease evolution. In this study, we explore novel biomarkers and show that their presence in patient blood samples can be detected and utilised for serial monitoring of treatment efficacy. Furthermore, this study dives beyond cancer detection and looks into the possibility of developing novel therapeutic targets for OC. Using high-definition image flow cytometry, we demonstrate the ability to detect circulating cancer-related cells (CCs) from blood samples of patients with advanced epithelial OC (aEOC). We report that the presence of AE1/AE3+ and WT1+ cells is significantly higher in-patient samples compared to controls (mean = 2914 and 547 CCs/ml, respectively). We also report the presence of CD34+ circulating endothelial cells in patients' peripheral blood.

We then investigated the mechanistic aspects of certain biomarkers and how informing on their functionality and involvement in OC could help discover new therapeutic targets; providing evidence for a novel role of surfactant protein D (SP-D) in ovarian cancer, as a biomarker and a therapeutic molecule. This thesis, completed with a pilot study investigating the shuttling effect of WT1, is important to understand the functional role of WT1 beyond just a biomarker used to confirm serous OC.

On the whole, information obtained from liquid biopsies can cater to a wide array of functions from diagnosis/prognosis, minimally invasive serial monitoring to identification of new targets for therapeutic purposes.

Contents

List of figures

List of tables

Acknowledgements

My research is incredibly meaningful to me; but I know I could not have done this alone. I would like to express my gratitude and mention those whose support and guidance made this possible.

Firstly, I would like to acknowledge my supervisor, Dr Emmanouil Karteris, whose immense patience, expertise, and motivation kept me going throughout my doctoral training. Manos, your supervision was instrumental to my growth and development as a researcher – you always encouraged me to achieve my goals and never stopped believing in me. I am fortunate to have been under your tutelage. I would also like to give a special mention to my second supervisor, Dr Amanda Harvey, for keeping me grounded and focused. I would like to thank Professor Marcia Hall, for providing me with clinical knowledge and experience which was crucial for this project. I would like to thank Dr Jayanta Chatterjee, for his input and expertise towards my research and my thesis. I am also very grateful for GRACE foundation, who supported my work. Thanks to you, I had the opportunity to experience the world of medical research.

To my colleagues in CBCEL, thank you for all your help and support over the last few years. To Dimple, Rooban, Sophie and Rachel – thanks for your support and for making labs manageable (and fun). To the Biosciences technical staff; Matthew Themis, Hassan Khonsari, Freya Crawford, and Helen Foster, thank you so much for all your help, from teaching/training to helping me troubleshoot issues. I appreciate all your support. And also, to Dr Emma Bourton and Dr Hussein Al-Ali for their (much needed) training and technical support with the ImageStream.

I am so lucky to have met some amazing people throughout this journey who've made this experience so unforgettable. A special mention to Aakila, Saqlain, Ruchira and Dorothee – for all the coffee/tea sessions, the food, chats, enduring my meltdowns and constantly reminding me that I can do this! This pandemic has been a tough one for everyone, but you taught me that we could get through it by supporting each other. Chrissi, I will never forget us singing along to the Beatles in the lab. Thanks for being so nice to me when I didn't know anyone around. Tina, I am so lucky to have met you – you have been an inspiring mentor and a source of support. Thank you for giving me somewhere to go for advice and clarity when I felt so lost.

Finally, the most important thank you goes out to my mother, father, and brother for encouraging me to pursue my dreams and taking that leap of faith with me. To my mother, who I think I got my smarts from – thank you for sticking with me through everything. Good and bad. This one is for you, ma. I hope you are proud of me

Declaration of Authorship

I, Juhi Kumar, declare that this thesis titled 'Exploration and validation of novel liquid biomarkers in ovarian cancer of diagnostic or prognostic value' and the work presented in it is my own. I confirm that:

- The work presented in this thesis was done while in candidature for a research degree at Brunel University London.
- Where I have consulted the published work of others, this is always clearly attributed.
- Where I have quotes from the work of others, the source is always given. With the exemption of such quotations, this thesis is entirely my own work.
- I have acknowledged all main sources of help.
- Where the thesis is based on work done in collaboration with others, I have made clear exactly what was done by others and what I have contributed myself.

Signed: 

Date: 17/12/2020

Publications, Presentation & Awards

Peer reviewed publications resulting from this work

- (Chapter 3 & 4) **Kumar J**, *et al* Detection of Abundant Non-Haematopoietic Circulating Cancer-Related Cells in Patients with Advanced Epithelial Ovarian Cancer. *Cells* (2019) doi:10.3390/cells8070732.

- (Chapter 5) **Kumar J** *et al* Surfactant Protein D as a Potential Biomarker and Therapeutic Target in Ovarian Cancer. *frontiers in Oncology* (2019) doi:10.3389/fonc.2019.00542.

- (Chapter 1) Katopodis P., Chudasama D., Wander G., Sales L., **Kumar J**., Pandhal M., Anikin V., Chatterjee J., Hall M., Karteris E. Kinase Inhibitors and Ovarian Cancer *Cancers* (2019) doi:10.3390/cancers11091357.

- (Chapter 1 & 5) Rodgers-Broadway K., **Kumar J**., Sisu C., Wander G., Mazey E., Jeyaneethi J., Pados G., Tsolakis D., Klonos E., Grunt T., Hall M., Chatterjee J., Karteris E Differential expression of mTOR components in endometriosis and ovarian cancer: Effects of rapalogues and dual kinase inhibitors on mTORC1 and mTORC2 stoichiometry *International Journal of Molecular Medicine* (2018) doi:10.3892/ijmm.2018.3967.

- Thomas J., Jeyaneethi J., **Kumar J**., Karteris E., Jones R., Hall M., *Cancers* (2020) Identification of Cancer-Associated Circulating Cells in Anal Cancer Patients doi: 10.3390/cancers12082229.

Conference poster presentations

- European Association of Cancer Research (EACR) - Cancer Genomics, Cambridge (UK), 2019

Awards

- **3rd Prize** (Poster Presentation) – 3rd Annual College of Health and Life Sciences Conference, Brunel University London, 2017

- **1st Prize** - 3-Minute Thesis competition, Brunel University London, 2018

- **People's Choice Awards** – 3-Minute Thesis competition, Brunel University London, 2018

Abbreviations

aEOC – Advanced Epithelial Ovarian Cancer

AKT - Protein kinase B or PKB

ANOVA - Analysis of variance

APS – Ammonium Persulphate

ARID1A - AT-rich interactive domain-containing protein 1A

ATP – Adenosine Triphosphate

ATP7A/B – Human copper-transporting P-type ATPase A/B

AUC – Area Under Curve

BAX - Bcl-2-like protein 4

BCT – Blood Collection Tube

BMI – Body Mass Index

BRAF - serine/threonine-protein kinase B-Raf

BRCA 1 – BR-east CAncer gene 1

BRCA 2 – BR-east CAncer gene 2

BREO – Brunel Research and Ethics Organisation

BRIP1 - BRCA1 interacting protein

BSA – Bovine Serum Albumin

CA125 – Cancer Antigen 125

CAR-T - Chimeric antigen receptor T cells

CCs – Circulating cancer-related Cells

CD45 - cluster of differentiation 45 or leukocyte common antigen

cDNA – complementary DNA

CEC – Circulating Endothelial Cells

ccfDNA – Circulating Cell-free DNA

CICATRIx - CIrculating tumour cells, Cell free DNA And leucocytes with imagesTReam analysIs in patients with various cancers

CK - Cytokeratins

CK20 – Cytokeratin 20

CK7 – Cytokeratin 7

CRD - Coding Region Determinant

CT scan – Computed Tomography Scan

CTC – Circulating Tumour Cell

ctDNA – Circulating tumour DNA

CTEC – Circulating Tumour-related Endothelial Cell

DAB - 3,3′-Diaminobenzidine

DAPI - 4′,6-diamidino-2-phenylindole

DMEM - Dulbecco's Modified Eagle Medium

DMSO - Dimethyl sulfoxide

DNA – Deoxyribonucleic Acid

dNTP - Deoxyribonucleotide triphosphate

DPX - Dibutylphthalate Polystyrene Xylene

ECL - Enterochromaffin-like cells

ECM – Extracellular Matrix

EDTA - Ethylenediamine tetra-acetic acid

EGF – Epidermal Growth Factor

EGFR - Epidermal growth factor receptor

ELISA – Enzyme Linked Immuno Sorbent Assay

EMT – Epithelial-to-Mesenchymal Transition

EOC – Epithelial Ovarian Cancer

ERBB 2 - v-erb-b2 avian erythroblastic leukaemia viral oncogene homolog 2 or HER2.

FADD – Fas-associated via death domain

FBS – Fetal Bovine Serum

FDA - U.S. Food and Drug Administration

FIGO – International Federation of Gynaecology and Obstetrics

FITC - Fluorescein isthiocyanate

GOG - Gynaecologic Oncology Group

GP – General Practice

HGSC – High Grade Serous Cancer

hnRNPs - Heterogeneous nuclear ribonucleoproteins

HRT – Hormone Replacement Therapy

HTA – Human Tissue Act

IBS – Irritable Bowel Syndrome

ICON-4 - International Collaborative Ovarian Neoplasm 4

IDS – Intermittent Debulking Surgery

IHC – Immunohistochemistry

IL-8 – Interleukin 8

IMS – Industrial Methylated Spirit

kDa – Kilodalton

KM – Kaplan Meier

KRAS - Kirsten RAS oncogene

LGSC – Low Grade Serous Cancer

MAPK - Mitogen-activated protein kinase

miRNA – micro-RNA

mRNA – Messenger Ribonucleic Acid

MRP2 - Multidrug resistance protein 2

MSH2 - MutS homolog 2

MSP - Merozoite surface protein

MTA – Materials Transfer Agreement

mTOR – Mechanistic Target of Rapamycin

mTORC1 - Mechanistic target of rapamycin complex 1

mTORC2 - Mechanistic target of rapamycin complex 2

MVCC – Mount Vernon Cancer Centre

NACT – Neo-adjuvant Chemotherapy

NES – Nuclear export signal

NF-κB - nuclear factor kappa-light-chain-enhancer of activated B cells

NGS – Next Generation Sequencing

NHS – National Health Service

NHSBSP – National Health Service Breast Screening Programme

NICE – National Institute of Health and Care Excellent

NRES - National Research Ethics Service

OC – Ovarian Cancer

OS – Overall Survival

PARP - poly-ADP ribose polymerase

PBS – Phosphate Buffered Saline

PCNA - Proliferating cell nuclear antigen

PCR – Polymerase Chain Reaction

PDS – Primary-debulking Surgery

PFA – Paraformaldehyde

PFS – Progression-free Survival

PI – Propidium Iodide

PI3K - Phosphoinositide 3-kinase

PIK3CA - Phosphatidylinositol-4,5-Bisphosphate 3-Kinase Catalytic Subunit Alpha

PLD - Phospholipase D

PS6K – Phospho S6 Kinase

PSA – Prostate Specific Antigen

PTEN - Phosphatase and tensin homolog

QC – Quality Control

RAPTOR - Regulatory-associated protein of mTOR

rfhSP-D – Recombinant fragment of human SP-D

RICTOR - Rapamycin-insensitive companion of mammalian target of rapamycin

RMI – Risk of Malignancy Index

RNA – Ribonucleic acid

ROC – Receiver Operating Curve

RPM – Rounds per minute

RPMI - Roswell Park Memorial Institute

RQ – Relative Quantification

RT-qPCR – Reverse Transcriptase quantitative Polymerase Chain Reaction

SDS PAGE - Sodium dodecyl sulphate polyacrylamide gel electrophoresis

SEM – Standard Error of Mean

SP-D – Surfactant Protein D

STIC – Serous Tubal Intraepithelial Cancer

TBS - Tris-buffered saline

TEC – Tumour-related Endothelial Cell

TGCA - The Cancer Genome Atlas

TGF-β – Tumour Growth Factor β

TKI – Tyrosine Kinase Inhibitor

TME – Tumour microenvironment

TNF-α – Tumour Necrosis Factor α

TP53 - Tumour protein p53

TUBB3 - Tubulin beta-3 chain

UKCTOCS - United Kingdom Collaborative Trial of Ovarian Cancer Screening

VEGF – Vascular Endothelial Growth Factor

WBC – White Blood Cell

WHO – World Health Organisation

WT1 – Wilms' Tumour protein 1

Chapter 1

Introduction

1.1 Introduction to Ovarian Cancer

Ovarian cancer (OC) is the 8th most common cause of cancer in women worldwide, accounting for over 295,000 cases annually (WHO, 2018). In the United Kingdom, OC accounts for 7,443 new cases annually which translates to roughly 20 cases every day. In comparison to breast and uterine cancer, the incidence of ovarian cancer within the UK and around the world is not as high. However, national statistics show that more than 50% of women diagnosed with OC every year will not be able to survive the disease. At present, the overall survival rate (10 years or more) of the disease is 35% and a mere 11% cases are considered preventable (Cancer Research UK, 2018). These numbers throw light on the severity and lethality of the disease.

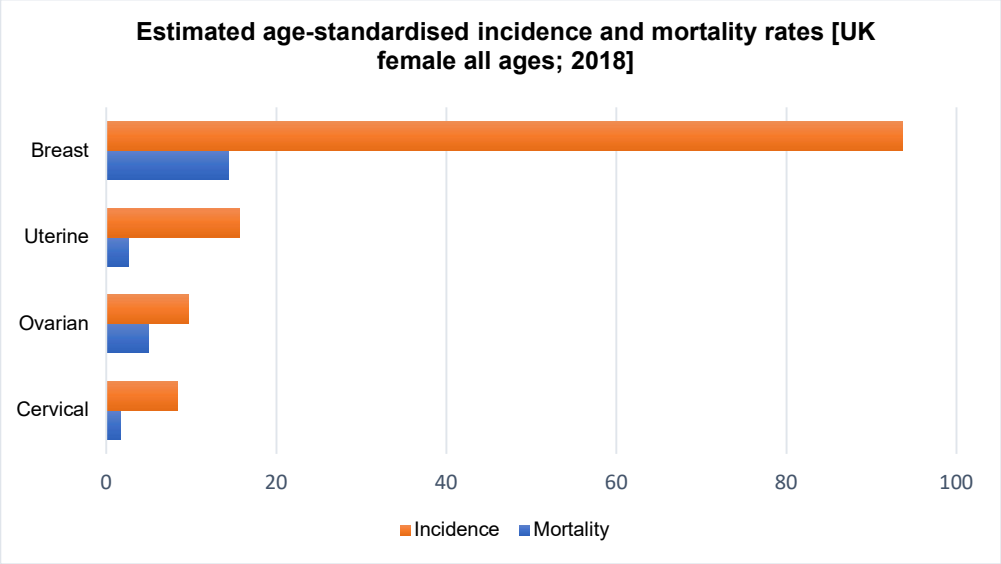

Figure 1.1 *- Latest estimated age-standardised rate (ASR) of incidence (orange) and mortality (blue) of various gynaecological cancers observed in the females in the United Kingdom. From top to bottom; Breast – I=93.6, M=14.4; Uterine – I=15.6 M=2.6; Ovarian – I=9.7, M=4.9; Cervical – I=8.4, M=1 (WHO, 2018).*

Over the past 20 years the incidence of OC has remained fairly static, however projections built on current statistics suggest a 15% increase in age-standardised mortality rates by 2035 (figure 2) (Cancer Research UK, 2018). On a positive note, OC mortality rate has seen a 17% drop within the last decade. Despite this improvement, not much has changed regarding the prognosis of

women diagnosed with the disease as overall survival rates are still below 50% (Doufekas and Olaitan, 2014)

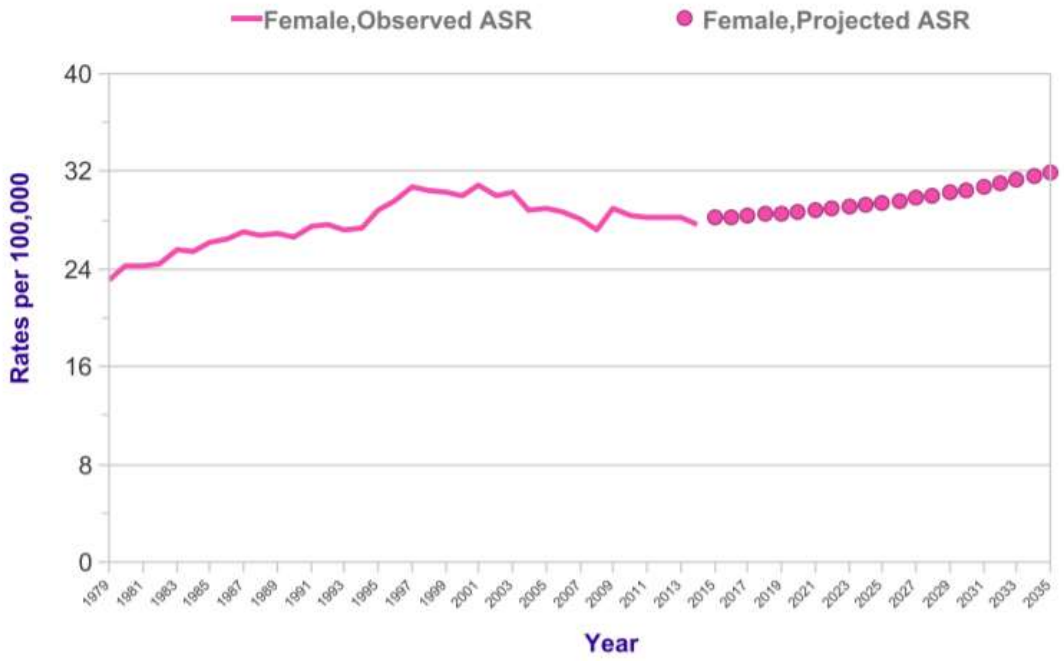

Figure 1.2 *– Observed (solid) and projected (dotted) age-standardised rates (ASR) of mortalities within the female population in the United Kingdom (Cancer Research UK, 2018).*

In most cases, women with OC are diagnosed at an advanced stage (FIGO stage III), translating to widely metastatic disease and low survival rates (Jayson *et al.*, 2014). If diagnosed at an earlier stage, the overall survival rate increases to over 90% with significantly better prognostic outcomes (Doufekas and Olaitan, 2014). Effective screening programs are shown to be a vital strategy in reducing mortality. This has been noted in the case of breast cancer through the UK NHS Breast Screening Programme (NHSBSP), the impact of which has resulted in a 20% reduction of breast cancer related deaths between 1991 to 2005. Similarly, cervical cancer screening programmes across the country have reported to save 4,500 lives per year, highlighting their importance in addressing the burden on our public health system (Marmot *et al.*, 2013; Johns *et al.*, 2017). The current landscape of diagnostics needs attention since the tests currently used to confirm presence of OC have limited sensitivity and specificity (Sundar *et al.*, 2016). These factors altogether have hindered any progress towards declining mortality rates in the UK and need to be addressed. Liquid biopsies have gained wide popularity within the last couple of decades as a means of providing a simple/quick but comprehensive method of disease detection. Liquid biopsies hold an enormous potential as a reliable test within the current clinical setting and is a topic that will be discussed extensively in this chapter .

1.2 Ovary – Anatomy and Physiology

The ovaries are primary female reproductive sex organs that are responsible for: 1) the development and release of ova (female germ cells) into the fallopian tube during ovulation and 2) the release of female sex hormones oestrogen and progesterone. A typical ovary is about 3 to 3.5 cm in length, 1.5 to 2.0 cm in width and weighs about 4 to 7 grams roughly, with a pearly grey appearance and a smooth consistency (Blaustein, 1983). The germinal epithelium also known as the visceral peritoneum (where "de novo" epithelial ovarian carcinomas generally arise from), covers the surface of each ovary, and consists of a layer of columnar epithelial cells that overlies a dense connective tissue layer called the tunica albuginea. The interior tissues of the ovary can be further sub-divided into the outer cortex and the inner medulla (Tortora and Derrickson, 2005).

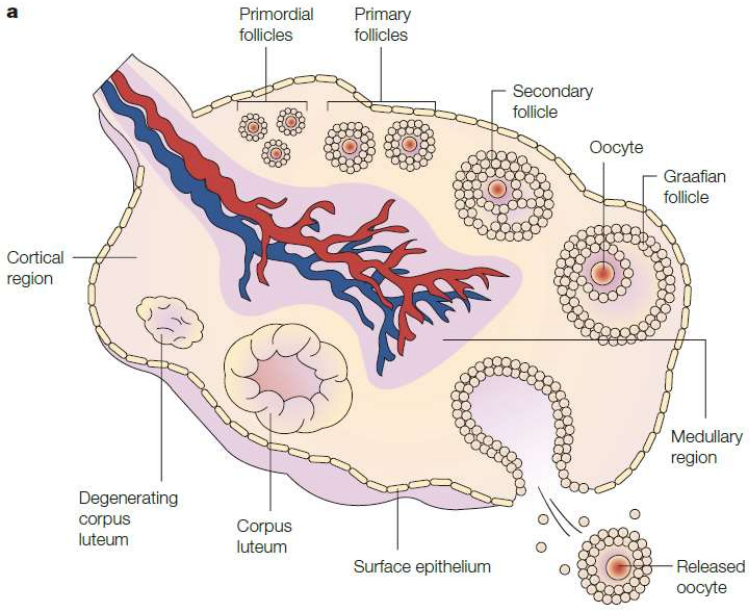

Figure 1.3 *– Anatomy of the adult human ovary - the free surface of the ovary is covered by a single layer of epithelial cells, the ovarian surface epithelium. The ovary has a large cortical and a small medullary region that are composed of fibroblast-like cells and smooth-muscle cells. The medullary region contains the larger blood vessels (shown in red and blue). The cortical region contains the follicles that each contain an oocyte. Primary follicles result from growth of primordial follicles, then develop into secondary follicles and mature into Graafian follicles. During ovulation, the ovarian surface is ruptured when the oocyte is released. After ovulation, the remnants of the follicle are transformed into the corpus luteum, a glandular structure that secretes female sex hormones. Different stages of oocyte maturation that take place during the 28-day menstrual cycle within the female ovary are shown in figure 1.3* (*Naora and Montell, 2005*) .

Oestrogen and progesterone levels fluctuate throughout the menstrual cycle with oestrogen peaking just before ovulation and progesterone steadily increasing after ovulation has occurred

(Tortora and Derrickson, 2005). If fertilisation fails to occur, oestrogen and progesterone return to basal levels, followed by menstruation, the process which involves the shedding of the mucosa or inner layer of the uterus with blood through the vagina. The ovaries cease to produce oestrogen and progesterone at menopause, at which time menstruation and fertility terminates (Tortora and Derrickson, 2005).

1.3 Origin and classification of Ovarian Cancer

OC is well established as a heterogenous disease composed of different types of tumours with widely differing clinicopathologic features and behaviours (Kurman and Shih, 2010). A substantial amount of effort has been made in the last few decades towards appropriate classification and elucidating the origin of these tumours for appropriate detection and care. Histologically, OC is classified into two broad categories: non-epithelial (originating from stromal and germ cells) and epithelial (originating from epithelial cells) OC. Non-epithelial OC is rare and forms a small proportion of cases, whereas over 90% of malignancies relate to the epithelial type (Reid *et al*, 2017; Kim *et al.*, 2018). Epithelial ovarian cancer is further sub-divided into five types, namely high-grade serous (HGSC), endometrioid, clear-cell, mucinous, and low-grade serous (LGSC) (Prat, 2012).

Based on distinct morphological and molecular heterogeneity that exists within epithelial OC, a dualistic model was proposed which broadly sub-divided epithelial OC into type I and type II tumours. Type I OCs tend to be low-grade, indolent tumours and include low-grade serous, endometrioid, mucinous, and malignant Brenner tumours. They are characterised by mutations of *KRAS*, *BRAF*, *ERBB2*, *PTEN*, *PIK3CA* and *ARID1A* and are relatively genetically stable (Kurman and Shih, 2010). Type II OCs are high-grade, aggressive tumours comprising of high-grade serous, high-grade endometrioid, malignant mixed mesodermal tumours (stromal and epithelial mixed tumours) and undifferentiated tumours. They are very frequently associated with *TP53* mutations and approximately 20% also carry a BRCA1/2 mutation due to a combination of germline and somatic mutations (Kurman and Shih, 2010, 2016; Rojas *et al.*, 2016). Invasive high-

grade serous carcinoma is the most common histological type accounting for up to ~80% of advanced ovarian cancers.

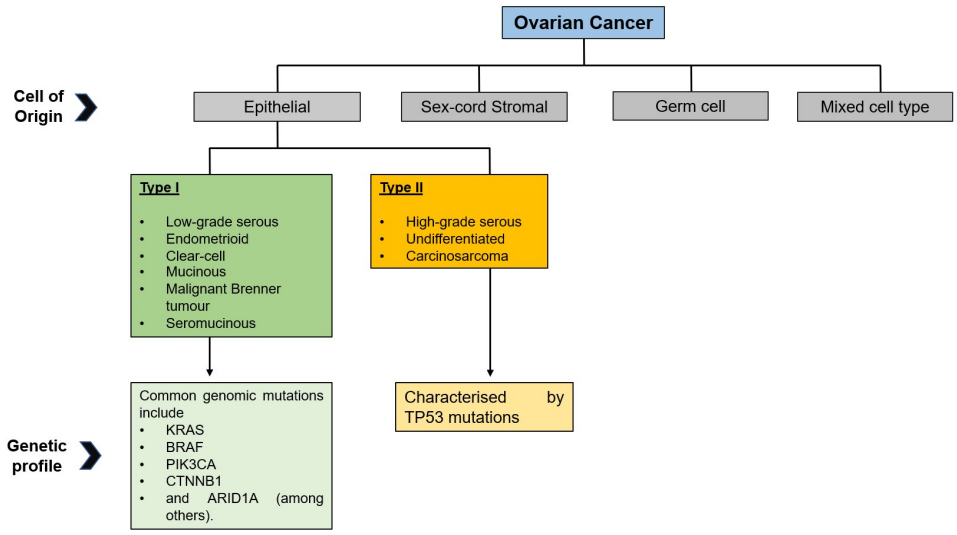

Figure 1.4 *- A simplified flowchart depicting the classification of OC based on cell of origin, histology, and genetic profile. Ovarian cancer sub-types are divided into type I and type II, with type I showing a set of common genetic mutations while majority of type II tumours are largely characterised by TP53 mutations. Figure adapted from* (Rojas et al., 2016).

The origin and mechanisms involved in the development of OC have been a subject of debate for many years. So far, there has been a lack of a definitive precursor lesion which can be accounted for the development of epithelial ovarian cancer (Kuhn *et al.*, 2012). All subtypes of epithelial OC were originally believed to arise from dysplastic epithelial cells covering the ovary, or inclusion cysts formed from invaginations of the ovarian surface epithelium. However, it was impossible to explain how various tumour sub-types, which did not morphologically resemble the ovarian surface epithelium, could arise from it (Kurman and Shih, 2010; Blagden, 2015). In addition, pre-malignant lesions found on the fallopian tube, also known as serous-tubal intraepithelial carcinomas (STICs) were shown to have a significant correlation with high-grade serous ovarian cancer (Perets et al 2013; Blagden, 2015). Therefore, the involvement of the fallopian tube in the development of OC was beginning to become apparent. A study conducted in 2007 analysed pathological results of specimen obtained from BRCA-positive women who underwent prophylactic surgery to reduce cancer risk, indicating a possibility for the distal fallopian tube to be the dominant site of origin for early malignancies (Callahan *et al.*, 2007). STIC lesions have also been identified in the fallopian tube of 70% patients with sporadic ovarian and serous peritoneal cancer, implying that its association is not limited to BRCA carriers (Kindelberger *et al.*, 2007). To corroborate morphological resemblances between the serous sub-type and the fallopian tube, an

expression array analysis between different histotypes of ovarian cancer with corresponding normal tissues revealed statistically significant correlations between gene expression in serous ovarian cancers and normal fallopian tube epithelium (P=0.0013) (Marquez et al 2005). Most STICs exhibit robust immunostaining of p53 and genomic instability, both features of HGSC, indicating genetic similarity between the two (Kim *et al.*, 2018). Gene expression profile of HGSC exhibits a greater similarity to the fallopian tube epithelium compared to the ovarian surface epithelium suggestive of the fallopian tube as a site of origin (Xiang *et al.*, 2018).

Although there is compelling evidence to support the 'STIC as a precursor' hypothesis, STICs and HGSCs were found to co-exist in a fraction of patients with or without BRCA mutations and does not provide an explanation of all HGSC occurrences (Chen *et al.*, 2017). Moreover, STICs are not exclusive to HGSC and are found in a proportion of patients with high-grade endometrial carcinoma or endometrial hyperplasia. This evidence suggests that STIC could be a risk factor for HGSC, but more causal evidence is required to affirm that STIC is a bona-fide precursor lesion for hereditary and sporadic HGSCs in women (Kim *et al.*, 2018).

1.4 Epidemiology

Based on most recent figures published by the WHO, approximately 295,000 new cases of OC were observed worldwide in 2018 (Bray *et al.*, 2018). As a result, OC is the 8th most common cause of cancer in women and the lifetime risk of developing OC is roughly 2.7% (Momenimovahed *et al.*, 2019). In the UK, OC is the 6th most common cause of gynaecological cancer, and it affects over 7,400 women per year or **20 cases per day.** Within the UK, the highest number of cases was recorded in England (over 6,000) followed by Scotland, Wales, and Northern Ireland (Cancer Research UK, 2018). Ovarian cancer cases make 2% of the total cancer cases detected within the UK (Cancer Research UK, 2018).

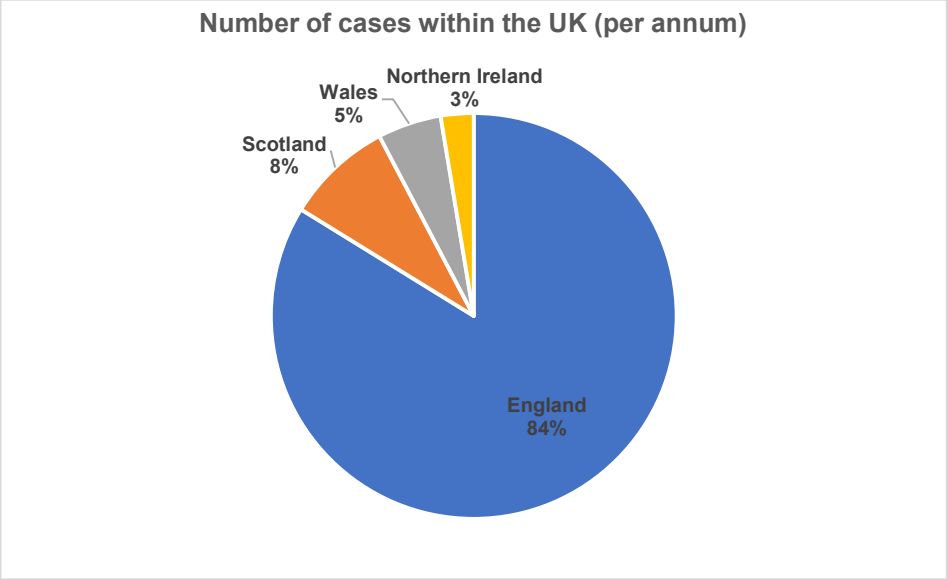

Figure 1.5 *- Pie-chart depicting the number of cases of OC within different parts of the UK recorded per annum* (*Cancer Research UK, 2020*).

The highest age-standardised incidence rates are observed in developed parts of the world, including North America, Central and Eastern Europe. It is worth noting that in most developed countries, largely North America and Europe, OC incidence and mortality have gradually declined since the 1990s (Reid *et al*, 2017) Despite this drop, the survival rates in the UK are still lower than other European countries such as Germany, Portugal, France, Spain as well as other countries like Australia and Canada. This is despite the UK having a similar health care system, having a similar percentage of women diagnosed at different stages of the disease to other developed countries, as well as being the centre for research and clinical trials on OC (Doufekas and Olaitan, 2014).

Based on ethnicity, white/Caucasian women have the highest incidence of OC within the UK (18.1 per 100,000), followed by Asian women (varying between 9.2 – 15.5 per 100,000). The rate of incidence seen within black women is significantly lower (between 6.6 – 12.1 per 100,000) (Cancer Research UK, 2018). This trend also holds true within North America where the incidence of OC in non-Hispanic white women is 5.2 per 100,000; followed by non-Hispanic blacks and Asian/Pacific Islanders (both at 3.4 per 100,000) (Torre *et al.*, 2018).

1.5 Risk factors

1.5.1 Age

Ovarian cancer mostly affects post-menopausal women. The incidence of OC is low in women under the age of 40 but rises steeply after the fifth decade. According to most recent data, the incidence rate peaks during the 75 to 80 age group, showing a strong correlation of OC with increasing age (Doufekas and Olaitan, 2014a; Cancer Research UK, 2018).

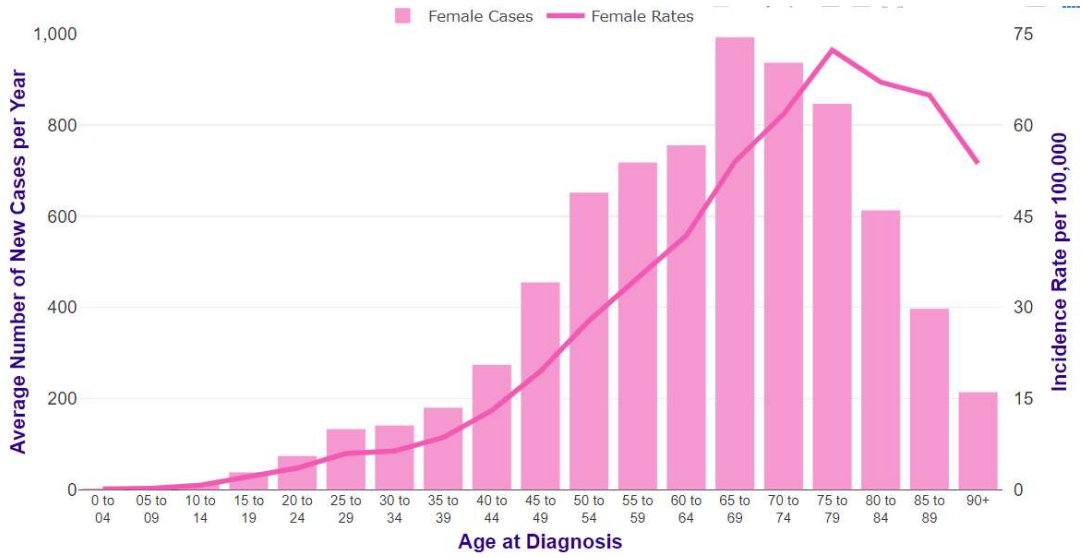

Figure 1.6 *– Graph depicting the correlation between age and OC diagnosis. Incidence rate increases with age, rising steeply from around age 35-39. The peak in female rates (represented by a pink solid line) is observed in the 75-79 age group* (*Cancer Research UK, 2020*).

1.5.2 Reproductive Factors

- **Parity and Breastfeeding -** Parity is shown to have a protective effect against OC and studies have reported that parous women had an estimated 26% lower risk of ovarian cancer than nulliparous women. The reduction in risk of OC was greatest for the first birth, with almost 20% risk reduction compared to nulliparous women. For every subsequent birth, risk reduction continued, however the protective effect was much smaller (<10% per birth) (Gaitskell et al., 2018; Sung et al., 2016). For miscarriage and abortion, most studies found a slightly reduced risk or no association with OC. Incomplete pregnancies seem to confer some protection from ovarian cancer, although the protection is weaker compared to full-term pregnancies. Lactation is also shown to have a protective effect. For each month of breast feeding, the relative risk decreased by 2% (Danforth et al., 2007; Sueblinvong and Carney, 2009; Doufekas and Olaitan, 2014).

- **Menarche and Menopause –** There is evidence that suggests a slight but non-significant reduction in OC risk in women who had their menarche after 12. However, no indicative patterns of potential risk have been detected based on age at menarche or at menopause (Hankinson et al., 1995). A meta-analysis conducted more recently concluded an inverse relationship between age at menarche and associated OC risk, possibly explained by the ''incessant ovulation hypothesis'', suggesting that the early beginning of damage to the ovarian lining to facilitate ovulation followed by the earlier release of associated hormones potentially increase OC risk (Gong et al., 2013).

- **Oral contraceptives –** The contraceptive effect of the combined pill, which contain both weak oestrogens and more potent progestins, is mediated by suppression of the mid-cycle gonadotrophin surge with a consequent inhibition of ovulation. Many epidemiological studies provide evidence for a protective effect of oral contraceptives against OC. Users of the contraceptive pill show a consistently lower risk of OC compared to those who do not in almost all case-control studies. Prolonged use of oral contraceptives is associated with a continual reduction in risk. In addition, the protective effect continues for a long time after cessation of use. Several studies have shown a 40-70% reduced risk even after 10 years have elapsed since the last use (Hankinson et al., 1995; Sueblinvong and Carney, 2009).

- **Hormone Replacement Therapy** – Hormone replace therapy (HRT) users are shown to carry a greater risk of developing OC in comparison to women who do not. A meta-analysis looking at the effect of oestrogen as HRT raised the risk of ovarian cancer by about 22% over 5 years (Hein et al., 2013). Furthermore, HRT use was associated with a higher risk of serous ovarian cancer compared to other histological types. Oestradiol-only therapy for 5 or more years was associated with an increased risk of both serous and endometrioid OC (Shi *et al*, 2016). Some studies have also shown that the risk related to oestrogen-only HRT is higher compared to oestrogen-progesterone therapy. Preliminary research suggests that progesterone may have a protective effect against neoplastic transformation, but this area needs to be explored further (Shi *et al*, 2016).

1.5.3 Body Mass Index (BMI)

A higher BMI is linked to an increased risk in OC. Obese women (BMI = 30+) carry a 30% higher risk of epithelial OC and overweight women (BMI = 25 – 29.9) carry a 16% risk when compared

to women with normal BMI, highlighting a positive correlation between BMI and OC development in adolescent/adult females (Engeland *et al*,, 2003; Olsen *et al.*, 2007). Furthermore, the link between obesity and OC may differ by stage, with decreased survival in case of localised disease although further investigation needs to be conducted to replicate and confirm this observation (Bandera et al., 2017).

1.5.4. Family History

Family history is a strong risk factor for OC. Mutations in **BR**east **CA**ncer gene 1 and 2 (BRCA1 and BRCA2) are associated with the highest percentage of familial risk, both of which carry a 59% and 16.5% risk respectively, in terms of developing OC by the age of 70 as reported by the Epidemiological study of BRCA1/2 mutation carriers (EMBRACE) in the UK (Mavaddat et al., 2013). In addition, germline alterations within BRCA1/2 were reported to be associated with high grade serous histology. Studies also indicate that OC could possibly be a manifestation of hereditary nonpolyposis colorectal cancer (HNPCC) syndrome, caused due to mutations in mismatch repair genes (MMR) such as **M**ut**S H**omolog **2** (MSH2) (Geary et al., 2008). Mutations in other genes such as **BR**CA1 **I**nteracting **P**rotein c-terminal helicase **1** (BRIP1), **RAD51** paralog **C** (RAD51C) and **RAD51** paralog **D** (RAD51D) also contribute to the development of hereditary OC (Norquist et al., 2016; Zheng et al., 2018). According to CRUK , 5 -15% of OC cases are caused due to inherited conditions, with majority of these cases linked to BRCA mutations. Other genetic conditions such as Lynch syndrome and Peutz-Jeghers syndrome are also linked to developing ovarian cancer with a 7% and 21% chance respectively (Cancer Research UK, 2020).

1.5.5. Underlying Medical Conditions

Endometriosis is a chronic condition characterised by the growth of endometrial tissue in sites other than the uterine cavity, most commonly in the pelvic cavity, including the ovaries, uterosacral ligaments, and pouch of Douglas. Common symptoms include dysmenorrhoea, dyspareunia, non-cyclic pelvic pain, and subfertility (Farquhar, 2007). As an underlying medical condition, endometriosis can increase the chances of developing OC. Multiple meta-analysis reports show a correlation of endometriosis with an increased risk of epithelial, endometrioid and clear cell OC (Pearce et al., 2012). Tubal ligation is shown to reduce the risk of epithelial OC by 34% (Wang et al., 2016). Unilateral oophorectomy, as well as radical resection of visible endometriosis aids in reducing the risk of later developing OC (Doufekas and Olaitan, 2014). Women with a history of breast cancer carry a twofold risk of developing OC. The risk increases to fourfold if breast cancer is diagnosed before the age of 40 and carry additional risk if they also have a family history of breast cancer or OC, as discussed earlier (Bergfeldt et al., 2002).

1.6. International Federation of Gynaecologic Oncology (FIGO) Staging

Based on degree of differentiation/tumour grade, OC can be classified using guidelines provided by various grading systems. Grading systems that are commonly used include those discussed and approved by FIGO, the World Health Organisation (WHO) and the Gynaecologic Oncology Group (GOG) (Prat, 2015).

Stage I tumours are confined to the ovaries or fallopian tube(s) (figure below). Stage I OC is further subcategorised into:

- **IA;** limited to one ovary (capsule intact) or fallopian tube surface, presenting no malignant cells in ascites or peritoneal washings.
- **IB;** tumour limited to both ovaries (capsules intact) or fallopian tubes. No tumour on ovarian or fallopian tube surface and no malignant cells in ascites or peritoneal washings.
- **IC:** tumour limited to one or both ovaries and fallopian tubes with any of the following:
  IC1: surgical spill
  IC2: capsule ruptured before surgery or tumour on ovarian or fallopian tube surface
  IC3: malignant cells in the ascites or peritoneal washings

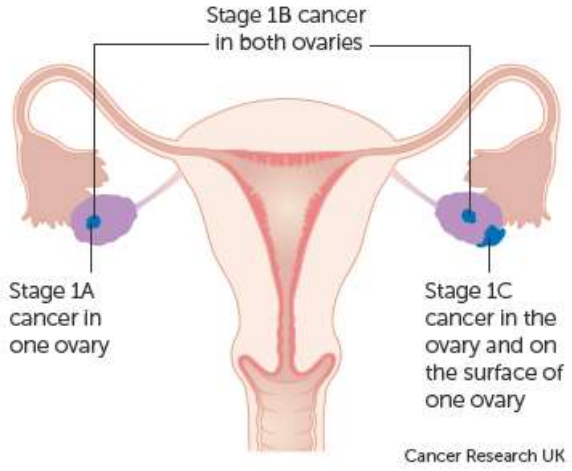

Figure 1.7 *– Sub-categories of stage I OC. Stage IA shows the presence of ovarian cancer confined to one ovary; Stage IB indicates the presence of ovarian cancer within both ovaries and stage IC is identified by the presence of the disease within both ovaries and in pelvic peritoneum (Cancer Research UK, 2020).*

Stage II tumours involve one or both ovaries or fallopian tubes with pelvic extension (below pelvic brim) or primary peritoneal cancer. Stage II tumours can be further sub-categorised into:

- **IIA;** extension and/or implants on uterus and/or fallopian tubes and/or ovaries.

- **IIB;** extension to other pelvic intraperitoneal tissues.

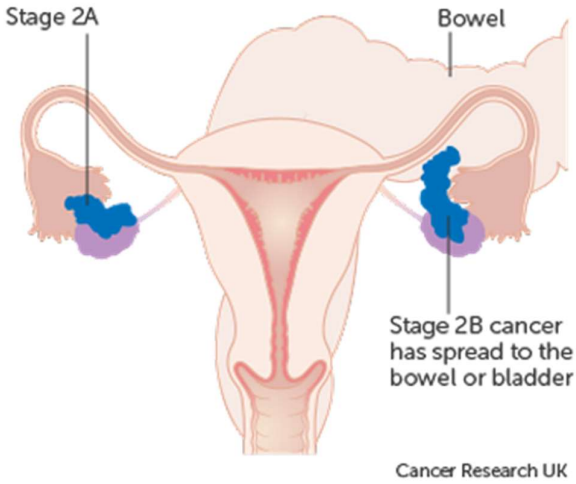

Figure 1.8 *- Sub-classifications of stage II OC. Stage IIA (left) showing the extension of disease from the ovaries to the fallopian tube and/or attachment to uterus. Stage IIB (right) showing the metastasis of ovarian cancer to other intraperitoneal tissues within the pelvic region (Cancer Research UK, 2020).*

Stage III tumours involve one or both ovaries or fallopian tubes, or primary peritoneal cancer, with cytologically or histologically confirmed spread to the peritoneum outside the pelvis and/or metastasis to the retroperitoneal lymph nodes. Stage III ovarian cancer is further sub-categorised as follows:

- IIIA; positive retroperitoneal lymph nodes only (cytologically or histologically proven):
    - **IIIA1(i)** Metastasis up to 10 mm in greatest dimension
    - **IIIA1(ii)** Metastasis more than 10mm in greatest dimension
    - **IIIA2** microscopic extra-pelvic (above the pelvic brim) peritoneal involvement with or without positive retroperitoneal lymph nodes.
- IIIB; macroscopic peritoneal metastasis beyond the pelvis up to 2 cm in greatest dimension with or without metastasis to the retroperitoneal lymph nodes.
- IIIC; macroscopic peritoneal metastasis beyond the pelvis more than 2 cm in greatest dimension, with or without metastasis to the retroperitoneal lymph nodes (includes extension of tumour to capsule of liver and spleen without parenchymal involvement of either organ)
-

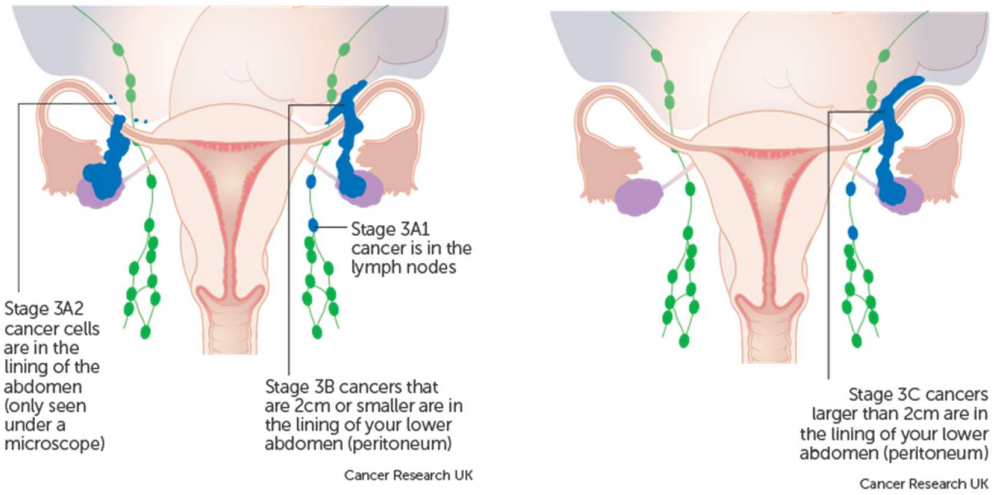

Figure 1.9- *Sub-classifications within stage III OC. Stage IIIA (left) showing that the cancer has now spread to the retroperitoneal lymph nodes and that the metastatic disease is equal to or more than 10mm in diameter. Stage IIIB (left) showing peritoneal metastasis with tumour size less than or equal to 2 cm and stage IIIC (right) showing peritoneal metastasis with tumour size greater than 2cm (Cancer Research UK, 2020).*

Stage IV results in distant metastasis excluding peritoneal metastases and is further sub-categorised into:

- **IVA;** pleural effusion with positive cytology
- **IVB;** parenchymal metastases and metastases to extra-abdominal organs (including inguinal lymph nodes and lymph nodes outside the abdominal cavity)

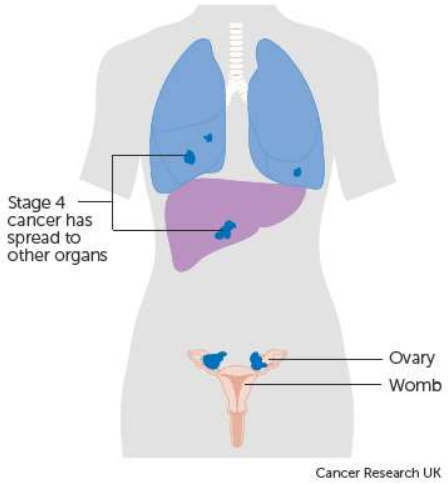

Figure 1.10 *- Conditions for stage IV OC. Stage IV, the most advanced stage of ovarian cancer, occurs when the tumour has moved from the pelvic/abdominal region and has affected the lymph nodes present outside the pelvic cavity. It is also characteristic of metastasis to other organs outside the pelvis (Cancer Research UK, 2020).*

According to FIGO guidelines, before classification into one of the above categories, the primary site should be designated. If impossible, then the primary site should be termed as 'undesignated', followed by recording the histological sub-type of the tumour. Changes that have been added to the most recent FIGO classification guideline include:

- Addition to sub-section IC, involving guidelines in the case of tumour rupture, surface involvement by tumour cells or presence of malignant cells in the ascites or peritoneal washings. Also, the possibility of having stage I peritoneal cancer has been eliminated.
- Deletion of sub-section IIC, about IIA or IIB but with tumour on surface has been eliminated due to it being considered redundant.
- Complete revision of stage III ovarian cancer, resulting in the assignment to stage IIIA1 based on spread to the retroperitoneal lymph nodes without intraperitoneal dissemination. Further sub-division of IIIA into IIIA (i) and IIIA (ii) based on metastasis being less than or greater than 10 mm in greatest dimension.
- Stage 4 includes the addition of IVA covering pleural effusion as part of the subdivision (Prat, 2015).

1.7 Procedure of diagnosis within the NHS

The UK National Health Service (NHS) follows detailed guidance provided by the National Institute for Health Care and Excellence to diagnose, treat, and manage patients with ovarian cancer. The guidelines were published in 2011 and were reviewed in 2017 (NICE, 2017).

Primary Care - At the primary care level, women (especially post-menopausal women) with gastro-intestinal symptoms or abdominal discomfort go through a physical examination and a routine blood test to record serum cancer antigen 125 (CA125) levels.

- If serum levels are low (≤ 35 U/mL), then the patient is assessed for other underlying clinical conditions and asked to return to GP if the symptoms are persistent (for at least 1 month) and/or frequent (at least 12 times). In case of high serum CA125 levels, the patient undergoes a pelvic and abdominal ultrasound to look for visible mass. Based on those results, the GP decides whether the patient needs to be referred to secondary care. CA-125 tests pose limitations which will be discussed later.
- In exceptional circumstances, if a physical examination confirms the presence of ascites or abdominal mass, the patient is immediately referred to secondary care, where additional tests are performed to confirm the diagnosis.

- England meets the standard for their country on the percentage of patients first seen by a specialist within two weeks of urgent GP referral for suspected cancer. This scheme supports early diagnosis as spotting cancer early is important for improving survival, therefore it is vital that patients with potential cancer symptoms are referred properly. Around a third (32%) of OC cases in England are diagnosed via the 'two-week wait' referral route (Cancer Research UK, 2020).

Secondary Care – At secondary care, results from blood tests and ultrasound examination is taken into consideration along with the patient's clinical status.

- If this suggests the presence of OC, then a computed tomography (CT) scan of the abdomen and pelvis is performed to confirm diagnosis.
- An accumulation of all these test results is used to calculate a Risk of Malignancy Index (RMI) score for each patient. If the RMI score is ≥ 250, the patient is referred to a specialist multi-disciplinary team within tertiary care (MDT).

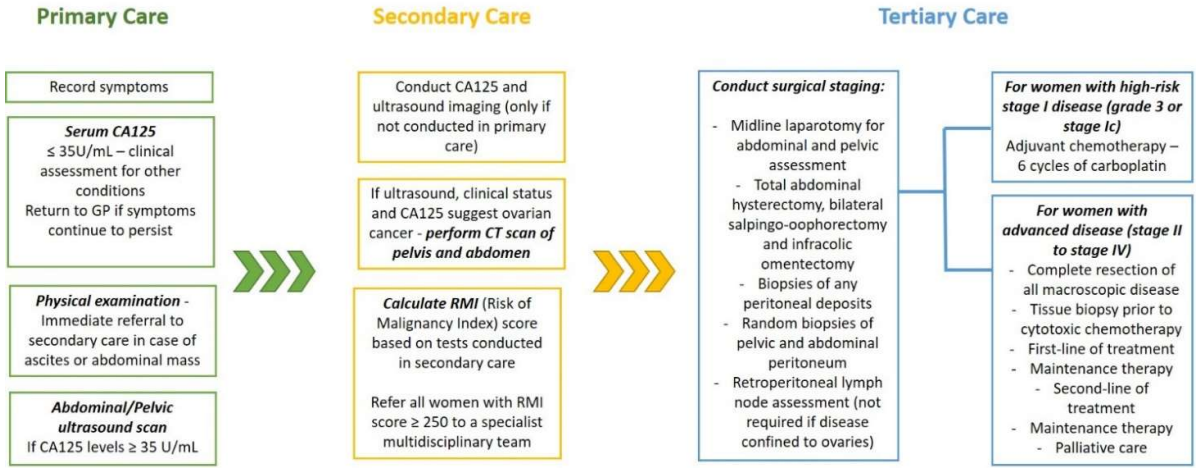

Figure 1.11 *- Summary of various steps involved in the diagnosis, treatment, and management of OC in the UK, according to the most recent NICE (National Institute for Health and Care Excellence) guidelines (NICE, 2017).*

Tertiary Care – The first step within tertiary care is to conduct surgical staging. This is mostly to obtain tissue samples from the tumour to confirm stage and grade through immunohistochemistry and discuss possible treatment options. Figure 1.11 shows the different procedures involved in surgical staging.

- For patients with early stage, low-grade cancer (confined to the ovaries), surgery alone is the recommended course of treatment. In case of high-risk stage I disease, adjuvant chemotherapy with carboplatin is accepted (see below).
- In case of advanced disease, surgery and chemotherapy is the accepted regimen. Before beginning chemotherapeutic treatment, a tissue biopsy is obtained to confirm cell type/grade of tumour, in order to assess the right course of treatment.

1.8. Treatment of OC

The current standard of care for patients with OC involves maximum surgical cytoreduction followed by combination chemotherapy (platinum-taxane) (Lheureux *et al*, 2019).

- **Surgery** - Surgery is pivotal to achieve the goal of improving survival. Not only does surgery help establish diagnosis and staging but is needed for maximal surgical cytoreduction. Removal of greater amounts of tumour has consistently been associated with better outcomes. Post-surgery patients with less than 1.5 cm disease had an additional 14 months added to their median overall survival whereas those with disease greater than 1.5 cm had only 12 months (Coleman et al., 2013). This shows the importance of residual disease as a prognostic factor for survival. Usually, primary debulking is performed prior to starting any kind of chemotherapeutic treatment. However, in neo-adjuvant chemotherapy, treatment is administered prior to surgical cytoreduction and is thought to benefit patients with significant medical comorbidities or those with non-debulkable tumours (Jenkins et al., 2013). Interval debulking surgery (IDS) after a short course of neo-adjuvant chemotherapy (NACT), usually three cycles of chemotherapy, has become a possible alternative treatment option to standard treatment in patients who are unable to undergo complete resection during primary debulking surgery (PDS) (Sato and Itamochi, 2014). Although NACT-IDS is considered an alternative, the progression-free survival (PFS) and overall survival (OS) rates are similar to those achieved during PDS (Gao et al., 2019).
- **Chemotherapy -** Platinum-based chemotherapy has helped manage OC to an extent. The most common chemotherapy regimen prescribed to patients with OC is a combination of carboplatin and paclitaxel (Jenkins et al., 2013). Unfortunately, a large proportion of patients become candidates for second-line treatments due to recurrent disease or loss of platinum sensitivity. Therefore, the second line of treatment is dependent on the level of platinum sensitivity (Kim et al., 2012). For platinum-sensitive patients, carboplatin monotherapy is a convenient option to administer as it is well-tolerated and produces relatively high response rates. However, the response from carboplatin-only treatment usually lasts for a few months until the disease slowly turns 'platinum resistant' which

each subsequent course of therapy (Luvero, Milani and Ledermann, 2014). The international collaborative ovarian neoplasm 4 trial (ICON-4) was the first to show that a combination of platinum and paclitaxel was more effective than single-agent platinum compounds in patients with relapsing platinum-sensitive ovarian cancer. The carboplatin/paclitaxel combination has shown to increase PFS by a median of 3 months and OS by 5 months compared to carboplatin alone, which is why a carboplatin/paclitaxel combination is more suitable (ICON and AGO Collaborators, 2003; Gabra, 2014). In case of platinum-resistant disease, taxanes such as paclitaxel and docetaxel are recommended. Topotecan, pegylated liposomal doxorubicin (PLD) and trabectedin are also utilised in case of recurrent disease (Monk et al, 2016).

1.9. Alternative chemotherapy options

High relapse rate and poor prognosis of advanced stage epithelial OC have led to the development of targeted molecular and biological therapies including anti-angiogenic agents, poly (ADP-ribose) polymerase (PARP) inhibitors, signalling pathway inhibitors and immunotherapies (Katopodis et al., 2019).

Anti-angiogenic therapy - Angiogenesis is a requirement to enable cancer growth; it is known to play a fundamental role in the pathogenesis of ovarian cancer, promoting tumour growth and progression through ascites formation and metastatic spread. Vascular endothelial growth factor (VEGF) and its receptor are expressed in OC cells and show a strong association with the development of malignant ascites and tumour progression (Monk et al, 2016). Bevacizumab (Avastin) is a humanised anti-VEGF monoclonal antibody currently approved for the treatment of OC (Keating, 2014). Bevacizumab is a human monoclonal antibody against the critical pro-angiogenic factor, vascular endothelial growth factor (VEGF) that contributes to angiogenesis, tumour growth and metastasis. (Matsuo et al., 2010). It works by targeting all isoforms of VEGF-A and preventing it from binding to VEGF receptors present on the surface of endothelial cell membranes. This results in a regression in tumour vascularisation which inhibits tumour growth (Keating, 2014). It has shown to improve PFS as a first-line treatment and in the case of recurrent platinum-sensitive or platinum-resistant disease (Keating, 2014). The introduction of anti-angiogenic agents has improved the outlook for those with high-risk disease (Hall et al., 2013)

PARP Inhibitors – In a landscape characterized by limited therapeutic options and a narrow range of drugs that improve survival, PARP inhibitors have emerged recently as an exciting option. PARP inhibitors promote cell death by trapping PARP1 on the damaged DNA, making this a possible therapy for BRCA-positive OC cases or instances where the malignancy shows

a BRCA-like phenotype (Konecny and Kristeleit, 2016). Multiple PARP inhibitors, including Olaparib, Veliparib, Niraparib, Rucaparib and Talazoparib have been evaluated in clinical trials (Mittica et al., 2018). In 2005, two seminal studies demonstrated that tumour cells lacking BRCA1 and BRCA2 (involved in double strand DNA break [DSB] repair by homologous recombination) are selectively sensitive to small molecular inhibitors of the PARP family of DNA repair enzymes. The model proposed was based on the concept of 'synthetic lethality' where the loss of either of the two genes is not lethal per se, but concomitant inactivation leads to cell death (Mateo et al., 2019).

- **Olaparib -** Clinical trials conducted on patients with BRCA mutations who received standard chemotherapy in the past showed a significant response to Olaparib. Further investigation comparing a higher and lower dose of Olaparib (400 mg and 200 mg respectively) and included a third arm of pegylated liposomal doxorubicin (PLD) showed a higher median PFS corresponding to a higher dose of Olaparib (median PFS was 6.5 months at 200mg, 8.8 months at 400mg and 7.1 for PLD cohorts) (Kaye et al., 2012). Building on this, a multicentre phase II study enrolled 65 patients with and without BRCA mutations. Response to Olaparib was seen in 41% of BRCA mutation carriers and 24% non-carriers, suggesting the presence of a target population beyond BRCA mutation carriers (Gelmon et al., 2011). Since all these studies were conducted in populations previously exposed to platinum chemotherapy, clinical trials in OC shifted towards using PARPi as a maintenance therapy. A key trial conducted after was carried out in HGSOC patients with platinum-sensitive relapse and indicated an improvement in PFS compared to placebo (8.4 months vs 4.8 months, respectively) which led to the approval of Olaparib as a maintenance treatment of BRCA1/2 patients. In 2018, the approval was expanded to all platinum-sensitive patients regardless of BRCA status (Pujade-Lauraine et al., 2017). Following this, Niraparib and Rucaparib have undergone testing in clinical studies, yielding promising results (Mateo et al., 2019).
- **Niraparib -** A phase III double-blind clinical trial (NOVA) investigating the efficiency of Niraparib against placebo in platinum-sensitive recurrent patients showed that patients receiving Niraparib (regardless of BRCA status) had a longer median duration of PFS (9.3 months compared to 3.9 months in placebo cohort). Patients without BRCA status and homologous recombination deficiency had a median PFS of 12.9 months (Kerliu et al., 2020). However, the BRCA cohort showed the highest median PFS of 21 months. As a result, Niraparib has gained FDA approval as a maintenance therapy for OC for patients who show complete or partial response to platinum-based chemotherapy (Kerliu et al., 2020).

- **Rucaparib –** Lastly, Rucaparib has also been developed and has shown positive results in patients with recurrent HGSOC. The ARIEL phase III trial evaluated Rucaparib as a maintenance treatment following platinum-based chemotherapy in recurrent high-grade OC in three cohorts: (i) BRCA1/2 germline or somatic mutations, (ii) homologous recombination deficiency and (iii) intent to treat population. The median PFS for all three cohorts recorded was higher (16.6 months) compared to the placebo cohort (5.4 months) (Coleman et al., 2017).

Tyrosine Kinase Inhibitors (TKIs) – Following the success of Bevacizumab, a VEGF1 receptor inhibitor, TKIs were seen as a potential alternate to target angiogenic pathways in OC (Marchetti et al., 2016). Tyrosine-kinases are classified as a group of enzymes that consist of a catalytic subunit, which transfers a phosphate from nucleotide triphosphate to the hydroxyl group of one or more tyrosine residues on signal transduction molecules, resulting in a conformational change affecting protein function. Upon activation, they function to auto-phosphorylate as well as phosphorylate other signalling molecules carrying out an important role in signal transduction and acting to activate/promote a variety of biological processes including cell growth, migration, differentiation, and apoptosis (Katopodis et al., 2019). The most important signalling pathways activated include the phosphoinositide 3-kinase/Akt pathway/mammalian target of rapamycin (PI3K/AKT/mTOR), the Ras/Raf mitogen-activated protein kinase (MAPK) pathway, the Raf/MEK/Erk pathway and the protein kinase C pathway (Marchetti et al., 2016). TKIs utilize different mechanisms, such as competing for the substrate to bind to within the ATP-binding pocket during an active conformation, to occupy a site adjacent to the ATP-binding pocket. This allows both the inhibitor and ATP to bind to the same protein and/or bind irreversibly to the protein kinase target. In some cases, TKIs can also block protein kinase recruitment leading, inhibiting oncogenic kinases to access the complex, resulting in the degradation of cancer cells (Figure 1.12)

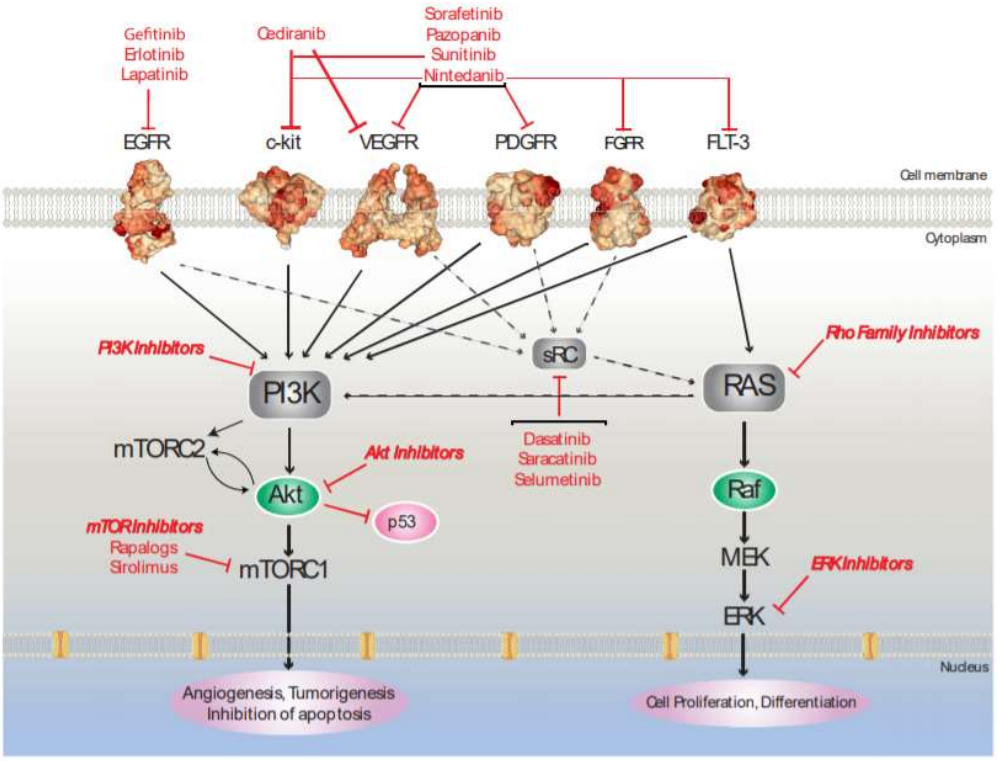

Figure 1.12 *– Overview of kinase inhibitors used as potential therapeutic targets against OC (Katopodis et al., 2019).*

TKIs have been tested clinically as a single agent as well as in combination with other chemotherapy drugs, most of which have undergone phase I or II trials as a monotherapy or in combination with Paclitaxel and Olaparib. It is worth noting that due to the heterogenous nature of OC, many treatments are rendered ineffective despite being broad-spectrum or targeted. Emerging evidence suggests that targeting multiple pathways may prove promising. Building on this, some of the most successful TKIs reported include Nintedanib, Cediranib and Pazopanib, are all multi-kinase inhibitors (Katopodis et al., 2019). PI3K/AKT/mTOR pathway is another prominent cellular pathway implicated in regulating cell growth, motility, survival, proliferation, protein synthesis, autophagy, transcription as well as angiogenesis. It is frequently active in clear-cell and endometrioid carcinoma; genetic aberrations linked to this signalling pathway are also found in epithelial OC (Cheaib *et al,* 2015). As single agents and combination therapies, the efficacy of PI3K/AKT/mTOR inhibitors in the treatment of a variety of cancers has generally not been satisfactory. Phase III clinical trials have not been reported yet in patients with OC, showing that they are not fully ready to be translated into clinical use and require further investigation (Katopodis et al., 2019).

1.10. Reliability of diagnostic tests

Based on the current mortality rate of the disease, it is evident that current diagnostic tests lack the necessary sensitivity required to diagnose this lethal disease early. Currently within the UK healthcare system, the techniques used for initial diagnosis of OC include:

- Physical examination
- Transvaginal ultrasound
- Serum CA125
- Immunohistochemistry

1.10.1. Physical Examination

Out of the three primary tests mentioned, physical examination is the least sensitive as a screening/diagnostic tool. Physical examinations are known to have limited accuracy, especially in the case of obese patients, where a mass could easily be missed or if detected, could be caused by conditions other than ovarian cancer (Doubeni *et al*, 2016). Furthermore, a prominent pelvic mass is not indicative of OC alone and could be a benign condition, which is why NICE guidelines recommend urgent referral to secondary care to perform additional tests to confirm diagnosis. This makes it an unreliable tool for early diagnosis or screening (NICE, 2017). Although ovarian cancer patients did have symptoms before diagnosis, the symptoms were often vague and not necessarily gynaecological in nature; with the most common symptoms experienced by patients being abdominal (increased size and abdominal pain), gastrointestinal (bloating, indigestion, constipation), pelvic pain, fatigue, and increased urinary frequency (Goff, 2012).

1.10.2 Transvaginal Ultrasound

Ultrasounds provide detailed images of the ovaries and the surrounding pelvis and is used to detect morphological changes to potentially detect a developing malignancy (Nash, Menon 2020). Women with suspected OC based on clinical presentation or a pelvic mass undergo transvaginal ultrasonography (Doubeni *et al*, 2016). Although having a visual element to aid in diagnosis is crucial, it does have limitations. Transvaginal ultrasounds can achieve anywhere from 86-94% sensitivity and specificity. Even in post-menopausal women, there is a possibility of capturing false positive results given that there is a high presence of benign lesions in this group (Doubeni *et al*, 2016). In the case of early-stage OC, a small tumour mass may not be picked up on an ultrasound scan, making it less reliable for screening and early detection, if considered by itself. Finally, many aggressive cases of OC metastasize before tumours can reach a visually detectable size which raises questions on its accuracy (Nash and Menon, 2020). Most recently, a phase II UKFOCSS trial aimed to establish the performance of screening with CA125 and

transvaginal sonography (TVS), using a risk of ovarian cancer algorithm (ROCA) to identify women with a high risk of OC and fallopian tube cancer. In this high-risk female population, ROCA screening took place every 4 months, followed by CA125 and TVS to detect disease. Based on this model, women enrolled in this study were significantly less likely to be diagnosed with stage IIIb to IV OC during UKFOCSS screening. Furthermore, the results suggest that in a high-risk population, this model of screening was associated with high sensitivity, significantly lower high-volume disease and a high zero residual disease rate after surgery. The overall findings also suggest a screening-mediated reduction in disease volume. The performance characteristics of screening every 4 months were encouraging; overall incident sensitivity was 94.7%, with occult cancer detection modelled, and positive predictive value (PPV) was 10.8% (i.e., greater than the suggested 10% level for general-population screening) (Rosenthal et al., 2017).

1.9.3 Serum CA125

CA125 is a glycoprotein that is highly expressed by epithelial ovarian cancers. It was first described by Bast and colleagues in 1981 and has become a well-established tumour marker over the years. However, its sensitivity and specificity have been in question for a quite some time (Rauh-Hain et al., 2011). To begin with, CA125 alone or in combination with other techniques is not enough to provide a robust screening or diagnostic tool for OC. In advanced disease, CA125 is elevated in about 85% of patients but it is not specific for OC. Elevated CA125 levels may also be found in non-gynaecological malignancies (e.g., breast, lung, colon, and pancreatic cancer) and in benign disease (e.g., endometriosis, pelvic inflammatory disease, and ovarian cysts) (Scholler and Urban, 2007; Dochez et al., 2019) leading to occurrences of false-positive results and misdiagnosis.

A randomised controlled trial (PLCO) studying the effect of ovarian cancer screening on mortality, including approximately 80,000 participants, showed that those who received OC screening did not have a reduced risk of death from the disease as compared to women who received usual care. Furthermore, 3000 patients on that trial received a false-positive diagnosis which was associated with further complications (Buys et al., 2011). An audit conducted by Moss et al in 2004 considered patients who were tested for CA125 levels between 2000 and 2002 and their results pointed out that 80% of the abnormal results in the female audit population undergoing investigation for suspected malignancy were not caused by OC. The elevated levels of CA125 was a result of malignancies present at other sites, inflammatory or benign gynaecological disease (Moss *et al,* 2005). A significant increase in the level of CA125 was found in adenomyosis, uterine myoma, endometrial pathology, and endometriosis of the ovary (Muinao, Deka Boruah and Pal, 2019). Moreover, CA125 is not only increased in about 80 % of ovarian cancer but also 50 % rises are observed in stage I epithelial ovarian cancers (Zurawski *et al.*, 1988; Muinao *et al,* 2019).

Therefore, using CA125 as the only biomarker for diagnosis will miss out positive cases that do not express the antigen. The UKCTOCS trial conducted across 13 specialist centres in the UK the largest cohort of women to date, testing the efficiency of CA125 and transvaginal ultrasound testing alone and in combination to reduce ovarian cancer mortality. This study concluded that the use of serum CA125 levels did not cause a significant reduction in mortality overall (Jacobs et al., 2016). However, data from 15 different studies showed that CA125 levels were increased in 90-94% patients suffering from stage II, III or IV ovarian cancer, which is why it is still used to monitor treatment response and detect recurrent disease in healthcare settings (Medeiros et al., 2009).

Patients with early ovarian cancer have few or no symptoms, making diagnosis at this stage very difficult. Currently, there is no established screening test. Clinical details and examination of patients with advanced OC is supported by ultrasound and multiple tumour markers (detected through blood test) including CA125, which established earlier, lacks the sensitivity for early stage EOC detection. Transvaginal ultrasonography improves visualization of ovarian structures, thus improving the differentiation of malignant versus benign conditions (Buys et al., 2011). In addition to CA125, HE4 (Human epididymis protein 4) has also been evaluated for diagnosing ovarian malignant tumours. HE4 was initially isolated in the epididymis and is weakly expressed in the epithelium of respiratory and reproductive organs, but is overexpressed in ovarian tumours (Dochez et al., 2019). HE4 shows a slightly superior performance in prediction of early stages, however CA125 is more sensitive generally and is more elevated in advanced staged of OC compared to early stages. Therefore, a combination of CA125 and HE4 may potentially be a useful screening tool in diagnosing specific histological subtypes and advanced stages (Ghasemi et al., 2014).

-

1.9.4 Immunohistochemistry/Tissue biopsy

Traditionally, tissue biopsies have been regarded as the gold standard for providing relevant data for appropriate cancer diagnosis, leading to positive health outcomes among patients in a variety of cancers (Arneth, 2018). Immunohistochemistry plays a vital role in the diagnosis and staging of OC. Additionally, histopathological samples are used to identify specific genetic signatures (such as the presence of cancer-type specific biomarkers like cytokeratins or TP53 mutations) that are characteristic of different types of tumours and can be indicative of metastatic potential (Lee et al., 2019). OC consists of distinct histological types, all having different clinical and biological characteristics, making accurate classification crucial and clinically relevant, given the differences in prognosis and potentially in therapy for different sub-

types (Köbel et al., 2014). Multiple biomarkers are used in clinical settings to identify various histological sub-types of OC, including general epithelial cancer markers such as cytokeratins, to those characteristically expressed within OCs (McCluggage, 2000). TP53 mutations are known to drive aggressive high-grade serous OCs and are also frequently present in fallopian tube precursor lesions (Kobel et al 2016). Immunohistochemical studies testing the efficiency of TP53 expression to detect HGSOC revealed its ability to detect more than 95% of HGSOC samples, highlighting potential to successfully differentiate between high-grade and low-grade serous OC (Köbel et al., 2016a). Cytokeratins have also been regarded as useful tumour markers due to their ability to indicate the presence of epithelial carcinomas. They constitute a sub-group of intermediate filaments, comprising of 20 different isotypes and are useful tumour markers, well-established for monitoring patients suffering from epithelial cell carcinomas (Barak et al., 2004). Epithelia from different sites differ in their cytokeratin expression patterns and can be used to distinguish between tumour types (McCluggage, 2000). Primary ovarian adenocarcinomas have a distinct cytokeratin expression pattern and show a CK7+/CK20- expression pattern, which has been used to detect malignant ovarian cancer cells (Stimpfl et al., 1999; Karantza, 2011). Wilms' Tumour protein 1 (WT1) has also useful in distinguishing serous tumours (both high- and low-grade serous OC) from other tumour types (Köbel et al., 2016b). WT1 is a transcription factor, initially identified in the genito-urinary system (kidney, ovary, and testes) and plays an important role in cell growth and differentiation. WT1 expression is characteristic of serous ovarian sub-type and is rarely expressed in other non-serous sub-types, making it specific to epithelial OC (Liliac et al., 2013). The frequency of WT1 expression in high grade serous ovarian cancer is approximately 97% (Casey et al., 2017).

Although tissue biopsies hold substantial diagnostic importance, its limitations need to be considered. Firstly, tissue biopsies are invasive as they require patients to undergo surgery in order to obtain a sample. This could be risk inducing for patients and some may not qualify as a result, posing a disadvantage. Surgical biopsies are expensive and time consuming. In some cases, where tumours are widespread and inaccessible, tissue biopsies are not an effective strategy. Most importantly, the heterogeneity of solid tumours is a major issue when sampling tissue biopsies as results may vary between sites. This is because tumours undergo genetic evolution over time and through treatment, making surgical options to obtain biopsies an improper method for serial monitoring (Strotman et al., 2016; Arneth, 2018; Lee et al., 2019; Domínguez-Vigil et al., 2018). In view of these hurdles, liquid biopsies are emerging as a means to provide a simple, fast and non-invasive method to detect biomarkers for diagnostic purposes as well for monitoring disease status/response to treatment, thereby offering the opportunity to access serial monitoring (Palmirotta et al., 2018).

1.11 Liquid Biopsies

Liquid biopsy is based on minimally invasive tests (usually involving blood, but can also include urine, cerebrospinal fluid, saliva, and ascites) and has a high potential to significantly change the therapeutic strategy in cancer patients, providing a powerful and reliable, minimally invasive clinical tool for individual molecular profiling of patients in real time (Lianidou and Pantel, 2018). The 'tumour circulome', defined as a subset of circulating components derived from cancer tissue hone the potential to be used directly or indirectly as a rich source of novel biomarkers (De Rubis *et al*, 2019). Liquid biopsies are based on the analysis of multiple biomarkers such as circulating tumour cells (CTCs), circulating tumour DNA (ctDNA), cell-free RNA, exosomes and free-floating proteins which have been shed by tumours and their metastatic sites into the bloodstream (Neumann et al., 2018).

Liquid biopsies offer a wide range of advantages over conventional tissue biopsies. Given their invasive nature, tissue biopsies are associated with many limitations including patient risk, sensitivity and accuracy, procedural costs, and its incompatibility for clinical longitudinal monitoring. Furthermore, they fail to capture intra-tumoral and inter-metastatic genetic heterogeneity (De Rubis *et al,* 2019). Many studies have shown the ever-changing genomic landscape of tumours and metastases in response to selective therapeutic effects that can suppress or promote the growth of cellular clones, a feature overlooked in the case of tissue biopsies (Palmirotta et al., 2018). Figure 1.13 shows an infographic depicting the various biomarker sources obtained from liquid biopsies and its applications in the current landscape of cancer diagnostics, treatment, and management.

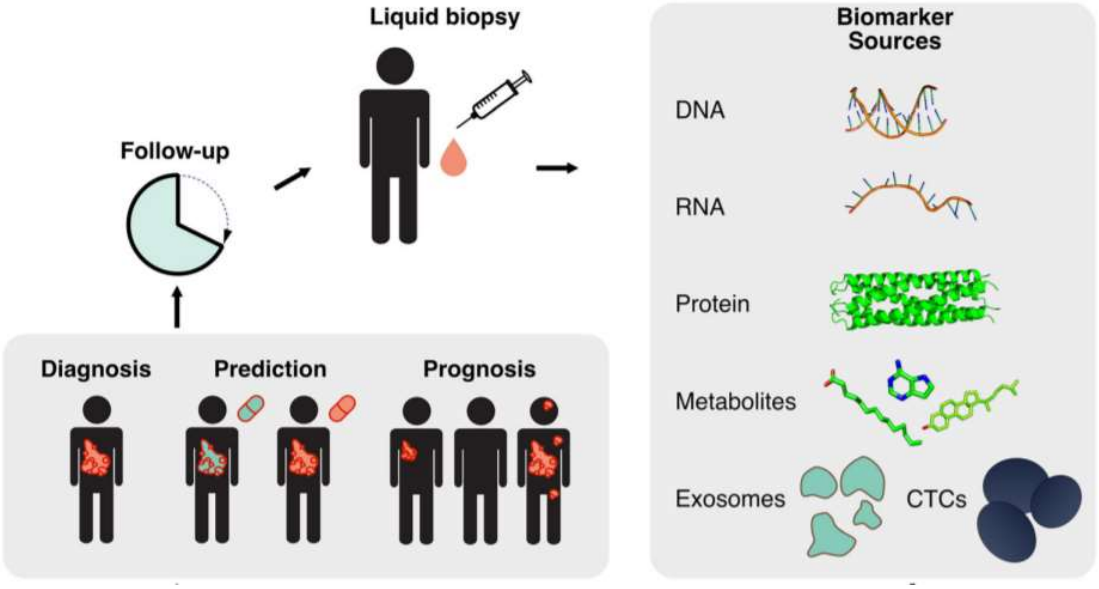

Figure 1.13 *- Pictographic representation highlighting the potential uses of liquid biopsies in cancer management and care. There are multiple biomarker sources identified in blood samples including DNA, RNA, free-floating proteins, metabolites, exosomes, and CTCs. Liquid biopsies can be collected from patients as a blood sample to either diagnose a patient, predict the success rate of treatment prescribed to a patient through serial monitoring or to determine patient prognosis. Blood samples can also be collected post-treatment for follow up purposes eliminating the need to undergo multiple invasive biopsies. (Bratulic et al, 2019).*

1.11.1. Circulating tumour cells (CTCs)

CTCs are living tumour cells that are released into the blood stream from the early onset of cancer development to advanced stage disease, both by primary and secondary lesions (Mari et al., 2019). CTCs contribute towards metastasis through the hematogenous route, using blood as a means of spreading and growth, as opposed to the transcoelomic passive dissemination of tumour spheroids in the peritoneal fluid and ascites (Giannopoulou *et al*, 2018). CTCs hone the ability to colonize distant sites and metastasize after going through various degrees of epithelial-to-mesenchymal transition (EMT) to detach from the tumour and mobilise (Mari et al., 2019). Thomas Ashworth, an Australian pathologist, first published about the presence of cancer-like cells in the blood of a patient with metastatic cancer while examining a sample post-mortem and proposed a hypothesis suggesting the role of circulating tumour cells (CTCs) as a fundamental prerequisite to metastasis (Palmirotta et al., 2018). Recent technological advances have enabled scientists to visualise and detect the presence of these cells which has brought about a substantial amount of attention and effort towards studying the potential of CTCs to provide a robust and reliable diagnosis/prognosis.

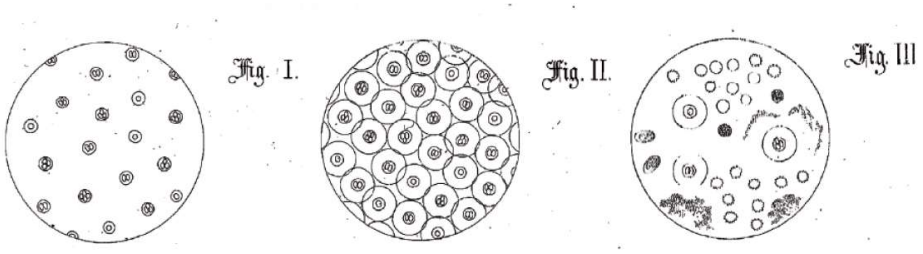

Figure 1.14 *- Drawings produced by Thomas Ashworth depicting the presence of cancer-like cells present in the blood of a patient post-mortem suggesting the possibility of hematogenous route of metastasis in cancer (Ashworth, 1869).*

CTCs can be detected after enrichment using various methods based on physical (size, density, electric charges, deformability) and/or biological markers (expression of epithelial markers and negative selection of haematopoietic markers). After enrichment, CTCs can be detected by immuno-cytological assays (i.e., epithelial protein expression), genomic assays (epithelial mRNAs) and functional methods. A summary of the methods and technologies currently used to detect, extract, and characterise CTCs is shown in figure 1.15.

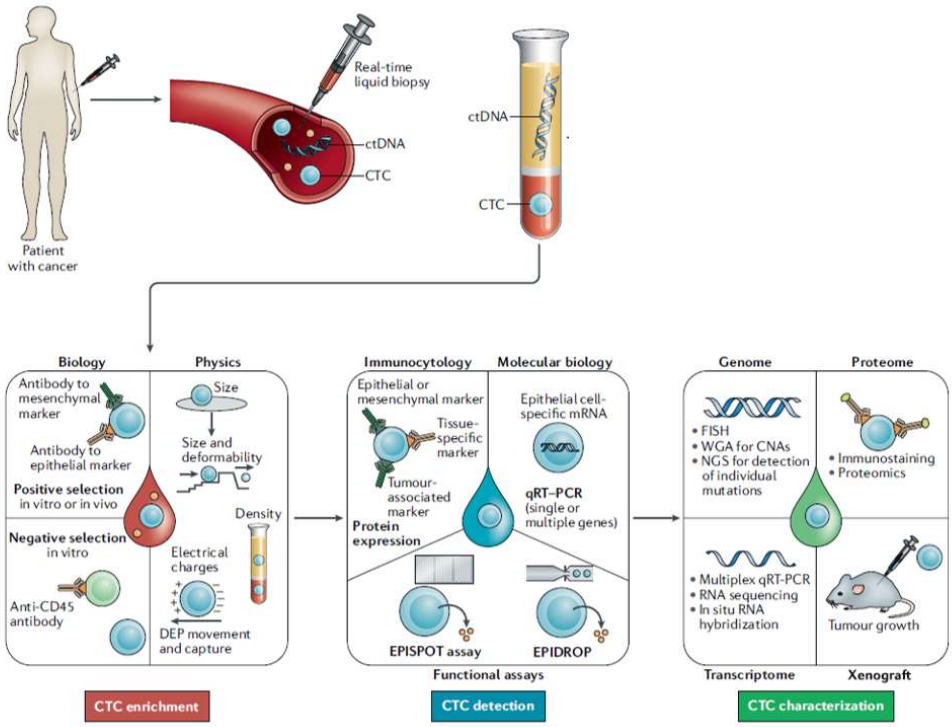

Figure 1.15 *- Technologies for CTC enrichment, detection, and characterization. CTCs in blood can be enriched using marker-dependent techniques: CTCs can be positively selected in vitro or in vivo using antibodies to epithelial and/or mesenchymal proteins (such as epithelial cell adhesion molecule (EpCAM) and/or*

cytokeratins and mesenchymal vimentin or N-cadherin) or negatively selected for through depletion of leukocytes using anti-CD45 antibodies. Positive enrichment of CTCs can also be performed in vitro using assays based on CTC characteristics including size, deformability, density, and electrical charge. Following enrichment, the isolated CTCs can be identified using immuno-cytological, molecular, or functional assays. With immuno-cytological platforms, CTCs are identified by membrane and/or intra-cytoplasmic staining with antibodies to detect expression of epithelial, mesenchymal, tissue-specific, or tumour-associated markers (Pantel and Alix-Panabières, 2019).

Post-enrichment, samples may still contain many white blood cells (WBCs), requiring the use of reliable methods to identify individual CTCs. The predominant approach involves direct immunological detection using antibodies to membrane and cytoplasmic antigens, including epithelial, mesenchymal, tissue-specific and tumour associated markers (Pantel and Alix-Panabières, 2019). The CellSearch platform developed by Veridex was the first cytometric CTC technology to gain FDA approval and is the most widely used platform to enumerate CTCs in samples from patients with breast, prostate, and colorectal cancers (Krebs et al., 2010; Lim et al., 2019). CellSearch™ uses magnetic beads bound to antibodies specifically targeting EpCAM-expressing cells to target CTCs of epithelial origin, a method referred to as immunomagnetic separation. Most current assays use CTC identification steps very similar to the CellSearch™ platform; cells positively stained with fluorescent antibodies for epithelial cytokeratins are marked as CTCs, whereas CD45 is used to identify and exclude white blood cells. Some markers (including cytokeratins) are expressed in a majority of cancers, however tissue-specific markers such as prostate-specific antigen (PSA) or breast-specific mammaglobin, can also be used (Pantel and Alix-Panabières, 2019). A table summarising other technologies developed for the purpose of CTC identification is shown below.

Table 1.1 *– A brief summary of various of CTC capturing technologies developed based on physical properties (label-free techniques) such as size, gradient and electrical charge and biological properties (affinity-based methods) including the direct detection of surface-based antibodies or separation of cells using antibodies allowing for immunomagnetic separation of cells of interest. Antibodies using immunomagnetic separation allow for a select number of cells to be isolated from a mixed population found in blood samples, followed by additional staining to detect specific protein expression.*

Label-Free		Affinity Based	
Function	Platform	**Function**	Platform
Gradient based	Ficoll Paque RareCyte	**Immunomagnetic**	CellSearch Adna Test MACs
Size based	Circulogix ISET ScreenCell Parsortix	**Microfluidic**	CTC-chip GEDI chip OncoCEE Clearbridge
Dielectrophoresis	ApoSTream DEPArray	**Surface based**	Herringbone chip ImageStream

Imaging flow cytometry is a new technology that carries the potential of accurately identifying potential CTCs and other cancer related cells by utilising multiple biomarkers for their identification. The ImageStream™ system developed by Amnis Corporation is the first commercially available imaging flow cytometer with full integration of modern image analysis system, combining the features of fluorescence microscopy and flow cytometry (Zuba-Surma et al., 2007). The current commercial embodiment simultaneously acquires six images of each cell, with fluorescence sensitivity comparable to conventional flow cytometry and the image quality of 40X-60X microscopy. The six images of each cell comprise of: a side-scatter image, a transmitted light (brightfield) image, and four fluorescence images corresponding to four separate spectral bands (Basiji et al., 2007). The ImageStream Mark II possesses unique features such as multi-magnifications (20x, 40x and 60x) as well as the extended depth of field (EDF) technology, which combines the use of specialised optics and special imaging processing algorithms allowing for all information about a captured cell to be grouped onto a single focal plane using focus stacking (Parris et al., 2015). Its data analysis software, known as IDEAS, can calculate over 40 quantitative features per image, resulting in approximately 250 features per cell. These features can be utilised to create histograms and scatter plots much like a standard flow cytometry data analysis program but with added image-based features to identify cell

populations based on size, shape, texture, probe distribution heterogeneity, co-localization of multiple probes etc. (Basiji et al., 2007).

CTC identification can discriminate healthy individuals and patients with benign adnexal tumours from cases with OC, therefore carrying diagnostic significance. In a recent study, 87 patients with indeterminate adnexal mass underwent sample collection for CTC enrichment and detection using a combination of immunocytochemistry and detection based on physical properties. Results indicate that combination of the two methods was able to discriminate benign tumours from OC with a 77.4% sensitivity and 100% specificity. Another study comparing CTC detection in early and late-stage patients found the frequency of CTCs to be significantly lower in stage I compared to stage III and IV. Compared to benign controls, early stage (I and II) and late stage (III and IV) were 8.4 and 16.9 times more likely to have CTCs respectively (Pearl et al., 2014). As a prognostic/predictive tumour biomarker in patients with OC, studies have reported that CTC numbers significantly decline after chemotherapy and high CTC numbers post-chemotherapy is suggestive of platinum-resistance (Asante et al., 2020). In addition, multiple studies have reported a significant association between presence of CTCs and negative impact on OS and PFS. The first ever study to report a prognostic significance of CTCs in primary ovarian cancer linked the presence of CTCs with significant decrease in progression free survival (PFS) (Fan et al., 2009). The same group conducted another study in 129 pre-surgery OC patients and reported a significant association between the presence of CTCs and worse outcomes of OS and PFS (Pearl et al., 2014). Another study sought to investigate the prognostic value of CTCs pre-surgery and after platinum-based chemotherapy in OC patients. CTCs were detected in 19% patients before surgery and 27% after platinum-based therapy. They also show that the presence of CTCs significantly correlated with shorter OS before surgery and after chemotherapy (Aktas et al., 2011). Overall, it is consistent that patients with persistently high CTCs have worse prognosis compared to those with negative CTCs (Giannopoulou *et al,* 2018; Asante *et al.*, 2020). Furthermore, post-operative OC CTC count was significantly associated with advanced stage than early stage, possibly indicating that higher CTC numbers correspond to a higher tumour burden (Kim et al., 2019).

1.11.2. Circulating tumour DNA (ctDNA)

Circulating cell-free DNA (cfDNA) can be extracted from blood plasma and is highly fragmented DNA, mainly derived from apoptotic/necrotic cells, perhaps predominantly from apoptotic leukocytes (Pantel and Alix-Panabières, 2019). cfDNA is normally found in healthy subjects and was first detected in 1948 by Mandel and Metais.

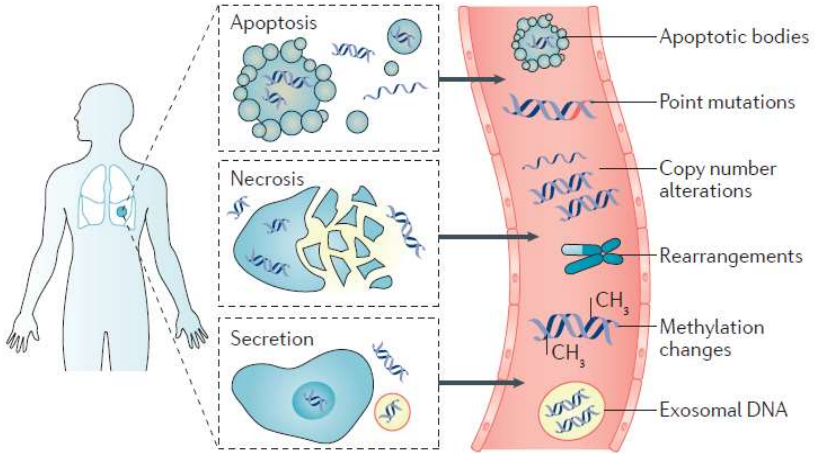

Figure 1.16*- Various sources of cell-free DNA, which can be found within the bloodstream. Cells release cell-free DNA (cfDNA) through a combination of apoptosis, necrosis, and secretion. cfDNA originates from either cancer cells or other cells included in the cancer microenvironment, immune cells, or other body organs. cfDNA found in blood could either be free-floating or associated with extracellular vesicles such as exosomes.* (Wan et al., 2017).

cfDNA was first linked to cancer in 1977, when a study demonstrated an increased amount of cfDNA detected in patients with pancreatic cancer, which decreased after receiving chemotherapy. In 1994, RAS gene mutations were detected in blood samples from cancer patients, highlighting a potential clinical utility for cfDNA (Palmirotta et al., 2018; Siravegna et al., 2019). Although majority of cfDNA comes from normal cells in the body, a small part of this population originates from primary tumours, metastatic sites, or CTCs – this population is called ctDNA or circulating tumour DNA. ctDNA carries tumour-specific molecular alterations, such as mutations, translocations, loss of heterozygosity, copy number alterations and methylations, reflecting an advantage of being able to better inform about tumour heterogeneity in comparison to tissue biopsies (Mari et al., 2019). In addition, ctDNA levels are also influenced by disease burden, tumour location, vascularity, and cellular turnover. ctDNA has been detected in multiple types of cancers including liver, ovarian, stomach, breast, and pancreatic cancer . Notably, in the case of brain tumours, ctDNA has been detected in cerebrospinal fluid samples, providing an alternative source and potential to gather information on surgically inaccessible tumours (Siravegna et al., 2019). Most studies involved in plasma ctDNA analysis capitalises on the identification of cancer-specific mutations by technologies such as digital PCR and next generation sequencing (NGS). Alternatively, assays based on the detection of DNA methylation patterns have also been developed with methylation-specific PCR (MSP) being the main detection method employed to detect ctDNA levels in OC patients (Asante et al., 2020). Analysis of methylated DNA has several advantages, including good reproducibility rates at various time

points because the methylation pattern of a single gene is conserved throughout disease progression (Mari et al., 2019).

In the case of OC, ctDNA shows the potentially to perform as a better diagnostic tool compared to CA125. Meta-analyses conducted on ctDNA as a tool for detection of OC revealed relatively high specificity (>88%) but varied in specificity (27-100%) (Cheng et al., 2017; Asante et al., 2020). Additionally, a few studies have also evaluated the utility of ctDNA as a prognostic biomarker for HGSOC. A study evaluated the correlation between ctDNA dynamics and response to adjuvant chemotherapy, concluding that undetectable levels of ctDNA at 6 months following initial primary treatment was associated with significantly improved PFS and OS and that ctDNA detection has a predictive lead time of 7 months over CT scans (Pereira et al., 2015). ctDNA levels were further shown to correlate with the timing of recurrence. In a study of 144 patients with epithelial OC treated with bevacizumab, both PFS and OS were found to be significantly shorter in patients with high levels of cfDNA in blood (Steffensen et al., 2014). Persistently detectable ctDNA levels post-surgery was also consistent with disease burden and the risk of recurrence in OC patients, while undetectable ctDNA levels were consistent with the absence of detectable disease. Undetectable rates of ctDNA six months after treatment completion were associated with better PFS and OS. The median PFS was 32 months for ctDNA-negative patients vs 6 months for patients with detectable ctDNA after treatment. In addition, TP53 mutations detected through ctDNA using digital PCR have been used to monitor tumour burden and follow treatment response in patients with HGSOC. Studies have shown that high mutant TP53 allele counts correspond to quicker disease progression. TP53 allele fraction concentration was also associated with tumour volume, assessed using CT scans and time-to-progression. TP53 detection in ctDNA was also able to show a more reliable response to chemotherapy compared to CA125 (Mari et al., 2019).

1.11.3. Exosomes

Exosomes are a subtype of EVs formed by an endosomal route and are typically 30-150 nm in diameter (Doyle and Wang, 2019). Exosomes consist of a range of molecules including but not limited to proteins (i.e., cytoskeletal proteins, membrane and fusion proteins and heat shock proteins), cell surface receptors and miRNA (Tkach and Théry, 2016). Exosomes were originally thought to be a source of cellular waste disposal; however, it has since been found that exosomes participate in cell-to-cell communication, cell maintenance and tumour progression (Doyle and Wang, 2019). Recent reports suggest that the presence of hypoxia induced cancer-derived exosomes are used to deliver signals to both tumour cells and the tumour microenvironment, including in OC (Nakamura et al., 2019). Like CTCs, circulating exosomes can be isolated through ultracentrifugation, density-based separation and magnetic separation using antibodies for surface antigens like EpCAM (Mari et al., 2019). In comparison to ctDNA, exosomes have more

stability and a longer circulating half-life which can be advantageous in their potential role as biomarkers (Cheng et al., 2017; Doyle and Wang, 2019). To date, over 2000 species of proteins have been identified from OC-derived exosomes, majority of which have been linked to tumour progression and metastasis (including membrane proteins and enzymes) (Cheng et al., 2017). A study conducted by Liang et al found both overexpressed proteins and signal pathways in OC-derived exosomes that are associated with carcinogenesis. The subset of overexpression proteins included EpCAM, proliferation cell nuclear antigen (PCNA), tubulin beta-3 chain (TUBB3), epidermal growth factor receptor (EGFR) and ERBB2 (Liang et al., 2013). Exosomal proteins also have the potential to serve as markers for tumour staging and prognostic indicators post-treatment. Studies have shown that plasma collected from OC patients contained a higher level of exosomal proteins compared to controls and that exosomal protein content was significantly higher in advanced stages as compared to early-stage disease (Cheng et al., 2017; Mari et al., 2019). Although this information is promising, this area of research is in its developmental stages and larger studies are required to confirm the results.

1.12 Surfactant proteins in OC

Immune surveillance has been recognised for long as an important element of host anti-cancer response. In some circumstances, these inflammatory and immune responses can potentially eliminate a tumour. However, oncogenic pathways activated in the tumour appear to organise the immunologic component of the microenvironment in a way that not only protects itself from the anti-tumour immune response but can also shift it to promote tumour growth (Pardoll, 2015). Cancer-immune system interactions have been used to develop successful immunotherapies like CAR T and have also been used to determine prognosis through T cell expression (Liu and Guo, 2018). Surfactant proteins are collagen containing C-type (calcium type) lectins. Of the C-type lectins, surfactant protein-D (SP-D) in particular appears to be a potent innate immune molecule involved in neutralisation, clearance of pathogens, removal of apoptotic/necrotic cells and downregulation of allergic reactions and inflammation (Nayak et al., 2012). Its primary structure is organised into a cysteine-containing N-terminal region, a triple helical collagen region composed of repeating Gly-X-Y triplets, an α-helical coiled neck region and a C-terminus comprising of a C-type lectin of CRD region (Nayak et al., 2012). SP-D can bind to various self and non-self-ligands (via CRD) on the target surface in a carbohydrate or calcium dependent manner, while the collagen region can recruit and activate immune cells for the clearance of pathogens or necrotic/apoptotic cells (Kishore et al., 2006). SP-D is composed of oligomers of a 130 kDa subunit comprising of three identical polypeptide chains of 43 kDa. Human SP-D is assembled into a 521 kDa tetrameric structure with four of the homo-trimeric subunits linked via their N-

terminal regions but multimers, trimers, dimers and monomers are also possible (Nayak et al., 2012). A visual representation of the multimerization of SP-D is shown in figure 1.17.

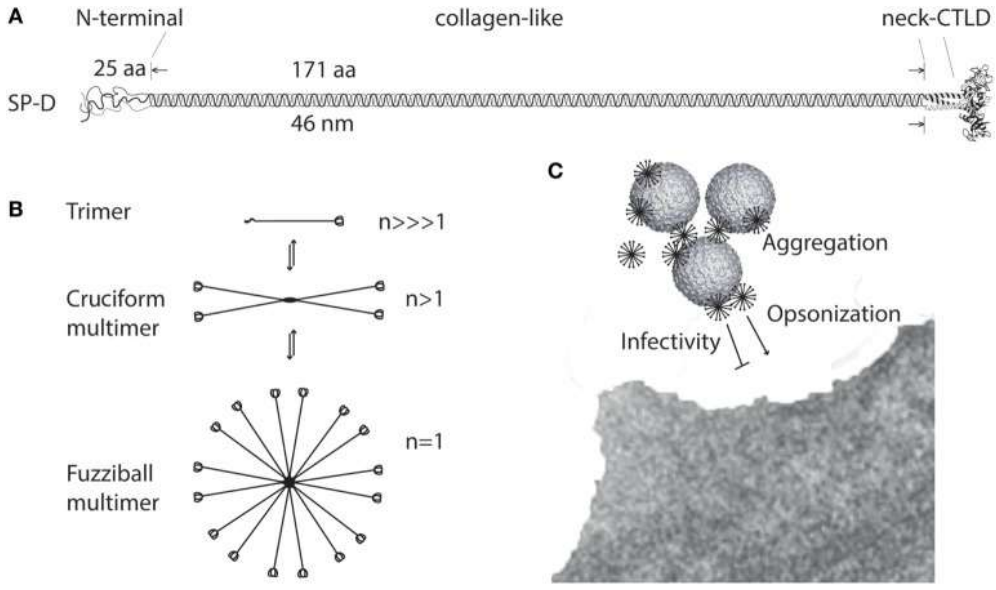

Figure 1.17 - *Multimerization of surfactant protein D (SP-D).* ***(A)*** *Regions of the trimeric SP-D subunit. The subunit structure has been drawn to the approximate dimensions of the protein domains.* ***(B)*** *Multimerization of the trimeric SP-D subunit (3 chains) into 4-subunit cruciform (12 chains) or fuzziball >4-subunit (>12 chains) structures of SP-D.* ***(C)*** *Schematic overview of how multimeric SP-D is implicated in antimicrobial defence. Binding of multimeric SP-D to microbe-associated glycans may block interaction of the microbe with its receptors, aggregate the microbes, or SP-D may act as an opsonin, enhancing endocytic uptake of the microbe in host cells. Only fuzziball SP-D multimers are shown here for simplicity. CTLD, C-type lectin domain (Sorensen, 2018).*

Although SP-D expression was known to be limited to the lungs, recent studies have established its extrapulmonary existence in a range of tissues and is shown to control inflammatory response and helper T-cell polarization. SP-D can also induce apoptosis in activated eosinophilic and T-cells via the p53 pathway (Kaur et al., 2018a; Thakur et al., 2019). Within the female reproductive system, SP-D expression has been localised in the uterus, cervical tissue, vagina, epithelium of fallopian tube, theca interna cells of ovarian follicles and the amniotic epithelium (Sorensen, 2018). Moreover, SP-D has shown to exhibit anti-cancer effects. In lung cancer, studies have shown that SP-D downregulated epidermal growth factor (EGF) signalling and supressed the progression of lung cancer cells by binding to EGF-receptors via lectin activity (Hasegawa et al., 2015). In another study, a recombinant fragment of human SP-D (rfhSP-D) was shown to induce apoptosis in pancreatic adenocarcinoma cell lines via a Fas-mediated pathway (Kaur et al., 2018a). Another study looking at the effects of rhfSP-D in prostate cancer established its ability to induce apoptosis via the intrinsic pathway in explants, primary tumour cells isolated from

tissue biopsies of metastatic prostate cancer patients and in prostate cancer cell lines (Thakur et al., 2019). Since SP-D is naturally expressed in various parts of the female reproductive system, it would be relevant to investigate the potential role of SP-D and immune response in OC.

1.13 Hypothesis and aims

Current diagnosis and staging of epithelial ovarian cancer (EOC) have important limitations and better biomarkers are needed. We hypothesise that liquid biopsies (i.e., blood in this study) can offer a promising alternative to tissue biopsies, providing novel, non-invasive diagnostic approaches and/or serial monitoring of OC evolution. This research aims to address the following objectives:

- Validate liquid biopsy handling
- Investigate the performance of non-haematopoietic circulating cells (CCs) at the time of disease presentation and relapse in OC patients.
- Assess the role of surfactant protein-D (SP-D) as biomarker in OC.
- Study the shuttling of WT-1 in response to chemotherapy.

Chapter 2

Materials and methods

2.1 Tissue culture

2.1.1 Cell culture

SKOV3 (moderately well-differentiated serous adenocarcinoma) and PEO1 (poorly differentiated serous adenocarcinoma) human adherent epithelial cell lines were used as in-vitro models representing human ovarian cancer. The details for each cell line are summarized in table 2.1.

Table 2.1 *– Details of ovarian cancer cell lines cultured in vitro and used for experiments conducted for this project; listing origin, subtype, grade, chemotherapeutic resistance, and gene mutations. Both the cell lines were characterised by (Beaufort et al., 2014) and (Hernandez et al., 2016).*

Cell line	Background/Origin	Subtype	Grade	Chemotherapeutic Resistance	Key gene mutations
SKOV3	Ascites	Serous	1/2	None	TP53 PIK3CA
PEO1	Ascites	High-grade serous	3	None	TP53 BRCA-2

SKOV3 cells were grown in DMEM (Dulbecco's Modified Eagles Medium, Gibco) supplemented with 10% FBS (fetal bovine serum, Gibco), 1% penicillin-streptomycin (Gibco) and 1% L-Glutamine (Gibco). PEO1 cells were grown in RPMI-1640 (Roswell Park Memorial Institute 1640, Gibco) supplemented with 10% FBS (fetal bovine serum, Gibco), 1% penicillin-streptomycin (Gibco) and 1% L-Glutamine (Gibco). All cell lines mentioned above were grown at 37°C in the presence of 5% CO_2 to mimic the conditions maintained within the human body. Cells were sub-cultured appropriately when approaching 80% confluency, roughly three times a week.

2.1.2 Tissue culture practice

Cells were carefully maintained in an aseptic environment with the use of a HERAsafe laminar flow cabinet (Heraeus). The flow hood was repeatedly sterilized using 2% TriGene Advance (Medimark Scientific) and 70% industrial methylated spirit (IMS) diluted in H_2O. Pre-packaged and pre-sterilized items were used wherever possible. All plasticware was sterilized using autoclave prior to use within the flow hood.

2.1.3 Thawing cryopreserved cells

Prior to retrieving cryopreserved cells to initiate culture, 10 mL of complete medium (supplemented with additives as mentioned above) was added to a T-25 flask and stored in the incubator for at least one hour in order to allow media to equilibrize to the temperature and CO_2 conditions. Cells were then removed from liquid nitrogen quickly and kept on ice, while being transported to the tissue culture facility. The frozen vial was instantly defrosted in a pre-warmed water bath at 37°C and transferred within the pre-prepared flask immediately; after which the flask was left undisturbed for 12 hours to allow cells to attach to the surface of the flask. The media within the flask was then replaced with pre-warmed fresh media, removing the DMSO present from the cell freezing medium and supplementing the cells with nutrients necessary for proper growth.

2.1.4 Sub-culturing cells

Cells were sub-cultured to continue healthy growth when they reached approximately 80% confluency rate. Firstly, the media from the flask was removed and cells were washed with 5mL sterile PBS (phosphate buffered saline, Gibco). 3mL of TrypLE™ Express (Gibco) was added per T-75 flask and incubated at 37°C for 3 to 5 minutes. The flask was gently disturbed to allow detachment of cells and resuspended in 17 mL of fresh medium (DMEM or RPMI depending on cell line). 15 mL of this stock was aspirated and 5mL was re-suspended into each of three new T-75 flasks. 15 mL of fresh new media was then added to each flask containing detached cells and placed carefully within the incubator to allow re-attachment and growth. All media used to sub-culture cells was pre-warmed in a water bath at 37°C. All cell lines required a 1 in 4 split approximately three times a week.

2.1.5 Cryopreserving cells

Cell lines were cryopreserved appropriately to maintain stocks within liquid nitrogen for future research. Cells were prepared for cryopreservation when in their exponential growth rate (approximately 70-80% confluency). Media from cells was removed and 3 mL of TrypLE™ Express was added to each T-75 flask. The flask was incubated at 37°C (as mentioned above) and gently disturbed to detach cells from the surface of the flask. This cell suspension was added to a 15 mL Falcon centrifuge tube (Thermo Fisher) and spun down in a centrifuge for 5 minutes at 1500 RPM (21 x g). The supernatant was aspirated, and the resultant pellet was re-suspended in 1-2 mL of Recovery™ cell culture freezing medium supplemented with 10% DMSO (Gibco). The cryovials were stored at -80°C for 24 hours before being transferred into liquid nitrogen.

2.1.6 Seeding cells

Cells were seeded in 6-well plates prior to treatments and extractions. Cells were counted using a Countess® Automated Cell Counter (Invitrogen) after adding an equal amount of Trypan Blue stain (0.4%) to 10µL of cell suspension to observe cell viability. The seeding volume was calculated as shown below:

Total number of cells = Viable cells/mL x volume (in mL) of suspension.

Number of cells/µL = Total number of cells/volume (in µL) of suspension.

Volume of suspension to add to each well = Seeding density required/number of cells per µL.

2.2. Clinical Samples

2.2.1 Ethical approval process

Prior to collecting samples from patients, ethical approval was sought and approved via the Human Tissue Act (HTA) and the National Research Ethical Service (NRES). Ethical approval was already in place for the collection of blood and plasma samples from ovarian cancer patients participating in the CICATRix trial in collaboration with Mount Vernon Cancer Centre (MVCC) [IRAS ID 198179]. Ethical approval was also sought after at Brunel University London by submitting of an application through BREO (Brunel Research Ethics Online). A Materials Transfer Agreement (MTA) was put in place for the transfer of ovarian cancer blood and plasma samples from Mount Vernon Cancer Centre to Brunel University London.

2.2.2 Whole blood samples

Blood samples were collected from ovarian cancer patients enrolled on the CICATRix trial at Mount Vernon Hospital, London (ethical approval was in set in place). All patients participating in the trial were diagnosed with advanced stage (III & IV) ovarian serous adenocarcinoma. Patient consent was sought prior to collection of any blood sample for the trial. Patient cohorts were divided into three categories depending on the treatment regimen set by the clinician before collecting blood samples. Further details on patient cohorts are provided in Table 2.2.

Table 2.2 – *Details provided for each cohort that patients were divided into after being enrolled on to the CICATRix trial.*

Patient Cohort	Details
NACT (Neo-adjuvant chemotherapy)	Patients belonging to this cohort had been diagnosed with advanced stage (III and IV) ovarian cancer and had received no prior chemotherapeutic treatment or surgical debulking.
PDS (Primary debulking surgery)	Patients belonging to this cohort had been diagnosed and had undergone surgery to remove majority of the tumour mass prior to being given any chemotherapeutic treatment.
Relapse	Patients belonging to this cohort has been diagnosed, had undergone chemotherapeutic/surgical treatment of the disease and did not respond to treatment or developed resistance.

Blood samples were collected prior to starting any treatment (during screening) and after receiving surgery plus every cycle of chemotherapy. Patients were followed through till the end of their treatment and blood samples were collected when they returned to the clinic for their follow-up tests. Blood was also collected (with signed consent) from healthy female volunteers as controls.

All blood samples were collected in Roche™ Cell-free DNA collection tubes in order to preserve blood for up to 7 days, allowing samples to be collected on days after clinics were run and to successfully process blood for CTC enumeration. For comparison purposes, blood was initially collected in Roche™ cell-free DNA collection tubes, EDTA (ethylenediaminetetraacetic acid) tubes and PAXgene blood DNA collection tubes (Qiagen) to investigate the efficacy of maintaining blood sample integrity for more than 1-2 days to allow efficient collection and processing.

2.3 Isolation and imaging of cells

2.3.1 ImageStream™ Mark II

Expression of various biomarkers of interest was visualized using ImageStream™ Mark II (Amnis), a high-resolution imaging flow cytometry machine. This work included studying the expression and cellular localization of AE1/AE3 (or pan-cytokeratin – a general marker of cancer, used extensively in tissue histopathology), WT1 (highly expressed in OC tumours) and CD45

(commonly used to identify the presence of white blood cells; used to differentiate WBCs from circulating tumour cells) using imaging flow cytometry.

2.3.2 Preparation of cultured cells for imaging flow cytometry

Cells were cultured in T-75 flasks until they reached up to 90% confluency rate. At this point, media within the flask was aspirated and cells were washed with pre-warmed 5 mL sterile PBS. 3 mL of TrypLE™ Express was added per T-75 flask and allowed to incubate at 37°C for 3-5 minutes, followed by gentle agitation to detach cells from the surface of the flask. The cell suspension was transferred to a 15 mL Falcon tube (Thermo Fisher) and centrifuged for 5 minutes at 1500 RPM (21 x g) to form a cell pellet. The supernatant was removed, and cells were immediately fixed on ice as described in section 2.3.4.

2.3.3 Preparation of whole blood samples from patients for imaging flow cytometry

One mL of whole blood was transferred into a 15 mL falcon tube. 9 mL of red blood cell lysis buffer was added to the aliquot of whole blood. The tube was inverted multiple times and incubated at room temperature for 10 minutes with gentle agitation. The tubes were centrifuged at 2500 RPM for 10 minutes. The supernatant was discarded, and the resultant cell pellet was resuspended in 3 mL of red blood cell lysis buffer. The samples were incubated for 10 minutes at room temperature with gentle agitation before being centrifuged again at 2500 RPM (60 x g) for 10 minutes. After discarding the supernatant, the cells were immediately fixed as described in section 2.3.4.

2.3.4 Fixing and permeabilization of cells

Cultured cells as well as pellets derived from patient samples were transferred to a 1.5 mL microcentrifuge, suspended in 1 mL of ice-cold 4% paraformaldehyde (diluted in PBS) and kept on ice for 5 minutes to allow cross-linking of proteins within the cells. The cell suspension was centrifuged and PFA was aspirated, followed by centrifugation at 3600 RPM (94 x g) for 3.5 minutes. The cell pellet was washed with 1 mL of PBS to wash away any remnants PFA thoroughly and the samples were re-centrifuged at 3600 RPM (94 x g) for 3.5 minutes.

In order to visualize nuclear proteins, 1 mL of 0.5% Triton-X (Sigma Aldrich) in PBS was mixed with the cell pellet and incubated for 10 minutes to allow permeabilization of cell membrane in order to access inter-cellular proteins. The samples were then centrifuged for 3.5 minutes at 3600 RPM (94 x g), washed again with PBS to remove traces for Triton-X and re-centrifuged as before.

2.3.5 Staining cells

After the fixing and permeabilization process, cells were incubated in blocking buffer (10% bovine serum albumin, Gibco, in PBS) for 1 hour with gentle agitation at room temperature in order to minimize non-specific binding of proteins. This was followed by centrifugation of cells at 3600 RPM (94 x g) for 3.5 minutes. The blocking buffer was removed, and cells were incubated in an appropriate dilution of the primary antibody in blocking buffer after which they were incubated overnight at 4°C with gentle agitation. In the case of conjugated antibodies (i.e., primary antibodies pre-conjugated with fluorophores), the micro centrifuge tubes were covered in aluminium foil and incubated in the dark. All subsequent steps were done under minimal light whilst covering the sample tubes to ensure that the fluorescence was not affected.

In the case of unconjugated antibodies, after the primary incubation, the samples were retrieved and centrifuged for 3.5 minutes at 3600 RPM (94 x g). After the supernatant was discarded, the cell pellet was washed thoroughly in 1 mL of 0.1% Tween in PBS and centrifuged as before. PBS-Tween was removed, and the cell pellet was resuspended in an appropriate dilution of secondary antibody containing light-sensitive fluorophores and incubated at room temperature for 1 hour. From this step onwards, samples were protected from light. The samples were washed once again in 0.1% PBS-Tween and centrifuged at 3600 RPM (94 x g) for 3.5 minutes. Finally, after discarding the supernatant, the cell pellet was suspended in 99 µL of Accumax (Innovative Cell Technologies) to deter cells from forming aggregates. 1 µL of DRAQ5 (Biostatus Ltd.) nuclear stain was added prior to visualisation of sample using the ImageStream X™. Data analysis was carried out on the IDEAS software supplied by Amnis.

Table 2.3 *– Details of antibodies used to identify cell population using imaging flow cytometry/immunofluorescence.*

Primary Antibody	Dilution	Species	Supplier	Fluorophore
Anti- AE1/AE3 (Conjugated)	1:100	Mouse	Cell Signalling	AlexaFluor 488
Anti- CD45 (Conjugated)	1:100	Rat	Thermo Fisher	Texas-Red
Anti-Wilms Tumour Protein 1 (Conjugated)	1:100	Rabbit	Abcam	AlexaFluor 488
Anti-CD34 (Conjugated)	1:100	Mouse	Thermo Fisher	AlexaFluor 488
Anti-Wilms Tumour Protein 1 (Conjugated)	1:100	Rabbit	Abcam	AlexaFluor 647
Anti-SP-D (Unconjugated)	1:100	Rabbit	Supplied by Dr Kishore's lab	AlexaFluor 488

2.4. Parsortix™ – size-based cell separation

A proof of principle blood spiking experiment and patient sample were run through the Parsortix (ANGLE plc) size-based separation platform. For the proof of principle experiment, 1000 SKOV3 cells were spiked in 5 ml of blood collected from a healthy volunteer. The sample tube was then attached to the Parsortix system to allow 'harvesting', during which the blood sample is taken up from the tube and allowed to pass through a cassette using microfluidics technology. The microfluidics cassette that sits within the apparatus contains multiple channels through which the cells (within the sample) pass through. A 'critical gap' of variable size captures potential circulating tumour cells (which are assumed to be much larger than other cell populations found in blood), allowing red blood cells and white blood cells to pass thorough and filter. The filtrate (containing cell populations of interest) was collected post-harvesting in a suspension with PBS. As an additional step, if red blood cells were present within the sample, 500 µL of RBC lysis buffer (Gibco) was added to the final filtrate to remove them.

The sample was then centrifuged at 3000 RPM (66 x g) for 3 minutes to pellet the cells collected. To this, 500 µL of 4% PFA (in PBS) was added and kept on ice for 5-7 minutes to allow the cells to fix for membrane staining. The cells were centrifuged again at 3000 RPM (66 x g) for 3 minutes and the supernatant was discarded carefully to retain the majority of the pellet. For nuclear staining, the pellet was suspended in 500 µl of 0.5% Triton-X (in PBS) and incubated on ice for 7 minutes, after which the tube was centrifuged (as before) and the supernatant was discarded. The pellet was resuspended in 10% BSA (in PBS) for one hour to allow blocking with gentle agitation at room temperature, after which the cells were centrifuged again (as above) and the same dilutions of antibodies (AE1/AE3, CD45 and WT1) were used as mentioned in table 2.3. The sample was then left to incubate at 4°C overnight. The next day, the sample was centrifuged at 3000 RPM (66 x g) for 3 minutes, the supernatant was discarded, and the cells were washed once in 500 µl of 0.1% Tween (in PBS) to wash any excess fluorescent antibodies. After centrifugation, the resultant pellet was resuspended in 50 µl of Accumax and 0.5 µl of DRAQ5 was added as a nuclear stain. The cells within the sample were viewed using the ImageStream X™.

2.5 Annexin V/PI Staining – flow cytometry

Fluorescently conjugated Annexin-V/Propidium Iodide (PI) Apoptosis Detection Kit (BioLegend) was used to detect and quantify apoptotic cell populations in treated and untreated samples. Prior to sample preparation, cells were cultured and treated as per experimental requirements. A list of contents provided in the kit are listed in table 2.4.

Table 2.4 *- List of materials and volumes supplied within the apoptotic/necrotic assay kit for flow cytometry.*

Materials provided	Amount
FITC Annexin-V	0.5 mL
Propidium Iodide solution	1 mL
Annexin-V Binding Buffer	50 mL

Post-treatment, cells were washed twice with 1mL of cold Cell Staining Buffer (BioLegend), after which they were centrifuged and resuspended in 1mL of Annexin-V binding buffer. 100 µL of the resultant cell solution was transferred into a 5 mL flow cytometry test tube and 5µL of FITC-conjugated Annexin-V antibody was added to it, followed by 10 µL of PI solution supplied with the kit. The test tubes containing sample solutions were briefly and gently vortexed to allow antibodies to mix thoroughly. The tubes were then incubated for 30 minutes at room temperature, away from light. Finally, 400µL of fresh Annexin-V binding buffer was added to each

incubated sample and kept covered before analysis. All samples were subjected to flow cytometry using the ACEA Novoflow Flow Cytometry unit and subsequent analysis of samples was carried out using the ACEA NovoExpress software (version 1.4.1).

2.6 RNA extraction

mRNA extraction was carried out from cells cultured in vitro to examine gene expression levels. To maintain sterility, all surfaces were cleaned thoroughly with 70% IMS and 2% TriGene solution. After extraction, RNA was stored at -80°C and was continuously kept on ice when required to avoid sample degradation.

2.6.1 Extracting RNA from cells cultured *in vitro* using GenElute™ (Sigma Aldrich)

The GenElute™ mammalian total RNA kit uses a silica-based system with a micro-spin format, providing high yields of RNA without the use of hazardous compounds such as phenol and chloroform.

Cells in culture were washed with 1 mL of phosphate buffered saline (PBS). 500uL of RNA lysis buffer (with 1% β-mercaptoethanol) was added to each well and a cell scraper was used to gently scrape the cells from the surface of the plate and incorporate with the lysis buffer. The resultant solution was transferred into a blue filtration column enclosed within a 2 mL collection tube and centrifuged for 2 minutes at 14,000 x g to remove cellular debris. The filtration column was discarded, and the filtered lysate was mixed with 500 µL of 70% ethanol. This mixture was added to a silica-based binding column enclosed within a collection tube and centrifuged for 15 seconds at 14,000 x g. The flow through was discarded and the RNA was now bound to the membrane. Next, multiple washes were carried out to remove contaminants. The membrane was first washed with Wash Solution I followed by two washed with Wash Solution II (both supplied with the kit) and centrifuged for 15 seconds at 14,000 x g. After the second wash with Wash Solution II, the samples were centrifuged for 2 minutes at 14,000 x g to remove ethanol. Finally, the column was transferred to a fresh, new collection tube to which 50 µL of elution solution was added. The tubes were spun down for 1 minute at 14,000 x g. The eluted RNA was stored at -80°C and kept on ice when used.

2.6.2 RNA quantification

RNA samples were quantified using the Nano Drop 2000C (Thermo Fisher Scientific). 1 uL of RNA per sample was used to analyse the purity and concentration. Concentration was calculated from absorbance at 280 nm and purity was calculated by A260/A280 ratio, for which a range of 1.7-2.1. was considered acceptable.

2.6.3 cDNA synthesis

Complementary DNA (cDNA) was synthesised from extracted RNA to use as a template to monitor gene expression using qPCR. All surfaces were cleaned thoroughly with 70% IMS and 2% TriGene and a flow hood was used to prior to conducting cDNA synthesis. A kit containing random primers was chosen, ensuring efficient first strand synthesis with any species of RNA molecules present (in this case, mRNA). The amount of RNA required for cDNA synthesis was calculated using the formula below:

RNA input = desired cDNA concentration/RNA concentration (ng/µL).

2.6.4. High throughput cDNA synthesis kit by Applied Biosystems (Thermo Fisher)

RNA input was calculated as mentioned above and diluted with molecular grade H_2O to make up to 10 µL mixture in a 0.6 mL polypropylene PCR tube per sample. The reverse transcription master mix was made using the reagents provided within the kit in the volumes mentioned in table 2.5.

Table 2.5 *– List of reagents and volumes used for reverse transcription used per sample with the high-throughput cDNA reverse transcriptase kit (Thermo Fisher).*

Reagent	Volume
10x RT Buffer	2.0 µL
25x dNTP Mix (100 mM)	0.8 µL
10x Random Primers	2.0 µL
MultiScribe™ Reverse Transcriptase	1.0 µL
RNase Inhibitor	1.0 µL
Nuclease-free H_2O	3.2 µL
Total per reaction	10 µL

10 µL of the master mix was then incorporated with the diluted RNA samples to constitute a final volume of 20 µL. Samples were briefly vortexed and kept on ice, after which they were incubated within a thermal cycler and incubated at conditions mentioned in table 2.6.

Table 2.6 *– Thermal protocol followed during cDNA synthesis.*

	Incubation temperature (°C)	Time (min)
Step 1 (Annealing)	25°C	10
Step 2 (Extension)	37°C	120
Step 3 (Inactivation)	85°C	5
Step 4	4°C	∞

Processed cDNA samples were stored at -20°C until further use.

2.7 Quantitative PCR (qPCR)

qPCR (quantitative polymerase chain reaction) was used to assess gene expression relative to housekeeping genes i.e., genes that are normally expressed in cells (RQ; relative quantification). All qPCR experiments were carried out in a qPCR-dedicated hood, sterilised with 2% Trigene (Medimark scientific) and 70% IMS throughout preparation to avoid contamination. Reagents and samples used for this experiment were defrosted and kept on ice when needed, to avoid degradation. qPCR mix containing SYBR® Green was kept in light-proof storage when possible. Applied Biosystems™ SYBR™ Green Master Mix (Thermo Fisher) was used to carry out qPCR gene expression experiments as per manufacturer's instructions. The master mix is optimized for SYBR® Green reactions and contains SYBR® Green I Dye, AmpliTaq Gold® DNA Polymerase, dNTPs with dUTP, Passive Reference, and optimized buffer components. Primers (sequences listed in table 2.7) used for the qPCR experiments were ordered from Sigma Aldrich and were supplied lyophilised. The tube was initially centrifuged to recollect all the dry components to the bottom of the tube and were then rehydrated with pure H_2O, as per manufacturer's instructions. Samples were loaded in triplicates, so master mixes were made for each primer used. The content of each individual sample loaded onto the qPCR plate are shown in table 2.8.

Table 2.7 – *List of genes and their sequences for forward and reverse primers used for RT-qPCR to quantify gene expression.*

Gene	Forward Primer	Reverse Primer
YWHAZ	5'-AGACGGAAGGTGCTGAGAA-3'	5'GAAGCATTGGGGATCAAGA-3'
FAS	5'- ACACTCACCAGCAACACCAA-3'	5'- TGCCACTGTTTCAGGATTTAA-3'
BAX	5'-TGCTTCAGGGTTTCATCCAGG-3'	5'- GGAAAAAGACCTCTCGGGGG-3'
TNFα	5′-GTATCGCCAGGAATTGTTGC-3′	5′-AGCCCATGTTGTAGCAAACC-3′

Table 2.8 *– Contents and volumes of master mix (per one sample) containing cDNA in preparation for RT-qPCR to analyse gene expression.*

Reagent	Volume/sample (µL)
Primer Mixture (Forward and Reverse)	1 (0.5 each)
SYBR™ Green Master Mix	10
Pure H_2O	9
cDNA	1
Total	20

cDNA samples were diluted to a concentration of 4ng/µL. 19µL of master mix containing primers, SYBR™ Green and pure water was added to each well in triplicates of a MicroAmp® Fast Optical 96-Well Reaction Plate (Life Technologies), followed by addition of 1µL of cDNA. The wells were then sealed with a transparent, adhesive film and the plate was centrifuged briefly to ensure the solution was collected at the bottom of the well and to avoid air bubbles.

The contents were then loaded, and the thermal protocol followed is shown in table 2.9.

Table 2.9 *– Thermal protocol used during RT-qPCR on the QuantStudio 7 (Life Technologies) using he SYBR Green MasterMix (Applied Biosciences).*

Stage	Temperature	Time	No. of cycles
Hold stage	50°C	2 minutes	1
	95°C	10 minutes	
PCR stage	95°C	15 seconds	40
	60°C	1 minute	
Melt curve stage	60-95°C	-	1

2.8 Western Blotting

Caspase–3, Phospho-S6 Kinase, RICTOR and RAPTOR expression was analysed in SKOV-3 cells using Western Blotting. Protein lysates were separated by mass using SDS-PAGE (Sodium-Dodecyl-Sulphate Polyacrylamide gel electrophoresis). During this process, heavier proteins stay near the top of the gel and smaller proteins shift towards the bottom due to negative charge.

Table 2.10 *-List and details of primary antibodies used for western blot analysis.*

Primary Antibody	Species	Supplier
Caspase 3	Rabbit	Cell Signalling Technology
PS6K	Rabbit	Cell Signalling Technology
RICTOR	Mouse	Abcam
RAPTOR	Rabbit	Abcam
GAPDH	Rabbit	Cell Signalling Technology

Protein lysates were extracted from cultured cells in 6-well plates in order to determine expression patterns of Caspase -3, PS6K, RICTOR and RAPTOR. Post-treatment with 20µg/mL of SP-D, the media was aspirated, and cells were washed with 500-1000 µL of PBS (Gibco). 250 µL of 2x Laemmli Buffer (Sigma Aldrich) was added to each well and gently rotated to allow the solution to cover the surface. Cells were then scraped using a cell scraper and the lysate was transferred into a sterile Eppendorf tube. Lysates were denatured by boiling at 95°C for 10 minutes using a heat block and transferred for storage at 20°C (or -80°C for long term storage) until required for further use.

A 10% resolving and 5% stacking gels were used and were prepared as follows. The gels were poured at a thickness of 1mm between glass plates according to the recipes in table 2.11 and 2.12.

Table 2.11 *– List of contents used to prepare the stacking gel for western blotting.*

Stacking Gel – contents	1 GEL (2 ml)	2 GELS (4 ml)
dH_2O	1.4	2.7
30% Acrylamide Mix	0.33	0.67
1.0M Tris (pH 6.8)	0.25	0.5
10% SDS	0.02	0.04
10% Ammonium Persulfate (APS)	0.02	0.04
TEMED	0.002	0.004

Table 2.12 *– List of contents used to prepare the resolving gel for western blotting.*

Resolving Gel – contents	1 GEL (5 ml)	2 GELS (10 ml)
dH_2O	1.9	4.0
30% Acrylamide Mix	1.7	3.3
1.5M Tris (pH 8.8)	1.3	2.5
10% SDS	0.05	0.1
10% Ammonium Persulfate (APS)	0.05	0.1
TEMED	0.002	0.004

100% methanol was added on top of the resolving gel (to eliminate any air bubbles) and allowed to set for 20-30 minutes at room temperature. Once the resolving gel had set, the methanol was poured away, and any excess was discarded using a filter paper. The stacking gel was poured over the resolving gel at an approximate height of 2cm, and a comb placed between the glass plates to form wells. The stacking gel was left to set for a further 20-30 minutes at room temperature.

Cell lysates were incubated at 100°C for at least 10 minutes to linearise the protein, break down disulphide bonds and remove tertiary structures. The SDS in the protein buffer and gel serves to coat the protein in a consistent negative charge to avoid the varying charges on amino acids to affect migration of the protein through the gel. 7µl of each sample was loaded into each appropriate well. 3µl of PageRuler™ Prestained Protein Ladder (Life Technologies) was used as a reference of mass. The gels were run in 1x Running Buffer at 300V and 40mA per gel until the visible blue band of LaemmLi buffer was almost at the bottom of the gel and the ladder was fully separated. The separated proteins were then electrophoretically transferred onto a nitrocellulose membrane (Thermo Scientific) in Wet-Transfer Buffer.

For transfer, two sponges, four pieces of filter paper and one piece of nitrocellulose membrane were required. The membrane and gel were secured between two sponges and filter paper and placed in a cassette prior to being placed in a tank filled with transfer buffer. An ice block was added to the tank to raise the buffer solution and keep the tank cool. The tank was transferred to a tray and surrounded by more ice. The set up was then allowed to run at 300V and 400mA for 1.5 hours.

After successful transfer, the membrane was carefully extracted from the cassette and placed into a tray containing 1gm of cow's milk powder (Marvel milk powder) in 20 ml of TBS-Tween 20 to allow blocking. This was left on a shaker (20-25 oscillations per minute) for a minimum of one hour at room temperature. After blocking, the membrane was rinsed with 1x TBS-Tween20

solution. The primary antibody (1:1000 dilution) diluted in 5% bovine serum albumin (BSA)/TBS Tween20 was applied to the membrane in a plastic pouch. Before sealing the pouch, visible air bubbles were removed. The pouch was sealed securely using heat and placed in the cold room overnight on an orbital shaker at 4°C.

The next day, the membrane was washed in TBS-Tween20 solution by adding it to a tray containing the solution and leaving it on a shaker for 15 minutes. This was repeated three times; therefore, the washes altogether took 45 minutes to ensure any and all unbound proteins were removed. Next, the secondary antibody (1:2000 dilution) was appropriately diluted in 5% BSA/TBS Tween20 and added with the membrane into a separate plastic pouch. The membrane was incubated for one hour at room temperature. This was followed by washes in TBS-Tween20 (3 times) for 10 minutes to remove any unbound secondary protein. The membrane was then stored in TBS Tween, while reagents are prepared for visualisation of the proteins by enhanced chemiluminescence (ECL).

Development of the membranes was carried out in a dark room so as not to expose the light-sensitive X-ray films. Solution A and B (recipes shown in table 2.13) were prepared beforehand, mixed, and applied to the drained membranes in a dark room immediately prior to developing.

Table 2.13 *– Contents and quantities used to prepare solutions A and B.*

Solution A		**Solution B**	
	Quantity		**Quantity**
TRIS (pH 8.0, 100 mM)	5 ml	**TRIS (pH 8.0, 100 mM)**	5 ml
Coumaric Acid	22 µl	**H_2O_2**	3 µl
Luminol	50 µl		

Once the solutions were added, the tray containing the membrane was rocked gently, allowing the mixture to completely cover the film. The membranes were incubated for 1-2 minutes, blotted on filter paper, and exposed to X-ray film within a light impermeable cassette (AutoRad) for a range of times (usually 30 seconds to 1 minute, depending on the strength of the antibody). The films were developed on a Curix60 (AGFA) automatic developing machine.

In case of further analysis/repeats, the membrane was sealed and stored at 4°C, enclosed in a pouch containing PBS to be reused at a later date.

2.9 Enzyme-linked Immunosorbent assay (ELISA)

Human surfactant protein-D levels were detected advanced-stage OC patient plasma samples using a sandwich ELISA immunoassay (BioVendor). Samples were incubated in a 96-well microplate coated with monoclonal anti-human surfactant protein D antibody and visualised using the ClarioSTAR® microplate reader. For the purpose of this assay, plasma samples stored at -80°C were thawed once and diluted 5.5x with the dilution buffer provided in the kit. Samples required to plot the standard curve were prepared through serial dilution of a concentrated stock. Two vials of quality control (QC) (upper and lower limit concentration) were provided within the kit, and a combination of the values obtained from the standards and QC were used to validate the functioning of this assay.

Table 2.14 *– List of contents and quantities provided in the SP-D ELISA-based detection kit supplied by BioVendor.*

Kit components	Quantity
Antibody-coated microtiter strips	96 wells
Biotin-labelled antibody	13 ml
Streptavidin-HRP conjugate	13 ml
Master standard	1 vial
Quality control (HIGH)	2 vials
Quality control (LOW)	2 vials
Dilution buffer	50 ml
Wash solution (concentrate)	100 ml
Substrate solution	13 ml
Stop solution	13 ml

100 µl of prepared samples including standards, QC and diluted patient plasma samples were added to the microplate in duplicates, followed by the incubation of the plate for two hours at 25°C, shaking at 300 rpm on an orbital shaker setting. The same temperature and shaker settings were used throughout the remainder of the experiment. Microwells were washed with 350µl/well of wash solution 5 times and the plate was inverted and tapped strongly against a paper towel to ensure complete removal of residual liquid from the wells. 100µl of Biotin-labelled antibody solution was added to each well. The plate was incubated for 1 hour under the aforementioned conditions. The wells were washed again with 350µl of wash solution, inverted and tapped strongly against a paper towel. Next, 100µl of Streptavidin-HRP conjugate was added to each well and incubated for 1 hour. The wells were washed again with 100µl of wash solution,

followed by the addition of 100µl of Substrate solution to each well. After this step, the plate was covered in aluminium foil to avoid contact with direct sunlight. At this step, the plate was incubated at 25°C for 15 minutes without shaking. Finally, the plate was retrieved and 100µl of Stop solution was added on top to restrict further colour development. The absorbance of each sample was recorded within 5 minutes of adding the stop solution at 450nm and 630nm.

2.10 Immunohistochemistry (IHC)

Immunohistochemistry and DAB (3,3'-Diaminobenzidine) staining was used to visualise SP-D expression in paraffin embedded OC tissue samples. A paraffin-embedded tissue microarray (US Biomax Inc) was used for this experiment, consisting of 60 cases of ovarian carcinoma with 10 adjacent normal ovarian tissues as control.

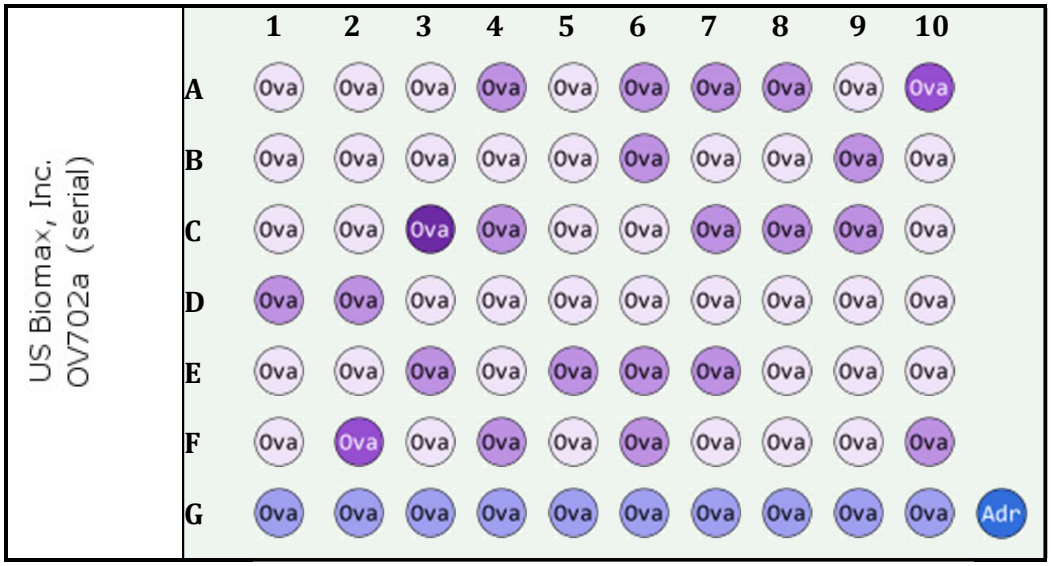

Figure 2.1. *Microarray panel display of the ovarian carcinoma tissue test slide. Ova – Ovary, Adr – Adrenal Gland, used as a negative control,* ● *- Malignant tumour,* ○ *- Malignant tumour (stage I),* ○ *- Malignant tumour (stage IA),* ○ *- Malignant tumour (stage IB),* ○ *- Malignant tumour (stage IC),* ● *- Malignant tumour (stage II),* ● *- Malignant tumour (stage IIA),* ● *- Malignant tumour (stage IIB),* ● *- Malignant tumour (stage III),* ● *- Malignant tumour (stage IIIC),* ● *- Malignant tumour (stage IV),* ● *- NAT (US Biomax, Inc, 2018). Further information on each tissue sample is provided in table 2.11.*

Firstly, tissue samples were deparaffinised and rehydrated by incubating them in Coplin jars containing Histoclear (National Diagnostics), then in decreasing concentrations of ethanol as shown in table 2.15.

Table 2.15 *– Step-by-step rehydration of tissue array slide stating solutions used during the process and the duration of each incubation.*

Solution	Time
Histoclear	2 x 5 min
Histoclear:Ethanol (1:1)	3 min
100% Ethanol	3 min
95% Ethanol	3 min
70% Ethanol	3 min
50% Ethanol	3 min
Running Tap Water	1 min

For antigen retrieval, the microarray slide was boiled in sodium citrate-Tween solution (2.94g sodium citrate in 1L distilled water, 500 µl Tween, pH6) using a microwave for 20 minutes without boil-drying. The slide was allowed to cool and then washed under running tap water for 10 minutes. Next, the slide was washed in PBS 0.025% Triton-X 2 times for 5 minutes on a shaker. It was then incubated in 3% hydrogen peroxide solution for 15 minutes on a shaker. After the incubation, the slide was washed 3 times for 5 minutes each time in PBS-Triton X. To block the tissue, 5% rabbit serum (in PBS-tween) was prepared and approximately 200 µL was dispensed onto the slide. Parafilm was used to evenly distribute the serum onto the slide and the slide was incubated for an hour within a humidity chamber. Then, the primary antibody was prepared in a 1:100 dilution and 200 µl was dispensed onto the slide after which it was incubated overnight at 4°C. On the following day, the slide was washed with PBS-Triton X solution 3 times for 5 minutes each and a secondary antibody was added in a 1:200 dilution, followed by incubation for 1 hour under humid conditions. The slide was washed 3 times for 5 minutes and 200 µl of DAB solution was dispensed onto the slide. At this step, the slide was to be incubated for approximately 10 minutes, until the samples started to develop a brown colour atop the tissue samples. After the colour development is visible, the slide is washed with distilled water once for 5 minutes. A few drops of haematoxylin are dispensed onto the slide (for nuclear staining) and covered with parafilm for approximately 1 minute, followed by staining with 0.1% sodium bicarbonate for approximately 1 minute followed by a rinse under water. Once the staining is complete, the slide is dehydrated using ethanol as shown in table 2.16.

Table 2.16 *– Solutions involved in step-by-step dehydration (and the duration for each step) of tissue array slide in preparation for staining and immunohistochemical analysis.*

Solution	Time
50% Ethanol	3 minutes
70% Ethanol	3 minutes
95% Ethanol	3 minutes
100% Ethanol	3 minutes
Histoclear:Ethanol (1:1)	3 minutes
Histoclear	3 minutes

Finally, a few drops of DPX were added to a coverslip and the slide was placed face down onto the coverslip. After this, the slide was allowed to dry overnight at 4°C prior to scoring. Images of the tissue samples were captured using the Leica DMi1 inverted microscope at 40x magnification. For analysis purposes, the tissue was split into three sections and positively stained cells were counted within each section and the average score of all three sections was considered to be the overall score of the tissue.

Table 2.17 *– Clinical information on paraffin-embedded tissue samples (total =71 samples; 60 ovarian cancer; 11 controls [10 positive and 1 negative control]) from the OV702a array chip ordered from Biomax U.S.*

Position	No.	Age	Sex	Pathology diagnosis	Grade	Stage	Type
A1	1	26	F	Serous papillary cystadenocarcinoma	1	IC	Malignant
A2	2	34	F	Serous papillary cystadenocarcinoma	1	IA	Malignant
A3	3	58	F	Serous papillary cystadenocarcinoma	2	IA	Malignant
A4	4	65	F	Serous papillary cystadenocarcinoma	1	IIA	Malignant
A5	5	65	F	Serous papillary cystadenocarcinoma	1	IA	Malignant

A6	6	50	F	Serous papillary cystadenocarcinoma	1	IIA	Malignant
A7	7	40	F	Serous papillary cystadenocarcinoma (sparse)	1	IIA	Malignant
A8	8	61	F	Serous papillary cystadenocarcinoma	3	IIB	Malignant
A9	9	53	F	Serous papillary cystadenocarcinoma	3	IA	Malignant
A10	10	58	F	Serous papillary cystadenocarcinoma	3	IIIC	Malignant
B1	11	52	F	Serous papillary cystadenocarcinoma	3	IA	Malignant
B2	12	68	F	Serous papillary cystadenocarcinoma	3	IA	Malignant
B3	13	36	F	Serous papillary cystadenocarcinoma	3	IB	Malignant
B4	14	50	F	Serous papillary cystadenocarcinoma	3	IB	Malignant
B5	15	59	F	Serous papillary cystadenocarcinoma	3	IC	Malignant
B6	16	62	F	Serous papillary cystadenocarcinoma	2	IIB	Malignant
B7	17	60	F	Serous papillary cystadenocarcinoma	2	IB	Malignant
B8	18	65	F	Serous papillary cystadenocarcinoma	3	IA	Malignant
B9	19	27	F	Serous papillary cystadenocarcinoma	2	IIB	Malignant
B10	20	53	F	Serous papillary cystadenocarcinoma	2	I	Malignant
C1	21	48	F	Serous papillary cystadenocarcinoma	2	IC	Malignant
C2	22	58	F	Serous papillary cystadenocarcinoma	2	I	Malignant

C3	23	64	F	Serous papillary cystadenocarcinoma	2	IV	Malignant
C4	24	58	F	Serous papillary cystadenocarcinoma	2	IIB	Malignant
C5	25	51	F	Serous papillary cystadenocarcinoma	2	IA	Malignant
C6	26	66	F	Serous papillary cystadenocarcinoma	3	IC	Malignant
C7	27	47	F	Serous papillary cystadenocarcinoma	3	IIA	Malignant
C8	28	57	F	Serous papillary cystadenocarcinoma	3	IIA	Malignant
C9	29	69	F	Serous papillary cystadenocarcinoma	2	II	Malignant
C10	30	54	F	Serous papillary cystadenocarcinoma	3	IB	Malignant
D1	31	52	F	Serous papillary cystadenocarcinoma	2	II	Malignant
D2	32	57	F	Serous papillary cystadenocarcinoma	3	IIB	Malignant
D3	33	51	F	Serous papillary cystadenocarcinoma	3	IB	Malignant
D4	34	40	F	Serous papillary cystadenocarcinoma	3	I	Malignant
D5	35	60	F	Serous papillary cystadenocarcinoma	3	I	Malignant
D6	36	54	F	Serous papillary cystadenocarcinoma	3	IC	Malignant
D7	37	63	F	Serous papillary cystadenocarcinoma	3	IB	Malignant
D8	38	52	F	Serous papillary cystadenocarcinoma	3	IC	Malignant
D9	39	41	F	Serous papillary cystadenocarcinoma	3	IA	Malignant

D10	40	60	F	Serous papillary cystadenocarcinoma	3	IA	Malignant
E1	41	70	F	Serous papillary cystadenocarcinoma	3	I	Malignant
E2	42	51	F	Serous papillary cystadenocarcinoma	3	IC	Malignant
E3	43	53	F	Serous papillary cystadenocarcinoma	3	IIA	Malignant
E4	44	37	F	Serous papillary cystadenocarcinoma	3	IB	Malignant
E5	45	48	F	Serous papillary cystadenocarcinoma	3	IIA	Malignant
E6	46	59	F	Serous papillary cystadenocarcinoma	2	IIB	Malignant
E7	47	44	F	Serous papillary cystadenocarcinoma	3	IIA	Malignant
E8	48	48	F	Mucinous adenocarcinoma	1	IB	Malignant
E9	49	45	F	Mucinous adenocarcinoma	1	IA	Malignant
E10	50	34	F	Mucinous adenocarcinoma	1	I	Malignant
F1	51	41	F	Mucinous adenocarcinoma	3	IB	Malignant
F2	52	29	F	Mucinous adenocarcinoma (sparse)	3	III	Malignant
F3	53	60	F	Mucinous adenocarcinoma	3	IA	Malignant
F4	54	47	F	Endometrioid adenocarcinoma	1	IIA	Malignant
F5	55	54	F	Endometrioid adenocarcinoma	1	IB	Malignant
F6	56	46	F	Endometrioid adenocarcinoma	2	II	Malignant

F7	57	49	F	Endometrioid adenocarcinoma	2	I	Malignant
F8	58	43	F	Endometrioid adenocarcinoma	3	IC	Malignant
F9	59	60	F	Endometrioid adenocarcinoma	3	IB	Malignant
F10	60	53	F	Endometrioid adenocarcinoma	3	IIA	Malignant
G1	61	39	F	Cancer adjacent normal ovary tissue	-	-	NAT
G2	62	53	F	Cancer adjacent normal ovary tissue	-	-	NAT
G3	63	48	F	Cancer adjacent normal ovary tissue	-	-	NAT
G4	64	39	F	Cancer adjacent normal ovary tissue	-	-	NAT
G5	65	17	F	Cancer adjacent normal ovary tissue	-	-	NAT
G6	66	45	F	Cancer adjacent normal ovary tissue	-	-	NAT
G7	67	48	F	Cancer adjacent normal ovary tissue	-	-	NAT
G8	68	44	F	Cancer adjacent normal ovary tissue	-	-	NAT
G9	69	41	F	Cancer adjacent normal ovary tissue	-	-	NAT
G10	70	69	F	Cancer adjacent normal ovary tissue	-	-	NAT
-	0	42	M	Adrenal Gland (Pheochromocytoma - tissue marker)	-		Malignant

2.11 Immunofluorescence (IF)

In preparation of treatment of adhered, cultured cells, 1 coverslip was placed in each well of a 12-well plate. A solution containing approximately 100,000 cells of desired cell line (SKOV-3 or PEO1) was dispensed in complete medium and incubated overnight at 37°C and 5% CO_2 overnight. After 24 hours, complete medium containing appropriate concentrations of cytotoxic drugs was added to wells as per protocol. The cells were then allowed to incubate under standard conditions for 24 hours, exposed to treated media.

After a 24-hour time point, treated media was aspirated and discarded appropriately, and the cells were washed with 500 µL of PBS to remove any remnants of cytotoxic treatments. 500 µL of 4% PFA solution was added to each well and left at room temperature for 10 minutes to facilitate fixing. The PFA was then aspirated and washed well with PBS to remove any remnants of PFA. For cells to permeabilise, 500 µL of 0.1% Triton-X (diluted in PBS) was added to each well and incubated for 15 minutes at room temperature, followed by aspiration and a wash with PBS. 500 µL of 5% bovine serum albumin (BSA) (diluted in PBS) was added to each well and incubated at room temperature for 1 hour to allow blocking. Post-blocking, BSA solution was aspirated and 100 µL of fluorescently conjugated antibody solution was carefully dispensed over the coverslip to ensure that all cells were submerged. The plate was then carefully covered and placed in the dark, overnight and at 4°C.

The next day, cells were washed with 500 µL of 0.1% PBS-Tween solution, followed by aspiration and an additional wash with 500 µL of PBS to ensure that all excess antibody solution has been washed off. The PBS was aspirated and the coverslip containing adherent cells were dehydrated as shown in table 2.18.

Table 2.18 *-Steps involved in dehydration of adherent cells in preparation for immunofluorescence analysis, providing details of dilutions and durations for each step.*

Solution	Time
Step 1 - 70% Ethanol	10 - 15 minutes
Step 2 – 90% Ethanol	10 minutes
Step 3 – 100% Ethanol	up to 10 minutes

After dehydration, the coverslips were ready to be mounted over a slide prior to viewing. 6-8 µL of mounting medium with DAPI nuclear stain (Vectashield) was added to the slide. A pair of forceps were used to pick the coverslip from the bottom of the well. The corner of the coverslip was first allowed to come in contact with the mounting medium, before gently placing it over the

remaining mounting medium. The coverslips were allowed to settle for 15 minutes in the dark to allow the mounting medium to dry. The coverslips were finally sealed with clear nail varnish to avoid any movement or air bubbles prior to viewing. All slides were viewed under a LEICA DM4000 Fluorescent Microscope, and all analysis was carried out using the LAS-X analysis software (version 3.7.0)

2.12 Bioinformatics (In Silico) Analyses

In silico analyses was carried out using various online tools (details below).

1. **Oncomine** was used to access data regarding gene expression levels of existing microarray data for specific genes noted in cancer and control tissue samples across various cancer types. Oncomine is a cancer microarray database and web-based data mining platform aimed at facilitating discovery from genome-wide expression analyses (Rhodes *et al.*, 2004).
2. **Kaplan Meier (KM)** plotter was used primarily as a meta-analysis tool for the discovery and validation of survival biomarkers, capable of assessing the effect of 54,000 genes (mRNA, miRNA and protein) on survival in various types of cancer (Nagy et al., 2018).
3. **CBioportal** is a web resource for exploring, visualising, and analysing multidimensional cancer genomics data, reducing molecular profiling data from cancer tissues and cell lines into readily understandable genetic, epigenetic, gene expression and proteomic events (Cerami et al., 2012).

2.13 Statistical Analyses

All statistical analyses conducted on data was performed using GraphPad Prism® software (version 5.00.288). A student's t-test was used to assess statistical significance of any changes observed. One-way ANOVA (analysis of variances) was carried out to compare the means of two or more independent groups to identify statistical significance. All p-values were represented using an asterisk (see table 2.19).

Table 2.19 *– Denotations associated with various P values used to denote statistically significant data.*

P-value	Denotation
0.01 – 0.05	*
0.001-0.009	**
<0.0009	***

Chapter 3

Optimisation and development of potential biomarkers for OC

3.1. Introduction

Although there is a growing interest in the use of CTCs for non-invasive diagnosis, prognosis and monitoring of treatment, there are a variety of important factors that could affect the integrity of collected samples (Qin et al., 2014). The conditions under which the sample is collected, the manner of transportation from the clinic to the laboratory, and pre-analytic sample processing procedures are insufficiently characterised which can potentially lead to issues regarding clinical interpretation. Thus, assessing and controlling the pre-analytic handling of biospecimens is essential for their optimal use (Rodriguez-Lee et al., 2018). CTCs are generally isolated from whole blood, and a major problem is the stability of this cell population; highlighting the need for blood to be handled with care, as any mechanical trauma can be detrimental to the viability of the cells (Apostolou *et al.,* 2017).

Similar to any procedure involving live tissues, blood degradation during the handling of samples and laboratory manipulations imposes practical constrains. Once removed from its native environment, a host of degenerative processes including haemolysis, platelet activation, cytokine and oxidative bursts, and neutrophil extracellular trap formation inflict damage to the entire blood specimen. Controlled studies using spiked tumour cells have documented a >60% loss in CTC yield within 5 hours of blood draw and significant RNA degradation occurring within 2-4 hours (Wong et al., 2017). During blood draw, whole blood is anticoagulated in order to prevent clotting of cellular components, a process for which EDTA (ethylenediaminetetraacetic acid) is commonly used (Parpart-Li et al., 2017). In order to maintain sample purity, it is important to consider the type of blood collection device, especially while working with CTC samples. Cell-free DNA blood collection tubes have addressed this issue by developing a propriety stabilisation buffer, intended for collection, shipping and storage of whole blood for further CTC/ctDNA analysis. These tubes have been extensively validated against standard EDTA tubes and can keep samples stable at varying temperatures over a span of 1-2 weeks (Parackal et al., 2019).

Apart from the fragility, CTC populations in blood are claimed to be present in very low numbers, therefore being classified as a 'rare' population. A possible explanation is that majority of enrichment-based platforms utilise EpCAM expression to identify CTCs (Schneck et al., 2015).

However, it is now well established that cancer cells undergo epithelial-to-mesenchymal transition (EMT) which results in a loss of a cell's epithelial markers.

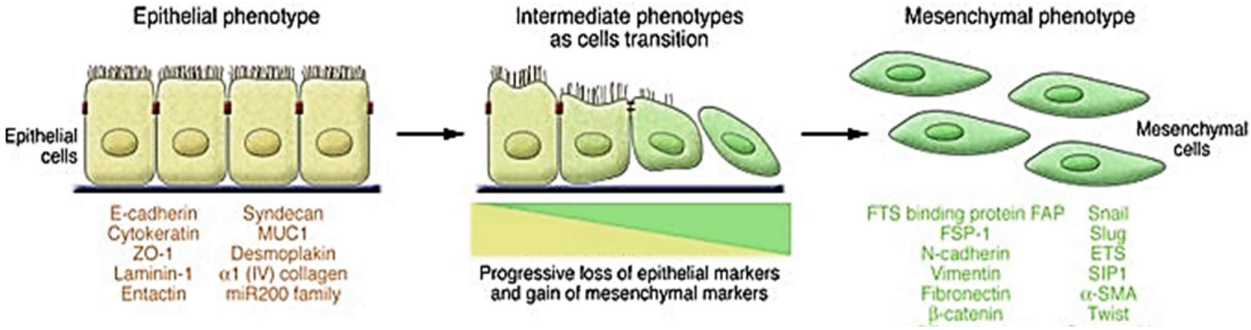

Figure 3.1 – *shows the process of epithelial-to-mesenchymal transition in cancer cells (EMT). Conversion of epithelial cells into mesenchymal cells results in the active loss of epithelial cell markers (listed in yellow) and gain of mesenchymal cell markers including N-Cadherin and Vimentin (listed in green). Cells that exhibit both epithelial and mesenchymal markers are within an 'intermediate state'. (Kalluri and Weinberg, 2009).*

Epithelial cells are normally held together by lateral cell-cell junctions and interact with the underlying basement membrane via hemidesmosomes and a6β4 integrins. Epithelial cells also express cytokeratins that stabilise desmosomes to ensure the resilience of epithelial cell layers to various physical stresses. Activation of the epithelial-mesenchymal process involves the loss of polarity, disruption of cell-cell junctions, degradation of the underlying basement membrane and reorganisation of the extracellular matrix (ECM). This change results in the loss of expression of classic epithelial markers such as cytokeratins and E-cadherin and the expression of mesenchymal markers such as N-cadherin, vimentin, fibronectin and β1 and β3 integrins. The resultant effect of this process is the reduced intercellular adhesion and increased motility exhibited by cells that have undergone the process giving them the ability to break through the basal membrane and migrate over long distances. Since EMT results in the loss of key epithelial cell-cell adhesion molecules, EpCAM is no longer able to bind to their membrane hence leaving them undetected exposing a problematic limitation of technologies that are heavily reliant on epithelial markers for CTC detection (Dongre and Weinberg, 2019; Kyung-A Hyun et al., 2016).

Experiments in this chapter are based on optimising the entire CTC identification process from sample collection to cellular identification, all the way to testing different methods used for CTC isolation thereby developing key aspects that are crucial for the optimal use of liquid biopsies within research-laboratory and clinical settings.

3.2. Aims

- To assess a variety of collection tubes for proper storage and preservation of cancer-related cellular material in patient blood sample
- To test and establish appropriate fluorescent antibodies for successful identification of potential CTCs via imaging flow cytometry.
- To illustrate the technical capability of ImageStream Mark II (Imaging flow cytometry technology) in capturing and identification of potential CTCs.
- To assess the performance of a size-based CTC identification platform (Parsortix™)

3.3 Results

3.3.1. Testing the validity of specialised blood collection tubes (BCTs) for optimal storage of blood samples

Blood collection and sample storage are two pre-analytic factors that are important to maintain sample integrity. Constant agitation and fluctuating temperatures can affect the purity of the blood sample and the condition of the analytes within the sample. Therefore, to ensure proper preservation of samples transported from the hospital to the lab, specialised blood collection tubes were tested in comparison to EDTA collection tubes that are routinely used in clinics. Although the sample storage period within EDTA tubes can be extended by refrigerating samples (at 4-6°C), temperature fluctuations and constant agitation can negatively affect the sample (Parackal et al., 2019). To address this issue, BCTs manufactured by Roche Diagnostics, Streck and PAXgene were tested and compared to EDTA tubes. The blood collection tubes advertised by Roche Diagnostics and Streck claim to minimize the degradation of CTCs and provide CTC stability for up to 7 days at 15 – 30°C. PAXgene tubes were developed specifically to obtain cell-free circulating DNA from whole blood and claim to allow transport and storage of sample for 7 days between 2-30°C.

In order to test the validity of these tubes, blood samples were collected into 2 EDTA tubes, 6 Roche cell-free DNA BCTs, 6 Streck cell-free DNA BCTs and 6 PAXgene ccf-DNA tubes. Each tube was then prepared for analysis every day over the course of 7 days to test their ability to maintain sample quality by analysing cell morphology using nuclear staining (DRAQ5) and brightfield images of samples using the ImageStream Mark II imaging flow cytometry system.

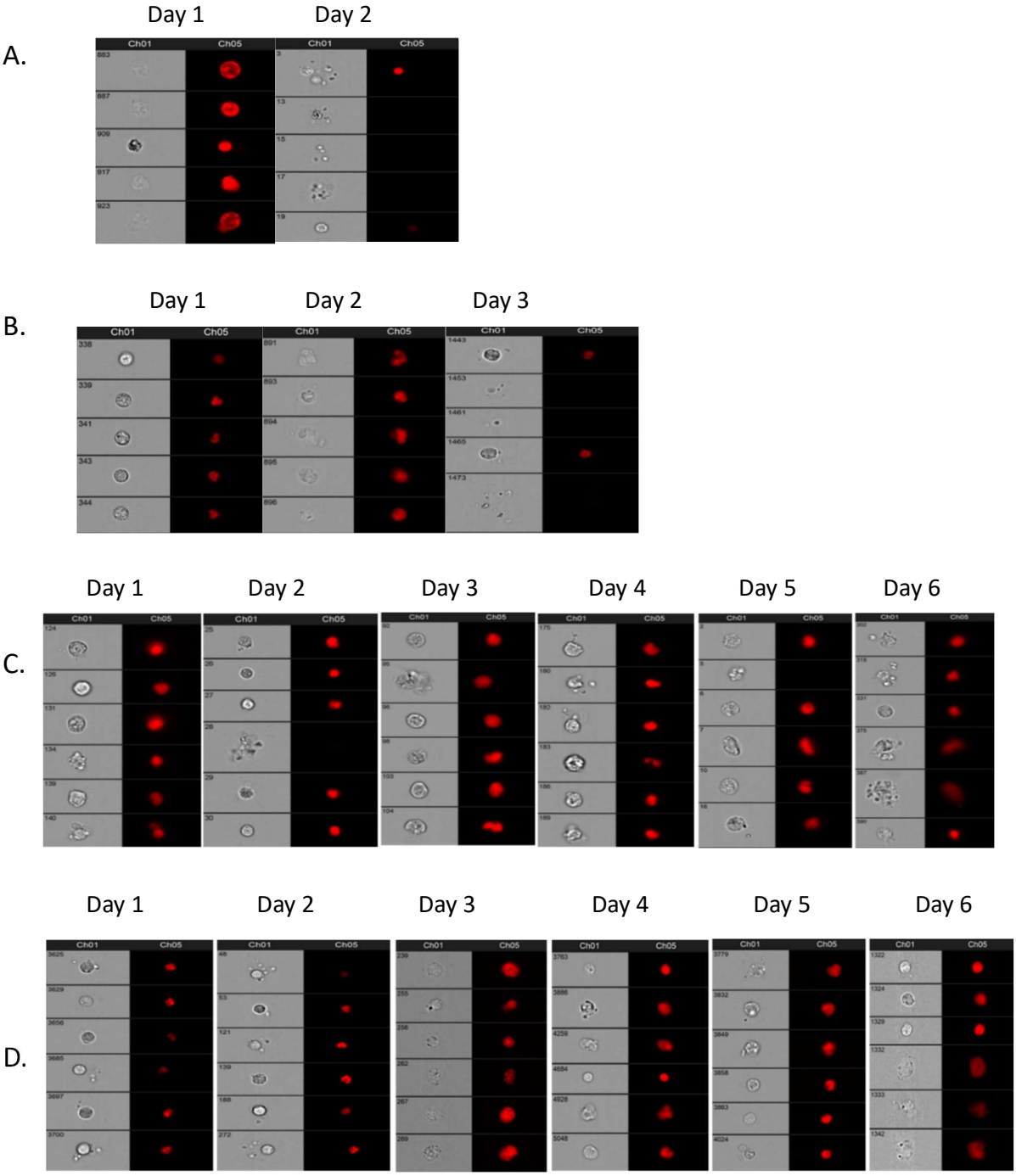

Figure 3.2 *- Circulating cell integrity observed over the course of 6 days using brightfield images (Ch01) and nuclear staining (Ch05) captured using ImageStream Mark II. The EDTA tubes (A) contained a very high amount of cell debris with a low number of intact cells remaining after being stored at 4°C on day 2, after which the blood sample was coagulated to continue further analyses. Cells within PAXgene tubes (B) showed strong nuclear staining till day 2, after which the sample coagulated. Streck (C) and Roche (D) cell-free DNA*

tubes did not coagulate blood over the course of 6 days, however, brightfield images from Roche tubes show intact cells over the course of 5 days with some cells showing low nuclear staining and irregular cell shape on day 6. Streck tubes, in comparison, showed early signs of some cellular material undergoing apoptosis as early as day 2 (Kumar et al., 2019).

From these results, it is evident that EDTA tubes were not able to preserve cell morphology as brightfield images from day 2 show cell debris and a lack of DRAQ5 staining compared to day 1. Contrary to studies, in this experiment, the blood samples stored in PAXgene tubes showed healthy cells until day 2 after which the sample coagulated and was unable to be processed any further. While both Roche and Streck tubes are capable of maintaining sample stability, based on cell morphology over 6 days, Roche tubes were able to maintain cell morphology over the course of 6 days compared to Streck tubes.

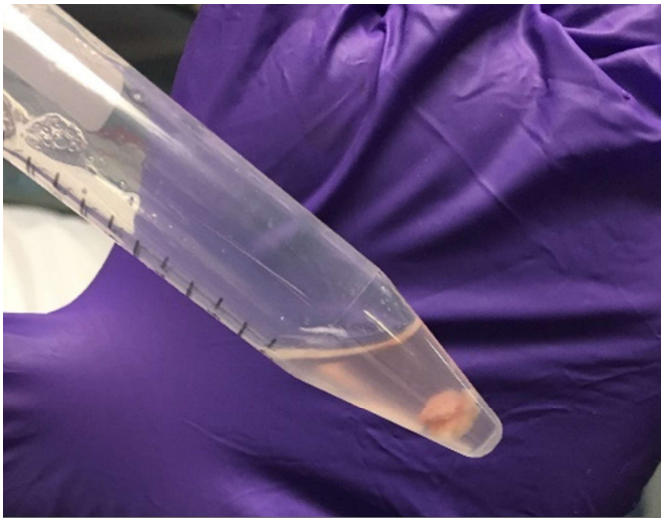

Figure 3.3 *– A coagulated cell pellet extracted from blood samples stored in PAXGene tubes during preparation for ImageStream testing on day 3. The pellet remained intact despite resuspension in cell dissociation buffer and was therefore unfit for further analysis.*

3.3.2. Testing antibodies to target both epithelial and mesenchymal cancer cells using *in vitro* models

A robust method for identifying cancer cells in a given sample would require multiple antibodies for the detection of multiple sub-populations of cancer cells. As established in the introduction, current methods of CTC identification are heavily reliant on the use of epithelial markers, leaving out cells that have undergone the process of EMT. The first step to developing this method was to choose the right antibodies that could target both epithelial cancer cells and cells undergoing EMT. For this purpose, two cancer-related antibodies were chosen – pan-cytokeratin (AE1/AE3)

and Wilms' tumour protein 1 (WT1). Pan-cytokeratin (AE1/AE3) combines multiple keratins which are expressed by CTCs with an epithelial phenotype whereas WT1 is a nuclear protein, specifically expressed in ovarian cancer cells, regardless of phenotype, meaning it would identify any cancer-related cells regardless of their EMT transition.

Firstly, antibody concentrations were tested using ovarian cancer cell lines to determine the dilution for optimum staining of cells. Conclusively, a 1:100 dilution of both AE1/AE3 and WT1 antibodies on SKOV3 cells showed the desired positive staining (shown in figure 2).

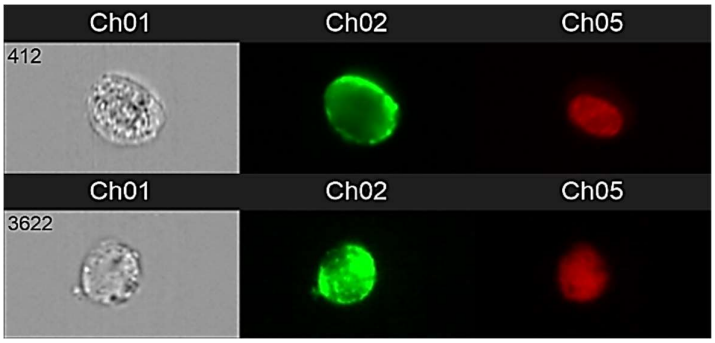

Figure 3.4 *- (top) SKOV3 cell stained with AE1/AE3 and (bottom) SKOV3 cell stained positively for WT1 using ImageStream Mark II at 40x magnification. Both antibodies use an Alexa Fluor AF488 conjugated antibody with green fluorescence shown in Ch02 and DRAQ5 nuclear stain shown in Ch05.*

Next, a proof of principle experiment was carried out using two ovarian cancer cell lines, exhibiting different phenotypes. These cells were stained with AE1/AE3 and WT1 and analysed using fluorescent microscopy. PEO1 cells strongly express E-cadherin, cyto-keratins and lack the expression of vimentin. SKOV3 cells, however, express vimentin and lack E-cadherin expression. They also express cyto-keratins, however PEO1 cells show a stronger expression in comparison which is why SKOV3 cells have an intermediate mesenchymal phenotype (Kwon *et al.*, 2011).

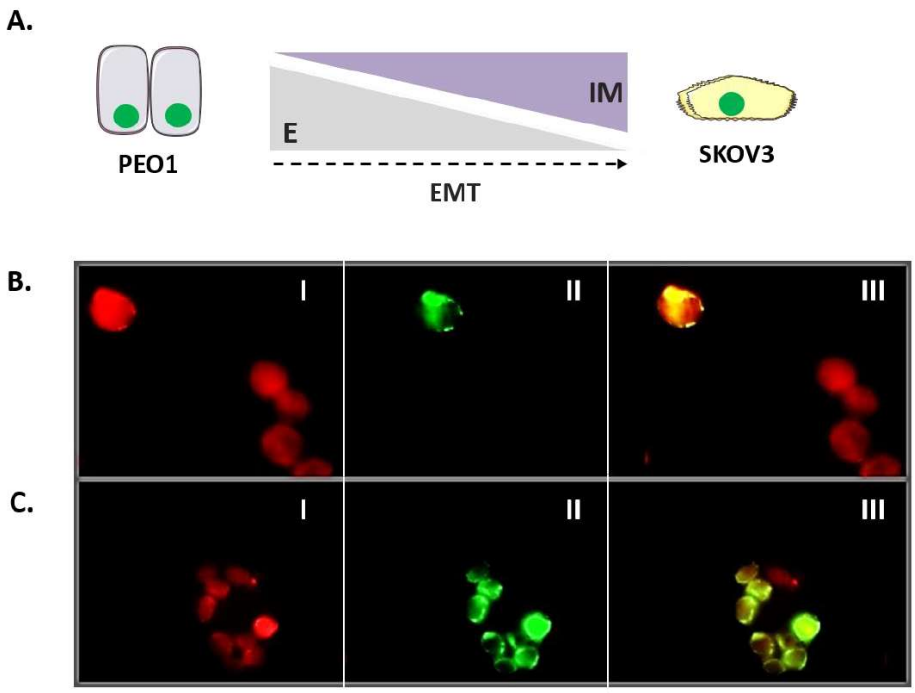

Figure 3.5 *– Proof of principle experiment involving testing biomarker efficiency to target epithelial and mesenchymal OC cells. SKOV3 (intermediate mesenchymal phenotype) and PEO1 (epithelial phenotype) were stained with cytokeratins (AE1/AE3) and WT1 to quantify the number of positive cells using fluorescent microscopy. Cytokeratin is expressed in cells with an epithelial phenotype, whereas WT1 would appear positive in ovarian cancer cells irrespective of epithelial-to-mesenchymal transitioning. (A) Diagrammatic representation of EMT dynamics between SKOV3 and PEO1 ovarian cancer cell lines. (B) SKOV3 cells and (C) PEO1 cells stained with WT1 (red; I), AE1/AE3 (green; II) and merged images (III) Images taken at 40x magnification using immunofluorescence (Kumar et al., 2019).*

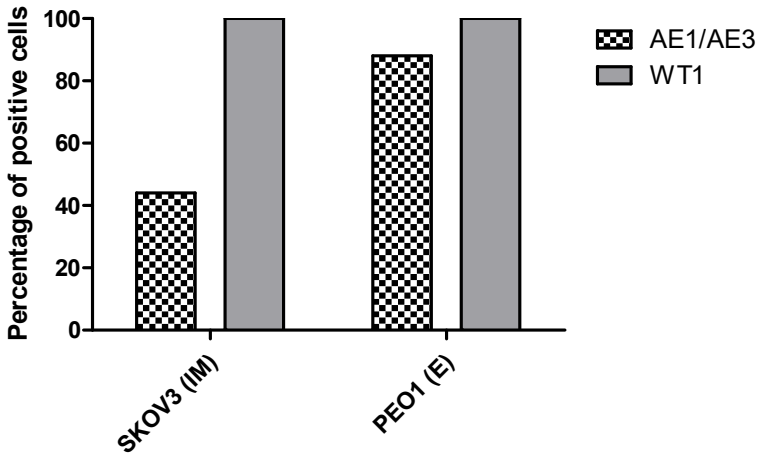

Figure 3.6 *– Graph depicting the percentage of cells stained positively for AE1/AE3 (blue) and WT1 (grey) using fluorescent microscopy out of 100 cells counted at random for SKOV3 cells with an intermediate mesenchymal phenotype (left) and PEO1 cells with an epithelial phenotype (right).*

100 SKOV3 and PEO1 cells stained with fluorescently conjugated antibodies for AE1/AE3 and WT1 were measured and analysed for positive staining. All cells (100/100) stained positive for WT1. 88/100 PEO1 cells expressed AE1/AE3 staining whereas 41/100 SKOV3 cells were stained positive for cytokeratin at almost a 1:2 ratio (Kumar et al 2019). This datum shows that regardless of EMT, WT1 had the ability to detect ovarian cancer cells. However, cytokeratins are currently a well-established CTC identification antibody, therefore, using both these biomarkers should improve reliability.

3.3.3. Testing a size-based separation method to detect the presence of ovarian cancer cells

In order to test the efficiency of a size-based cell separation platform, Parsortix™ cell separation system was used. Parsortix™ utilises a microfluidic cassette with a 'critical gap' of varying widths to optimally capture larger cancer cells based on size, while allowing red and white blood cells to flow through (Miller et al., 2018). The system is configured to either allow staining of cells captured within the cassette or to harvest them from the cassette into a small volume of buffer for subsequent evaluation and downstream interrogation (Miller et al., 2018). In order to run preliminary experiments, 1000 SKOV3 cells were spiked into 5 ml of healthy volunteer blood, as suggested on the protocol provided by the manufacturer. The tube containing spiked blood was attached directly to the machine, allowing the fluidics system to run the entire sample through the cassette to capture cells of interest.

The resultant sample collected after a complete run was approximately 200 µL and contained a significant amount of red blood cells. The sample needed to be washed with red blood cell lysis

buffer to eliminate the contaminants, after which 100uL was stained with WT1 as a separate sample and the other was stained with a combination of AE1/AE3 and CD45 (to eliminate any WBCs). Both samples were analysed using imaging flow cytometry to record the yield and visualise accuracy of staining. Although the cells stained positively, the overall yield was low with only a few cells detected in each run (shown in figure 3.7).

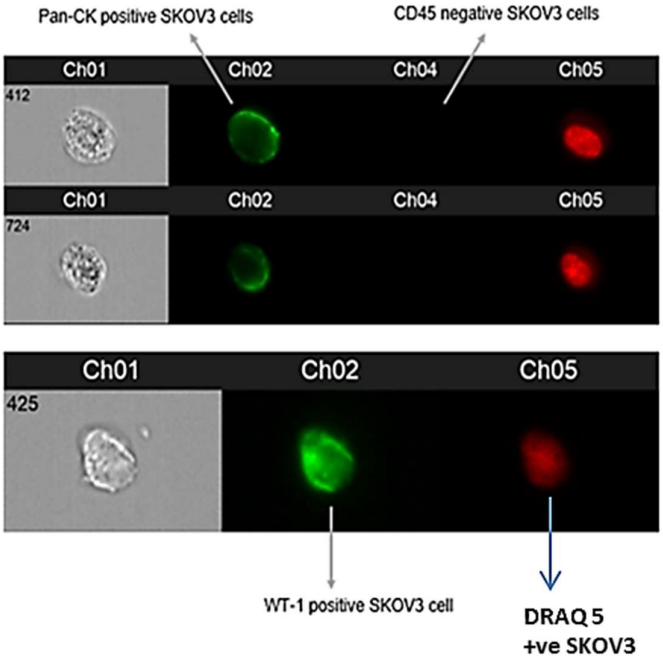

Figure 3.7 *– Cultured OC cells captured using size-based technology. (top) SKOV3 cells positively stained for AE1/AE3 (green) shown in Ch02 and negative for CD45 shown in Ch04 after harvesting the sample using Parsortix™ size-based cell separation; (bottom) SKOV3 cell positive for WT1 (green) in channel 2. All images under Ch05 are positive for DRAQ5 nuclear staining. Ch01 show images in brightfield.*

In the interest of investigating the efficacy of this method in a clinical setting, a blood sample was collected from an ovarian cancer patient (enrolled on the CICATRix trial). After running the prepared sample on Imagestream post-staining, only one positive cell was detected (as seen in figure 3.8).

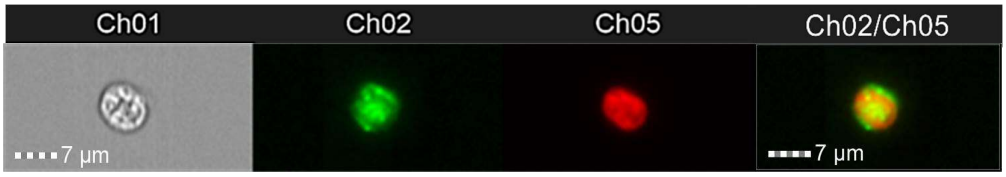

Figure 3.8 *- Picture captured using ImageStream IDEAS software showing a positively stained circulating tumour cell (CTC) harvested using the Parsortix™ cell separation system. Ch01 shows image of the captured cell in brightfield, Ch02 shows AE1/AE3 expression (green), Ch05 shows DRAQ5 nuclear staining and Ch02/Ch05 shows an overlay image of the two channels.*

3.3.4 Using ImageStreamX Mark II (imaging flow cytometry) to detect and visualise cancer cells

To test the potential of imaging flow cytometry in detecting ovarian cancer cells, various concentrations (ranging from 200,000 to 20 cells/mL) of SKOV3 and PEO1 cells were spiked into blood collected from a healthy volunteer as a representative model to simulate detection using patient samples. Each concentration of cells was spiked in 1ml of blood and the protocol for cell detection was followed, as described in the methodology chapter.

For each sample, 5000 events were recorded using the ImageStreamX Mark II flow cytometry machine. The events were represented using a scatterplot to identify the population of interest. As shown in figure 3.9, the scatterplot generated shows three distinct populations based on area of the cell and the aspect ratio, which depicts the circularity (or morphology) of the cells in the marked population.

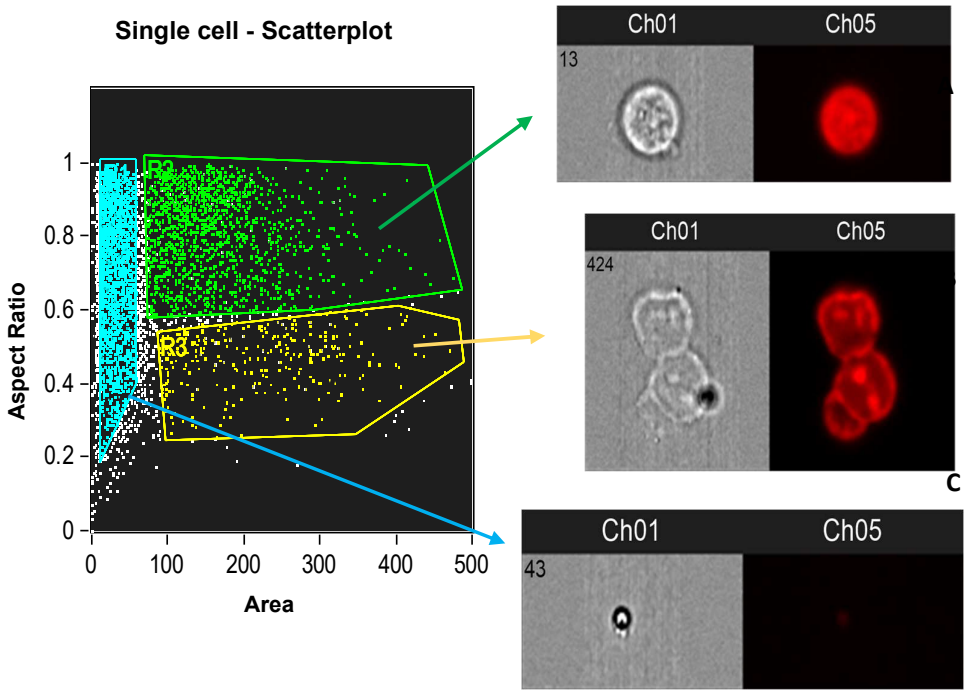

Figure 3.9 *- Scatterplot extracted from the IDEAS analysis software representing the various populations found within the sample including the single cell of interest (A), doublets which are counted by the system as single events (B) and cellular debris (C). Aspect ratio is plotted on the y axis, with dots plotted closer to 1 having more circularity, while area of the cell is plotted on the x axis. Ch01 shows images in brightfield and Ch05 shows cells stained with DRAQ5 nuclear stain.*

Once the population of interest is identified, a histogram is created (figure 3.10) to capture cells within focus – showing a clear picture of the nuclear staining, depicted using DRAQ5 fluorescent dye captured in Ch05, which targets nuclear matter and brightfield images in Ch01. From figure 8, the population showing cells in clear focus have a gradient measure of 40 and above.

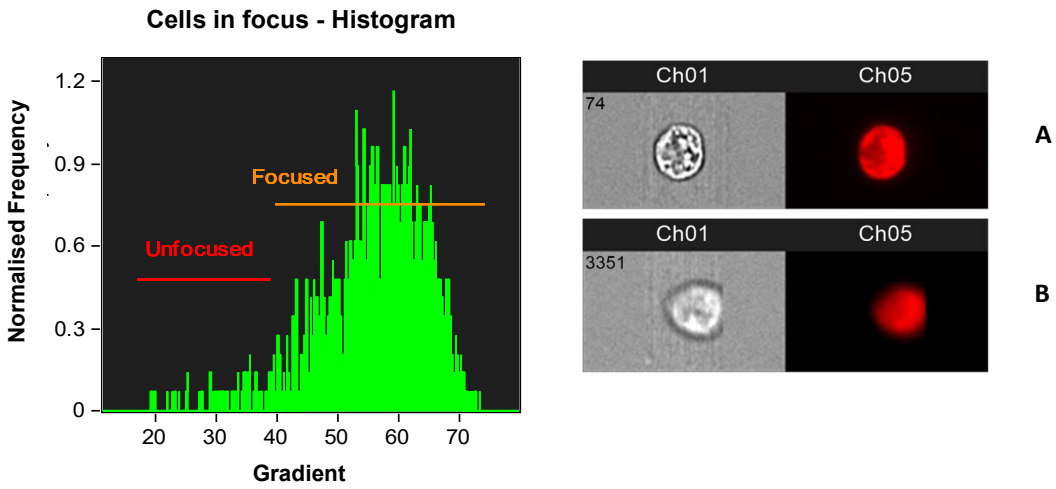

Figure 3.10 *- Histogram showing gating required to identify the population of cells in focus. (A) shows cells identified to be in focus while (B) shows cells that are unfocussed. Ch01 shows images in brightfield and Ch05 shows cells stained with DRAQ5 nuclear stain.*

Once the cells in focus are gated, this population is further gated based on intensity of the fluorescent signal emitted by the antibody of interest. For these experiments, two antibodies were used; a green, fluorescent dye conjugated with AE1/AE3 antibody (detected in Ch02) , targeting cyto-keratins that are expressed by ovarian cancer cells and an orange, fluorescent dye conjugated with CD45 antibody (detected in Ch04) targeting white blood cell (WBC) populations. Individual snapshots from each gated population are targeted for specific staining patterns to determine a true positive. As seen in figure 3.11, ovarian cancer cells are stained with pan-cytokeratin (AE1/AE3), an epithelial membrane marker and CD45 to distinguish WBCs from cancer cell lines. The characteristic membrane staining of both antibodies helps distinguish between the two populations of interest.

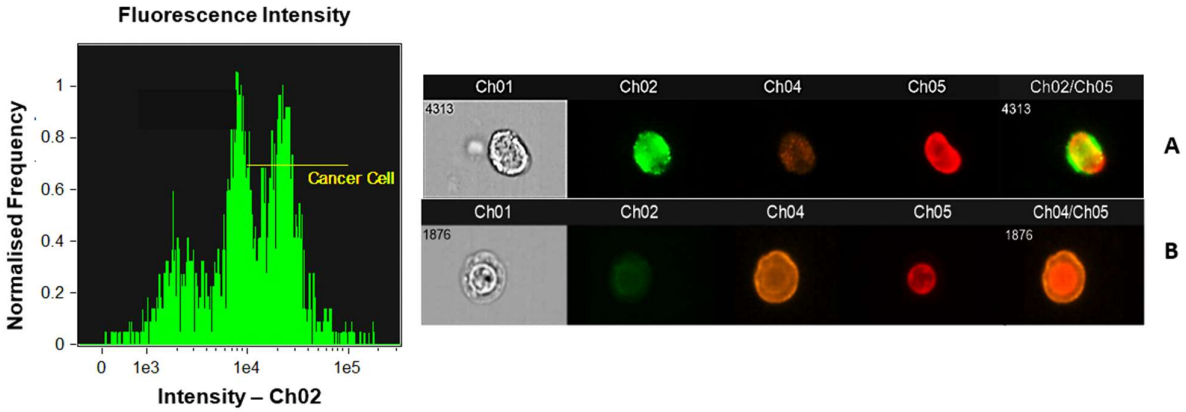

Figure 3.11 *- Graph used to identify various populations of cells based on fluorescence intensity. (left) In this graph, cancer cells are identified by gating cells with a high intensity of AF488 (green) identified in Ch02, while the population with a fluorescence intensity closer to 0 are usually positive for other antibodies (in this case is positive for CD45 shown in Ch04). In either case, cells gated are visualised and evaluated individually to identify cells with accurate staining. Panel A depicts a AE1/AE3+ and CD45- cell and panel B shows an AE1/AE3- and CD45+ cell. Both cells show a positive DRAQ5 nuclear staining (Ch05). Composite images (Ch02/Ch05) show superimposed images of fluorescent images from two channels.*

Based on the number of cells adhering to the staining pattern, each event is counted as a positive cell and the total number of cells pertaining to each population are then counted. Tables 3.1 and 3.2 (respectively) show the varying concentrations of SKOV3 and PEO1 cells spiked in blood, followed by the number of cells retrieved using the method explained above. Both these cell lines were used to detect AE1/AE3 and WT1 expression after blood spiking.

Table 3.1 *– Number of spiked cells (per 1mL of volunteer blood) and the number of SKOV3 and PEO1 cells positively identified for AE1/AE3 staining using ImageStream analysis with percentage retrieval in parentheses next to each value.*

Number of spiked cells (per 1mL)	SKOV3 (AE1/AE3+)	PEO1 (AE1/AE3+)
200,000	10,500 (5.25%)	11,000 (5.5%)
20,000	7,500 (37.5%)	9,000 (45%)
2,000	600 (30%)	1,250 (62.5%)
200	142 (71%)	181 (90.5%)
20	3 (15%)	16 (80%)

Table 3.2 *– showing the number of spiked cells (per 1mL of volunteer blood) and the number of SKOV3 and PEO1 cells positively identified for WT1 staining using ImageStream analysis with percentage retrieval in parentheses next to each value.*

Number of spiked cells (per 1mL)	SKOV3 (WT1+)	PEO1 (WT1+)
200,000	12,000 (6%)	9,667 (4.8%)
20,000	7,200 (36%)	6,000 (30%)
2,000	1,300 (65%)	667 (33%)
200	90 (45%)	125 (62.5%)
20	0 (0%)	8 (40%)

The results shown in table 3.2 show a relatively higher number of AE1/AE3 positive PEO1 cells compared to SKOV3 which correlates with the proof of principle experiment conducted earlier based on epithelial/mesenchymal phenotypes. In each case, when compared to a size-based platform, imaging flow cytometry was able to detect a significant amount of positive cell population within blood showing the potential of this being an effective method to identify these cell populations in patient samples.

3.4 Discussion

This chapter focuses on the development and validation of various aspects involved in liquid biopsy testing in order to for it to be clinically relevant and provide a degree of robustness.

Pre-analytical variables such as sample collection and storage require special attention, especially for protecting the integrity of the sample to carry out reliable further downstream analysis (Parackal et al., 2019). With this in mind, various blood collection tubes were tested for their ability to maintain sample integrity, specifically in terms of cellular morphology. In this case, the blood samples were collected and stored in tubes and tested every day for 6 days to account for the time it would take from blood collection at the clinic, transportation from the clinic to the laboratory and further analysis. These blood collection tubes (BCTs) were also compared with standard EDTA tubes used routinely within clinical practice to assess performance. Results from this experiment show that Roche tubes were better able to preserve cellular morphology over 6 days as compared to other tubes, showing signs of apoptotic cells on day 6. In comparison, the Streck tubes showed presence of cellular debris much earlier, on day 2. Previous experiments conducted to compare Roche and Streck tube performance have shown that while both tubes are capable of maintaining blood sample integrity for 7 days, Streck tubes were found to do so successfully over 14 days (Parackal et al., 2019). Contrary to these findings, the Roche cell-free DNA tubes performed better in our experiments and were used to collect blood samples from patients and healthy volunteers over the course of the clinical trial. In this study, PAXgene tubes could not be tested past day 3 due to sample coagulation. Blood samples stored past day 3 continued to show sample coagulation and could not be processed any further. Based on these data, Roche BCT were used hereafter to collect and store samples for processing.

The next step was to validate biomarkers that are reliable and can be used to identify circulating tumour cell populations in blood samples. Selection of cells expressing the cell surface epithelial cell adhesion molecule (EpCAM) is popularly used in CTC detection as it shows little to no expression in leukocytes and is expressed by epithelial-derived cancers (de Wit *et al,* 2014). To date, CellSearch platform is the only FDA approved CTC detection platform which uses enrichment by EpCAM-targeted immunomagnetic selection (Li et al., 2020). EpCAM mRNA expression in patient tumour samples showed high EpCAM expression in a majority of tumour types, however there was a subset of samples with lower EpCAM expression. In particular, lung and ovarian cancer samples had a greater percentage of tumour cells with very low EpCAM expression, while a similar analysis in breast cancer cell lines showed that 20% of those cells showed little of no EpCAM expression and a high expression of mesenchymal markers such as Vimentin (Punnoose et al., 2010). The same study also used CellSearch to detect spiked samples containing EpCAM high and EpCAM low expressing cancer cells and showed that while high

EpCAM expressing cells show a 75% recovery rate, low EpCAM expressing cells showed a significantly lower recovery rate of 42%, demonstrating a downward trend towards decreased recovery after 48 hours (Punnoose et al., 2010). For this purpose, one epithelial (AE1/AE3) and one ovarian-specific (WT1) marker were subsequently used for the study. A majority of advanced ovarian cancers are of epithelial phenotype, justifying the use of an antibody targeting a wide array of cytokeratins traditionally expressed by epithelial OC cells. And due to EMT, circulating tumour cells tend to lose their expression of epithelial markers and express mesenchymal markers, for which WT1 was picked, which is a nuclear marker, is overexpressed in OC and would help identify circulating tumour cells that have undergone EMT. As seen in the *in vitro* proof of principle experiment on PEO1 and SKOV3, WT1 expression was seen in cells from both epithelial (PEO1) and intermediate mesenchymal (SKOV3) phenotypes.

To compare the efficiency of CTC detection based on methodology i.e., physical properties (in this case cell size) and biological properties (detection using fluorescent antibodies), Parsortix™ cell separation platform and the ImageStream X imaging flow cytometer by Amnis Corporation were used. Experiments conducted in this chapter using OC cell lines showed a minimal retrieval of cells using the microfluidics chip compared to the results that were obtained using imaging flow cytometry. This could be due to the width of the 'critical gap' within the microfluidics chip through which the sample is passed allowing for smaller cells such as RBCs and WBCs to pass by and entrapping larger cancer cells. The critical gap within these chips is now available in various widths ranging from 10µm down to 4.5µm, which could make CTC isolation more efficient based on size (Miller et al., 2018) and is something that could be utilised in future size-based experiments on CTCs. The width of the critical gap (where CTCs are captured) used for this assay ranged from 7 to 10µm, which subsequently may have affected the number of cells that were captured. From size-based analysis conducted in patient blood samples (further discussed in chapter 4), there seems to be a size overlap between white-blood cells and potential CTCs with cell size noted at an average of 7-8µm (Kumar *et al.*, 2019). Therefore, a size-based assay would be more successful in capturing cell populations with a smaller critical gap, however, antibody-based identification would still be needed to differentiate between WBCs and CTCs due to the size overlap. Compared to this two-step process, imaging flow cytometry provided a better alternative of processing the entire sample in a non-biased way.

Finally, another proof of principle experiment was conducted to mimic the conditions of a patient blood sample wherein varying concentrations of OC cell lines were spiked into 1ml of blood collected from a healthy volunteer using serial dilution. This was done to study the frequency of cell retrieval for each biomarker used. In corroboration with previous results, AE1/AE3+ cells were higher in PEO1 cell compared to SKOV3. The percentage proportion of cells detected was

mostly greater as the number of spiked cells decreased, meaning that the smaller the spiked CTC population, the more detectable the cells were. However, it is worth noting that 100% of the cells were not detected in samples spiked with the lowest dilution of CTCs (20 cells), which shows that it may not be a very sensitive assay for diagnostic purposes, possibly because not many cells may be disseminating through blood during early stages, so this technique may possibly not pick up very minute populations of cells.

Chapter 4

Identification of cancer-related circulating cells (CCs) in blood extracted from patients with OC

4.1 Introduction

Circulating tumour cells (CTCs) have received enormous attention as a novel biomarker for a variety of malignant diseases, including ovarian cancer. They appear as individual cells or clusters of cells that enter into the bloodstream through intravasation from primary tumours and reach a distant organ, where they can eventually grow into an overt metastasis (Kim et al., 2019). CTCs are not the only tumour derivatives in circulation, but they contain a population of metastatic precursors that are of paramount importance for the accomplishment of disease progression (Castro-Giner et al., 2018). Patients with positively identified CTCs are shown to have worse prognoses, a phenomenon confirmed in the case of breast, prostate, and colorectal cancer. Particularly in the case of OC, evidence suggests that CTC detection translates to lower progression-free and overall survival (Kim et al., 2019). Progress has been hindered until quite recently due to technical challenges posed by CTC detection, analogous to looking for the proverbial 'needle in a haystack' (Krebs et al., 2010). Furthermore, as discussed before, a vast majority of cancers are of epithelial origin, hence the identification of CTCs based on epithelial antigen expression became the initial approach, however, this approach does not account for cells that undergo EMT leaving a significant population of CTCs undetected (Thiery, 2002; Keller *et al,* 2019). As mentioned earlier, the most widely used method for CTC analysis i.e., the CellSearch™ CTC test has been used in patients with OC in multiple publications with conclusively very low yields (e.g., single CTC in 7.5 mL of whole blood, which may contain 75 million leucocytes and 50 billion erythrocytes), posing a significant technical challenge, translating to limited clinical utility (Kumar *et al.*, 2019). Furthermore, the instrument used for CTC detection is also important, and a microscope or flow cytometer is typically selected for this task. However, there are trade-offs between speed and specificity. While the microscope can identify CTCs based on images and is highly specific, images must be acquired at a low magnification to maintain high throughput. Flow cytometers provide high throughput but do not generate cell images to examine molecular localization or morphology, reducing accuracy (Takahashi et al., 2020). In addition to CTCs, all modes of tumour angiogenesis induce shedding of endothelial cells into the blood stream, subsequently known as circulating endothelial cells (CECs) (Rahbari et al., 2017). Tumour vascularisation is induced and regulated by hypoxia and facilitates the release of angiogenic factors such as VEGF that promotes the proliferation of endothelial cells. Endothelial cells are

directly involved in tumour vasculature and are at the centre of diverse processes involved in the pathogenesis of malignant neoplasms; potentially being of importance as a biomarker in cancer (Lin, 2020). This chapter utilises the potential of imaging flow cytometry to quantify cancer-related circulating cells ranging from CTCs to other derivates such as CECs. Together, these populations are combined under an umbrella term called cancer-related circulating cells (CCs). This term will be used for the remainder of our studies.

4.2 Aims

- To quantify and compare the number of AE1/AE3+ and WT1+ CCs in OC patients undergoing chemotherapeutic treatments.
- To compare the cell size of AE1/A3 and WT1+ CCs with white blood cells to determine whether CTCs can be detected solely based on size.
- To quantify the number of CD31+ CECs detected in OC patients as a pilot study.

4.3 Results

4.3.1 Analysing OC patient blood samples using imaging flow cytometry

Advanced stage OC patients from two clinical trials (CICATRix and TRANS-METROBIBF) were included in this study; the study was performed in accordance with the Declaration of Helsinki. Blood samples were collected from patients attending Mount Vernon Cancer Centre (East and North Hertfordshire NHS Trust) for biomarker identification and analysis. Specimen collected under the TRANS-METROBIBF trial was conducted by Dimple Chudasama during the course of her PhD and the results were published as a combined study. Both these studies aimed to collect blood samples to explore the predictive role of circulating tumour cells (CTCs) in OC.

5–10 mL of whole blood was taken from patients at regular intervals with a tissue diagnosis of high-grade serous ovarian cancer (HGSOC); patients were categorised into three groups:

(1) Relapse—patients whose aEOC had relapsed following prior remission, and who required further chemotherapy treatment.

(2) NACT—patients whose primary treatment at diagnosis was **N**eo-**A**djuvant **C**hemo**T**herapy.

(3) post-PDS—patients who underwent **P**rimary **D**ebulking **S**urgery as their first treatment for aEOC.

39 healthy female volunteers donated 5–10 mL of whole blood, which was also screened for cells that would stain with pan-cytokeratin and WT1 antibodies. Whole blood samples were assayed within 6 days of venesection. Patients and volunteers provided a written consent form to

participate in this study and for the use of their donated blood specimen. Further details regarding patients included in this study is provided in tables 4.1 – 4.3.

Table 4.1 – *Clinical information of patients belonging to Neoadjuvant chemotherapy and interval surgery (NACT) cohort (n=13).*

		Total number in cohort = 13
Age at diagnosis	<60y	3
	>60y	10
Radiological Staging	III	11
	IV	2
Neoadjuvant chemo	Carboplatin/Paclitaxel	13
	Bevacizumab	2
Residual Disease*	0	10
	<1cm	-
	>1cm	-
	>2cm	-
	No interval surgery	3
Adjuvant chemo	Carboplatin/Paclitaxel	13
	Bevacizumab	7

Table 4.2 – *Clinical information of patients belonging to the Primary debulking surgery (PDS) cohort (n=9).*

		Total number in cohort = 9
Age at diagnosis	<60y	2
	>60y	7
Radiological Staging	I	-
	II	1
	III	8
	IV	-
Residual Disease	0	6
	<1cm	1
	>1cm	1
	>2cm	1
Adjuvant chemo	Carboplatin/Paclitaxel	9
	Bevacizumab	3

Table 4.3 – *Clinical information for OC patients placed within the Relapse treatment cohort (n=15).*

		Total number in cohort = 15
First treatment	Chemotherapy (NACT)	5
	Surgery (PDS)	10
Age	<60y	7
	>60y	8
Residual Disease	R0	10 (NACT x 4)
	<1cm	-
	>1cm	2 (NACT x 1)
	>2cm	3
Adjuvant chemo	Carboplatin/Paclitaxel	13 (NACT x 5)
	Carboplatin alone	1
	No adjuvant	1
Line of relapse for CC*	First relapse	3
	Second relapse	5
	Third relapse	5
	Fourth relapse	2

Blood samples were collected from patients before beginning treatment (screening), after each cycle of chemotherapy and at the end of treatment (EOT). Red blood cells were removed from the sample and prepared for ImageStream™ analysis as described in section 2.3.1 in methodology. White blood cells within the sample were identified using CD45 antibody which detects B cells, T cells and macrophages among other types of white blood cells (BD Biosciences CD marker handbook). In order to identify potential circulating tumour cells (CTCs) or cancer-related circulating cells (CCs), a cocktail of cytokeratin markers called AE1/AE3 was used to target epithelial CCs. WT1 was in this study as an OC specific marker with the intention of detecting non-epithelial CCs affected by EMT. DRAQ5 was used to stain the nucleus.

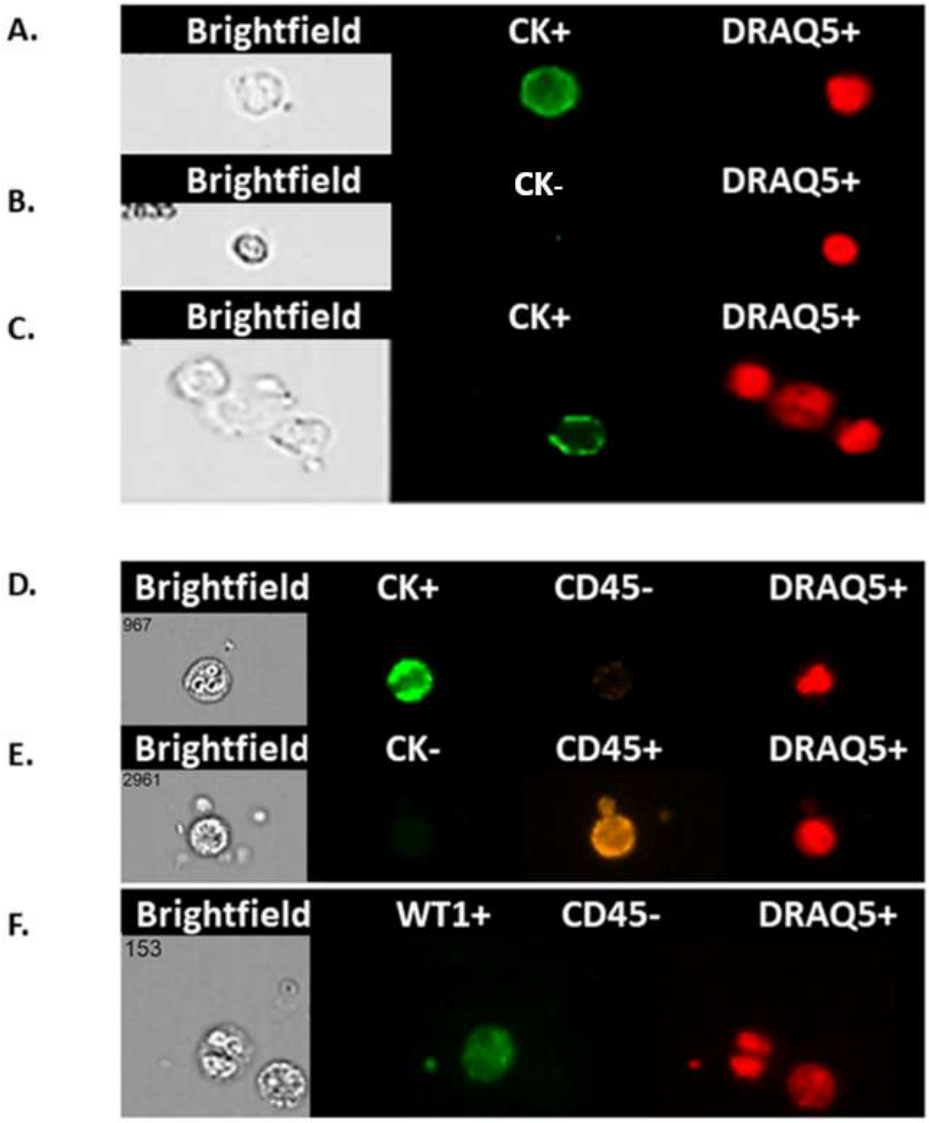

Figure 4.1 - *Circulating cells from an ovarian cancer patient blood sample based on staining in a scatter image generated by the Imagestream Mark II. The micrograph shows images of single cells from ovarian cancer patients with: (A): positive staining for CK and nuclear staining (DRAQ5) identifying a potential circulating ovarian cell (CC), (B): negative staining for CK but positive for DRAQ5 identifying a potential white blood cell (WBC), (C): combination of 2 potential WBCs (CK-) with a circulating ovarian CC (CK+); all three were stained positive for DRAQ5, (D): positive staining for CK, negative for CD45 and nuclear staining (DRAQ5) identifying a CC, (E): negative staining for CK, positive for CD45 and nuclear staining (DRAQ5) identifying a WBC, (F): a combination of 2 cells; one WT1 positive and one negative, both negative for CD45, but positive for nuclear staining (DRAQ5) identifying two potentially different CCs, but not WBCs (Kumar et al., 2019).*

Comparison between aEOC and volunteer blood samples showed a significant increase in CK+ and WT1+ CCs in patients (*P <0.05; see figure 4.2). For CK+ cells, the mean number of positively identified cells per 1 mL of blood was 547 CCs/mL (n=37) in aEOC, compared to 47 CCs/mL (n=39) found in control samples. Similarly, the mean WT1+ cells in aEOC patients were 2914 CCs/mL (n=27) compared to 667 CCs/ml in healthy female volunteers (n=15). Histopathological data collected from patient tissue samples at the time of diagnosis was also compared to corresponding blood CC results. In the case of WT1, out of 29 patients, 19 (65% tissue/blood overlap) showed WT1+ outcome in both blood and tissue samples, whereas 2 samples showed WT1+ CCs in blood only. 15 (38% tissue blood overlap) patients (out of 37) showed CK+ outcome in both blood and tissue samples. Overall, there appears to be a correlation between histopathological outcomes and immunostaining analysis using imaging flow cytometry (Kumar *et al.*, 2019).

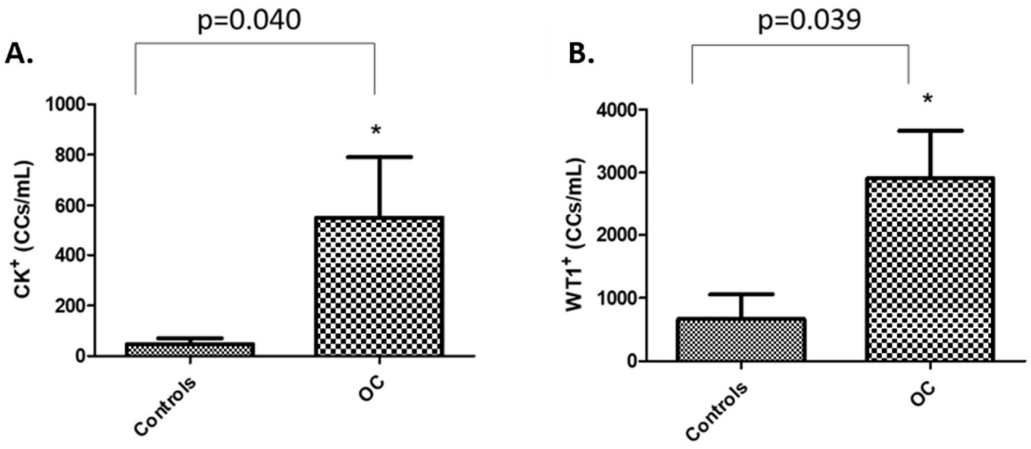

Figure 4.2 *– Comparing positively identified CCs in volunteers and patient blood samples. CK+ CCs (left) and WT1+ CCs (right) identified in blood samples collected from healthy volunteers (controls) and aEOC patients (OC). Unpaired student t test result shows both AE1/AE3+ and WT1+ identified CCs are significantly higher in aEOC patient blood compared to controls (*P < 0.05; ± SEM) (Kumar et al., 2019).*

To measure the validity of this test in a diagnostic/prognostic setting, a ROC (receiver operating characteristic) curve was generated. ROC curves compare sensitivity versus specificity across a range of values to predict a dichotomous outcome. The area under the ROC curve (AUC) is used as a measure of test performance (Florkowski, 2008).

- Sensitivity ("positivity in disease") refers to the proportion of subjects who have the target condition (reference standard positive) and give positive test results.

- Specificity ("negativity in health") is the proportion of subjects without the target condition and give negative test results.

Positive predictive value is the proportion of positive results that are true positives (i.e., have the target condition) whereas negative predictive value is the proportion of negative results that are true negatives (i.e., do not have the target condition).

ROC curves were generated using GraphPad Prism for both CK and WT1 and the AUC was used to measure accuracy for each test to identify presence or absence, in an OC context.

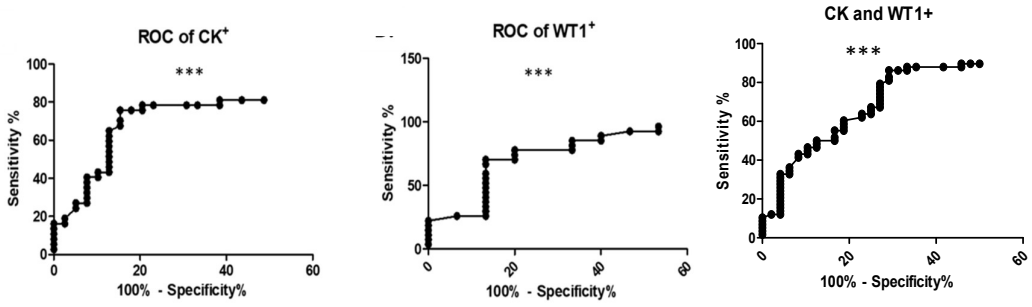

Figure 4.3 *- ROC curve analysis used to measure percentage of sensitivity and specificity. AUC calculated for CK+ was 0.78 (***P < 0.0001), for WT1+ was 0.82 (***P < 0.0006) and for CK+ and WT1+ combined was 0.79 (***P <0.0001) (Kumar et al., 2019).*

ROC curve analyses show a strong capability for both CK and WT1 to function as a positive predictor of disease, which is useful in a prognostic context. In terms of specificity i.e., to deduce true negatives, both tests are similar (specificity % - CK+ = 50; WT1+ = 53.3) and this remains similar despite combining both these biomarkers.

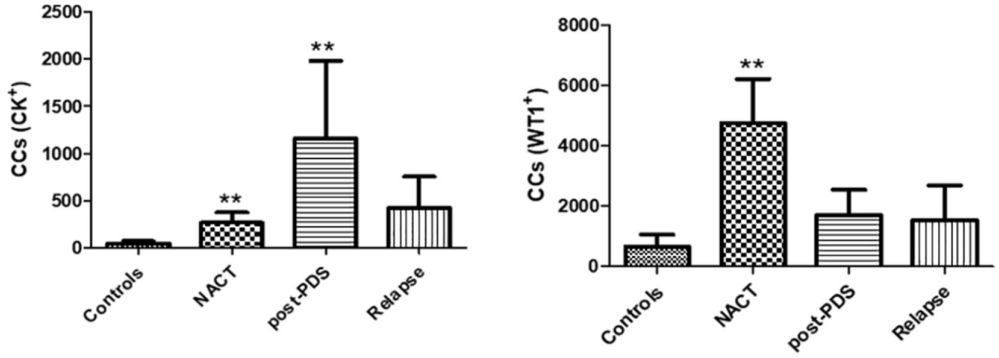

Figure 4.4 *– Comparing CC levels in volunteers and patient samples based on specified cohorts. CK+ CCs (left) and WT1+ CCs (right) was quantified in healthy volunteers and in the three identified aEOC patient cohorts (NACT, PDS and Relapse). For CK+ CCs, patients classified as NACT and PDS showed significantly higher positively identified CCs compared to controls (**P <0.001). For WT1+ CCs, NACT patients showed significantly more CCs compared to controls (**P <0.001). Significance was determined using unpaired student t test method (Kumar et al., 2019).*

From figure 4.4, it is evident that there is a difference in the number of CCs based on patient cohorts. For the CK+ patients, the number of CCs was significantly high in NACT and post-PDS cohorts when compared to controls. Whereas, for the WT1+ patients, the NACT cohort showed a significant increase in CCs compared to controls. It is noteworthy that the number of WT1+ CCs in the NACT cohort is higher compared to CK+ CCs. Also, the post-PDS cohort showed more CK+ CCs compared to WT1+ CCs. Considering the fact that CK+ targets cells of epithelial origin whereas WT1 also targets cells undergoing EMT, it is possible that in the case of NACT patients, more EMT-related cancer cells are found in blood post-chemo, whereas a higher proportion of epithelial cancer cells are seen after surgery, possibly because the tumour site has been disturbed, releasing more epithelial CCs. Although, presence of CTCs in patient samples collected one week post-op correlated with poor prognosis and disease recurrence (Zhang et al., 2018; Kim et al., 2019). It may be worth investigating whether the same trend emerges in a larger patient cohort.

CA125 is routinely used within the NHS to diagnose OC and its ability to perform as an accurate test has been discussed extensively in the main introduction. Four patients were followed during their chemotherapy treatment and the number of CCs was compared to their recorded serum CA125 level after every treatment cycle.

Overall, CCs varied in broad alignment with serum CA125 response; for example, patient 14 had a similar drop in CCs and CA125 levels following the first 3 treatments. However, when we performed correlation analysis (Pearson and Spearman) no apparent significance was reached. As it can be seen, patient 13 *(post-PDS cohort)* had adjuvant chemotherapy after primary surgery for stage IIB ovarian cancer and there was a good response that correlated with a drop in CC level, although no apparent change was noted for CA125 levels. A similar pattern was evident for patient 25 *(relapse),* who received chemotherapy for first relapse ovarian cancer with a good clinical response. Patient 14, was a *NACT* patient who received 4 cycles of chemotherapy, followed by an unexpected 50-day delay prior to interval surgery. It is evident that although CA125 remained stable, CCs rose in line with disease relapse/progression during this period. Patient 29 is a *post-PDS* (post-surgery) patient who showed early relapse during adjuvant chemotherapy at 130 days, which was preceded by a rise in CC level at 60–70 days. If this was known earlier, the chemotherapy treatment may well have been withheld after 2–3 cycles due to it being ineffective. CC levels decreased dramatically following treatment with letrozole and subsequent tamoxifen (relapse therapy). A one month follow up demonstrated a rapid surge of CCs concomitant with the diagnosis of brain metastases and relatively early death of this patient (Kumar *et al.*, 2019).

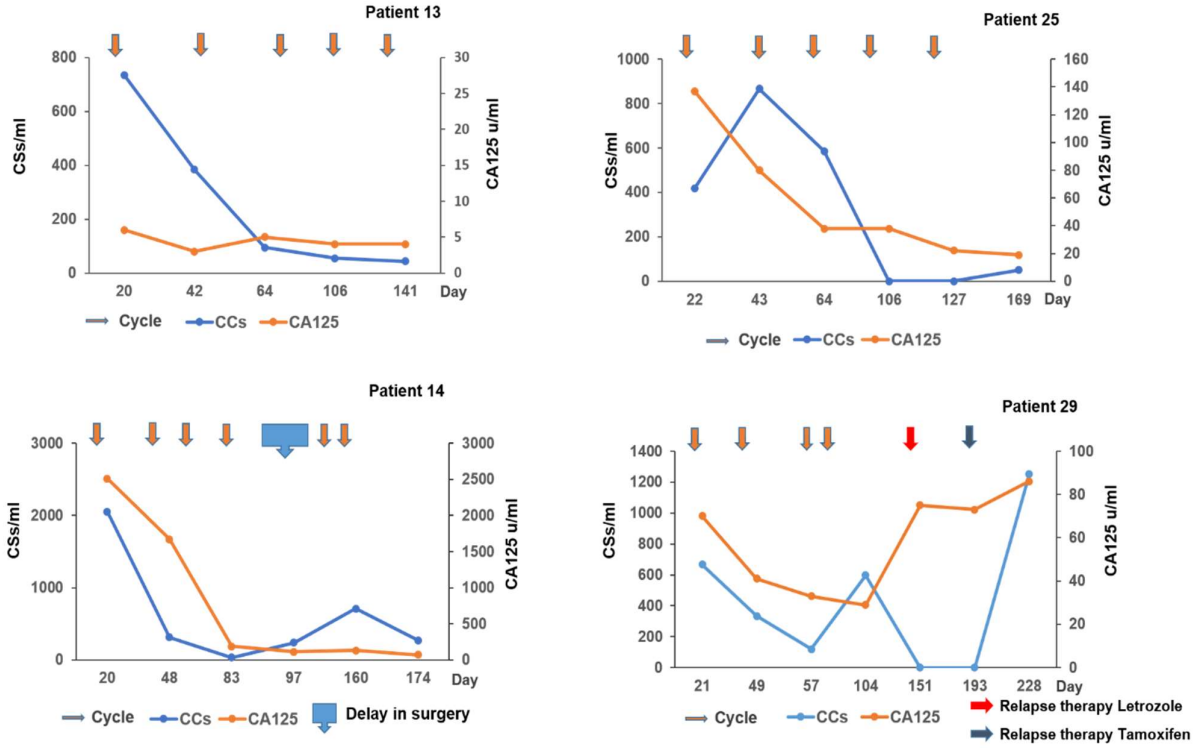

Figure 4.5 *– Serial monitoring of CCs in aEOC patients. CCs (CK+ and WT1+) measured in 1 mL of patient blood during chemotherapeutic treatment for 4 aEOC patients. Blue lines represent CC levels and orange lines represent recorded CA125 levels at each cycle. Chemotherapy treatments are represented with arrows (Kumar et al.*, 2019).

This study also included a size-based analysis of positively identified CCs to explore the potential of using size-based technologies for the detection of CCs in OC. Results (figure 4.6) show that even though WT1+ CCs showed a slightly larger diameter compared to CK+ CCs and CD45+ cells, there still remains an overlap. A combined analysis comparing the size of CK+/WT+ CCs and CD45+ cells did not show any significance. This suggests that size-based platforms, at least in the case of OC, may not be as helpful and would require additional immunofluorescence-based assays to distinguish between the different population of cells.

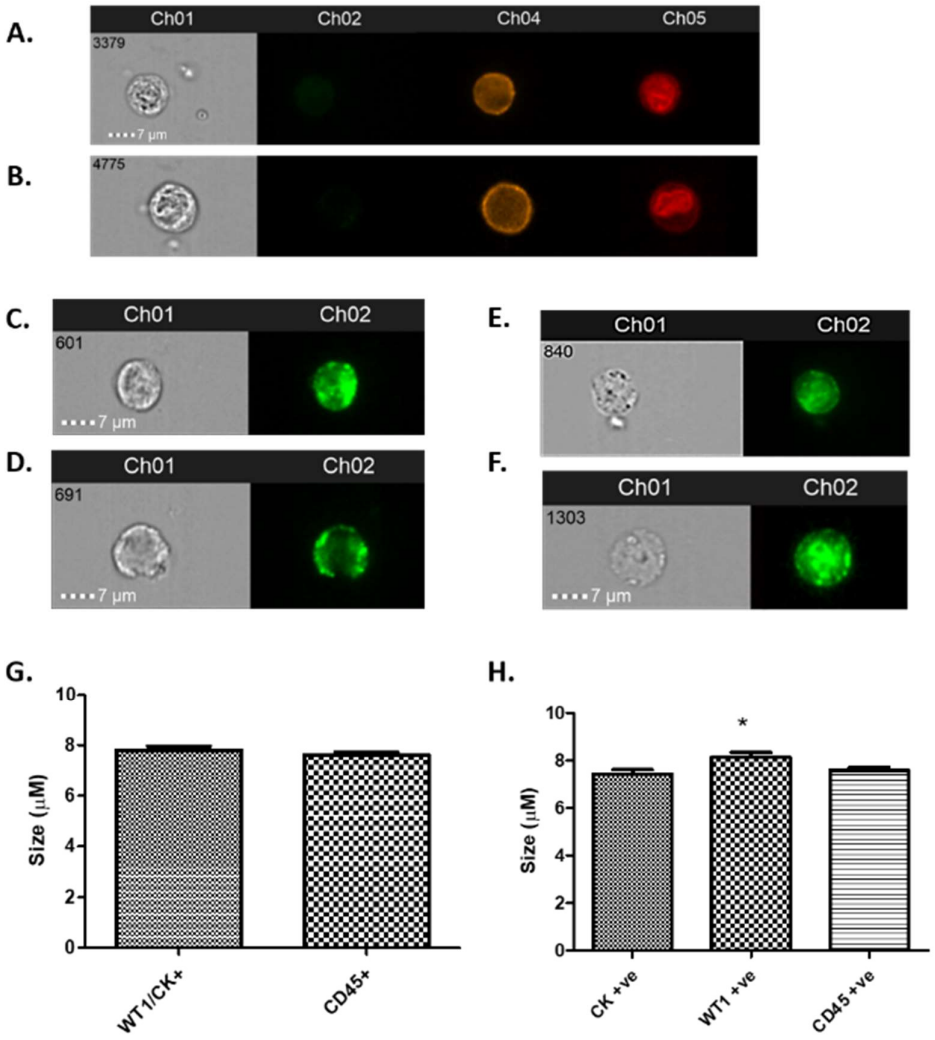

Figure 4.6 *– Size-based analysis of CCs and WBCs. Different sizes of WBCs (**A**: 8µM; **B**: 10µM), CK⁺ CCs (**C**: 7µM, **D**: 8.5 µM), WT1⁺ CCs (**E**: 7µM; **F**: 8µM). (**G**): No apparent differences in size were detectable when combined CK⁺ and WT1⁺ CCs were measured and compared to controls. However, WT1⁺ CCs were larger compared to CK⁺ CCs; but not by a great margin (**H**; * p < 0.05) (Kumar et al 2019).*

4.3.2 Identifying additional CC populations in blood – cancer-related circulating endothelial cells (CECs) – pilot study

Hematogenous cancer metastasis is significantly impacted by tumour neovascularisation, which in turn is regulated by hypoxia. Hypoxia facilitates the release of angiogenic factors such as VEGF, TNF-α and IL-8 that promote the proliferation of quiescent endothelial cells. Endothelial cells that make up the lining of the tumour vasculature are at the centre of diverse processes involved in the pathogenesis of malignant neoplasms. A majority of endothelial cells in the tumour vasculature are tumour-derived endothelial cells (TECs) exhibiting cytogenetic abnormalities of aneuploid chromosomes (Lin, 2020).

Morphologically abnormal tumour vasculature, contributed by TECs, possesses loosened junctions between endothelial cells, leading to an increase in vascular permeability and trans-endothelial intravasation as well as extravasation during tumour metastasis. Following their shedding into peripheral blood, TECs turn into circulating tumour-derived endothelial cells (CTECs). From previous experiments, it was evident that despite using WBC and CC biomarkers, there remained a population of cells within the sample that was not picked up by these antibodies. Therefore, as a pilot study, six patient samples were simultaneously incubated with anti-CD34 antibody (Sidney et al., 2014; BD Biosciences, 2011); primarily to study the morphological features of the CD34+ cell population recorded and to note the number of positively identified cells per/ml.

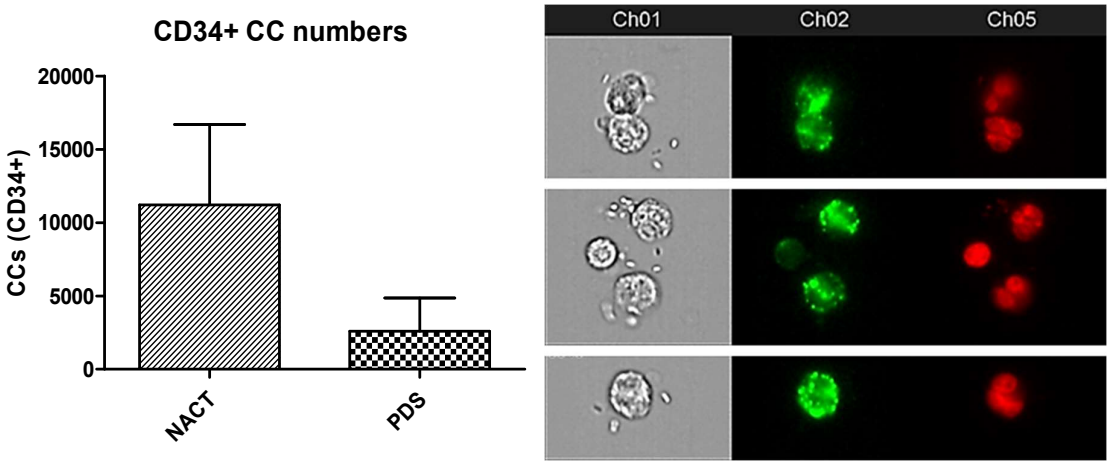

Figure 4.7 – *Analysing the presence of CD34+ CECs in aEOC patient blood samples.* ***(left)*** *Graph comparing the number of CD34+ CCs identified in patients with aEOC (n=6). Patients belonging to NACT cohort (n=4; Mean = 11216) and PDS cohort (n=2; Mean =2595) were compared and an unpaired student's t-test was conducted. No statistical significance was observed between the two groups (p value = 0.2).* ***(Right)*** *CD34+ circulating endothelial cells (CECs) identified in advanced EOC patient blood samples using ImageStream. Ch01 shows image of cells in brightfield, Ch02 shows CD34+ staining and Ch05 shows nuclear image using DRAQ5™. CD34+ CECs were seen in clusters with each other (top), with other cells (middle) and as single cells (bottom). Of note, these cells have a bigger nucleus or are multi-nucleated.*

CD34+ CCs were identified and compared in 6 patients belonging to two patient cohorts (NACT [n=4] and PDS [n=2]). Patients with aEOC belonging to the NACT cohort showed higher number of CD34+ endothelial cells compared to patients in the PDS cohort, however, no significance was noted. A larger study needs to be conducted in order to validate these results and investigate the role/significance of additional populations (such as CECs) in peripheral blood.

4.4 Discussion

This chapter aimed to investigate the potential of liquid biopsies, specifically circulating cancer-related cells (CCs), as a biomarker to determine prognosis in advanced OC patients. CTC identification has the potential to discriminate between healthy individuals, patients with benign tumours, and patients with advanced OC.

Our data demonstrates that AE1/AE3+ and WT1+ cell populations are significantly higher in blood samples collected from patients with advanced OC compared to healthy volunteers. The ROC curves generated were significant, suggesting that these readouts are of potential diagnostic value. ROC curves generated for CA125 for OC have low sensitivity (70%) and high specificity (90%) (Sánchez Vega et al., 2018); which is quite similar to the results from the analysis done here. However, it is worth noting that CC detection, with further improvements, could target the issue of CA125 being non-specifically upregulated in the case of benign conditions such as liver cirrhosis and pregnancy. Surprisingly, in two female volunteer samples, >4000 WT1+ CCs/mL were detected. On further investigation, it was noted that these volunteers were young and the positively identified cells is consistent with the presence of circulating endothelial cells found in females during the menstrual phase. Other healthy volunteers included in the study were post-menopausal women and did not show WT1+ CCs in blood. Future studies should include a larger age-matched control cohort, in order to determine the reliability of WT1 as a biomarker in pre-menopausal women. It is also worth noting that the number of positive CCs found in patients during screening is much higher compared to cell numbers reported using enrichment techniques like CellSearch™. There are two possibilities that may explain this; the method utilised here to identify CCs does not use EpCAM enrichment, a biomarker we know to be downregulated in CCs when they go through epithelial-to-mesenchymal transition.

There is also a possibility that a fraction of the population may be circulating endothelial cells (CECs). The presence of CECs is noted as a potential biomarker for vascular damage in cancer including OC (Kumar et al., 2019). Although promising, there are challenges involved in identifying an antibody specific enough to target CECs. For the purpose of this pilot study, CD34 antibody was used to distinguish CECs from other cell populations. CD34 (alternatively known as haematopoietic progenitor cell antigen 1 [HPCA1]) was chosen since it specifically targets precursor stem cells and endothelial cells (BD Biosciences, 2011). From figure 4.7, we can see that the endothelial CCs identified show giant or multiple nuclei; similar to cells identified when identifying AE1/AE3 and WT1 positive cells. Tumour blood vessels differ from normal counterparts, by changes in their morphology, therefore tumour-related endothelial cells appear to be structurally abnormal and can acquire cytogenetic abnormalities while in the tumour microenvironment (Hida et al., 2004).

Furthermore, cells containing multiple nuclei, or a giant nucleus are known to promote cancer 'stem cell' like properties through processes including nuclear budding, in addition to secreting growth factors and affecting the cells around them. These giant cells are capable of rapid proliferation through a budding process; this mode of cell division is called 'neosis' and the somatic reduction division of these giant cells have been reported in different cancer cell types including OC (Mirzayans *et al*, 2018). In addition to quantification of CCs, having technology that focuses not just on cell size, but also morphological characteristics such as multi-nuclear properties may be helpful in identifying chemoresistance much earlier compared to sole reliance on CA125 levels throughout treatment. Techniques to carry out simultaneous expression of AE1/AE3 and WT1 were not sufficiently developed during the course of this trial; however, the obvious next step would be to optimise multiple biomarker staining of CC populations in blood samples to study the different populations (epithelial and mesenchymal) of cells and the expression overlap (if any) of cells that co-express both markers.

Chapter 5

Investigating the role of rfhSP-D as a potential biomarker and drug target in ovarian cancer

5.1 Introduction

Human surfactant protein-D (SP-D), a soluble collagen containing C-type lectin (Collectin), is a potent innate immune molecule, and is mainly considered to possess anti-microbial and inflammation modulatory properties (Kishore et al., 2006). SP-D, which is primarily produced within the lungs by type II pneumocytes and Clara cells, is involved in viral neutralisation, clearance of bacteria, fungi, apoptotic and necrotic cells, down-regulation of allergic reactions, and modulation of inflammation (Nayak et al., 2012). Although its homeostatic role within the lungs has been widely studied, its specific functions in extra-pulmonary tissues such as kidney, trachea, brain, testes, heart, or ovaries are being investigated now.

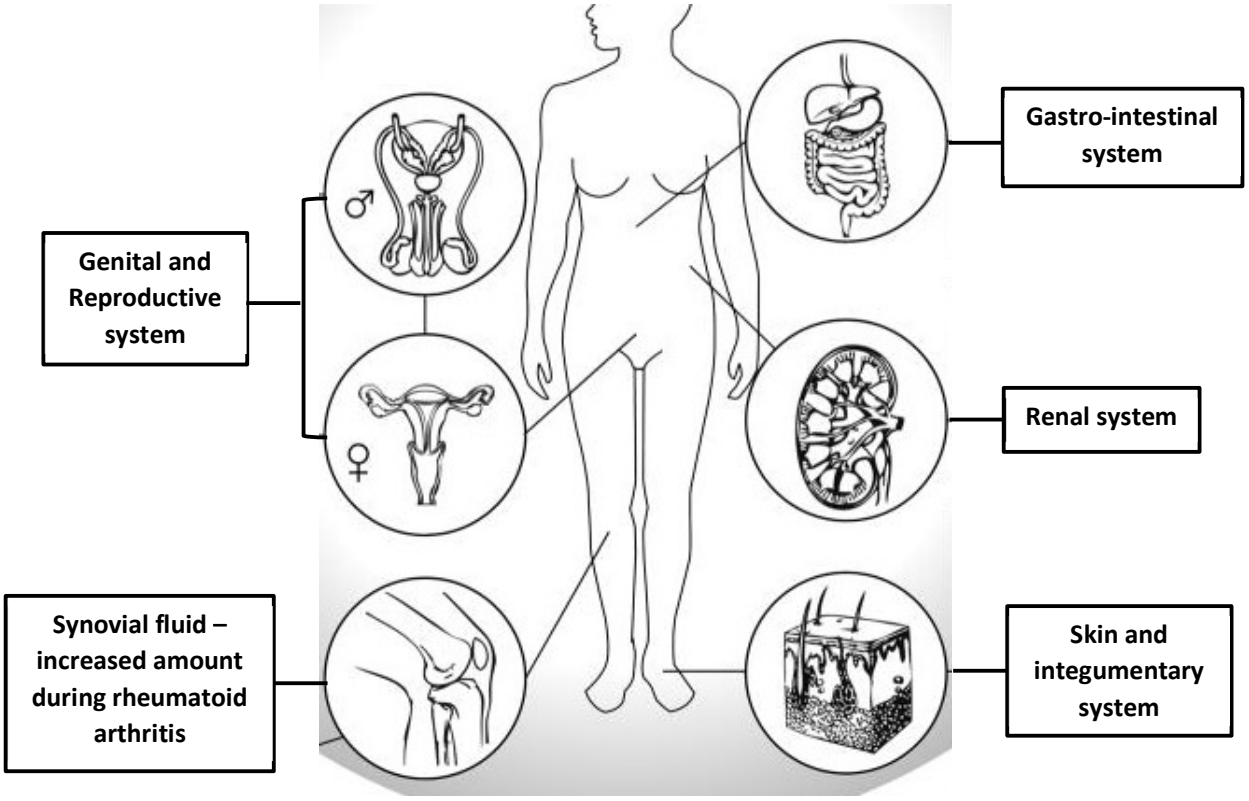

Figure 5.1 *- SP-D expression in some extra-pulmonary tissues and cells; adapted from* (Vieira *et al,* 2017).

Other than playing an important role within the innate immune system, SP-D expression is shown to affect cancer cell progression. As a primary site of production, the effects of SP-D have largely

been studied within lung cancer, where it has shown the ability to downregulate the EGF pathway by directly binding to EGFR and affecting cell proliferation, invasion, and metastasis *in vitro* (Hasegawa et al., 2015). A comparison of mRNA levels between neoplastic and healthy lung tissue revealed a lower expression of SP-D in lung adenocarcinoma, squamous cell carcinoma, large cell carcinoma and tumour carcinoid compared to normal lung tissue. In addition, immunohistochemical staining for SP-D confirmed a differential expression, with lower expression in neoplastic pulmonary parenchyma compared to healthy samples (Mangogna et al., 2018). Results from a clinical trial with 71 lung cancer patients showed an increased incidence of lung cancer associated with lower levels of SP-D, indicating the potential of SP-D in bronchoalveolar fluid as a biomarker (Sin et al., 2008). This suggests that a lower expression of SP-D in the lung correlates to an increase in cancer progression, therefore having a plausible protective effect. Other than the lung, SP-D expression has also been investigated in pancreatic cancer, wherein introducing a recombinant fragment of human SP-D (rfhSP-D) induced apoptosis in multiple pancreatic cancer cell lines independent of p53 status. Of note, an upregulation of pro-apoptotic genes Fas and TNF-α was reported after 24 hours, followed by the cleavage of caspases 8 and 3 at 48 hours, indicating that SP-D induced apoptosis via the TNF-α/Fas-mediated pathway (Kaur et al., 2018a). SP-D also inhibited TGF-β expression in a range of pancreatic cell lines, affecting their invasive potential by suppressing epithelial-to-mesenchymal transition (EMT) (Kaur, Riaz, Singh, *et al.*, 2018). A similar picture emerged in prostate cancer cell lines, where treatment with rfhSP-D reduced cell viability in a time and dose dependent manner and induced apoptosis in androgen dependent and independent cancer cells via p53 and pAkt pathways (Thakur et al., 2019).

SP-D is also found to be expressed within the human female reproductive system, including the uterus, ovaries, and oviduct. Within the uterus, SP-D expression is confined to the endothelium and epithelium. The ciliated epithelium in the fallopian tube and the cuboidal epithelium covering the ovarian surface also express SP-D (Leth-Larsen et al., 2004). SP-D mRNA is reported to be overexpressed in OC and could function as a potential indicator of prognosis (Mangogna et al., 2018). However, further research is necessary to elucidate the role of SP-D at an ovarian level in health and disease. Given that rfhSP-D expression has shown pro-apoptotic and anti-invasive effects in various *in vitro* cancer models, this chapter focused on the hypothesis that exposure to rfhSP-D could produce similar effects in OC, proving to be a potential therapeutic agent. We also hypothesised that potential changes in the expression of SP-D might be of additional value as a biomarker for diagnosis or prognosis for the disease.

5.2 Aims

- To elucidate the effects of rfhSP-D using SKOV3 and PEO1 cell lines as *in vitro* OC models
- To investigate the role of SP-D as a potential biomarker by analysing expression in clinical samples from OC patients.
- To inform on/delineate the role of SP-D in OC using bioinformatics analyses such as gene expression profiles and KM plot generators.

5.3 Results

5.3.1 Analysing the effects of a recombinant fragment of human SP-D (rfhSP-D) *in-vitro* using SKOV3 and PEO1 ovarian cancer cell lines

The migratory and proliferative capacity of ovarian cancer cells was investigated after exposure to rfhSP-D for 24 and 48 hours. For this and other experiments that follow, the concentration of rfhSP-D used (20 μg/ml) was kept constant after referring through previously published material. While varying concentrations of rfhSP-D were used for similar studies in other cell lines, the highest concentration (20 μg/ml) was noted to have measurable effects in cell lines (Kaur et al., 2018b; a; Mahajan et al., 2013). SKOV3 and PEO1 cells were seeded in 6-well plates (~10cm^2 growth area) to create a confluent monolayer. An artificial 'wound' was created in the monolayer using a fine pipette tip and images were taken at 0, 24- and 48-hour time points using a LEICA DMi1 inverted microscope configured at 40x magnification.

Untreated SKOV3 cells showed a visible growth into the wound which became more prominent after 48 hours. Contrary to this, the gap created within rfhSP-D treated SKOV3 cells grew wider at 24- and 48-hours. Therefore, treatment of SKOV3 cells with rfhSP-D affects cell growth and motility (see figure 5.2).

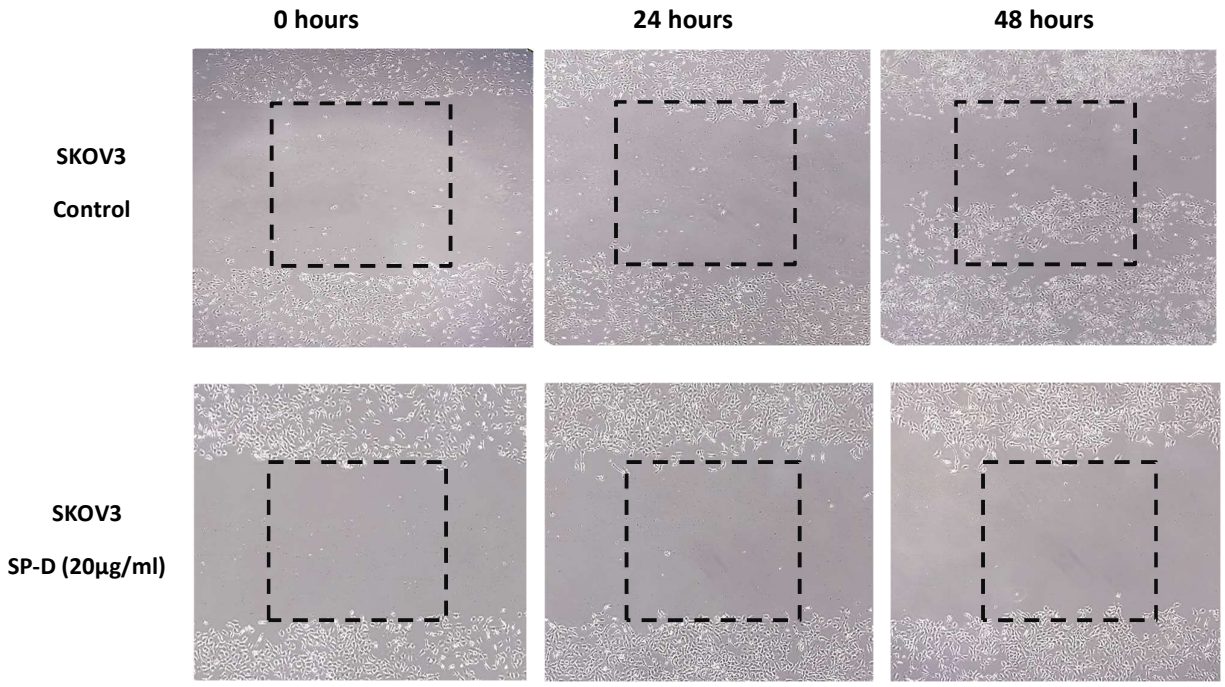

Figure 5.2 – *Wound healing experiments conducted on SKOV3 cells under untreated conditions (control – top panel) and cells treated with 20 µg/ml of rfhSP-D (SP-D – bottom panel). An artificial 'wound' was created in the monolayer and the width of the wound was used as a measure for proliferative capacity of cells (as represented by black squares within the figure). Images were taken at 0-, 24- and 48- hour time-points (from left to right). SKOV3 cell images from the 'control' panel on top show cells growing within the gap at 48 hours, in comparison to treated SKOV3 cells with a much wider gap in comparison, indicating lower proliferation rate in cells treated with rfhSP-D.*

Conflictingly, PEO1 cells did not follow the same pattern as SKOV3 cells, showing continued growth and proliferation into the wound at both time points. However, at 48-hours, PEO1 cells within the intact monolayer had spaces with attached cells in the gap of the wound, suggesting a displacement of cells. Although cells were also seen in the wound gap for untreated cells at 48-hours, the monolayer was intact (see figure 5.3).

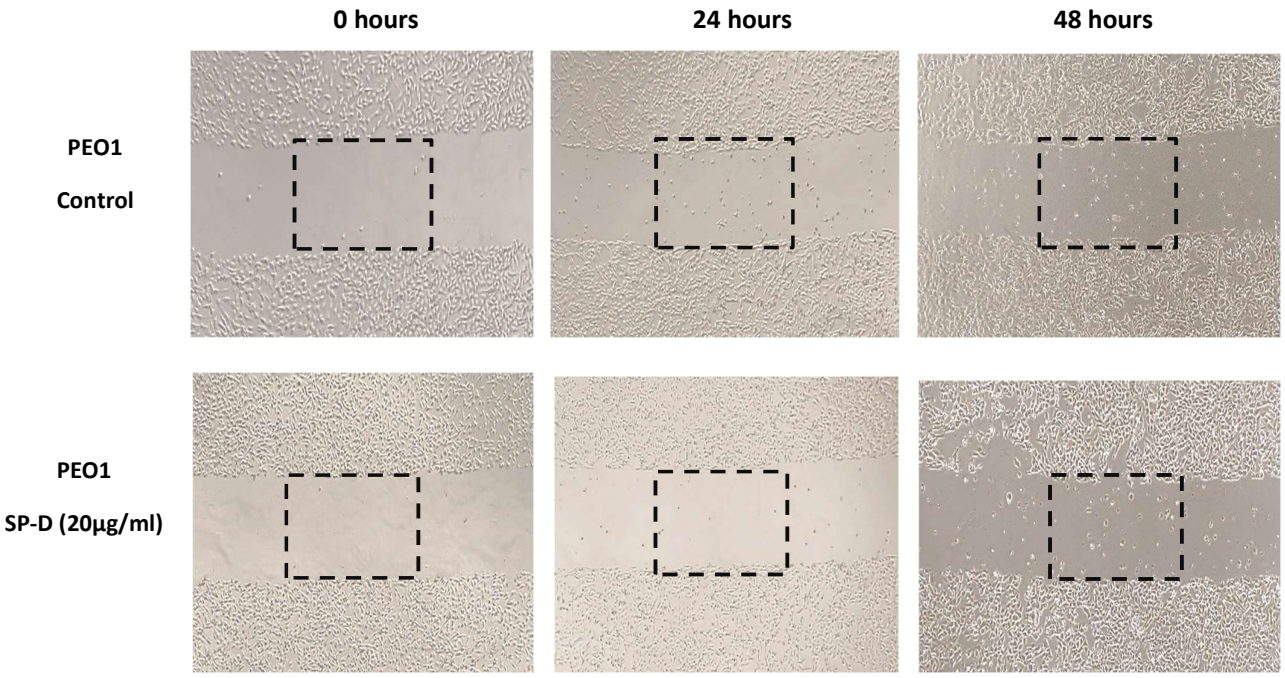

Figure 5.3 –*Wound healing experiments conducted on PEO1 cells under untreated conditions (control – top panel) and cells treated with 20 µg/ml of rfhSP-D (SP-D – bottom panel). An artificial 'wound' created to measure proliferative capacity of cells is represented by black squares within the figure. Images were taken at 0-, 24- and 48- hour time-points (from left to right). In case of PEO1, both control and treated sample images look quite similar at recorded time points, with cells growing within the gap at 48 hours.*

To further examine the effects of rfhSP-D on ovarian cancer cells, cell viability experiments were performed on both SKOV3 and PEO1 cell lines using trypan blue cell counting and an Annexin/PI assay. Conducting cell counts using trypan blue was used to measure cell viability and cell death, while an Annexin/PI staining assay was conducted as a more robust method to confirm results.

Table 5.1 *– Table showing the number of live cells, dead cells, and percentage of viable cells of SKOV3 and PEO1 cells following treatment with 20 µg/ml of rfhSP-D at a 24-hour time point. Following treatment, cells were stained with Trypan Blue dye and analysed using the Countess machine by Thermo Fisher Scientific.*

Cell Line	Live Cells	Dead Cells	Viability %
SKOV3 – 24hr	3.9 x 10^5	1.2 x 10^5	76%
PEO1 – 24hr	5.3 x 10^5	3 x 10^4	96%

Approximately 0.5 x 10^6 cells of SKOV3 and PEO1 were separately seeded in a 6-well plate in triplicates. Cells were treated with 20µg/ml of SP-D; cells untreated with rfhSP-D were used as control . Cells were stored in an incubator at 37°C at 5% CO_2 for 24 hours. When compared to PEO1, SKOV3 cells showed a lower cell viability and a higher number of dead cells after being

treated with SP-D for 24 hours (shown in table 5.1). In order to validate these observations, an apoptosis/cell death assay was performed. Control samples (untreated) and treated cells (with 20µg/ml SP-D for 24 hours) were stained with Annexin V and PI. Annexin V binds to phosphatidylserine (PS), a lipid that is usually present on the inner leaflet of the plasma membrane. PS is exposed when lipid symmetry is lost during apoptosis, making it a reliable marker to detect apoptotic cell populations (Crowley et al., 2016). PI is commonly used to detect cells undergoing late apoptosis and necrosis, when the integrity of the plasma membrane is severely affected, allowing fluorescently conjugated PI dye to interact with nucleic acids and identify these cells (Vermes *et al*, 2000).

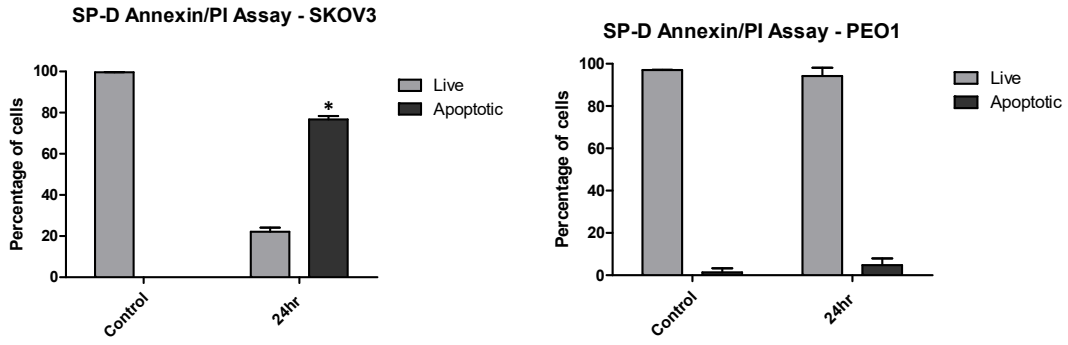

Figure 5.4 *- Annexin-V/PI fluorescence assay was used to record apoptotic SKOV3 and PEO1 cell populations in untreated/control conditions and after treatment with 20µg/ml of rfhSP-D. Percentage of live cells (grey) and apoptotic cells (black) were recorded at 0- and 24-hour time points. Apoptotic cell counts were much higher in SKOV3 cells after rfhSP-D treatment for 24 hours, compared to PEO1. Error bars indicate ± SEM; *p<0.05.*

rfhSP-D treated SKOV3 cells have a higher apoptotic/dead cell population after 24 hours but treated PEO1 cells do not (See figure 5.4). This indicates that exposure to rfhSP-D has cytostatic and cytotoxic effects in SKOV3 cells post-treatment .

To further investigate the mechanism through which SP-D induced apoptosis/necrosis within SKOV3 cell lines, qPCR was performed on cDNA extracted from control samples and both cell lines treated with SP-D at two time points: 24- and 48-hours. Fas, Bax and TNF-α gene expression levels were measured and YWHAZ was used as a housekeeping gene. SP-D has shown to induce cell death using a Fas-mediated pathway in pancreatic cancer cells and seemed to show a similar mechanism within SKOV3 cells treated in this study.

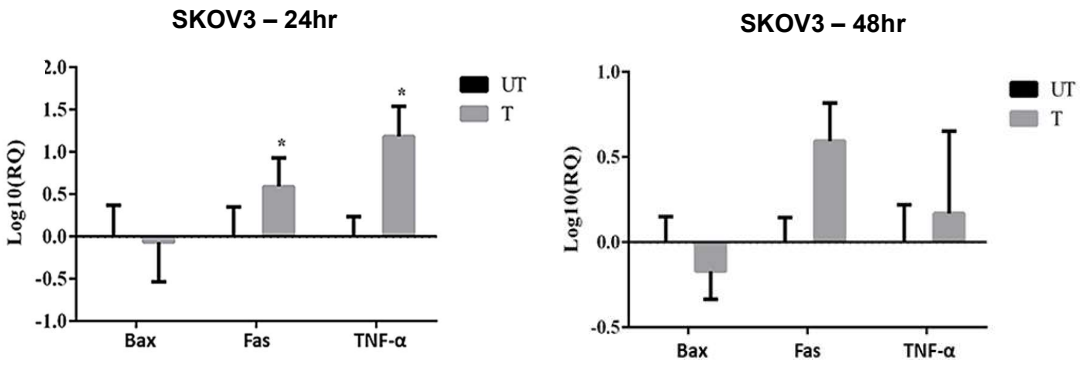

Figure 5.5 *– Gene expression results from RT-qPCR performed on SKOV3 cells; analysing the effects of SP-D on Bax, Fas and TNF-α gene expression at 24-hours (left) and 48-hours (right) SKOV3 cells treated with SP-D show a statistically significant upregulation in Fas and TNF-α expression compared to controls (*P<0.05). After 48 hours, although there is a marked upgregulation of FAS and TNF-α, it is not statistically signficant. Bax expression is downregulated at both time points* (Kumar *et al.*, 2019)*. Bars in black represent values from untreated samples (UT) and grey bars represent values from SP-D treated (T) samples.*

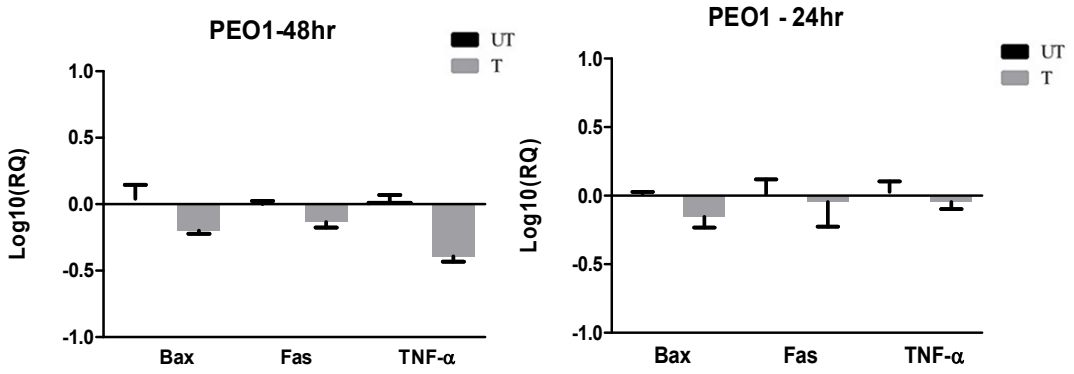

Figure 5.6 *– Gene expression results from RT-qPCR performed on PEO1 cells; analysing the effects of SP-D on Bax, Fas and TNF-α gene expression at 24-hours (left) and 48-hours (right). At both time points, all three genes are downregulated, albeit non-significantly. Bars in black represent values from untreated (UT) samples and grey bars represent values from SP-D treated (T) samples. No significance was noted in comparison to controls.*

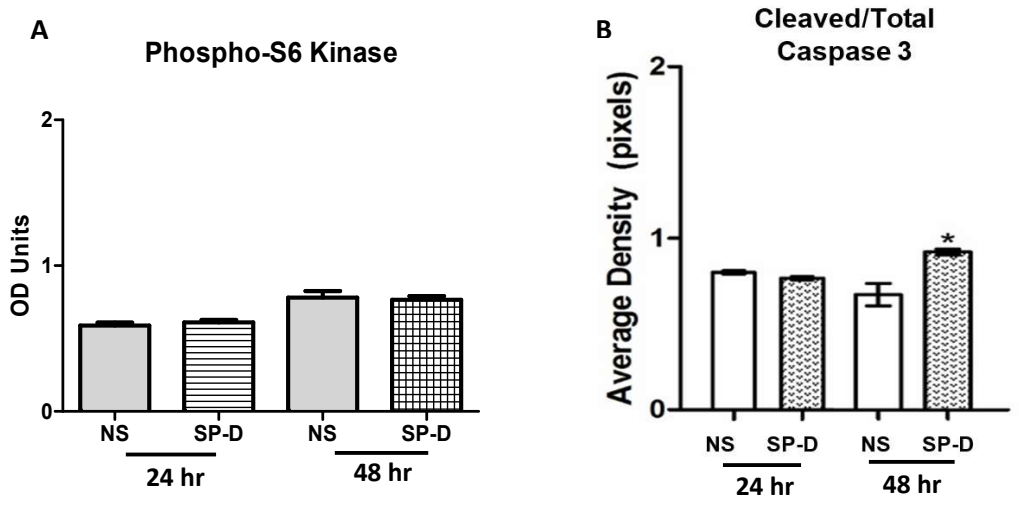

Figure 5.7 – *(A) phospho-S6-kinase (PS6K) and (B) cleaved/total caspase-3 levels measured in SKOV3 untreated and treated cells after treatment with 20µg/ml of rfhSP-D for 24 and 48 hours. There was no significant change in PS6K levels in treated samples compared to controls. However, cleaved/total caspase 3 levels increase in treated SKOV3 cells after 48 hours. (*P <0.005) (Kumar et al., 2019) .*

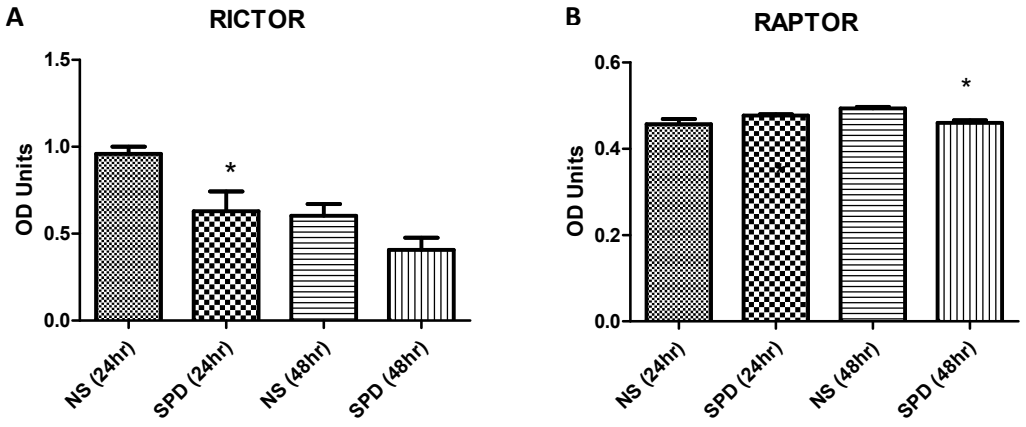

Figure 5.8 – *RICTOR (A) and RAPTOR (B) levels measured in SKOV3 untreated and treated cells after treatment with 20µg/ml of rfhSP-D for 24 and 48 hours. RICTOR expression is downregulated in rfhSP-D treated SKOV3 cells after 24 hours, whereas RAPTOR levels lower in treated cells after 48 hours. ±SEM; significance calculated using unpaired student's t test with Welch's correction (*P <0.005) (Kumar et al., 2019).*

Finally, mTOR components' (RICTOR and RAPTOR) protein expression was analysed to examine whether or not SP-D expression affected pathways established within OC to promote cell proliferation, using SKOV3 cells. Western blot analyses showed that RICTOR expression was

significantly lower in rfhSP-D treated cells compared to untreated cells after 24-hours, whereas RAPTOR expression was negatively affected in treated cells after 48-hours. This not only highlights the capability of SP-D to induce apoptosis through Fas and caspase 3 expression, but also its potential involvement in negatively affecting signalling pathways that promote cancer growth. Interestingly, CCs (cancer-related circulating cells) also express RAPTOR and RICTOR, the two key components of mTORC1 and mTORC2 complexes, respectively.

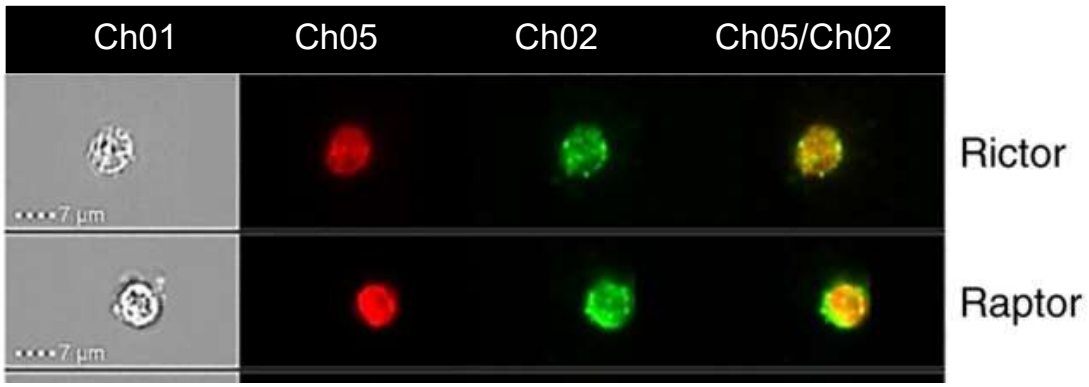

Figure 5.9 – *CD45 negative circulating tumour-related cells (CCs) with positive RICTOR and RAPTOR expression. Images were taken using ImageStream™ imaging flow cytometer. Ch01 shows brightfield image, Ch05 shows DRAQ5 stained-nuclear image, Ch02 shows Rictor and Raptor staining and Ch05/Ch02 shows a composite image of the fluorescent signals captured within the two channels (Rogers-Broadway et al., 2019).*

5.3.2 Exploring the role of SP-D as a biomarker for OC using clinical samples

As mentioned, although SP-D is an innate molecule known to interact with pathogens and has also been implicated in the clearance of apoptotic and necrotic cells, its role in cancer is poorly understood. *In silico* analyses have shown that SP-D expression in OC is indicative of unfavourable prognosis (Mangogna et al., 2018). Therefore, there is a potential that SP-D could serve as a biomarker for OC. In order to investigate this, SP-D expression was examined in tissue as well as liquid biopsies.

Cellular distribution and protein expression of SP-D was analysed at different stages and grades of OC and compared between various sub-types using immunohistochemistry. Three areas of each tissue sample were selected, and cells positively stained for SP-D were counted in each area, calculating a final average percentage of positively stained cells. All images were taken using a Leica DMi1 inverted microscope (40x magnification).

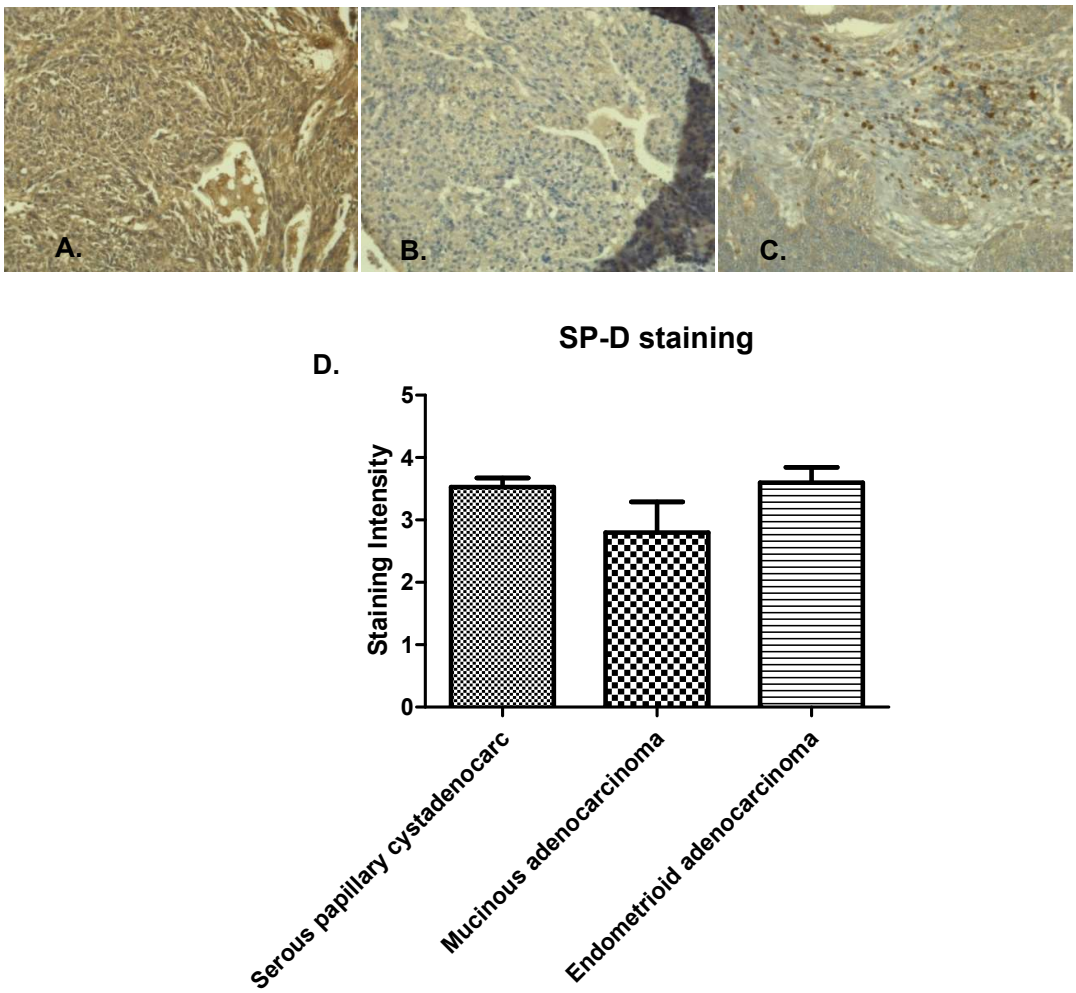

Figure 5.10 - *Immunohistochemistry for SP-D expression in different pathologies of ovarian tissue array clinical samples (40x magnification). The figure shows representative images of serous papillary cystadenocarcinoma (**A.**, location on the slide: D7), mucinous adenocarcinoma (**B.**, location on the slide: F1) and endometrioid adenocarcinoma (**C.**, location on the slide: F9). ANOVA test was used to assess significance. Error bars depict standard error. No significant change was seen between different types of OC (p=0.2235).*

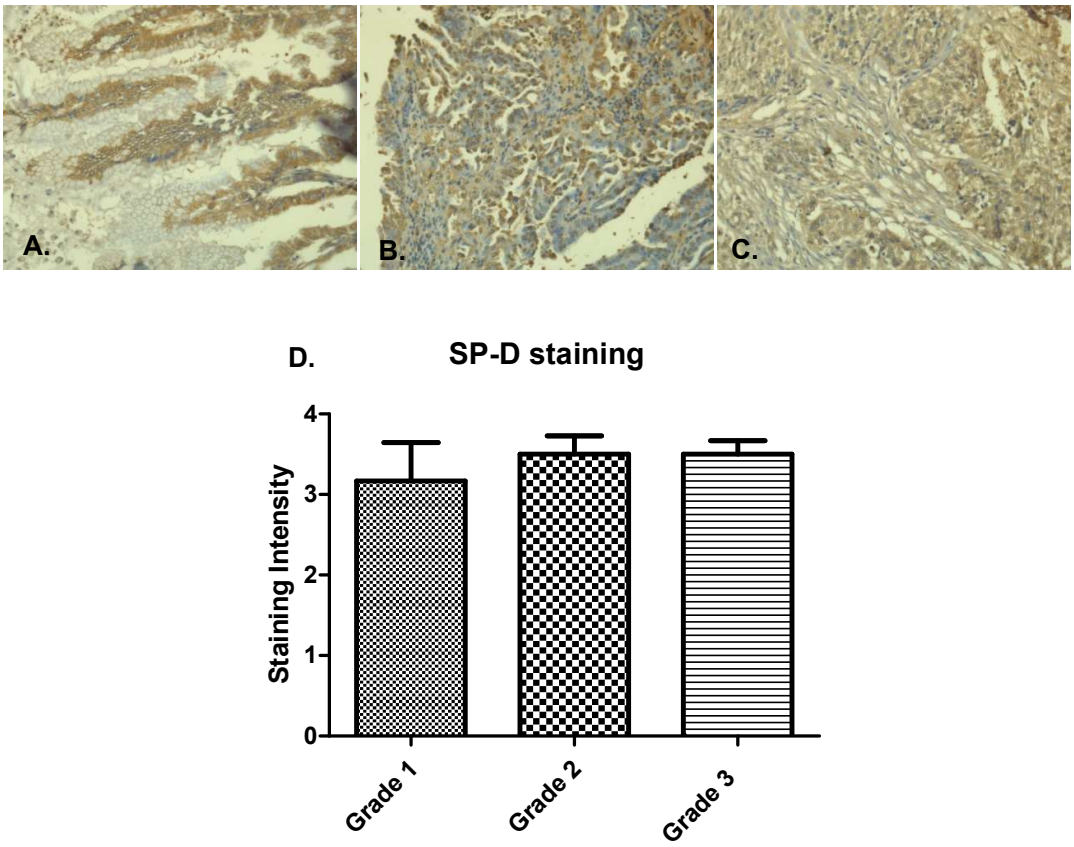

Figure 5.11 - *Immunohistochemistry for SP-D expression in different grades of ovarian tissue array clinical samples (40x magnification) depicting representative images of mucinous cystadenocarcinoma grade 1 (**A.**, location on the slide: E10), serous papillary cystadenocarcinoma grade 2 (**B.**, location on the slide: A3) and serous papillary cystadenocarcinoma grade 3 (**C.**, location on the slide: B3). Significance was measured using ANOVA test. Error bars depict standard error. No significant change was seen between different grades of disease (p=0.7055).*

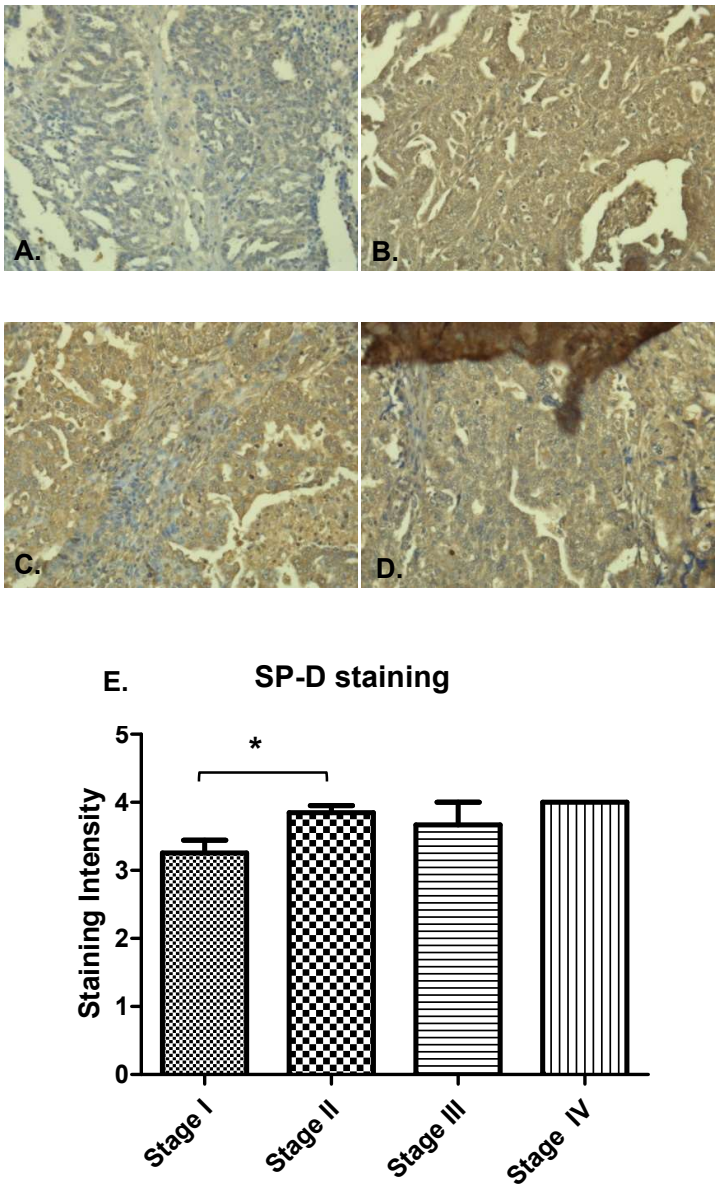

Figure 5.12 *- Immunohistochemistry for SP-D expression in different stages of ovarian tissue array clinical samples (40x magnification). The figure shows representative images of serous papillary cystadenocarcinoma stage I (A., location on the slide: C2), serous papillary cystadenocarcinoma stage II (B., location on the slide: C7), serous papillary cystadenocarcinoma stage III (C., location on the slide: A8) and serous papillary cystadenocarcinoma stage IV (D., location on the slide: C3). Student's t-tests were used to assess significance. Error bars depict standard error. A nearly significant up-regulation of SP-D was observed in stage II OC compared to stage I OC (*p=0.05).*

Immunohistochemical analyses of OC tissue samples showed high SP-D expression when considering sub-classifications and/or grading. However, SP-D staining was much stronger in serous papillary cystadenocarcinoma and endometroid adenocarcinoma compared to mucinous

carcinoma, despite the non-significance in staining intensity between various sub-groups. It is worth noting that during the SP-D expression analyses based on stage, the difference in expression levels between stage I and stage II was significant (p=0.05). Stage II samples showed stronger staining compared to stage I, however, the differences between stages II, III and IV were negligible.

To determine whether SP-D holds any potential as a biomarker within liquid biopsies, an ELISA assay was performed to detect SP-D in plasma samples collected from patients undergoing treatment for advanced stage OC. Plasma samples collected and stored from patients enrolled on the CICATRix trial was used in this ELISA assay. Plasma samples were collected from four patients at various stages of their chemotherapy treatment and the ELISA assay was performed to analyse if there were any changes in SP-D concentrations in response to treatment.

Firstly, SP-D was detected in every patient plasma sample collected during their treatment, indicating that SP-D is secreted and is found to be circulating in OC patients. Next, SP-D concentrations were recorded for three patients, one undergoing neo-adjuvant chemotherapy (NACT), one undergoing primary debulking surgery (PDS) prior to chemotherapy and one patient receiving a second course of treatment after experiencing relapse. Interestingly, the concentration of SP-D in plasma was much lower in the Relapse patient compared to PDS and NACT. A one-way ANOVA test conducted gave a highly significant result with a p value of 0.007 (see figure 5.13).

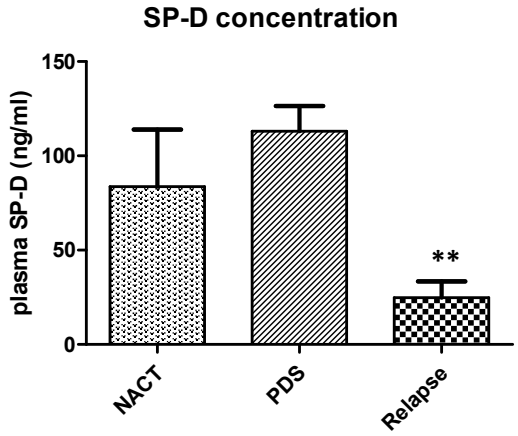

Figure 5.13 *- SP-D concentrations recorded across different cycles during chemotherapy treatment of 3 patients; one undergoing neoadjuvant chemotherapy (NACT) after diagnosis, one underwent primary debulking surgery (PDS) prior to chemotherapy and one relapse patient (n = 3). One-way analysis of variance (ANOVA) analysis show that SP-D plasma levels is significantly lower in Relapse patient compared to NACT and PDS (P value = 0.0072).*

Due to limitations relating to time and samples available to run per plate, there were only a handful of patients whose SP-D levels could be recorded and used for further analysis. Extensive studies including more patients are necessary in order to establish a more robust correlation between CTCs and SP-D concentration in liquid biopsies. However, the variation observed between patients receiving first-line chemotherapy vs relapse patients clearly shows that SP-D levels are high initially and there is a possibility that they could be affected by a successful treatment. A possibility lies in investigating whether high SP-D levels throughout treatment could be an indicator of an unsuccessful treatment or not.

Furthermore, an additional experiment was conducted to investigate whether cells extracted from OC patient blood samples expressed SP-D or not. A small population of CD45 negative CTCs showed a positive staining for SP-D with a predominantly cytoplasmic staining, which was also seen during the immunohistochemical analyses of ovarian cancer tissue samples discussed earlier.

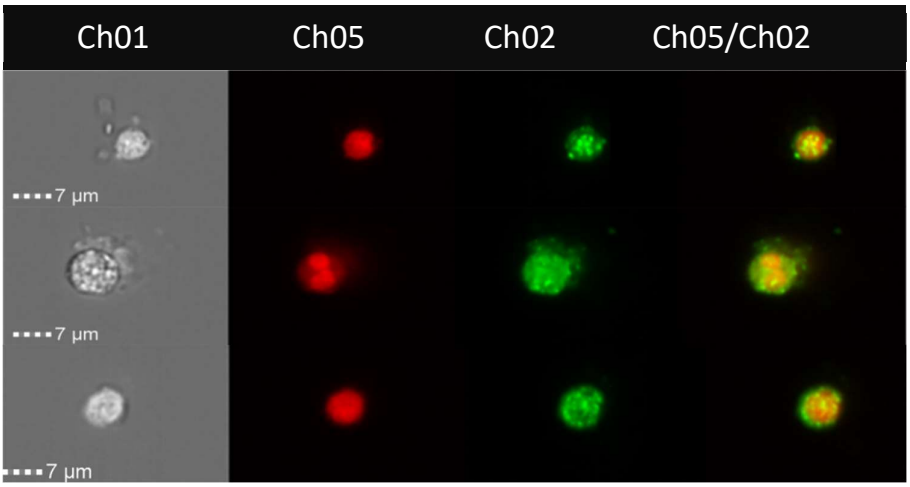

Figure 5.14 *– ImageStream analysis showing SP-D expression in CCs from 3 ovarian cancer patients visualised at 40x magnification. Channel 1 shows images in brightfield, channel 2 shows cells stained with DRAQ5 (red), channel 3 shows SPD expression using an Alexa Fluor AF488 secondary antibody and channel 4 shows a merged image taken from channels 5 and 2. SP-D shows a strong cytoplasmic expression (Kumar et al., 2019).*

Collectively, the detection of SP-D in OC tissue samples, patient plasma samples and in potentially in CTCs builds a foundation for further research to be conducted in order to test its potential as a possible biomarker.

5.3.3 *In silico* analyses of SP-D expression in OC

To compare immunohistochemistry-based SP-D expression data generated within this chapter with other studies, datasets were accessed using Oncomine™, to compare SP-D expression profiles between (i) controls and OC samples and (ii) across the main sub-types of OC.

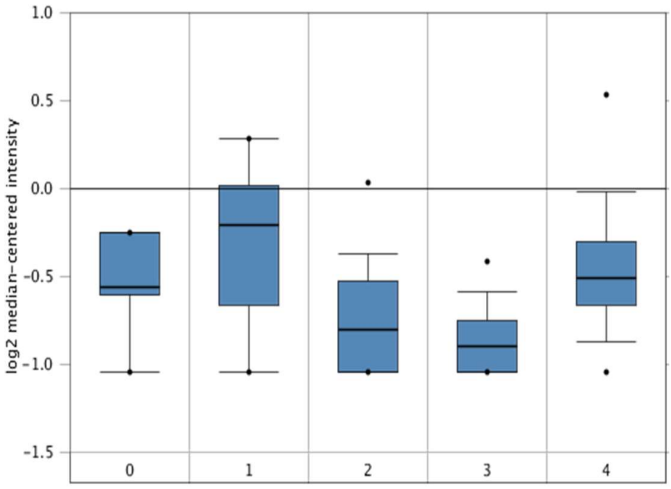

Figure 5.15 - *SP-D gene expression from the Hendrix et al. dataset plotted by Oncomine™. The figure shows the mean SP-D gene expression in control normal ovaries (0, n=4), ovarian clear cell adenocarcinoma (1, n=8), ovarian endometrioid adenocarcinoma (2, n=37), ovarian mucinous adenocarcinoma (3, n=13) and ovarian serous adenocarcinoma (4, n=41). Boxes represent the 25th-75th percentile (with median line), bars show the 10th-90th percentile and dots show the complete spread of data. Fold change in SP-D expression was 1: 1.217 (p=0.123), 2: -1.109 (p=0.782), 3: -1.201 (p=0.897) and 4: 1.086 (p=0.266) when compared to normal respectively (ONCOMINE, 2020; Hendrix et al., 2006).*

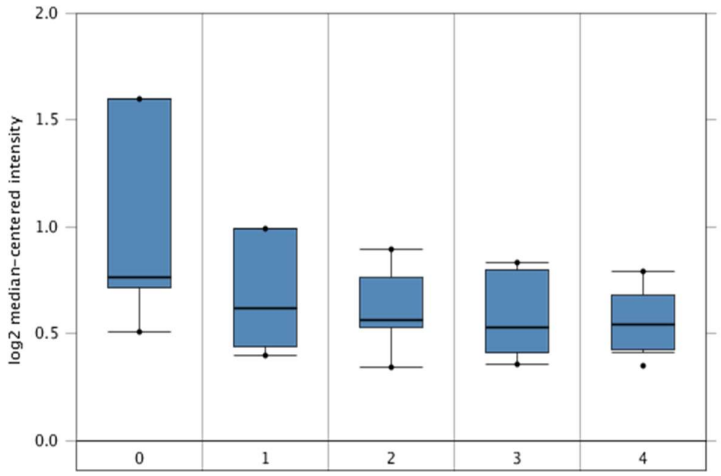

Figure 5.16 *- SP-D gene expression from the Lu et al. dataset plotted by Oncomine™. The figure shows the mean SP-D gene expression in control normal ovaries (0, n=5), ovarian clear cell adenocarcinoma (1, n=7), ovarian endometrioid adenocarcinoma (2, n=9), ovarian mucinous adenocarcinoma (3, n=9) and ovarian serous adenocarcinoma (4, n=20). Boxes represent the 25th-75th percentile (with median line), bars show the 10th-90th percentile and dots show the complete spread of data. Fold change in SP-D expression was 1: -1.179*

(p=0.855), 2: -1.214 (p=0.893), 3: -1.255 (p=0.922) and 4: -1.257 (p=0.924) when compared to normal respectively (ONCOMINE, 2020; Lu et al., 2004).

The datasets accessed using Oncomine corroborates with the data acquired from the immunohistochemistry experiment, showing that there are no significant changes in SP-D gene expression based on OC sub-types. SP-D expression levels between normal peritoneum and serous OC samples show an elevated expression in cancer samples compared to controls.

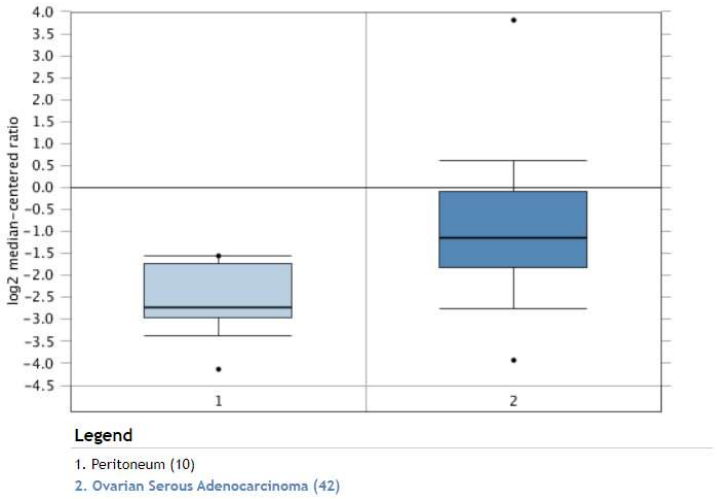

Figure 5.17 *- SP-D gene expression from the Yoshihara et al. dataset plotted by Oncomine™. The figure shows the mean SP-D gene expression in control normal ovaries (0, n=10) and ovarian serous adenocarcinoma (2, n=42). Boxes represent the 25th-75th percentile (with median line), bars show the 10th-90th percentile and dots show the complete spread of data. Fold change in SP-D expression was: 3.059 (p=0.003***) when compared to normal respectively (ONCOMINE, 2020; Yoshihara et al., 2009).*

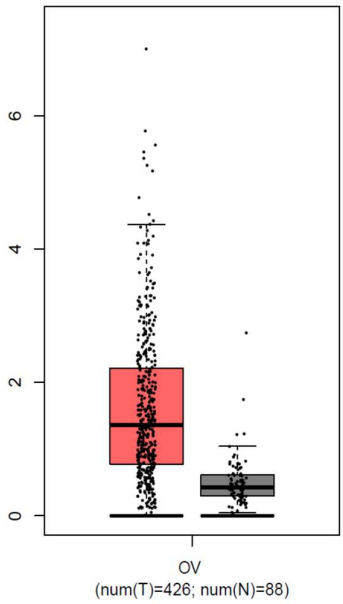

Figure 5.18 *– Box plot graph showing SP-D transcript expression in OC samples (red; n=426) and control samples (grey; n=88). This dataset was accessed using CBioPortal* (Gao et al., 2013).

SP-D transcript expression was elevated in tumour samples compared to normal samples. Furthermore, SP-D expression was also explored within the TGCA dataset based on cancer stage and tumour grade (figure 5.19). Based on cancer staging, there is an upregulation of SP-D expression between stage I and stage II OC samples which corroborates with the tissue histology discussed earlier. Based on cancer grade, higher grades of OC show higher expression of SP-D with the highest seen in grade 4 OC, however the dataset only factors SP-D transcription datum from one sample. The histology microarray did not contain grade 4 samples, so further experiments should aim to compare SP-D transcription in grade 4 samples compared to lower grades.

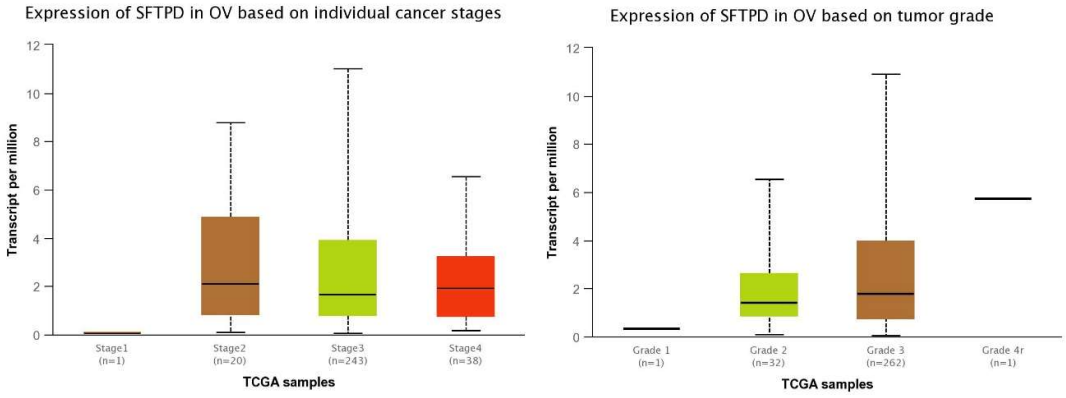

Figure 5.19 *- SP-D transcript expression in OC tissue samples based on individual cancer stages (left) and tumour grade (right) from samples recorded in the TGCA dataset Accessed from CBioPortal* (Cerami et al., 2012).

Kaplan-Meier plots were used to investigate the effects of SP-D expression on overall survival (OS) and progression-free survival (PFS) in OC patients. KM plots for OS show a negative relationship between SP-D expression and prognosis in OC patients.

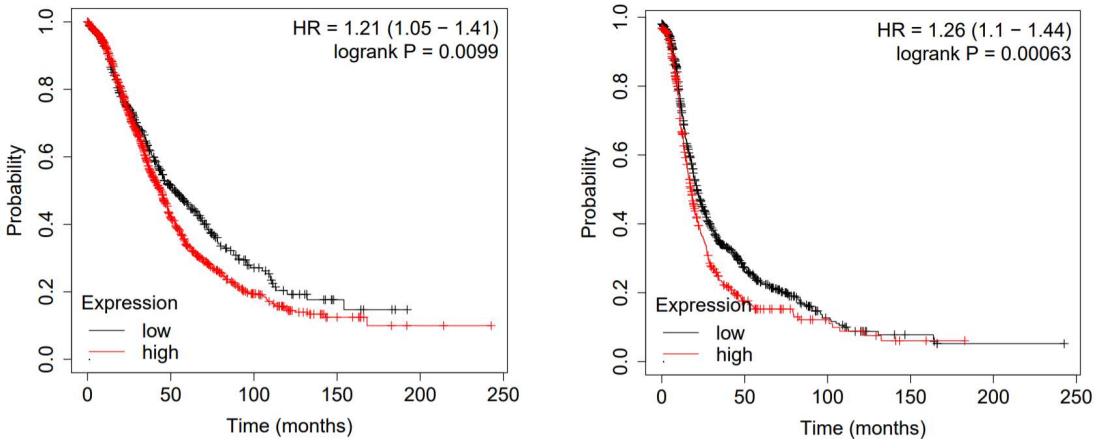

Figure 5.20 *– KM plot for OS (left) and PFS (right) in OC patients based on SP-D expression. N=1657 and 1463, respectively. Plot points in red represent cohort of patients with high SP-D expression and in black show cohort with low SP-D expression. Median survival for OS and PFS is lower in the high expression cohort compared to the low expression cohort. Median survival (in months) for OS (high exp. vs low exp.) 44.03/52.63. Median survival (in months) for PFS is 12.13/17.5.*

5.4 Discussion

SP-D is a potent immune molecule and is considered to be a modulator of inflammatory response (Kaur et al., 2018b). Recent studies suggest it may play a promising role as an immune surveillance molecule in cancer. Although the exact role of SP-D in cancer is still being investigated, evidence suggests that mRNA and protein expression levels may hold some prognostic value. In the case of OC, SP-D expression was shown to be higher in OC samples compared to healthy controls using PCR and immunohistochemistry (IHC) techniques, associating high expression with unfavourable prognostic outcomes (Mangogna et al., 2018). Based on this information, the current study was aimed at investigating the possibility of SP-D as a functional biomarker for OC, focusing on both tissue and liquid biopsies.

Immunohistochemical analyses included samples ranging from stages, grades, and subtypes of OC in order to provide a complete picture. Results concluded that SP-D protein expression is high in OC tissue samples irrespective of type and grade, with a significant increase in expression at stage II when compared to stage I. These conclusions not only corroborate expression data acquired from Oncomine but are also concurrent with another study that used IHC to compare expression levels between four control samples and four OC samples (Mangogna et al., 2018). Liquid biopsies were exclusively included in this study due to their minimally invasive nature to detect cancer without the delay, cost, and risk associated with tissue biopsies (Tanos and Thierry, 2018). This analysis was purely exploratory and included blood samples (for detection of CCs) and plasma samples (for detection of SP-D protein). The ELISA assay was crucial for two main reasons; 1. it validated the assumption that OC cells did not secrete any SP-D *in vitro* and 2. SP-D protein is present in detectable amounts in patient plasma samples, which was previously unknown. This conclusion opens the doors to further test the validity of SP-D as a biomarker, possibly in a diagnostic or a prognostic setting. The scope of this study was limited (in both time and resources), since plasma samples collected throughout multiple treatment cycles belonged to a small group of patients (n=3), however, provides the basis to proceed towards larger, more conclusive studies in the future. The identification of SP-D+/CD45- cells in patient blood samples is further builds a case to explore the potential of SP-D as a biomarker for OC, and its wider role in potential metastatic events

Previous studies have shown that a recombinant fragment of human SP-D (rfhSP-D) can induce apoptosis, either through a Fas-mediated pathway (shown in pancreatic cancer cell lines) or in activated eosinophilic and T-cells via p53 pathway (Kaur et al., 2018a; Mahajan et al., 2014). The *in vitro* experiments in this study examined the effects of rfhSP-D on ovarian cancer cell lines SKOV3 and PEO1 to determine its capability as a therapeutic target. In the case of SKOV3 cells,

exposure to rfhSP-D lead to cell death through upregulation of Fas. In the Fas/FasL pathway, association of Fas with FasL (Fas Ligand) can activate the Fas-associated death domain (FADD) and make mitochondrion release cytochrome C, eventually initiating the key caspase-3 in catalysing the specific cleavage of important cellular protein required during apoptosis (Zheng et al., 2003). Results obtained from wound healing assays, Annexin-V staining and trypan blue assay show a cytotoxic effect of SP-D on SKOV3 cells. For further confirmation, qPCR and Western blot analysis was utilised, the results from which show caspase-3 expression in treated SKOV3 cells, with a significant upregulation noted after 48-hours.

While SKOV3 cells have a response similar to other *in vitro* models published in current literature, PEO1 cells do not mirror this effect. In chapter 3, it has been shown that PEO1 and SKOV3 exhibit a slight phenotypic difference, i.e., PEO1 cells are epithelial whereas SKOV3 cells show an intermediate mesenchymal phenotype. RfhSP-D has shown to suppress EMT transition in pancreatic cell lines by downregulating TGF-β (Kaur et al., 2018b) which raises the possibility that rfhSP-D may only be able to induce apoptosis in cells with an active EMT dynamic, thereby being ineffective in cells with a strong epithelial phenotype. Another notable difference between the two cell lines is that PEO1 cells carry a BRCA2 mutation in addition to a TP53 mutation. BRCA2 is a mediator of homologous recombination and interacts with proteins (including TP53, BRCA1, RAD51) associated with the cell cycle and DNA damage response pathways. The absence of an effective repair mechanism allows DNA damage to occur at many sites, including genes required for cell cycle checkpoint expression. In humans, the tumours that develop in patients with germline heterozygous mutations involving BRCA2 are defective in HR-mediated repair (Roy *et al*, 2012). DNA damage, especially a double strand break, activates the NF-κB dependent repair pathway, which would usually target BRCA2 to induce homologous recombination. (Volcic et al., 2012). rfhSP-D treatments have shown to increase NF-kB expression causing growth arrest in pancreatic cell lines (Kaur et al., 2018a). However, PEO1 cells may evade this because of the BRCA mutation, resulting in a downregulation of apoptosis. So, there is a possibility that BRCA-associated mutations may hinder rfhSP-D induced apoptosis, which affects its therapeutic potential. Further experiments to validate these hypotheses would include similar experiments on PEO4 cell lines, which carry a silent BRCA2 mutation.

Chapter 6

Investigating the functional role of Wilms' Tumour Protein 1 in OC

6.1 Introduction

The mammalian Wilms' tumour protein 1 (WT1) gene is located on the short arm of chromosome 11 (11p13) and spans ~50 kb (Hastie, 2017). WT1 contains four C-terminal zinc-finger motifs and an N-terminal DNA binding domain which allows it to function as a transcription factor (Maki et al., 2017). The N-terminal domain comprises of proline-glutamine rich sequences and is involved in RNA and protein interactions, critical for transcriptional regulatory function.

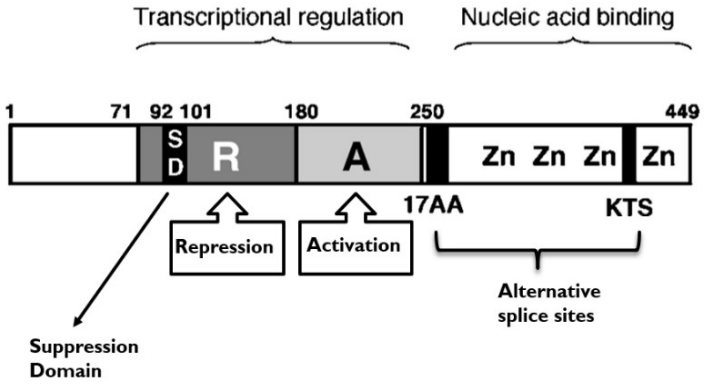

Figure 6.1 *- WT1 gene structure; highlighting the various regions in the N-terminus showing locations of the repression, activation, and suppression domain in the gene. The zinc fingers are located in in the C-terminus of the gene. The two common alternative splice variation sites (17AA and KTS) are also highlighted in the nucleic-acid binding region of the gene; figure adapted from (Hartkamp et al., 2010).*

The C-terminal domain contains four Krüpple-like C2H2 zinc fingers, which permit binding to target DNA sequences but are also involved in RNA and protein interactions (Yang et al., 2007). There are at least 36 potential isoforms, the diversity created through a combination of alternative transcription sites, translation start sites, splicing and RNA editing (Hastie, 2017). However, there are two predominant alternative splicing events; these include splicing of exon 5 (17 amino acids or 17AA) and of three amino acids (lysine, threonine and serine or KTS) in the 3' end of exon 9 (shown in figure 6.2) (Yang et al., 2007).

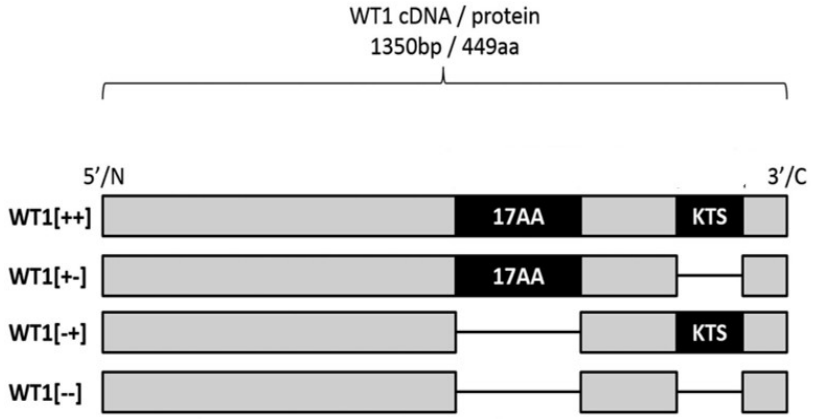

Figure 6.2 *- WT1 splice variants; based on the presence or absence of 17AA region corresponding to the entire sequence of exon 5 and the KTS region corresponding to nine base pairs of the C-terminus in exon 9. WT1(++) indicates the wild-type, full length protein; WT1(+ -) indicates WT1 gene without the KTS region on the 3' end; WT1 (- +) shows the gene without the 17AA region and WT1 (- -) corresponds to the WT1 gene with both 17AA and KTS deletions* (Maki et al., 2017).

WT1 was first identified in 1990 as a strong candidate predisposition gene for Wilms' tumour, a form of paediatric kidney cancer that affects 1 in 10,000 children (Charlton and Pritchard-Jones, 2016). Although, subsequent research over the years indicates that WT1 may play a role in other cancer-related malignancies. High WT1 expression is found in a variety of tumours including breast, ovarian, mesothelioma, renal cell cancer and leukaemia (Yang et al., 2007; Qi et al., 2015). Immunohistochemical analysis of ovarian cancer tissue samples report a high frequency of WT1 expression, specifically in serous OC samples (Hylander et al., 2006). WT1 staining also proved to be valuable in differentiating serous OC from serous uterine cancers, showing a 97% positive staining of WT1 in serous OC samples compared to no positive staining in serous uterine cancer samples (Al-Hussaini et al., 2004). Therefore, WT1 is additionally utilised as a diagnostic marker for serous ovarian cancer detection. Furthermore, high WT1 mRNA expression was found in patients diagnosed with advanced stage of OC and was positively correlated with more aggressive clinical features such as lymph node and omentum metastasis (Liu et al., 2014). Despite the amount of evidence supporting the involvement of WT1 as an oncogene, there is a gap in the current literature regarding its' exact function. Immunohistochemically, WT1 is generally detected within the nucleus and any cytoplasmic staining would be regarded as non-specific (Nakatsuka et al., 2006). However, emerging evidence shows that WT1 can shuttle to the cytoplasm, and by doing so can be involved in RNA metabolism and translational regulation (Nakatsuka et al., 2006; Niksic et al., 2004). This chapter explores this phenomenon of WT1 protein movemement *in vivo* and *in vitro* and utilises expression and mutational analyses using bioinformatics to explore beyond the role of WT1 as a diagnostic marker to a more functional role it could play within ovarian cancer.

6.2 Aims

1. Using WT1-positive CCs to study protein distribution and determine whether WT1 movement occurs in cells under treatment conditions.
2. Investigate whether chemoterapeutic treatments (i.e., Paclitaxel and Cisplatin) can alter WT1 localisation *in vitro.*
3. Use *in silico* analyses to provide a more in-depth picture of the role of WT1 in cancer including expression, methylation and mutation data.

6.3 Results

6.3.1 WT1 localisation *in vivo* and *in vitro* after treatment of OC with common chemotherapeutic agents

Although initial proof of principle experiments (conducted *in vitro*) confirmed the presence of WT1 in the nucleus, a number of cancer-related circulating cells (CCs) detected in blood samples collected from patients undergoing chemotherapy showed additional cytoplasmic expression of WT1, especially during early cycles of treatment. Blood samples were acquired prior to beginning treatment, during treatment (after every treatment cycle) and after completion of chemotherapy, from 14 patients undergoing treatment for advanced epithelial ovarian cancer (aEOC) and enrolled on the CICATRix trial. Patients enrolled on this trial were prescribed to treatment with either a platinum-based drug (Carboplatin) or a combination of Carboplatin with Paclitaxel.

To analyse protein localisation in CCs (either within the nucleus or cytoplasm), positively stained cells were grouped and analysed using the 'nuclear localisation' wizard on IDEAS data analysis software developed for ImageStream (Amnis). The wizard uses nuclear staining to create a mask, specifically covering the nuclear image. The fluorescent signal from the translocating protein of interest is detected and the area covered by that signal is marked by the wizard. If the protein expression is detected within the area of the nuclear mask (i.e., if the protein is expressed within the nucleus), the images are said to be 'similar', and a score > 0 is allocated. If the translocating protein is not found within the nucleus, then a score < 0 is given to the image.

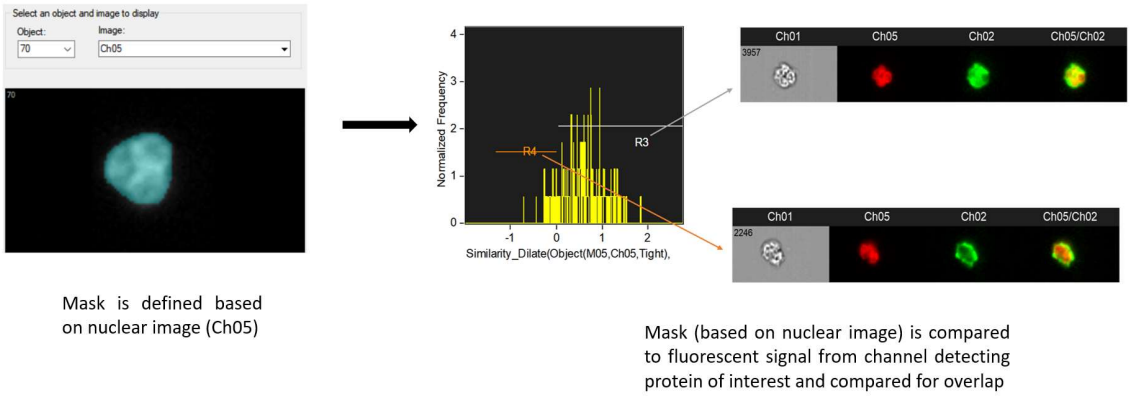

Figure 6.3 *– The ImageStream translocation wizard used to detect fluorescent signals from a protein of interest within the nucleus. Within the wizard, a mask is created, covering the nuclear image and this mask is then compared to signals detected from the protein of interest. If the protein is detected within the nucleus, the fluorescent signals would be detected within the boundaries of the mask and a score > 0 will be allocated to the image. If the protein is outside the nucleus, the fluorescent signals would be detected outside the boundaries of the mask and a score < 0 will be given. Based on this analysis, the number of cells with and/or without the protein present in the nucleus can be measured to detect translocation.*

Results from figure 6.4 (A) show that the number of WT1 positive cells with cytoplasmic expression is higher at the beginning of treatment and goes lower with subsequent treatment cycles. At EOT, cytoplasmic expression of WT1 in cells is significantly lower compared to cells identified after treatment cycle 1.

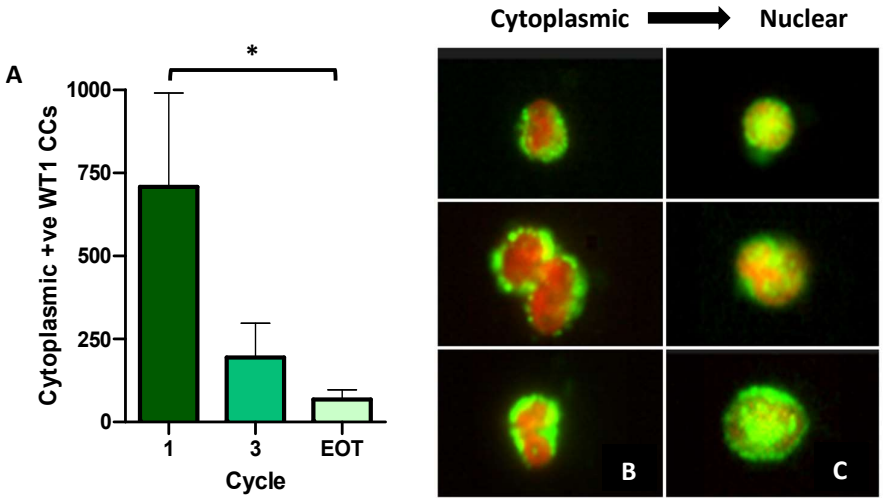

Figure 6.4 *– Analysis of aEOC blood samples showing CCs with cytoplasmic WT1 expression. (A) Bar graph depicting cytoplasmic positive WT1 CCs recorded in patients (n=14) undergoing treatment for EOC at cycle 1 (beginning), cycle 3 (mid-treatment) and EOT (end of treatment). The number of WT1 positive CCs showing cytoplasmic expression was significantly higher compared to EOT (p=0.042). Error bars represent standard*

*deviation and asterisks denote significance (*p<0.05). Panels in (B) and (C) show pictures of WT1 positive CCs from 3 patients after treatment cycle 1 and at EOT, respectively.*

Results from this experiment indicate that CCs depict potential changes in the localisation of WT1 throughout treatment. The frequency of cells with cytoplasmic WT1 is high during early stages of treatment in comparison to EOT, which suggests that this movement potentially occurs as a response to treatment.

SKOV3 cells were used as an in vitro model to determine whether the movement of WT1 is affected by exposure to chemotherapeutic agents. SKOV3 cells were seeded in 6-well plates at a density of 3 x 10^5 cells per well. Two different concentrations of Paclitaxel and Cisplatin were selected to examine WT1 protein localisation within SKOV3 cells. Based on the standard treatment concentrations of Paclitaxel and Cisplatin given to OC patients, the concentrations in circulation stay between 50-100 nM (for Paclitaxel) and 7-10 µM (for Cisplatin) (Telleria, 2013). Using these ranges, a higher and lower concentration of each chemotherapeutic agent was diluted appropriately in media and used to treat SKOV3 and PEO1 cells over 24 hours. After 24 hours of exposure to Paclitaxel and Cisplatin at standard incubation conditions (37°C temperature and 5% CO_2), the cells were prepared for immunofluorescence analysis. All images were captured using the DM-4000 microscope by LEICA microsystems and corresponding LAS X software version 3.7.0. 100 cells were picked and counted at random based on the localisation of WT1 and nuclear staining. Futhermore, SKOV3 cells were quantified to determine the proportion of live and apoptotic cell populations under the influence of Paclitaxel, Cisplatin, and their combination.

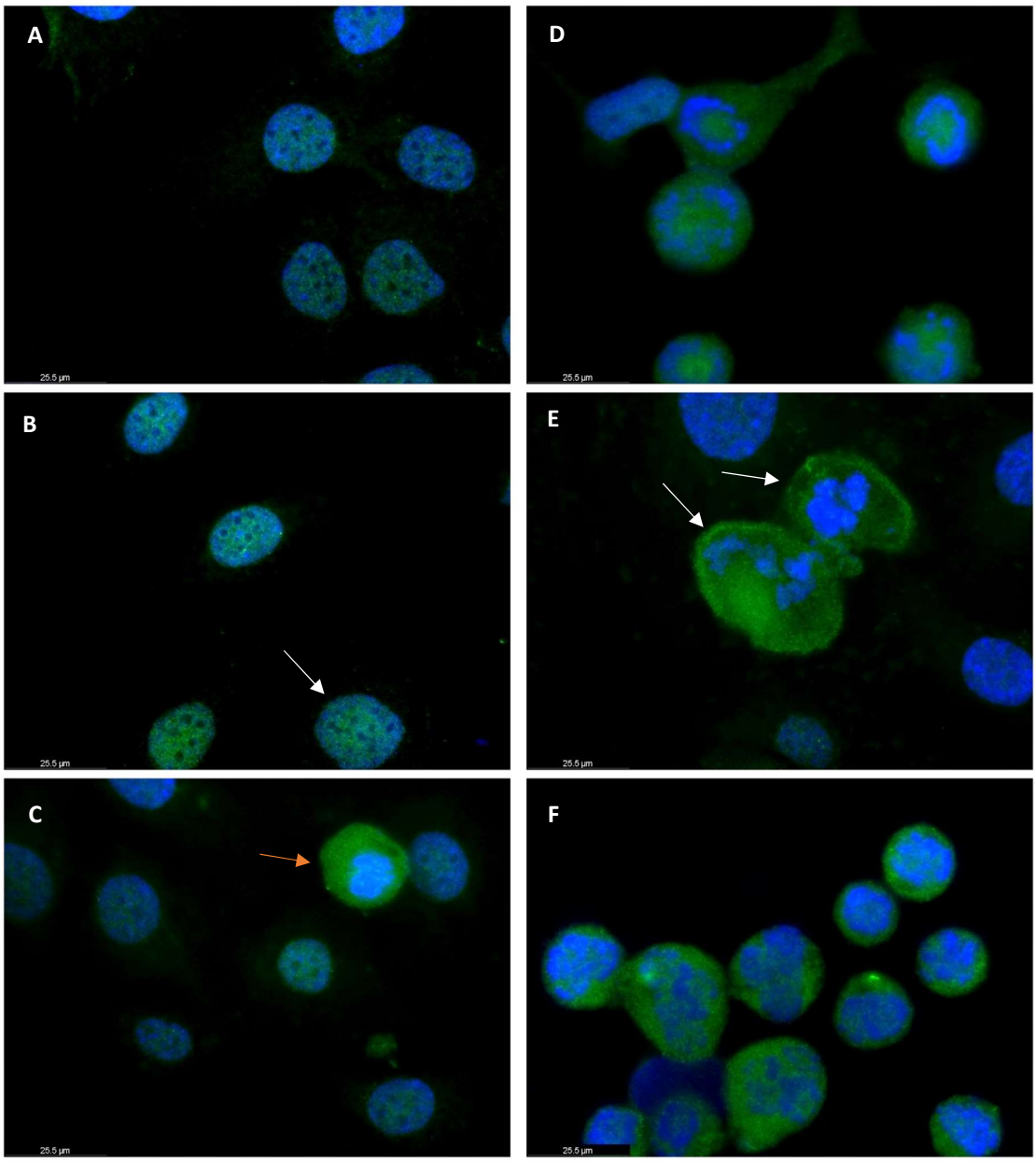

Figure 6.5 – *Fluorescence microscopy to analyse WT1 expression/localisation in SKOV3 and PEO1 cells untreated and treated with Paclitaxel, Cisplatin, and a combination of the two for 24 hours. WT1 protein is depicted in green (AF488) and nuclear image is depicted in blue (DAPI). A, B and C show composite images of untreated cells with WT1 present in the nucleus. An arrow (in orange) shows an untreated cell with strong WT1 in the cytoplasm during cell division. D, E and F show SKOV3 cells treated with Paclitaxel, Cisplatin, and a combination of the two, respectively. Arrows (in white) show cells with a disintegrated nucleus and WT1 detected around the nucleus, as opposed to untreated cells, where the WT1 is predominantly nuclear. All images were captured at 60x magnification.*

Images from figure 6.5 (A,B and C) show that most untreated SKOV3 cells show strong nuclear expression of WT1, however, in one case during cell division, strong cytoplasmic WT1 expression is noted. In figure 6.5 (D,E and F), images are captured after SKOV3 cells are exposed to Paclitaxel (D), Cisplatin (E) and a combination of the two (F). In all three images, the nucleus is showing signs of disintegration leading to apoptosis in response to chemotherapy and WT1 is expressed in the cytoplasm. A large population of cells exposed to Paclitaxel and combination treatments showed signs of apoptosis, however, Cisplatin-treated cells showed very little nuclear disintegration, despite being Cisplatin-sensitive. To confirm the presence of apoptotic cell populations, an Annexin-V/PI assay was used. SKOV3 cells were exposed to the same treatment concentrations for 24 hours and stained with Annexin V and PI, both well-established markers used to detect apoptotic populations in a sample (as explained in chapter 5).

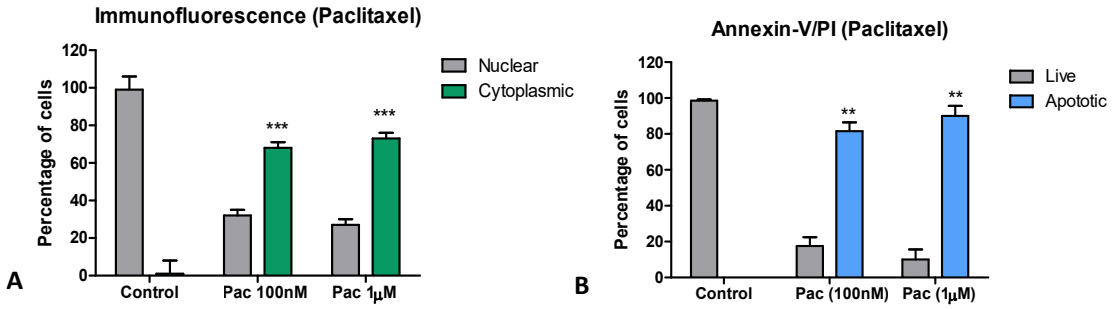

Figure 6.6 - *Immunofluorescence and Annexin-V/PI assay analyses on SKOV3 cells treated with varying concentrations of paclitaxel.* ***(A)*** *– SKOV3 cells untreated and treated with varying concentrations of Paclitaxel (100nM and 1μM, respectively ; ***P<0.0001). Error bars indicate standard deviation and asterisk represent significance, calculated using a two-tailed unpaired Students t-test with Welch's correction for unequal variances. Results show that both concentrations of Paclitaxel showed a similar number of cytoplasmic positive WT1 cells and induced apoptosis in a similar sized population (as confirmed visually through DAPI staining of the nucleus).* ***(B)*** *shows the percentage population of live and apoptotic cells after treatment with 100nm and 1μM Paclitaxel for 24 hours. Compared to the immunofluorescence results, the Annexin-V/PI assay detected a higher population of apoptotic cells at both concentrations, which is significantly higher compared to live cell populations (P= 0.006 and 0.005, respectively). However, the increase in apoptotic cells was not significant between the two concentrations. This corroborates with the pattern noted during the immunofluorescence-based cell count.*

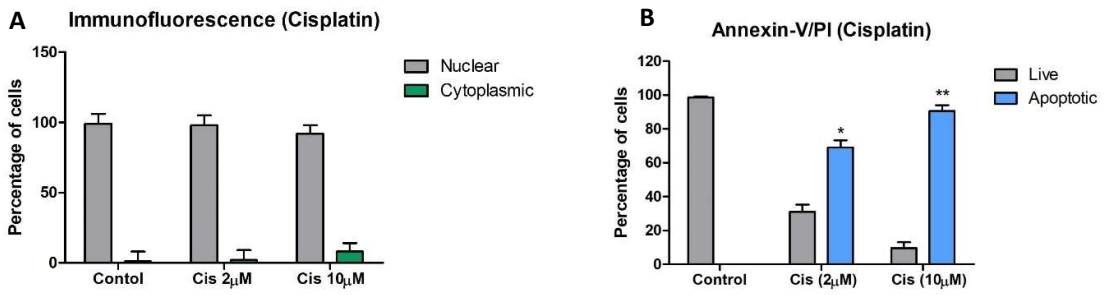

Figure 6.7- *IF and Annexin-V/PI assay analysis on SKOV3 cells treated with varying concentrations of cisplatin.* ***(A)*** *– SKOV3 cells untreated and treated with varying concentrations of Cisplatin (2μM and 10μM, respectively). Error bars indicate standard deviation and asterisk represent significance, calculated using a two-tailed unpaired Students t-test with Welch's correction for unequal variances. Although SKOV3 cells are sensitive to Cisplatin, immunofluorescence-based cell counts revealed that most cells had an intact nucleus with strong nuclear WT1 expression, with very few cells undergoing apoptosis.* ***(B)*** *shows the percentage population of live and apoptotic cells after treatment with 2μM and 10μM Paclitaxel for 24 hours. Compared to the immunofluorescence results, the Annexin-V/PI assay detected a higher population of apoptotic cells at both concentrations, which is significantly higher compared to live cell populations (P= 0.122 and 0.0019, respectively). More cells undergo apoptosis when treated with a higher concentration of Cisplatin, but the increase is not significant.*

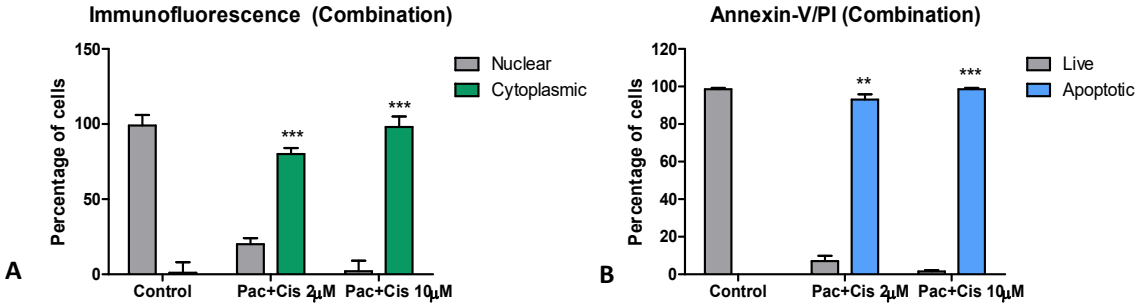

Figure 6.8 - *IF and Annexin-V/PI assay analysis on SKOV3 cells treated with a combination of paclitaxel and cisplatin.* ***(A)*** *– SKOV3 cells untreated and treated with a combination of Paclitaxel (100nM) and varying concentrations of Cisplatin (2μM and 10μM; ***P<0.0001). Error bars indicate standard deviation and asterisk represent significance, calculated using a two-tailed unpaired Students t-test with Welch's correction for unequal variances. Immunofluorescence cell counts showed a large number of cells with cytoplasmic WT1. When combined with a higher concentration of Cisplatin, the combination treatment showed mostly apoptotic cells with a minute number of cells showing no nuclear disintegration.* ***(B)*** *population (%) of live and apoptotic cells after a combination treatment with Paclitaxel and Cisplatin for 24 hours. Compared to the immunofluorescence results, the Annexin-V/PI assay detected a higher population of apoptotic cells at both concentrations, which is significantly higher compared to live cell populations (**P= 0.001 and ***P<0.0001,*

respectively). However, the increase in apoptotic cells was not significant between the two concentrations. This corroborates with the pattern noted during the immunofluorescence-based cell count.

The Annexin-V/PI assay was required to validate the immunofluorescence experiment, due to the low numbers of apoptotic cells visualised after treatment with Cisplatin in a known Cisplatin-sensitive cell line.

6.3.2 Gene expression and mutational analyses of WT1 in OC

A variety of bioinformatics analysis methods were used to gain further insight into the role of WT1, specifically in OC. CBioPortal for cancer genomics is an open-access resource for exploring multi-dimensional genomics datasets. This portal supports and stores non-synonymous mutations, DNA copy number data, mRNA and microRNA expression data, protein level and phosphoprotein level data, DNA methylation data and de-identified clinical data. It also acts as an exploratory tool to access large scale genomic datasets and view genomic alterations across various patients and cancer types (Cerami et al., 2012; Gao et al., 2013).

Firstly, WT1 gene expression data from the TGCA dataset showed elevated levels of WT1 in OC samples when compared to other cancer types.

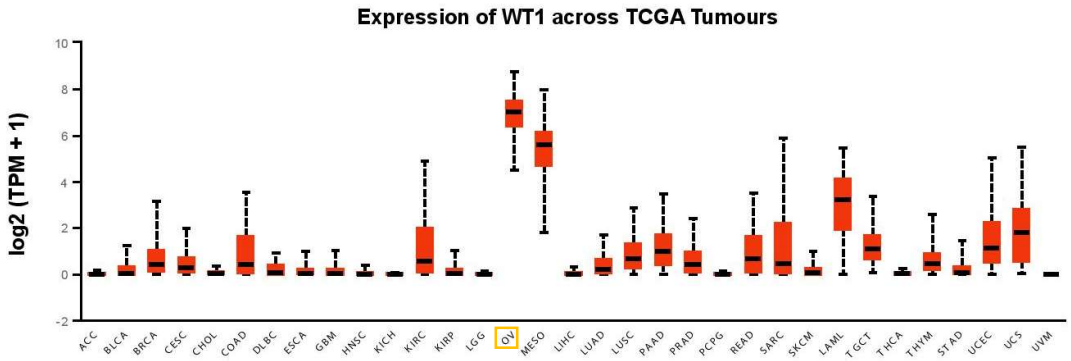

Figure 6.9 – *WT1 gene expression shown across various cancers (OC highlighted in yellow) acquired using CBioPortal. OC samples, in comparison to other cancer types, show a high expression of WT1, which corroborates with lower methylation rates, further explained in figure 6.12 below.*(Cerami et al., 2012).

Genetic alterations in the WT1 gene were recorded in a wide variety of cancers included in the PanCancer dataset using multiple methods to detect mutations in the gene, including RNA sequencing (figure 6.10) and mutation frequency (figure 6.11). These figures show that WT1 gene is more amplified within ovarian cancer when compared to other different types of cancer.

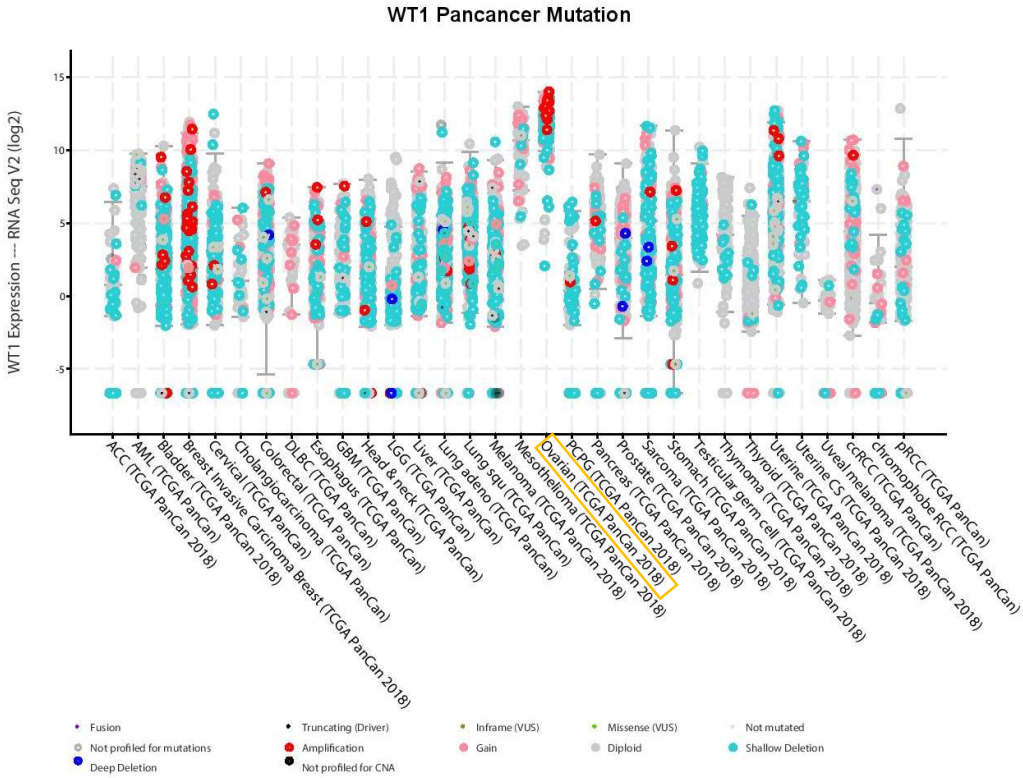

Figure 6.10 – *WT1 expression data recorded using RNA sequencing of different types of cancers including OC (highlighted in yellow). OC samples show higher WT1 amplification in comparison to other cancer samples.*

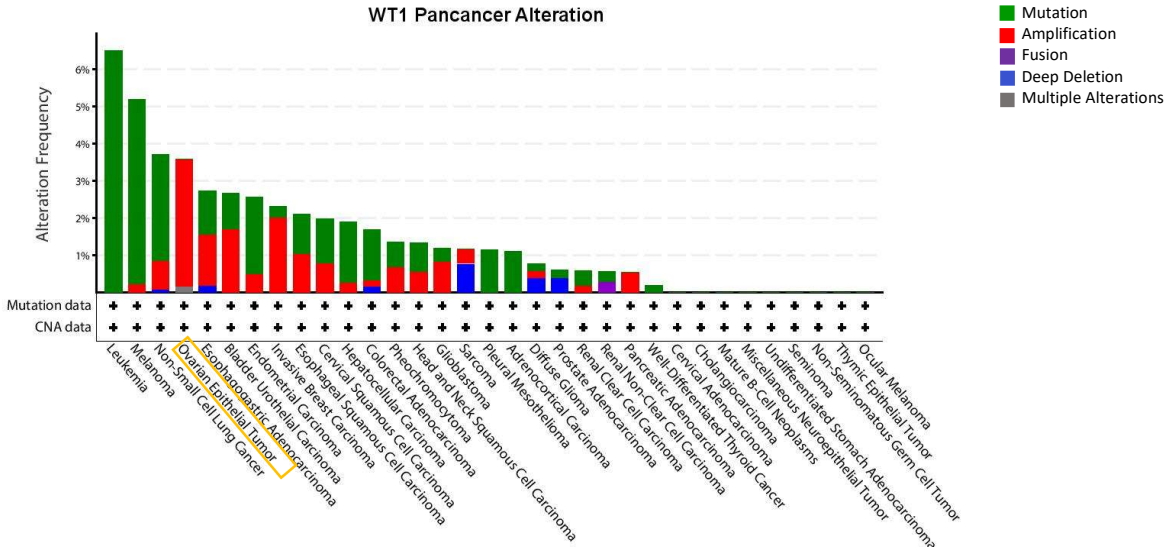

Figure 6.11*- Mutation frequency data recorded in a variety of cancers (including OC – highlighted in yellow). Epithelial OC tumour samples show a high frequency of WT1 amplification compared to other cancer types, with an occurrence of multiple alterations (shown in grey). Data acquired from the PanCancer dataset.*

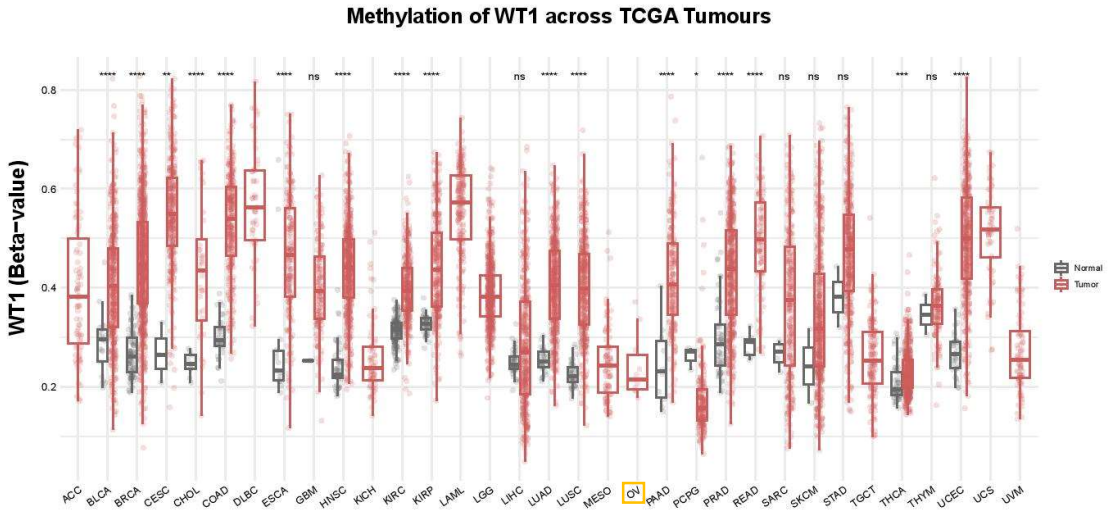

Figure 6.12 - *WT1 gene methylation status displayed across various types of cancers (OC highlighted in yellow), comparing normal and cancer samples (normal shown in grey and tumour samples shown in red). OC samples show a lower methylation of WT1, indicating that gene expression in tumour cells is not repressed as compared to other samples shown in the dataset.*

CBioportal also stored information on the methylation status of WT1 in various types of cancers. DNA methylation is an epigenetic mechanism wherein the transfer of a methyl group onto the C5 position of cytosine to form 5-methylcytosine and the resultant complex inhibits or represses gene expression (Moore et al 2013). This indicates that a high methylation status translates to increased repression of the gene. Methylation datum accessed from the TGCA dataset (shown in figure 6.12) indicate a very low frequency of methylation within OC samples compared to other cancer types. The fact that WT1 is overexpressed in OC, indicates that hypomethylation plays a role in its transcription at the ovarian level. Furthermore, WT1 expression levels (recorded in the TGCA cancer dataset) shows high WT1 expression levels compared to other cancer types, in corroboration with the hypomethylation data described above.

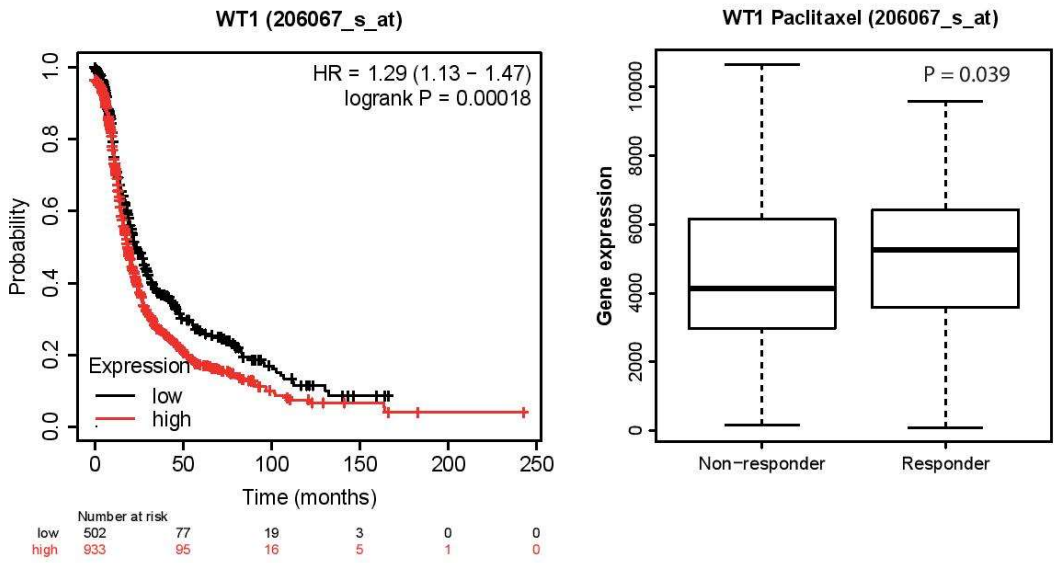

Figure 6.13 *– Effects of WT1 expression on OS and PFS in OC. KM plot (left) showing samples with high WT1 expression (in red) and low WT1 expression (in black). These data shows that high WT1 expression in patients correlates to lower PFS compared to samples showing lower WT1 expression. Furthermore, the boxplot indicating patient response to Paclitaxel treatment (right) show that responders have a higher WT1 gene expression compared to non-responders (*P<0.05). No data was available for Cisplatin.*

Furthermore, regarding the effect of WT1 (206067_s_at) expression in OC patients, KM-plot generated for progression-free survival (PFS) indicate that a higher expression level translates to significantly lower PFS in patients suffering OC. In addition, WT1 gene expression is significantly higher in patients responding to Paclitaxel compared to patients that do not. It could be possible to use WT1 expression data as a means of predicting response to treatment.

6.4 Discussion

This study intended to investigate the possibility of WT1 shuttling in ovarian cancer in accordance with previously published studies in other cellular models. As mentioned, WT1 was initially identified as a tumour suppressor involved in the development of Wilms' tumour, however, it has also exhibited oncogenic properties in haematological malignancies as well as solid tumours (Nakatsuka et al., 2006). WT1 expression is characteristic of serous sub-type of OC and is rarely found in non-serous subtypes (Liliac et al., 2013). While immunohistochemical studies have established the role of WT1 as a reliable diagnostic marker for OC, the mechanism behind why WT1 expression is pertinent to OC development and the specific role it plays in cancer progression is still unclear. WT1 shows a strong nuclear expression in most cancers, including OC, where multiple studies have reported nuclear expression of serous ovarian tumour cells is around 90-95% (Salvatorelli et al., 2020). Since WT1 expression is traditionally considered to be nuclear-positive, any cytoplasmic staining is often regarded as non-specific (Nakatsuka et al., 2006). Hence, this chapter aimed to explore the hypothesis that both nuclear and cytoplasmic expression of WT1 can be potential diagnostic or prognostic significance in OC. Furthermore, we investigated whether therapeutic treatments could affect shuttling *in vivo* and *in vitro*.

6.4.1 WT1 cytoplasmic expression in malignancy

Most studies currently published have used tumour tissue to detect the presence of WT1 in OC, however, in this study, both cytoplasmic and nuclear WT1 expression is seen in circulating cancer-related cells (CCs) extracted from liquid biopsies during and at the end of treatment. This observation corroborates with previous studies that have reported both nuclear and cytoplasmic WT1 staining not just in epithelial OC but also in a variety of other cancers (Nakatsuka et al., 2006; Hylander et al., 2006). CCs expressing cytoplasmic WT1 were detected in large numbers at the beginning of chemotherapy treatment and began to fall as the patients responded to treatment. Cytoplasmic WT1+ CCs were significantly lower at EOT compared to treatment cycle 1. It may be helpful to analyse CCs in a larger cohort of patients and analyse whether the localisation of WT1 is indicative of a positive or negative response to current treatment, making it a potentially reliable prognostic factor. Studies looking at a variety of cancers have noted that cytoplasmic expression of WT1 is higher in malignant cells compared to normal cells. This is the case in lung, breast, and endometrial cancer (Oji et al., 2002; Loeb et al., 2001; Ohno et al., 2009). WT1 expression in pancreatic ductal adenocarcinoma was detected both in the nucleus and cytoplasm, however, weaker cytoplasmic expression translated to prolonged OS and relapse-free survival (Kanai et al., 2018). Interestingly, WT1 cytoplasmic expression has been documented in reparative neo-angiogenesis and in most benign and malignant vascular tumours (Al Dhaybi et

al., 2010; Trindade et al., 2011). These findings are also in line with the proposed WT1 involvement in tumour vascularization where it may participate in the regulation of endothelial cell proliferation and migration (Parenti et al., 2014). Endometrial tumours showing strong cytoplasmic WT1 staining were associated with advanced FIGO stage, myometrial invasion, and high-grade histological differentiation, suggesting that upregulation of WT1 cytoplasmic expression is linked to tumour progression (Ohno et al., 2009).

6.4.2 WT1 shuttling – potential novel roles

Heterokaryon assays, which involves the fusion of two cells, is used in publications as an effective method used to detect steady-state or dynamic protein localisations and is helpful in studying nucleo-cytoplasmic shuttling (Gammal *et al.*, 2011; Wang *et al.*, 2013) This technique has been used to show that WT1 undergoes nucleo-cytoplasmic shuttling, with studies successfully identifying a nuclear export sequence (NES) and interactions with nuclear transport proteins (Vajjhala et al., 2003; Depping et al., 2012). WT1 is known to function as a transcriptional regulator: as an activator, repressor, or co-activator. It is reported to be rapidly re-imported and is mentioned to shuttle in and out of the cell together with heterogenous ribonuclear particles (hnRNPs), strengthening the idea of its involvement in RNA metabolism. In addition, using Western blot analysis, WT1 was found in polyribosomes, suggesting association with translation machinery (Niksic et al., 2004; Vajjhala et al., 2003). These findings propose that WT1 may contribute as a multi-functional component within protein complexes that regulate transcription, RNA processing and translation. These data also raise the possibility that oncogenic potential of WT1 could be regulating translation rather than nuclear processes (Niksic et al., 2004). Nuclear translocation of WT1 involves importins α and β and is facilitated through a nuclear localisation sequence identified in the third zinc finger of the protein. Besides its role as a tumour suppressor gene and putative oncogene, WT1 is necessary for normal embryonic development. A common feature of WT1-expressing cells is their capability to switch between mesenchymal and epithelial states. A failure of EMT in the absence of WT1 may lead to programmed cell death thereby impeding normal development (Martínez-Estrada et al., 2010). Therefore, it may be possible that in order for the cell to harness its 'growth and development' (or metastatic) potential in an oncogenic context, it may exploit EMT.

Finally, bioinformatics analyses provide a complete picture highlighting the importance of WT1 in OC. WT1 shows a high level of mutational alteration and gene expression in OC samples compared to various other types of cancer, pinpointing its unique relevance, specifically in OC. The data discussed in this chapter highlights the potential of WT1 as a prognostic indicator and as an active element, potentially beyond transcriptional regulation. The evidence supporting nucleo-cytoplasmic shuttling within scientific literature and in this study push the necessity to

explore the implications of this molecular mechanism and its link to OC progression; showing that supposedly 'non-specific' cytoplasmic localization of WT1 may be a more reliable as diagnostic/prognostic staining tool. For example, drug effectiveness can be monitored by assessing the rate of WT1 shuttling. Future studies with a wider repertoire of therapeutic agents used in clinic and with additional cell lines are necessary to gain a better insight into this complex regulation.

Chapter 7

Discussion and concluding remarks

What is ovarian cancer (OC) and why is it important?

Ovarian cancer (OC) is a lethal malignancy caused as a result of uncontrolled growth on the ovary, a primary reproductive organ located in the pelvis, in females. According to Cancer Research UK, the estimated lifetime risk of being diagnosed with OC in the UK is 1 in 50 for females born after 1960. In comparison to other malignancies, OC has a low survival rate. Although the improvement in OC survival rate has doubled over the last 4 decades, it still remains low at 35%.

Table 7.1 *– A list of various cancer type, current survival rate and survival rate improvement noted in the last four decades and their comparisons to OC (in bold) (Cancer Research UK, 2020).*

Cancer Type	Survival rate (10-year)	Survival rate improvement (in the last 40 years)
Breast	76%	38%
Cervical	51%	17%
Uterine	72%	23%
Prostate	78%	59%
Testicular	91%	29%
Ovarian	**35%**	**17%**

OC is sometimes referred to as the 'silent killer', due to the low predictive value of the symptoms associated with this malignancy, which tend to overlap with those of more common abdominal and gastrointestinal diseases (Goff et al., 2004; Gajjar et al., 2012). This complicates timely diagnosis and referral of the condition, driving patients towards late diagnosis (stage III/IV), precisely when survival rates drop. Late diagnosis is also a major driver of NHS cancer treatment costs. Treatment for stage III and IV OC costs the NHS nearly two and a half times the amount spent on stage I and II services, respectively. Early-stage diagnosis in patients could result in the NHS saving up to £16 million annually, benefitting over 1,400 patients (Cancer Research UK, 2014). Once diagnosed, treatment options are fairly limited. Although, a combination of surgery and chemotherapy result in high incidence of remissions, the recurrence rate of OC is also quite high, resulting in patients experiencing a continuum of symptom-free periods and recurrence episodes (Cortez et al., 2018). Current therapeutic options are limited, meaning that patients who develop resistance to treatment do not have access to many alternatives. On a positive note,

recent technological advances have helped identify novel therapeutic targets; PARP inhibitors have recently gained FDA approval, providing an alternative approach to the management of recurrent OC, and addressing novel strategies focused on exploiting DNA repair deficiencies (Loizzi et al., 2020). This therapy will at least benefit OC patients that carry BRCA1/2 mutations. Additionally, the introduction of anti-angiogenic drugs such as Bevacizumab to standard chemotherapy and as a maintenance therapy have helped improve overall survival (Pignata et al., 2017). However, it is now apparent that tumour heterogeneity represents a fundamental property of many solid tumours, presenting a major obstacle to effective cancer therapy. Tumours continue to undergo molecular evolution as a result of host genetics, the tumour micro-environment and even in response to chemotherapy (El-Deiry *et al.,* 2017).

The latest statistics available show 5-year survival rate for stage I OC patients at 93%, which is much more promising in comparison to stage III and IV patients at 27% and 13% respectively (CRUK 2020; ONS 2019).

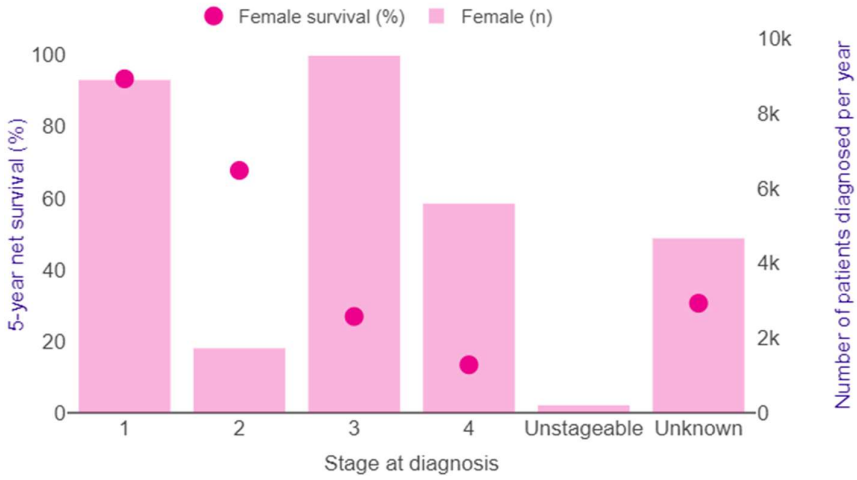

Figure 7.1 *– Bar graph showing the number of OC patients diagnosed per annum at various stages. Data points (denoted in dark pink) denote percentage of female survival at each stage (stage 1 = 93.3%; stage 2 = 67.7%; stage 3 = 26.9%; stage 4 = 13.4%; unknown = 30.6%) (Cancer Research UK, 2020).*

Can OC be detected earlier?

Currently, only a small number of cases of OC are detected in its early stages (stage I and II). Earlier detection is required since survival rates increase up to 90% when diagnosed earlier. Successful ways to detect OC earlier is through effective screening and diagnosis. Screening programmes have worked effectively to decrease mortality rates in other cancers including cervical and breast cancer. For example, the NHS breast cancer screening programme offered to women aged 50-69 has helped save 1,300 lives a year (Marmot et al., 2013). Similarly, cervical

screening (using liquid-based cytology) has helped save 4,500 lives annually (Peto et al., 2004; Marmot et al., 2013). Although screening methods have been studied to help detect OC earlier and more accurately, no significant progress has been made till date. As a stand-alone test, trans-vaginal ultrasounds have shown to lack the required sensitivity and specificity needed for screening (Loud and Murphy, 2017). CA125 and transvaginal ultrasound (TVS) techniques have been tested in combination as a multi-modal screening (MMS) strategy to test efficiency as a long-term screening tool in an effort to reduce OC-related deaths. As of 2021, this strategy did not result in significant reduction of OC-related mortality and therefore, could not be recommended as an optimum screening method (Menon et al., 2021). This is in line with the PLCO randomised controlled trial which also showed no statistically significant reduction in mortality from OC for women screened using a combination of CA125 and TVS (Buys et al., 2011). This highlights the need for effective screening, possibly using novel, more robust biomarkers that can help reduce mortality and save lives.

Serum CA-125 tests are carried out initially as a diagnostic test for OC, followed by a transvaginal ultrasound if the blood tests show a higher-than-normal level of CA-125 (> 35 U/ml). However, it is not necessarily elevated in early-stage disease and is also known to be high in the case of non-malignant conditions providing limited efficiency (refer to table 7.2) (Dochez et al., 2019).

Table 7.2 - *Benign and malignant conditions other than OC which may cause elevations in serum CA125 that may result in incorrect interpretation (Sturgeon, Duffy and Walker, 2011).*

Benign Conditions	Malignancies
Chronic liver diseases (e.g., Cirrhosis)	Breast cancer
Endometriosis	Cervical cancer
Menstruation	Endometrial cancer
Pancreatitis	Liver cancer
Peritoneal inflammation	Lung cancer
Pleural inflammation	Pancreatic Cancer
Surgical procedures	Uterine Cancer

Once again, this shows that while CA125 is currently available as a means of OC diagnosis, it does not achieve the required sensitivity and specificity. In published studies to date, more than 35 different biomarkers have been reported to improve the sensitivity of CA125 for detecting early-stage disease, particularly the combination of CA125 with HE4, which is slightly less sensitive than CA125 but shows better specificity for distinguishing malignant masses from benign ones (Bast et al., 2020). Recently, the FDA approved the use of the OVA1 panel that includes testing

serum biomarker levels of CA125, Apolipoprotein A1, Transthyretin, Transferrin and β2-microglobulin. OVA1 provided 96% sensitivity at 28% specificity in post-menopausal women and was able to detect 76% of the malignancies that had been missed by CA125 (Kumari, 2018). Going forward, the strategy seems to involve the development of robust multi-marker panels that aid in the detection of early-stage cases.

What are tissue and liquid biopsies? How do they compare?

Tissue biopsies involve the surgical retrieval of a biological sample from a suspicious mass to establish a diagnosis and determine possible treatment options. Tissue biopsies currently represent the standard procedure for cancer detection, capable of providing reliable results but this procedure poses its own limitations (Mannelli, 2019). It are relatively invasive, not always feasible and only provide information limited to a single point in space and time, failing to capture tumour heterogeneity (Arneth, 2018; Russano et al., 2020). Liquid biopsies rely on the analysis of body fluids (e.g., blood, saliva, cerebrospinal fluid, urine), providing a minimally-invasive alternative that can be used to assess and serially monitor the genetic status of cancer tumours over time (Mannelli, 2019). Compared to tissue biopsies, liquid biopsies help capture disseminated cells and DNA released from tumours that may be inaccessible through surgery, providing the option for serial monitoring, and can be repeatedly performed to monitor disease progression (Mannelli, 2019). Liquid biopsies include circulating tumour cells (CTCs), circulating tumour DNA (ctDNA), free-floating proteins and exosomes. CTCs are found primarily in the bloodstream as individual cells or a cluster. They detach from the primary tumour and use hematogenous routes of transmission to facilitate metastasis and reach distant organs (Kim et al 2019). Particularly in the case of CTCs, CellSearch™ platform has gained FDA-approval for clinical testing for CTCs in cancer patients and it is likely that other instruments will follow in the near future. While liquid biopsies harness multiple advantages, there are some challenges that need to be considered. Before liquid biopsies can be used routinely within a clinical environment, they need to be standardized. Firstly, isolating CTCs from a blood sample poses a challenge since the number of CTCs present in a patient sample are much smaller compared to the number of white blood cells or red blood cells within the sample, however, enrichment and isolation have helped address this limitation (Morgan, 2019), although capturing all circulating cells, namely those undergoing EMT continues to pose a challenge (Keller *et al*, 2019). Additionally, CTCs can be used to gain phenotypic data through single cell genomic, transcriptomic and/or proteomic profiling (De Rubis *et al,* 2019). While this provides in-depth genetic information, single cell analyses pose a similar limitation as tissue biopsies, since genetic information from a single cell may not be able to provide a holistic view and address tumour heterogeneity.

In addition to CTCs, tumour DNA is also present in peripheral blood, in part due to the high apoptotic rate within the tumour microenvironment (TME), which results in the release of DNA from apoptotic cells into the bloodstream. Circulating tumour DNA (ctDNA) is the portion of circulating cell-free DNA (ccfDNA) specifically derived from cancer cells and has been estimated to range from 10 to 90% of the total ccfDNA in cancer patients (Elazezy and Joosse, 2018). ctDNA is a fraction of the cell-free DNA found in circulation that originate from tumour cells and contain cancer-related genomic variants (Merker et al., 2018). The mechanisms of cfDNA release are poorly understood. Although a large fraction has been shown to originate through apoptosis/necrosis, early studies indicate that cfDNA is also derived from active cellular secretions using *in vitro* cell culture studies (Bronkhorst *et al,* 2019). While currently available technologies like next generation sequencing (NGS) and PCR can detect ctDNA in blood, their sensitivity is sub-optimal due to low levels of ctDNA in blood (De Rubis *et al,* 2019).

Exosomes are a subset of extracellular vesicles (EVs), that are normally released by prokaryotes and eukaryotes to regulate intercellular communication in health/disease. We now know that they enable transfer of functional proteins, metabolites and nucleic acids to recipient cells and are involved in cancer progression through regulation of tumour growth, metastasis, angiogenesis, and mediation of drug resistance (Dai et al., 2020; Gurung et al., 2021). Exosomes have been isolated using various methods including size, morphology and surface protein content using techniques including ultracentrifugation, immunoaffinity, scanning electron microscopy and Western blotting (Wang et al., 2021).

What was the purpose of this study?

The purpose of this study was to explore the prognostic potential of liquid biopsies in OC through identification and testing of biomarkers, in a clinical and molecular perspective.

Chapters 3 and 4 focused mainly on the utility of circulating cancer-related cells (CCs) as a biomarker in advanced stage OC patients. Experiments in chapter 3 involved the validation of biomarkers using *in vitro* models of OC and addressed key aspects involved in successful clinical testing of CCs such as sample collection and comparison of technologies based on biological and physical properties for identifying CCs. Chapter 4 focused on detection of CCs in aEOC patient blood samples based on treatment as well as comparing the efficiency of CCs to inform on treatment success through serial monitoring, in comparison with CA-125. This chapter also included a pilot study, identifying the presence of circulating endothelial cells (CECs) and highlighting the presence of multiple cancer-related cell populations within blood samples, in addition to CTCs. Chapter 5 investigated the role of SP-D in OC and its reliability as a biomarker. Clinical experiments were conducted to explore the correlation of SP-D expression with OC stage

and grade, whereas experiments conducted on two OC cell lines (SKOV3 and PEO1) tested the therapeutic potential of rfhSP-D expression *in vitro*. Finally, chapter 6 included exploratory experiments studying the relevance of WT1 protein localisation in OC disease progression, highlighting the need of evaluating the mechanistic importance of cytoplasmic expression of WT1 in OC.

What are some of the limitations of current research? What are the future perspectives?

CTC identification method (biological vs physical properties) – Results from this study showed that imaging flow cytometry provided a higher yield of positive CCs compared to the size-based platform, Parsortix™. The reason behind a low yield of CCs from Parsortix™ was the width of the 'critical gap' within the microfluidics cassette. The size range of CCs identified with AE1/AE3 and WT1 was quite similar to CD45+ white blood cells, showing a size overlap between the two populations (Kumar *et al.*, 2019). The critical gap (which is used to capture 'larger' CTCs within) within the microfluidics cassette used was 10 μm, therefore, our population of interest would have easily passed through the cassette. Further experiments need to take place using smaller size pores in the filtration cassette. It is also worth noting that Parsortix™ has been successful in detecting CTCs in other types of cancers. In comparison to EpCAM-based CTC enrichment method, size-based CTC isolation using Parsortix™ performed better in isolating head and neck squamous cell carcinoma (HNSCC) cells from blood, stating that the system was more appropriate to remove leukocytes and allow for molecular analysis in a high purity of enriched cells (Zavridou et al., 2020). Furthermore, experiments involving a Parsortix™ cassette with a 6.5 μm gap dramatically improved capture efficiency of CTCs, both in volunteer blood spiked with breast cancer cell lines and patient blood samples (Koch et al., 2020). This shows that perhaps using a cassette with a smaller gap could increase CTC capture efficiency and provide much reliable results.

Biomarker performance - Although CC populations identified using imaging flow cytometry yielded a higher population of positive cells compared to size-based methods, there are a few limitations that need to be considered. For the purpose of this study, two cancer-related biomarkers were used. Patterns that have emerged from the assessment of clinical samples need to be validated in larger patient cohorts. Looking deeper, the volunteer vs patient WT1+ cell population analysis shows that post-menopausal women in the volunteer cohort had no WT1+ cells compared to pre-menopausal volunteers. This could possibly mean that a WT1+ CC identification test could be more specific and sensitive in post-menopausal OC patients and could potentially be developed for a more age-specific patient population. CA125 and CC correlation

throughout treatment was only done on four patients and varied in broad alignment with each other. Correlation analysis did not show any significance, however, there were instances where CCs were higher compared to CA125 and could have been more helpful in informing clinicians over further course of treatment. This shows that CCs could be a potentially helpful indicator, however, these need to be corroborated with a larger cohort of patients. CC-based quantification also sheds light on the use of multiple biomarkers within the same test to identify true CC populations accurately. Additional fluorescent channels can be used to incorporate multiple biomarkers in order to provide further confirmation. For example, adding mesenchymal markers like Vimentin could potentially help capture circulating tumour cells undergoing EMT.

Currently CellSearch™ is the only FDA approved platform that uses EpCAM coated ferrofluid particles for CTC detection. As mentioned before, solely relying on EpCAM for CTC detection could lead to overlooking a significant population of cells that have undergone EMT. AdnaTest® is another commercialised positive selection platform that relies on immunomagnetic beads coated with a cocktail of antibodies for enhanced capture and enrichment of CTCs in breast, prostate, ovarian and colon cancer. A clinical study to assess the prognostic validity of CTCs in metastatic prostate cancer showed better performance from the AdnaTest compared to CellSearch, with a higher detection rate of 62% compared to 45% respectively (Habli et al., 2020). However, CellSearch system outperforms the AdnaTest by its ability to accurately associate CTC numbers with OS and PFS. Other modalities designed to detect CTCs through immunomagnetic beads continue to use EpCAM and CK expression to confirm CTC presence.

In this case, either future platforms could include EMT-related biomarkers or perhaps size-based platforms could be optimised further to capture more CTCs. This was seen in the case of Parsortix, where chips with various 'critical gap' widths resulted in higher yields.

Immune-based biomarkers in OC – Tumour immune surveillance is the process wherein the immune system identifies cancerous and/or precancerous cells and eliminates them before they can cause harm (Swann and Smyth, 2007). *In vivo* and *in vitro* studies using cancer models have demonstrated a compelling involvement of effector immune cells, soluble factors, and signalling pathways in anti-tumour immune responses. However, the immune system can also aid in the progression of transformed cells by triggering immunosuppression and promoting angiogenesis and metastasis of tumour cells (Murugaiah et al., 2020). SP-D is an innate immune molecule that was found to be upregulated within OC samples (both in tissue and liquid biopsies). Furthermore, expression of rfhSP-D in SKOV3 cells induced cell death through the increase of caspase-3 levels. However, the same effect was not fully replicated in PEO1 cells, possibly due to its epithelial phenotype or BRCA2 mutation status. Future experiments would include PEO4, an OC cell line with a silent BRCA2 mutation, to test whether rfhSP-D related therapeutic effects are BRCA-

dependent or not. Larger cohort sizes are required to further investigate SP-D levels in patient plasma samples and blood and note any correlations based on stage/grade, to check whether the results corroborate with tissue biopsy results.

The role of WT1 in OC - Despite WT1 being a nuclear marker, experiments have shown a possibility to reconsider cytoplasmic staining of WT1 in cells and its relevance to OC progression. This leads us to rethink what constitutes a 'positive result'. The atypical cytoplasmic staining of WT1 noted in CCs probed us to conduct a pilot study to examine the correlation between WT1 protein sub-localisation in the cytoplasm and OC progression. WT1 is known to be overexpressed in OC, however, the mechanism of how it relates to OC progression is not fully understood. A 17AA-/KTS- splice variant introduced in mice models showed a significant increase of tumorigenic activity through the upregulation of VEGF, with an increase in tumour weight and production of ascites as a result (Yamanouchi et al., 2014).

STRING network analysis on WT1 revealed a strong association with TP53, a well-known oncogene. In an oncogenic context, WT1 has an experimentally determined association with TP53, a well-established and highly unregulated gene in cancer. Similar to TP53, WT1 is initially identified as a tumour suppressor gene in 1990 when it was found to cause a type of paediatric kidney cancer called Wilms' tumour (Hastie, 2017).

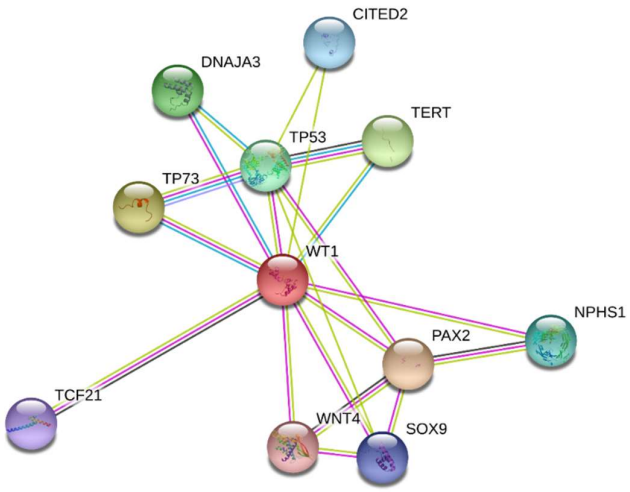

Figure 7.2 *– STRING analysis of the WT1 gene; showing a network of possible interactions collated from information on known and predicted protein-protein interactions using information sourced from genomic context, high throughput lab experiments and co-expression data.*

P53 and WT1 are shown to interact with one another physically and functionally. P53 can alter the transcriptional activity of WT1 (seen in the case of Wilms' tumours) and WT1 in turn, has shown to stabilise P53, affect it's transcriptional activity, and rescue cells from P53-induced

apoptosis (Menke et al., 2002). Co-expression of TP53 and WT1 have shown that WT1 interacts with p53 through zinc fingers 1 and 2 in order to stabilize TP53 and inhibit TP53-mediated apoptosis (Maheswaran et al., 1995). This might indicate a possibility for a synergistic role between the two. Immunohistochemical analysis on patient tissue samples have also shown that a high co-expression of TP53 and WT1 is correlated with high grade OC and poorer prognosis (Carter et al., 2018).

Interpatient variability – Interpatient variability is described as the difference in patient features/traits, pharmacokinetics and genetics that potentially impact the efficacy of treatment (Holliday et al., 2014). Our study followed four patients throughout treatment and correlated their CCs levels with CA125 levels and showed that CCs varied in broad alignment with CA125 levels, with no apparent significance between the two. Interpatient variability tends to mask general patterns due to individual genetic/physiological factors. Larger cohorts of patients are therefore required to study correlations not just generally across all aEOC patients, but also to study the effects based on treatment cohorts since CCs numbers may vary depending on treatment, biomarker of choice and individual patient (see figure 4.4). Multiple biomarkers can also be used for CC detection, since it could help identify multiple populations within the same sample and identify them with more precision. Epithelial markers (such as cytokeratins and EpCAM) can be paired with mesenchymal markers (such as Vimentin) to account for phenotypical variations in CC populations. Identifying and analysing other populations such as circulating endothelial cells (CECs), that disseminate from the tumour into the blood stream, may aid in providing patient specific prognostic/diagnostic information for a more informed clinical decision. This ties well with the need to develop multi-marker biomarker tests, which could also capture different cell populations that arise from tumour dissemination/metastasis. Conducting further experiments and collecting data on CEC+ cell numbers in liquid biopsies and comparing it with CTC+ populations could provide interesting insights into the volume of various cell populations that actually disseminate into the blood stream to facilitate metastasis. Future studies should also compare CC numbers in patients with other clinicopathological data such as CT scans to correlate the quantity of CCs found with visual data identifying tumour mass.

Conclusion

The need for biomarkers in OC is required as it can help account for disease heterogeneity, an aspect that is overlooked in the current clinical landscape due to the limited amount of information provided by tissue biopsies and the lack of specificity of current tests. In this study, we consider biomarkers that are directly related to cancer progression (such as AE1/AE3 and WT1) and explore further into immune-system related biomarkers (such as SP-D). Chapters 5 and 6 specifically look into the mechanistic aspects of biomarkers and how informing on their functionality and involvement in OC could help discover new therapeutic targets. Investigating the shuttling effect of WT1 is important to understand the functional role of WT1, beyond just a biomarker used to confirm serous OC.

Bibliography

Aktas, B., Müller, V., Tewes, M., Zeitz, J., Kasimir-Bauer, S., Loehberg, C.R., Rack, B., Schneeweiss, A. and Fehm, T., 2011. Comparison of estrogen and progesterone receptor status of circulating tumor cells and the primary tumor in metastatic breast cancer patients. *Gynecologic Oncology*, 122(2), pp.356–360.

Al-Hussaini, M., Stockman, A., Foster, H. and McCluggage, W.G., 2004. WT-1 assists in distinguishing ovarian from uterine serous carcinoma and in distinguishing between serous and endometrioid ovarian carcinoma. *Histopathology*, 44(2), pp.109–115.

Apostolou, P., Ntanovasilis, D.A. and Papasotiriou, I., 2017. Evaluation of a simple method for storage of blood samples that enables isolation of circulating tumor cells 96 h after sample collection. *Journal of Biological Research (Greece)*, 24(1), pp.1–11.

Arneth, B., 2018. Update on the types and usage of liquid biopsies in the clinical setting: a systematic review. *BMC Cancer*. [online] Available at: <https://pubmed.ncbi.nlm.nih.gov/29728089/>.

Asante, D.B., Calapre, L., Ziman, M., Meniawy, T.M. and Gray, E.S., 2020. Liquid biopsy in ovarian cancer using circulating tumor DNA and cells: Ready for prime time? *Cancer Letters*, 468(September 2019), pp.59–71.

Ashworth, T., 1869. A case of cancer in which cells similar to those in the tumours were seen in blood after death. *Australasian Medical Journal*, 14, pp.146–147.

Bandera, E. V., Lee, V.S., Qin, B., Rodriguez-Rodriguez, L., Powell, C.B. and Kushi, L.H., 2017. Impact of body mass index on ovarian cancer survival varies by stage. *British Journal of Cancer*, [online] 117(2), pp.282–289. Available at: <http://dx.doi.org/10.1038/bjc.2017.162>.

Barak, V., Goike, H., Panaretakis, K.W. and Einarsson, R., 2004. Clinical utility of cytokeratins as tumor markers. *Clinical Biochemistry*, 37(7), pp.529–540.

Basiji, D.A., Ortyn, W.E., Liang, L., Venkatachalam, V. and Morrissey, P., 2007. Cellular Image Analysis and Imaging by Flow Cytometry. *Clinics in Laboratory Medicine*, 27(3), pp.653–670.

Bast, R.C., Zhen, L., Han, C.Y., Lu, K.H., Anderson, K.S., Drescher, C.W. and Skates, S.J., 2020. *Biomarkers and Strategies for Early Detection of Ovarian Cancer*.

BD Biosciences, 2011. *CD Marker Handbook*.

Beaufort, C.M., Helmijr, J.C.A., Piskorz, A.M., Hoogstraat, M., Ruigrok-Ritstier, K., Besselink, N.,

Murtaza, M., Van IJcken, W.F.J., Heine, A.A.J., Smid, M., Koudijs, M.J., Brenton, J.D., Berns, E.M.J.J. and Helleman, J., 2014. Ovarian cancer cell line panel (OCCP): Clinical importance of in vitro morphological subtypes. *PLoS ONE*, 9(9).

Bergfeldt, K., Rydh, B., Granath, F., Grönberg, H., Thalib, L., Adami, H.O. and Hall, P., 2002. Risk of ovarian cancer in breast-cancer patients with a family history of breast or ovarian cancer: A population-based cohort study. *Lancet*, 360(9337), pp.891–894.

Blaustein, A., 1983. *Pathology of the Female Genital Tract*.

Bratulic, S., Gatto, F. and Nielsen, J., 2019. *The Translational Status of Cancer Liquid Biopsies*. *Regenerative Engineering and Translational Medicine*. Regenerative Engineering and Translational Medicine.

Bronkhorst, A.J., Ungerer, V. and Holdenrieder, S., 2019. The emerging role of cell-free DNA as a molecular marker for cancer management. *Biomolecular Detection and Quantification*, [online] 17(February), p.100087. Available at: <https://doi.org/10.1016/j.bdq.2019.100087>.

Buys, S.S., Partridge, E., Black, A., Johnson, C.C., Lamerato, L., Isaacs, C., Reding, D.J., Greenlee, R.T., Yokochi, L.A., Kessel, B., Crawford, E.D., Church, T.R., Andriole, G.L., Weissfeld, J.L., Fouad, M.N., Chia, D., O'Brien, B., Ragard, L.R., Clapp, J.D., Rathmell, J.M., Riley, T.L., Hartge, P., Pinsky, P.F., Zhu, C.S., Izmirlian, G., Kramer, B.S., Miller, A.B., Xu, J.L., Prorok, P.C., Gohagan, J.K. and Berg, C.D., 2011. Effect of screening on ovarian cancer mortality: The Prostate, Lung, Colorectal and Ovarian (PLCO) cancer screening randomized controlled trial. *JAMA - Journal of the American Medical Association*, 305(22), pp.2295–2302.

Cancer Research UK, 2014. Saving lives, averting costs. *A report prepared for Cancer Research UK*, [online] (September), p.79. Available at: <www.incisivehealth.com.>.

Cancer Research UK, 2020. *Cancer Research, UK (2020) Available at: http://www.cancerresearchuk.org/health-professional/cancer-statistics/statistics-by-cancer-type/ovarian-cancer/risk-factors (Accessed December 2015)*.

Carter, J.H., Deddens, J.A., Mueller, G., Lewis, T.G., Dooley, M.K., Robillard, M.C., Frydl, M., Duvall, L., Pemberton, J.O. and Douglass, L.E., 2018. Transcription factors wt1 and p53 combined: A prognostic biomarker in ovarian cancer. *British Journal of Cancer*, [online] 119(4), pp.462–470. Available at: <http://dx.doi.org/10.1038/s41416-018-0191-x>.

Casey, L., Köbel, M., Ganesan, R., Tam, S., Prasad, R., Böhm, S., Lockley, M., Jeyarajah, A.J., Brockbank, E., Faruqi, A., Gilks, C.B. and Singh, N., 2017. A comparison of p53 and WT1 immunohistochemical expression patterns in tubo-ovarian high-grade serous carcinoma before

and after neoadjuvant chemotherapy. *Histopathology*, 71(5), pp.736–742.

Castro-Giner, F., Gkountela, S., Donato, C., Alborelli, I., Quagliata, L., Ng, C., Piscuoglio, S. and Aceto, N., 2018. Cancer Diagnosis Using a Liquid Biopsy: Challenges and Expectations. *Diagnostics*, [online] 8(2), p.31. Available at: <http://www.mdpi.com/2075-4418/8/2/31>.

Cerami, E., Gao, J., Dogrusoz, U., Gross, B.E., Sumer, S.O., Aksoy, B.A., Jacobsen, A., Byrne, C.J., Heuer, M.L., Larsson, E., Antipin, Y., Reva, B., Goldberg, A.P., Sander, C. and Schultz, N., 2012. The cBio Cancer Genomics Portal: An open platform for exploring multidimensional cancer genomics data. *Cancer Discovery*, 2(5), pp.401–404.

Charlton, J. and Pritchard-Jones, K., 2016. WT1 mutation in childhood cancer. *Methods in Molecular Biology*, 1467, pp.1–14.

Cheaib, B., Auguste, A. and Leary, A., 2015. The PI3K/Akt/mTOR pathway in ovarian cancer: Therapeutic opportunities and challenges. *Chinese Journal of Cancer*, 34(1), pp.4–16.

Cheng, L., Wu, S., Zhang, K., Qing, Y. and Xu, T., 2017. A comprehensive overview of exosomes in ovarian cancer: Emerging biomarkers and therapeutic strategies. *Journal of Ovarian Research*, 10(1), pp.1–9.

Coleman, R.L., Brady, M.F., Herzog, T.J., Sabbatini, P., Armstrong, D.K., Walker, J.L., Kim, B.G., Fujiwara, K., Tewari, K.S., O'Malley, D.M., Davidson, S.A., Rubin, S.C., DiSilvestro, P., Basen-Engquist, K., Huang, H., Chan, J.K., Spirtos, N.M., Ashfaq, R. and Mannel, R.S., 2017. Bevacizumab and paclitaxel–carboplatin chemotherapy and secondary cytoreduction in recurrent, platinum-sensitive ovarian cancer (NRG Oncology/Gynecologic Oncology Group study GOG-0213): a multicentre, open-label, randomised, phase 3 trial. *The Lancet Oncology*, [online] 18(6), pp.779–791. Available at: <http://dx.doi.org/10.1016/S1470-2045(17)30279-6>.

Coleman, R.L., Monk, B.J., Sood, A.K. and Herzog, T.J., 2013. Latest research and treatment of advanced-stage epithelial ovarian cancer. *Nature Reviews Clinical Oncology*, [online] 10(4), pp.211–224. Available at: <http://www.nature.com/doifinder/10.1038/nrclinonc.2013.5>.

Crowley, L.C., Marfell, B.J., Scott, A.P. and Waterhouse, N.J., 2016. Quantitation of apoptosis and necrosis by annexin V binding, propidium iodide uptake, and flow cytometry. *Cold Spring Harbor Protocols*, 2016(11), pp.953–957.

Dai, J., Su, Y., Zhong, S., Cong, L., Liu, B., Yang, J., Tao, Y., He, Z., Chen, C. and Jiang, Y., 2020. *Exosomes: key players in cancer and potential therapeutic strategy*.

Danforth, K.N., Tworoger, S.S., Hecht, J.L., Rosner, B.A., Colditz, G.A. and Hankinson, S.E., 2007. Breastfeeding and risk of ovarian cancer in two prospective cohorts. *Cancer Causes and Control*,

18(5), pp.517–523.

Depping, R., Schindler, S.G., Jacobi, C., Kirschner, K.M. and Scholz, H., 2012. Nuclear transport of wilms′ tumour protein Wt1 involves importins α and β. *Cellular Physiology and Biochemistry*, 29(1–2), pp.223–232.

Al Dhaybi, R., Powell, J., McCuaig, C. and Kokta, V., 2010. Differentiation of vascular tumors from vascular malformations by expression of Wilms tumor 1 gene: Evaluation of 126 cases. *Journal of the American Academy of Dermatology*, 63(6), pp.1052–1057.

Dochez, V., Caillon, H., Vaucel, E., Dimet, J., Winer, N. and Ducarme, G., 2019. Biomarkers and algorithms for diagnosis of ovarian cancer: CA125, HE4, RMI and ROMA, a review. *Journal of Ovarian Research*, 12(1), pp.1–9.

Domínguez-Vigil, I.G., Moreno-Martínez, A.K., Wang, J.Y., Roehrl, M.H.A. and Barrera-Saldaña, H.A., 2018. The dawn of the liquid biopsy in the fight against cancer. *Oncotarget*, 9(2), pp.2912–2922.

Dongre, A. and Weinberg, R.A., 2019. New insights into the mechanisms of epithelial–mesenchymal transition and implications for cancer. *Nature Reviews Molecular Cell Biology*, [online] 20(2), pp.69–84. Available at: <http://dx.doi.org/10.1038/s41580-018-0080-4>.

Doubeni, C.A., Doubeni, A.R.B. and Myers, A.E., 2016. Diagnosis and Management of Ovarian Cancer. [online] 93(11). Available at: <www.aafp.org/afp>.

Doufekas, K. and Olaitan, A., 2014. Clinical epidemiology of epithelial ovarian cancer in the UK. *International Journal of Women's Health*, 6(1), pp.537–545.

Doyle, L.M. and Wang, M.Z., 2019. Overview of Extracellular Vesicles, Their Origin, Composition, Purpose and Methods for Exosome Isolation and Analysis. *Cells*.

El-Deiry, W.S., Taylor, B. and Neal, J.W., 2017. Tumor Evolution, Heterogeneity, and Therapy for Our Patients With Advanced Cancer: How Far Have We Come? *American Society of Clinical Oncology Educational Book*, (37), pp.e8–e15.

Elazezy, M. and Joosse, S.A., 2018. Techniques of using circulating tumor DNA as a liquid biopsy component in cancer management. *Computational and Structural Biotechnology Journal*, [online] 16, pp.370–378. Available at: <https://doi.org/10.1016/j.csbj.2018.10.002>.

Engeland, A., Tretli, S. and Bjørge, T., 2003. Height, body mass index, and ovarian cancer: A follow-up of 1.1 million Norweigian women. *Journal of the National Cancer Institute*, 95(16), pp.1244–1248.

Fan, T., Zhao, Q., Chen, J.J., Chen, W.T. and Pearl, M.L., 2009. Clinical significance of circulating

tumor cells detected by an invasion assay in peripheral blood of patients with ovarian cancer. *Gynecologic Oncology*, [online] 112(1), pp.185–191. Available at: <http://dx.doi.org/10.1016/j.ygyno.2008.09.021>.

Farquhar, C., 2007. Endometriosis. *British Medical Journal*, 334(7587), pp.249–253.

Florkowski, C.M., 2008. Sensitivity, specificity, receiver-operating characteristic (ROC) curves and likelihood ratios: communicating the performance of diagnostic tests. *The Clinical biochemist. Reviews*, [online] 29 Suppl 1(August), pp.S83-7. Available at: <http://www.ncbi.nlm.nih.gov/pubmed/18852864%0Ahttp://www.pubmedcentral.nih.gov/articlerender.fcgi?artid=PMC2556590>.

Gabra, H., 2014. Introduction to managing patients with recurrent ovarian cancer. *European Journal of Cancer, Supplement*, [online] 12(2), pp.2–6. Available at: <http://dx.doi.org/10.1016/S1359-6349(15)70003-0>.

Gaitskell, K., Green, J., Pirie, K., Barnes, I., Hermon, C., Reeves, G.K. and Beral, V., 2018. Histological subtypes of ovarian cancer associated with parity and breastfeeding in the prospective Million Women Study. *International Journal of Cancer*, 142(2), pp.281–289.

Gajjar, K., Ogden, G., Mujahid, M.I. and Razvi, K., 2012. Symptoms and Risk Factors of Ovarian Cancer: A Survey in Primary Care. *ISRN Obstetrics and Gynecology*, [online] 2012, pp.1–6. Available at: <http://www.hindawi.com/journals/isrn/2012/754197/>.

Gammal, R., Baker, K. and Heilman, D., 2011. Heterokaryon technique for analysis of cell type-specific localization. *Journal of Visualized Experiments*, (49), pp.4–7.

Gao, J., Aksoy, B.A., Dogrusoz, U., Dresdner, G., Gross, B., Sumer, S.O., Sun, Y., Jacobsen, A., Sinha, R., Larsson, E., Cerami, E., Sander, C. and Schultz, N., 2013. Integrative analysis of complex cancer genomics and clinical profiles using the cBioPortal. *Science Signaling*, 6(269).

Gao, Y., Li, Y., Zhang, C., Han, J., Liang, H., Zhang, K. and Guo, H., 2019. Evaluating the benefits of neoadjuvant chemotherapy for advanced epithelial ovarian cancer: a retrospective study. *Journal of ovarian research*, 12(1), p.85.

Geary, J., Sasieni, P., Houlston, R., Izatt, L., Eeles, R., Payne, S.J., Fisher, S. and Hodgson, S. V., 2008. Gene-related cancer spectrum in families with hereditary non-polyposis colorectal cancer (HNPCC). *Familial Cancer*, 7(2), pp.163–172.

Gelmon, K.A., Tischkowitz, M., Mackay, H., Swenerton, K., Robidoux, A., Tonkin, K., Hirte, H., Huntsman, D., Clemons, M., Gilks, B., Yerushalmi, R., Macpherson, E., Carmichael, J. and Oza, A., 2011. Olaparib in patients with recurrent high-grade serous or poorly differentiated ovarian

carcinoma or triple-negative breast cancer: A phase 2, multicentre, open-label, non-randomised study. *The Lancet Oncology*, 12(9), pp.852–861.

Ghasemi, N., Ghobadzadeh, S., Zahraei, M., Mohammadpour, H., Bahrami, S., Ganje, M.B. and Rajabi, S., 2014. HE4 combined with CA125: Favorable screening tool for ovarian cancer. *Medical Oncology*, 31(1).

Giannopoulou, L., Kasimir-Bauer, S. and Lianidou, E.S., 2018. *Liquid biopsy in ovarian cancer: recent advances on circulating tumor cells and circulating tumor DNA*. *Clinical chemistry and laboratory medicine*, .

Goff, B., 2012. Symptoms associated with ovarian cancer. *Clinical Obstetrics and Gynecology*, 55(1), pp.36–42.

Goff, B.A., Mandel, L.S., Melancon, C.H. and Muntz, H.G., 2004. Frequency of symptoms of ovarian cancer in women presenting to primary care clinics. *Journal of the American Medical Association*, 291(22), pp.2705–2712.

Gong, T.-T., Wu, Q.-J., Vogtmann, E., Lin, B. and Wang, Y.-L., 2013. Age at menarche and risk of ovarian cancer: a meta-analysis of epidemiological studies. *Int J Cancer*, [online] 132, pp.1–7. Available at: <https://www.ncbi.nlm.nih.gov/pmc/articles/PMC3806278/pdf/nihms516886.pdf>.

Gurung, S., Perocheau, D., Touramanidou, L. and Baruteau, J., 2021. The exosome journey: from biogenesis to uptake and intracellular signalling. *Cell Communication and Signaling*, [online] 19(1), pp.1–19. Available at: <https://doi.org/10.1186/s12964-021-00730-1>.

Habli, Z., Alchamaa, W., Saab, R., Kadara, H. and Khraiche, M.L., 2020. Circulating tumor cell detection technologies and clinical utility: Challenges and opportunities. *Cancers*, 12(7), pp.1–30.

Hall, M., Gourley, C., Mcneish, I., Ledermann, J., Gore, M., Jayson, G., Perren, T., Rustin, G. and Kaye, S., 2013. Targeted anti-vascular therapies for ovarian cancer: Current evidence. *British Journal of Cancer*, 108(2), pp.250–258.

Hankinson, S.E., Colditz, G.A., Hunter, D.J., Willett, W.C., Stampfer, M.J., Rosner, B., Hennekens, C.H. and Speizer, F.E., 1995. A prospective study of reproductive factors and risk of epithelial ovarian cancer. *Cancer*, 76(2), pp.284–290.

Hartkamp, J., Carpenter, B. and Roberts, S.G.E., 2010. The Wilms' Tumor Suppressor Protein WT1 Is Processed by the Serine Protease HtrA2/Omi. *Molecular Cell*, 37(2), pp.159–171.

Hasegawa, Y., Takahashi, M., Ariki, S., Asakawa, D., Tajiri, M., Wada, Y., Yamaguchi, Y., Nishitani, C.,

Takamiya, R., Saito, A., Uehara, Y., Hashimoto, J., Kurimura, Y., Takahashi, H. and Kuroki, Y., 2015. Surfactant protein D suppresses lung cancer progression by downregulation of epidermal growth factor signaling. *Oncogene*, [online] 34(7), pp.838–845. Available at: <http://www.ncbi.nlm.nih.gov/pubmed/24608429>.

Hastie, N.D., 2017. Wilms' tumour 1 (WT1) in development, homeostasis and disease. *Development (Cambridge)*, 144(16), pp.2862–2872.

Hein, A., Thiel, F.C., Bayer, C.M., Fasching, P.A., Häberle, L., Lux, M.P., Renner, S.P., Jud, S.M., Schrauder, M.G., Müller, A., Wachter, D., Strehl, J., Hartmann, A., Beckmann, M.W. and Rauh, C., 2013. Hormone replacement therapy and prognosis in ovarian cancer patients. *European Journal of Cancer Prevention*, 22(1), pp.52–58.

Hendrix, N.D., Wu, R., Kuick, R., Schwartz, D.R., Fearon, E.R. and Cho, K.R., 2006. Fibroblast growth factor 9 has oncogenic activity and is a downstream target of Wnt signaling in ovarian endometrioid adenocarcinomas. *Cancer Research*, 66(3), pp.1354–1362.

Hernandez, L., Kim, M.K., Lyle, L.T., Bunch, K.P., House, C.D., Ning, F., Noonan, A.M. and Annunziata, C.M., 2016. Characterization of ovarian cancer cell lines as in vivo models for preclinical studies. *Gynecologic Oncology*, 142(2), pp.332–340.

Hida, K., Hida, Y., Amin, D.N., Flint, A.F., Panigrahy, D., Morton, C.C. and Klagsbrun, M., 2004. Tumor-associated endothelial cells with cytogenetic abnormalities. *Cancer Research*, 64(22), pp.8249–8255.

Holliday, S.F., Kane-Gill, S.L., Empey, P.E., Buckley, M.S. and Smithburger, P.L., 2014. Interpatient variability in dexmedetomidine response: A survey of the literature. *The Scientific World Journal*, 2014.

Hylander, B., Repasky, E., Shrikant, P., Intengan, M., Beck, A., Driscoll, D., Singhal, P., Lele, S. and Odunsi, K., 2006. Expression of Wilms tumor gene (WT1) in epithelial ovarian cancer. *Gynecologic Oncology*.

Icon, T. and Collaborators, A.G.O., 2003. Paclitaxel plus platinum-based chemotherapy versus conventional platinum-based chemotherapy in women with relapsed ovarian cancer: The ICON4/AGO-OVAR-2.2 trial. *Lancet*, 361(9375), pp.2099–2106.

Jacobs, I.J., Menon, U., Ryan, A., Gentry-Maharaj, A., Burnell, M., Kalsi, J.K., Amso, N.N., Apostolidou, S., Benjamin, E., Cruickshank, D., Crump, D.N., Davies, S.K., Dawnay, A., Dobbs, S., Fletcher, G., Ford, J., Godfrey, K., Gunu, R., Habib, M., Hallett, R., Herod, J., Jenkins, H., Karpinskyj, C., Leeson, S., Lewis, S.J., Liston, W.R., Lopes, A., Mould, T., Murdoch, J., Oram, D., Rabideau, D.J., Reynolds, K., Scott, I.,

Seif, M.W., Sharma, A., Singh, N., Taylor, J., Warburton, F., Widschwendter, M., Williamson, K., Woolas, R., Fallowfield, L., McGuire, A.J., Campbell, S., Parmar, M. and Skates, S.J., 2016. Ovarian cancer screening and mortality in the UK Collaborative Trial of Ovarian Cancer Screening (UKCTOCS): A randomised controlled trial. *The Lancet*, 387(10022), pp.945–956.

Jenkins, V., Catt, S., Banerjee, S., Gourley, C., Montes, a, Solis-Trapala, I., Monson, K. and Fallowfield, L., 2013. Patients' and oncologists' views on the treatment and care of advanced ovarian cancer in the UK: results from the ADVOCATE study. *British journal of cancer*, [online] 55(55), pp.1–8. Available at: <http://www.ncbi.nlm.nih.gov/pubmed/23652312>.

Kalluri, R. and Weinberg, R.A., 2009. The basics of epithelial-mesenchymal transition. *Journal of Clinical Investigation*, pp.1420–1428.

Kanai, T., Ito, Z., Oji, Y., Suka, M., Nishida, S., Takakura, K., Kajihara, M., Saruta, M., Fujioka, S., Misawa, T., Akiba, T., Yanagisawa, H., Shimodaira, S., Okamoto, M., Sugiyama, H. and Koido, S., 2018. Prognostic significance of wilms' tumor 1 expression in patients with pancreatic ductal adenocarcinoma. *Oncology Letters*, 16(2), pp.2682–2692.

Karantza, V., 2011. Keratins in health and cancer: more than mere epithelial cell markers. *Oncogene*, 30(2), pp.127–138.

Katopodis, P., Chudasama, D., Wander, G., Sales, L., Kumar, J., Pandhal, M., Anikin, V., Chatterjee, J., Hall, M. and Karteris, E., 2019. Kinase inhibitors and ovarian cancer. *Cancers*, 11(9), pp.1–17.

Kaur, A., Riaz, M.S., Murugaiah, V., Varghese, P.M., Singh, S.K. and Kishore, U., 2018a. A Recombinant fragment of human surfactant protein D induces apoptosis in pancreatic cancer cell lines via fas-mediated pathway. *Frontiers in Immunology*, 9(JUN).

Kaur, A., Riaz, M.S., Singh, S.K. and Kishore, U., 2018b. Human surfactant protein D suppresses epithelial-to-mesenchymal transition in pancreatic cancer cells by downregulating TGF-β. *Frontiers in Immunology*, 9(AUG), pp.1–13.

Kaye, S.B., Lubinski, J., Matulonis, U., Ang, J.E., Gourley, C., Karlan, B.Y., Amnon, A., Bell-McGuinn, K.M., Chen, L.M., Friedlander, M., Safra, T., Vergote, I., Wickens, M., Lowe, E.S., Carmichael, J. and Kaufman, B., 2012. Phase II, open-label, randomized, multicenter study comparing the efficacy and safety of olaparib, a poly (ADP-ribose) polymerase inhibitor, and pegylated liposomal doxorubicin in patients with BRCA1 or BRCA2 mutations and recurrent ovarian cancer. *Journal of Clinical Oncology*, 30(4), pp.372–379.

Keating, G.M., 2014. Bevacizumab: A review of its use in advanced cancer. *Drugs*, 74(16), pp.1891–1925.

Keller, L., Werner, S. and Pantel, K., 2019. Biology and clinical relevance of EpCAM. *Cell Stress*, 3(6), pp.165–180.

Kerliu, L., Myruski, S., Bhatti, A., Soni, P., Petrosius, P., Pervanas, H.C. and Horton, E.R., 2020. Niraparib for the Treatment of Recurrent Epithelial Ovarian, Fallopian Tube, or Primary Peritoneal Cancer. *Annals of Pharmacotherapy*, 54(10), pp.1010–1015.

Kim, A., Ueda, Y., Naka, T. and Enomoto, T., 2012. Therapeutic strategies in epithelial ovarian cancer. *Journal of Experimental & Clinical Cancer Research*, [online] 31(1), p.14. Available at: <http://www.jeccr.com/content/31/1/14>.

Kim, M., Suh, D.H., Choi, J.Y., Bu, J., Kang, Y.T., Kim, K., No, J.H., Kim, Y.B. and Cho, Y.H., 2019. Post-debulking circulating tumor cell as a poor prognostic marker in advanced stage ovarian cancer: A prospective observational study. *Medicine*, 98(20), p.e15354.

Kishore, U., Greenhough, T.J., Waters, P., Shrive, A.K., Ghai, R., Kamran, M.F., Bernal, A.L., Reid, K.B.M., Madan, T. and Chakraborty, T., 2006. Surfactant proteins SP-A and SP-D: Structure, function and receptors. *Molecular Immunology*, 43(9), pp.1293–1315.

Köbel, M., Bak, J., Bertelsen, B.I., Carpen, O., Grove, A., Hansen, E.S., Levin Jakobsen, A.M., Lidang, M., Måsbäck, A., Tolf, A., Gilks, C.B. and Carlson, J.W., 2014. Ovarian carcinoma histotype determination is highly reproducible, and is improved through the use of immunohistochemistry. *Histopathology*, 64(7), pp.1004–1013.

Köbel, M., Piskorz, A.M., Lee, S., Lui, S., LePage, C., Marass, F., Rosenfeld, N., Masson, A.M.M. and Brenton, J.D., 2016a. Optimized p53 immunohistochemistry is an accurate predictor of TP53 mutation in ovarian carcinoma. *Journal of Pathology: Clinical Research*, 2(4), pp.247–258.

Köbel, M., Rahimi, K., Rambau, P.F., Naugler, C., Le Page, C., Meunier, L., De Ladurantaye, M., Lee, S., Leung, S., Goode, E.L., Ramus, S.J., Carlson, J.W., Li, X., Ewanowich, C.A., Kelemen, L.E., Vanderhyden, B., Provencher, D., Huntsman, D., Lee, C.H., Gilks, C.B. and Mes Masson, A.M., 2016b. An Immunohistochemical Algorithm for Ovarian Carcinoma Typing. *International Journal of Gynecological Pathology*, 35(5), pp.430–441.

Koch, C., Joosse, S.A., Schneegans, S., Wilken, O.J.W., Janning, M., Loreth, D., Müller, V., Prieske, K., Banys-Paluchowski, M., Horst, L.J., Loges, S., Peine, S., Wikman, H., Gorges, T.M. and Pantel, K., 2020. Pre-analytical and analytical variables of label-independent enrichment and automated detection of circulating tumor cells in cancer patients. *Cancers*, 12(2).

Konecny, G.E. and Kristeleit, R.S., 2016. PARP inhibitors for BRCA1/2-mutated and sporadic ovarian cancer: Current practice and future directions. *British Journal of Cancer*, [online] 115(10),

pp.1157–1173. Available at: <http://dx.doi.org/10.1038/bjc.2016.311>.

Krebs, M.G., Hou, J.M., Ward, T.H., Blackhall, F.H. and Dive, C., 2010. Circulating tumour cells: Their utility in cancer management and predicting outcomes. *Therapeutic Advances in Medical Oncology*, 2(6), pp.351–365.

Kumar, J., CHUDASAMA, D., Roberts, C., Kubista, M., Sjöback, R., Chatterjee, J., ANIKIN, V., Karteris, E. and Hall, 2019a. Detection of Abundant Non-Haematopoietic Circulating Cancer-Related Cells in Patients with Advanced Epithelial Ovarian Cancer. *Cells*, 8(7), p.732.

Kumar, J., Murugaiah, V., Sotiriadis, G., Kaur, A., Jeyaneethi, J., Sturniolo, I., Alhamlan, F.S., Chatterjee, J., Hall, M., Kishore, U. and Karteris, E., 2019b. Surfactant Protein D as a Potential Biomarker and Therapeutic Target in Ovarian Cancer. *Frontiers in Oncology*, 9(July), pp.1–14.

Kumari, S., 2018. Serum Biomarker Based Algorithms in Diagnosis of Ovarian Cancer: A Review. *Indian Journal of Clinical Biochemistry*, [online] 33(4), pp.382–386. Available at: <https://doi.org/10.1007/s12291-018-0786-2>.

Kurman, R. and Shih, I., 2010. The Origin and pathogenesis of epithelial ovarian cancer-a proposed unifying theory. *The American journal of surgical pathology*, [online] 34(3), pp.433–443. Available at: <http://www.ncbi.nlm.nih.gov/pmc/articles/PMC2841791/>.

Kwon, Y., Cukierman, E. and Godwin, A.K., 2011. Differential expressions of adhesive molecules and proteases define mechanisms of ovarian tumor cell matrix penetration/invasion. *PLoS ONE*, 6(4).

Kyung-A Hyun, Goo, K.B., Han, H., Sohn, J., Choi, W., Kim, S. Il, Jung, H. Il and Kim, Y.S., 2016. Epithelial-to-mesenchymal transition leads to loss of EpCAM and different physical properties in circulating tumor cells from metastatic breast cancer. *Oncotarget*, 7(17), pp.24677–24687.

Lee, K., Lee, S.J., Yoon, S., Ryoo, B.Y., Kim, S.W., Choi, S.H., Lee, S.M., Chae, E.J., Park, Y., Jang, S.J., Park, S.Y., Yoon, Y.K., Park, S.H. and Kim, T.W., 2019. Feasibility, safety, and adequacy of research biopsies for cancer clinical trials at an academic medical center. *PLoS ONE*, [online] 14(8), pp.1–12. Available at: <http://dx.doi.org/10.1371/journal.pone.0221065>.

Leth-Larsen, R., Floridon, C., Nielsen, O. and Holmskov, U., 2004. Surfactant protein D in the female genital tract. *Molecular Human Reproduction*, 10(3), pp.149–154.

Lheureux, S., Braunstein, M. and Oza, A.M., 2019. Epithelial ovarian cancer: Evolution of management in the era of precision medicine. *CA: A Cancer Journal for Clinicians*, pp.280–304.

Li, Y., Wu, G., Yang, W., Wang, X., Duan, L., Niu, L., Zhang, Y., Liu, J., Hong, L. and Fan, D., 2020.

Prognostic value of circulating tumor cells detected with the CellSearch system in esophageal cancer patients: A systematic review and meta-analysis. *BMC Cancer*, 20(1), pp.1–11.

Liang, B., Peng, P., Chen, S., Li, L., Zhang, M., Cao, D., Yang, J., Li, H., Gui, T., Li, X. and Shen, K., 2013. Characterization and proteomic analysis of ovarian cancer-derived exosomes. *Journal of Proteomics*, 80, pp.171–182.

Lianidou, E. and Pantel, K., 2019. Liquid biopsies. *Genes Chromosomes and Cancer*, 58(4), pp.219–232.

Liliac, L., Luisa Carcangiu, M., Canevari, S., Căruntu, I.D., Apostol, D.G.C., Danciu, M., Onofriescu, M. and Amălinei, C., 2013. The value of PAX8 and WT1 molecules in ovarian cancer diagnosis. *Romanian Journal of Morphology and Embryology*, 54(1), pp.17–27.

Lim, S. Bin, Di Lee, W., Vasudevan, J., Lim, W.-T. and Lim, C.T., 2019. Liquid biopsy: one cell at a time. *npj Precision Oncology*, [online] 3(1). Available at: <http://dx.doi.org/10.1038/s41698-019-0095-0>.

Lin, P.P., 2020. Aneuploid Circulating Tumor-Derived Endothelial Cell (CTEC): A Novel Versatile Player in Tumor Neovascularization and Cancer Metastasis. *Cells*, 9(6).

Liu, M. and Guo, F., 2018. Recent updates on cancer immunotherapy. *Precision Clinical Medicine*, 1(2), pp.65–74.

Liu, Z., Yamanouchi, K., Ohtao, T., Matsumura, S., Seino, M., Shridhar, V., Takahashi, T., Takahashi, K. and Kurachi, H., 2014. High levels of wilms' tumor 1 (WT1) expression were associated with aggressive clinical features in ovarian cancer. *Anticancer Research*, 34(5), pp.2331–2340.

Loeb, D.M., Evron, E., Patel, C.B., Sharma, P.M., Niranjan, B., Buluwela, L., Weitzman, S.A., Korz, D. and Sukumar, S., 2001. Wilms' tumor suppressor gene (WT1) is expressed in primary breast tumors despite tumor-specific promoter methylation. *Cancer Research*, 61(3), pp.921–925.

Loizzi, V., Ranieri, G., Laforgia, M., Gadaleta, C.D., Gargano, G., Kardhashi, A., de Liso, M., Naglieri, E., Del Vecchio, V., Cicinelli, E. and Cormio, G., 2020. Parp inhibitors and epithelial ovarian cancer: Molecular mechanisms, clinical development and future prospective (Review). *Oncology Letters*, 20(4), pp.1–9.

Loud, J. and Murphy, J., 2017. Cancer screening and early detection in the 21st century. *Seminal Oncology Nursing*, 33(2), pp.121–128.

Lu, K.H., Patterson, A.P., Wang, L., Marquez, R.T., Atkinson, E.N., Baggerly, K.A., Ramoth, L.R., Rosen, D.G., Liu, J., Hellstrom, I., Smith, D., Hartmann, L., Fishman, D., Berchuck, A., Schmandt, R.,

Whitaker, R., Gershenson, D.M., Mills, G.B. and Bast, R.C., 2004. Selection of potential markers for epithelial ovarian cancer with gene expression arrays and recursive descent partition analysis. *Clinical Cancer Research*, 10(10), pp.3291–3300.

Luvero, D., Milani, A. and Ledermann, J.A., 2014. Treatment options in recurrent ovarian cancer: Latest evidence and clinical potential. *Therapeutic Advances in Medical Oncology*, 6(5), pp.229–239.

Mahajan, L., Gautam, P., Dodagatta-Marri, E., Madan, T. and Kishore, U., 2014. Surfactant protein SP-D modulates activity of immune cells: Proteomic profiling of its interaction with eosinophilic cells. *Expert Review of Proteomics*, 11(3), pp.355–369.

Mahajan, L., Pandit, H., Madan, T., Gautam, P., Yadav, A.K., Warke, H., Sundaram, C.S., Sirdeshmukh, R., Sarma, P.U., Kishore, U. and Surolia, A., 2013. Human surfactant protein D alters oxidative stress and HMGA1 expression to induce p53 apoptotic pathway in eosinophil leukemic cell line. *PLoS ONE*, 8(12), pp.1–16.

Maheswaran, S., Englert, C., Bennett, P., Heinrich, G. and Haber, D.A., 1995. The WT1 gene product stabilizes p53 and inhibits p53-mediated apoptosis. *Genes and Development*, 9(17), pp.2143–2156.

Maki, T., Ikeda, H., Kuroda, A., Kyogoku, N., Yamamura, Y., Tabata, Y., Abiko, T., Tsuchikawa, T., Hida, Y., Shichinohe, T., Tanaka, E., Kaga, K., Hatanaka, K., Matsuno, Y., Imai, N. and Hirano, S., 2017. Differential detection of cytoplasmic Wilms tumor 1 expression by immunohistochemistry, western blotting and mRNA quantifcation. *International Journal of Oncology*, 50(1), pp.129–140.

Mangogna, A., Belmonte, B., Agostinis, C., Ricci, G., Gulino, A., Ferrara, I., Zanconati, F., Tripodo, C., Romano, F., Kishore, U. and Bulla, R., 2018. Pathological significance and prognostic value of surfactant protein D in cancer. *Frontiers in Immunology*, 9(AUG), pp.1–12.

Mannelli, C., 2019. Tissue vs Liquid Biopsies for Cancer Detection: Ethical Issues. *Journal of Bioethical Inquiry*, 16(4), pp.551–557.

Marchetti, C., Palaia, I., De Felice, F., Musella, A., Donfracesco, C., Vertechy, L., Romito, A., Piacenti, I., Musio, D., Muzii, L., Tombolini, V. and Benedetti Panici, P., 2016. Tyrosine-kinases inhibitors in recurrent platinum-resistant ovarian cancer patients. *Cancer Treatment Reviews*, [online] 42, pp.41–46. Available at: <http://dx.doi.org/10.1016/j.ctrv.2015.10.011>.

Mari, R., Mamessier, E., Lambaudie, E., Provansal, M., Birnbaum, D., Bertucci, F. and Sabatier, R., 2019. Liquid biopsies for ovarian carcinoma: How blood tests may improve the clinical management of a deadly disease. *Cancers*, 11(6), pp.1–23.

Marmot, M.G., Altman, D.G., Cameron, D.A., Dewar, J.A., Thompson, S.G. and Wilcox, M., 2013. The benefits and harms of breast cancer screening: An independent review. *British Journal of Cancer*, [online] 108(11), pp.2205–2240. Available at: <http://dx.doi.org/10.1038/bjc.2013.177>.

Martínez-Estrada, O.M., Lettice, L.A., Essafi, A., Guadix, J.A., Slight, J., Velecela, V., Hall, E., Reichmann, J., Devenney, P.S., Hohenstein, P., Hosen, N., Hill, R.E., Mũoz-Chapuli, R. and Hastie, N.D., 2010. Wt1 is required for cardiovascular progenitor cell formation through transcriptional control of Snail and E-cadherin. *Nature Genetics*, 42(1), pp.89–93.

Mateo, J., Lord, C.J., Serra, V., Tutt, A., Balmaña, J., Castroviejo-Bermejo, M., Cruz, C., Oaknin, A., Kaye, S.B. and De Bono, J.S., 2019. A decade of clinical development of PARP inhibitors in perspective. *Annals of Oncology*, 30(9), pp.1437–1447.

Matsuo, Y., Sawai, H., Ochi, N., Yasuda, A., Sakamoto, M., Takahashi, H., Funahashi, H., Takeyama, H. and Guha, S., 2010. Proteasome inhibitor MG132 inhibits angiogenesis in pancreatic cancer by blocking nf-κb activity. *Digestive Diseases and Sciences*, 55(4), pp.1167–1176.

Mavaddat, N., Peock, S., Frost, D., Ellis, S., Platte, R., Fineberg, E., Evans, D.G., Izatt, L., Eeles, R.A., Adlard, J., Davidson, R., Eccles, D., Cole, T., Cook, J., Brewer, C., Tischkowitz, M., Douglas, F., Hodgson, S., Walker, L., Porteous, M.E., Morrison, P.J., Side, L.E., Kennedy, M.J., Houghton, C., Donaldson, A., Rogers, M.T., Dorkins, H., Miedzybrodzka, Z., Gregory, H., Eason, J., Barwell, J., McCann, E., Murray, A., Antoniou, A.C. and Easton, D.F., 2013. Cancer risks for BRCA1 and BRCA2 mutation carriers: Results from prospective analysis of EMBRACE. *Journal of the National Cancer Institute*, 105(11), pp.812–822.

McCluggage, W.G., 2000. Recent advances in immunohistochemistry in the diagnosis of ovarian neoplasms. *Journal of Clinical Pathology*, 53(5), pp.327–334.

Medeiros, L.R., Rosa, D.D., da Rosa, M.I. and Bozzetti, M.C., 2009. Accuracy of CA 125 in the diagnosis of ovarian tumors: A quantitative systematic review. *European Journal of Obstetrics and Gynecology and Reproductive Biology*, 142(2), pp.99–105.

Menke, A.L., Clarke, A.R., Leitch, A., Ijpenberg, A., Williamson, K.A., Spraggon, L., Harrison, D.J. and Hastie, N.D., 2002. Genetic interactions between the Wilms' tumor 1 gene and the p53 gene. *Cancer Research*, 62(22), pp.6615–6620.

Menon, U., Gentry-Maharaj, A., Burnell, M., Singh, N., Ryan, A., Karpinskyj, C., Carlino, G., Taylor, J., Massingham, S.K., Raikou, M., Kalsi, J.K., Woolas, R., Manchanda, R., Arora, R., Casey, L., Dawnay, A., Dobbs, S., Leeson, S., Mould, T., Seif, M.W., Sharma, A., Williamson, K., Liu, Y., Fallowfield, L., McGuire, A.J., Campbell, S., Skates, S.J., Jacobs, I.J. and Parmar, M., 2021. Ovarian cancer population screening and mortality after long-term follow-up in the UK Collaborative Trial of Ovarian Cancer

Screening (UKCTOCS): a randomised controlled trial. *The Lancet*, [online] 397(10290), pp.2182–2193. Available at: <http://dx.doi.org/10.1016/S0140-6736(21)00731-5>.

Merker, J.D., Oxnard, G.R., Compton, C., Diehn, M., Hurley, P., Lazar, A.J., Lindeman, N., Lockwood, C.M., Rai, A.J., Schilsky, R.L., Tsimberidou, A.M., Vasalos, P., Billman, B.L., Oliver, T.K., Bruinooge, S.S., Hayes, D.F. and Turner, N.C., 2018. Circulating tumor DNA analysis in patients with cancer: American society of clinical oncology and college of American pathologists joint review. *Journal of Clinical Oncology*, [online] 36(16), pp.1631–1641. Available at: <https://doi.org/10.1200/JCO.2017.76.8671>.

Miller, M.C., Robinson, P.S., Wagner, C. and O'Shannessy, D.J., 2018. The Parsortix™ Cell Separation System—A versatile liquid biopsy platform. *Cytometry Part A*, 93(12), pp.1234–1239.

Mirzayans, R., Andrais, B. and Murray, D., 2018. Roles of polyploid/multinucleated giant cancer cells in metastasis and disease relapse following anticancer treatment. *Cancers*, 10(4).

Mittica, G., Ghisoni, E., Giannone, G., Genta, S., Aglietta, M., Sapino, A. and Valabrega, G., 2018. PARP Inhibitors in Ovarian Cancer. *Recent Patents on Anti-Cancer Drug Discovery*, 13(4), pp.392–410.

Monk, B.J., Minion, L.E. and Coleman, R.L., 2016. Anti-angiogenic agents in ovarian cancer: Past, present, and future. *Annals of Oncology*, 27(Supplement 1), pp.i33–i39.

Morgan, T.M., 2019. Liquid biopsy: Where did it come from, what is it, and where is it going? *Investigative and Clinical Urology*, 60(3), pp.139–141.

Moss, E.L., Hollingworth, J. and Reynolds, T.M., 2005. The role of CA125 in clinical practice. *Journal of Clinical Pathology*, 58(3), pp.308–312.

Muinao, T., Deka Boruah, H.P. and Pal, M., 2019. Multi-biomarker panel signature as the key to diagnosis of ovarian cancer. *Heliyon*, [online] 5(12), p.e02826. Available at: <https://doi.org/10.1016/j.heliyon.2019.e02826>.

Murugaiah, V., Agostinis, C., Varghese, P.M., Belmonte, B., Vieni, S., Alaql, F.A., Alrokayan, S.H., Khan, H.A., Kaur, A., Roberts, T., Madan, T., Bulla, R. and Kishore, U., 2020. Hyaluronic Acid Present in the Tumor Microenvironment Can Negate the Pro-apototic Effect of a Recombinant Fragment of Human Surfactant Protein D on Breast Cancer Cells. *Frontiers in Immunology*, 11(July), pp.1–17.

Nagy, Á., Lánczky, A., Menyhárt, O. and Gyorffy, B., 2018. Validation of miRNA prognostic power in hepatocellular carcinoma using expression data of independent datasets. *Scientific Reports*, 8(1), pp.1–9.

Nakamura, K., Sawada, K., Kobayashi, M., Miyamoto, M., Shimizu, A., Yamamoto, M., Kinose, Y. and Kimura, T., 2019. Role of the exosome in ovarian cancer progression and its potential as a therapeutic target. *Cancers*, 11(8), pp.1–16.

Nakatsuka, S.I., Oji, Y., Horiuchi, T., Kanda, T., Kitagawa, M., Takeuchi, T., Kawano, K., Kuwae, Y., Yamauchi, A., Okumura, M., Kitamura, Y., Oka, Y., Kawase, I., Sugiyama, H. and Aozasa, K., 2006. Immunohistochemical detection of WT1 protein in a variety of cancer cells. *Modern Pathology*, 19(6), pp.804–814.

Naora, H. and Montell, D.J., 2005. Ovarian cancer metastasis: Integrating insights from disparate model organisms. *Nature Reviews Cancer*, 5(5), pp.355–366.

Nash, Z. and Menon, U., 2020. Ovarian cancer screening: Current status and future directions. *Best Practice and Research: Clinical Obstetrics and Gynaecology*, [online] 65(xxxx), pp.32–45. Available at: <https://doi.org/10.1016/j.bpobgyn.2020.02.010>.

Nayak, A., Dodagatta-Marri, E., Tsolaki, A.G. and Kishore, U., 2012. An insight into the diverse roles of surfactant proteins, SP-A and SP-D in innate and adaptive immunity. *Frontiers in Immunology*, 3(JUN), pp.1–21.

Neumann, M.H.D., Bender, S., Krahn, T. and Schlange, T., 2018. ctDNA and CTCs in Liquid Biopsy – Current Status and Where We Need to Progress. *Computational and Structural Biotechnology Journal*, 16, pp.190–195.

NICE, 2017. *NICE Guidelines*. [online] Available at: <https://www.nice.org.uk/guidance/cg122>.

Niksic, M., Slight, J., Sanford, J.R., Caceres, J.F. and Hastie, N.D., 2004. The Wilms' tumour protein (WT1) shuttles between nucleus and cytoplasm and is present in functional polysomes. *Human Molecular Genetics*, 13(4), pp.463–471.

Norquist, B.M., Harrell, M.I., Brady, M.F., Walsh, T., Lee, M.K., Gulsuner, S., Bernards, S.S., Casadei, S., Yi, Q., Burger, R.A., Chan, J.K., Davidson, S.A., Mannel, R.S., DiSilvestro, P.A., Lankes, H.A., Ramirez, N.C., King, M.C., Swisher, E.M. and Birrer, M.J., 2016. Inherited mutations in women with ovarian carcinoma. *JAMA Oncology*, 2(4), pp.482–490.

Ohno, S., Dohi, S., Ohno, Y., Kyo, S., Sugiyama, H., Suzuki, N. and Inoue, M., 2009. Immunohistochemical detection of WT1 protein in endometrial cancer. *Anticancer Research*, 29(5), pp.1691–1695.

Oji, Y., Miyoshi, S., Maeda, H., Hayashi, S., Tamaki, H., Nakatsuka, S.I., Yao, M., Takahashi, E., Nakano, Y., Hirabayashi, H., Shintani, Y., Oka, Y., Tsuboi, A., Hosen, N., Asada, M., Fujioka, T., Murakami, M., Kanato, K., Motomura, M., Kim, E.H., Kawakami, M., Ikegame, K., Ogawa, H., Aozasa, K., Kawase, I.

and Sugiyama, H., 2002. Overexpression of the Wilms' tumor gene WT1 in de novo lung cancers. *International Journal of Cancer*, 100(3), pp.297–303.

Olsen, C.M., Green, A.C., Whiteman, D.C., Sadeghi, S., Kolahdooz, F. and Webb, P.M., 2007. Obesity and the risk of epithelial ovarian cancer: A systematic review and meta-analysis. *European Journal of Cancer*, 43(4), pp.690–709.

Oncomine, n.d. *ONCOMINE*. [online] Available at: <www.oncomine.org>.

Palmirotta, R., Lovero, D., Cafforio, P., Felici, C., Mannavola, F., Pelle, E., Quaresmini, D., Tucci, M. and Silvestris, F., 2018. Liquid biopsy of cancer: a multimodal diagnsotic tool in clinical oncology. *Therapeutic Advances in Medical Oncology*, 10, pp.1–26.

Pantel, K. and Alix-Panabières, C., 2019. Liquid biopsy and minimal residual disease — latest advances and implications for cure. *Nature Reviews Clinical Oncology*, [online] 16(7), pp.409–424. Available at: <http://dx.doi.org/10.1038/s41571-019-0187-3>.

Parackal, S., Zou, D., Day, R., Black, M. and Guilford, P., 2019. Comparison of Roche Cell-Free DNA collection Tubes® to Streck Cell-Free DNA BCT®s for sample stability using healthy volunteers. *Practical Laboratory Medicine*, [online] 16(June), p.e00125. Available at: <https://doi.org/10.1016/j.plabm.2019.e00125>.

Pardoll, D., 2015. Cancer and the Immune System: Basic Concepts and Targets for Intervention. *Seminal Oncology*, pp.523–538.

Parenti, R., Cardile, V., Graziano, A.C.E., Parenti, C., Venuti, A., Bertuccio, M.P., Lo Furno, D. and Magro, G., 2014. Wilms' tumor gene 1 (WT1) silencing inhibits proliferation of malignant peripheral nerve sheath tumor snf96.2 cell line. *PLoS ONE*, 9(12), pp.1–16.

Parpart-Li, S., Bartlett, B., Popoli, M., Adleff, V., Tucker, L., Steinberg, R., Georgiadis, A., Phallen, J., Brahmer, J., Azad, N., Browner, I., Laheru, D., Velculescu, V.E., Sausen, M. and Diaz, L.A., 2017. The effect of preservative and temperature on the analysis of circulating tumor DNA. *Clinical Cancer Research*, 23(10), pp.2471–2477.

Parris, C.N., Adam Zahir, S., Al-Ali, H., Bourton, E.C., Plowman, C. and Plowman, P.N., 2015. Enhanced γ-H2AX DNA damage foci detection using multimagnification and extended depth of field in imaging flow cytometry. *Cytometry Part A*, 87(8), pp.717–723.

Pearce, C.L., Templeman, C., Rossing, M.A., Lee, A., Near, A.M., Webb, P.M., Nagle, C.M., Doherty, J.A., Cushing-Haugen, K.L., Wicklund, K.G., Chang-Claude, J., Hein, R., Lurie, G., Wilkens, L.R., Carney, M.E., Goodman, M.T., Moysich, K., Kjaer, S.K., Hogdall, E., Jensen, A., Goode, E.L., Fridley, B.L., Larson, M.C., Schildkraut, J.M., Palmieri, R.T., Cramer, D.W., Terry, K.L., Vitonis, A.F., Titus, L.J.,

Ziogas, A., Brewster, W., Anton-Culver, H., Gentry-Maharaj, A., Ramus, S.J., Anderson, A.R., Brueggmann, D., Fasching, P.A., Gayther, S.A., Huntsman, D.G., Menon, U., Ness, R.B., Pike, M.C., Risch, H., Wu, A.H. and Berchuck, A., 2012. Association between endometriosis and risk of histological subtypes of ovarian cancer: A pooled analysis of case-control studies. *The Lancet Oncology*, [online] 13(4), pp.385–394. Available at: <http://dx.doi.org/10.1016/S1470-2045(11)70404-1>.

Pearl, M.L., Zhao, Q., Yang, J., Dong, H., Tulley, S., Zhang, Q., Golightly, M., Zucker, S. and Chen, W.T., 2014. Prognostic analysis of invasive circulating tumor cells (iCTCs) in epithelial ovarian cancer. *Gynecologic oncology*, 134(3), pp.581–590.

Pereira, E., Camacho-Vanegas, O., Anand, S., Sebra, R., Camacho, S.C., Garnar-Wortzel, L., Nair, N., Moshier, E., Wooten, M., Uzilov, A., Chen, R., Prasad-Hayes, M., Zakashansky, K., Beddoe, A.M., Schadt, E., Dottino, P. and Martignetti, J.A., 2015. Personalized circulating tumor DNA biomarkers dynamically predict treatment response and survival in gynecologic cancers. *PLoS ONE*, 10(12), pp.1–13.

Peto, P.J., Gilham, P.C., Fletcher, O. and Matthews, F.E., 2004. The cervical cancer epidemic that screening has prevented in the UK. *Lancet*, 364(9430), pp.249–256.

Pignata, S., Cecere, S.C., Du Bois, A., Harter, P. and Heitz, F., 2017. Treatment of recurrent ovarian cancer. *Annals of Oncology*, [online] 28(Supplement 8), pp.viii51–viii56. Available at: <http://dx.doi.org/10.1093/annonc/mdx441>.

Prat, J., 2015. FIGO Committee on Gynecologic Oncology. Staging classification for cancer of the ovary, fallopian tube, and peritoneum. *International Journal of Gynecology and Obstetrics*, [online] 124(1), pp.1–5. Available at: <http://www.pubmedcentral.nih.gov/articlerender.fcgi?artid=4397237&tool=pmcentrez&rendertype=abstract>.

Pujade-Lauraine, E., Ledermann, J.A., Selle, F., Gebski, V., Penson, R.T., Oza, A.M., Korach, J., Huzarski, T., Poveda, A., Pignata, S., Friedlander, M., Colombo, N., Harter, P., Fujiwara, K., Ray-Coquard, I., Banerjee, S., Liu, J., Lowe, E.S., Bloomfield, R., Pautier, P., Korach, J., Huzarski, T., Byrski, T., Pautier, P., Harter, P., Colombo, N., Scambia, G., Nicoletto, M., Nussey, F., Clamp, A., Penson, R., Oza, A., Poveda Velasco, A., Rodrigues, M., Lotz, J.P., Selle, F., Ray-Coquard, I., Provencher, D., Prat Aparicio, A., Vidal Boixader, L., Scott, C., Tamura, K., Yunokawa, M., Lisyanskaya, A., Medioni, J., Pécuchet, N., Dubot, C., de la Motte Rouge, T., Kaminsky, M.C., Weber, B., Lortholary, A., Parkinson, C., Ledermann, J., Williams, S., Banerjee, S., Cosin, J., Hoffman, J., Penson, R., Plante, M., Covens, A., Sonke, G., Joly, F., Floquet, A., Banerjee, S., Hirte, H., Amit, A., Park-Simon, T.W., Matsumoto, K.,

Tjulandin, S., Kim, J.H., Gladieff, L., Sabbatini, R., O'Malley, D., Timmins, P., Kredentser, D., Laínez Milagro, N., Barretina Ginesta, M.P., Tibau Martorell, A., Gómez de Liaño Lista, A., Ojeda González, B., Mileshkin, L., Mandai, M., Boere, I., Ottevanger, P., Nam, J.H., Filho, E., Hamizi, S., Cognetti, F., Warshal, D., Dickson-Michelson, E., Kamelle, S., McKenzie, N., Rodriguez, G., Armstrong, D., Chalas, E., Celano, P., Behbakht, K., Davidson, S., Welch, S., Helpman, L., Fishman, A., Bruchim, I., Sikorska, M., Słowińska, A., Rogowski, W., Bidziński, M., Śpiewankiewicz, B., Casado Herraez, A., Mendiola Fernández, C., Gropp-Meier, M., Saito, T., Takehara, K., Enomoto, T., Watari, H., Choi, C.H., Kim, B.G., Kim, J.W., Hegg, R. and Vergote, I., 2017. Olaparib tablets as maintenance therapy in patients with platinum-sensitive, relapsed ovarian cancer and a BRCA1/2 mutation (SOLO2/ENGOT-Ov21): a double-blind, randomised, placebo-controlled, phase 3 trial. *The Lancet Oncology*, 18(9), pp.1274–1284.

Punnoose, E.A., Atwal, S.K., Spoerke, J.M., Savage, H., Pandita, A., Yeh, R.F., Pirzkall, A., Fine, B.M., Amler, L.C., Chen, D.S. and Lackner, M.R., 2010. Molecular biomarker analyses using circulating tumor cells. *PLoS ONE*, 5(9), pp.1–12.

Qi, X.W., Zhang, F., Wu, H., Liu, J.L., Zong, B.G., Xu, C. and Jiang, J., 2015. Wilms' tumor 1 (WT1) expression and prognosis in solid cancer patients: A systematic review and meta-analysis. *Scientific Reports*, 5(Figure 1), pp.11–15.

Qin, J., Alt, J.R., Hunsley, B.A., Williams, T.L. and Fernando, M.R., 2014. Stabilization of circulating tumor cells in blood using a collection device with a preservative reagent. *Cancer Cell International*, [online] 14(1), pp.1–6. Available at: <Cancer Cell International>.

Rahbari, N.N., Schölch, S., Bork, U., Kahlert, C., Schneider, M., Rahbari, M., Büchler, M.W., Weitz, J. and Reissfelder, C., 2017. Prognostic value of circulating endothelial cells in metastatic colorectal cancer. *Oncotarget*, 8(23), pp.37491–37501.

Rauh-Hain, J. a, Krivak, T.C., Del Carmen, M.G. and Olawaiye, A.B., 2011. Ovarian cancer screening and early detection in the general population. *Reviews in obstetrics and gynecology*, 4(1), pp.15–21.

Rhodes, D.R., Yu, J., Shanker, K., Deshpande, N., Varambally, R., Ghosh, D., Barrette, T., Pander, A. and Chinnaiyan, A.M., 2004. ONCOMINE: A Cancer Microarray Database and Integrated Data-Mining Platform. *Neoplasia*, [online] 6(1), pp.1–6. Available at: <http://linkinghub.elsevier.com/retrieve/pii/S1476558604800472>.

Rodriguez-Lee, M., Kolatkar, A., Luttgen, M.M.C., Dago, A.D., Kendall, J., Carlsson, N.A., Bethel, K., Greenspan, E.J., Hwang, S.E., Waitman, K.R., Nieva, J.J., Hicks, J. and Kuhn, P., 2018. Effect of blood collection tube type and time to processing on the enumeration and high-content characterization

of circulating tumor cells using the high-definition single-cell assay. *Archives of Pathology and Laboratory Medicine*, 142(2), pp.198–207.

Rogers-Broadway, K.R., Kumar, J., Sisu, C., Wander, G., Mazey, E., Jeyaneethi, J., Pados, G., Tsolakidis, D., Klonos, E., Grunt, T., Hall, M., Chatterjee, J. and Karteris, E., 2019. Differential expression of mTOR components in endometriosis and ovarian cancer: Effects of rapalogues and dual kinase inhibitors on mTORC1 and mTORC2 stoichiometry. *International Journal of Molecular Medicine*, 43(1), pp.47–56.

Rojas, V., Hirshfield, K.M., Ganesan, S. and Rodriguez-Rodriguez, L., 2016. Molecular characterization of epithelial ovarian cancer: Implications for diagnosis and treatment. *International Journal of Molecular Sciences*, 17(12).

Rosenthal, A.N., Fraser, L.S.M., Philpott, S., Manchanda, R., Burnell, M., Badman, P., Hadwin, R., Rizzuto, I., Benjamin, E., Singh, N., Evans, D.G., Eccles, D.M., Ryan, A., Liston, R., Dawnay, A., Ford, J., Gunu, R., Mackay, J., Skates, S.J., Menon, U. and Jacobs, I.J., 2017. Evidence of stage shift in women diagnosed with ovarian cancer during phase II of the United Kingdom familial ovarian cancer screening study. *Journal of Clinical Oncology*, 35(13), pp.1411–1420.

Roy, R., Chun, J. and Powell, S.N., 2012. BRCA1 and BRCA2: Different roles in a common pathway of genome protection. *Nature Reviews Cancer*, 12(1), pp.68–78.

De Rubis, G., Rajeev Krishnan, S. and Bebawy, M., 2019. Liquid Biopsies in Cancer Diagnosis, Monitoring, and Prognosis. *Trends in Pharmacological Sciences*, [online] 40(3), pp.172–186. Available at: <https://doi.org/10.1016/j.tips.2019.01.006>.

Russano, M., Napolitano, A., Ribelli, G., Iuliani, M., Simonetti, S., Citarella, F., Pantano, F., Dell'Aquila, E., Anesi, C., Silvestris, N., Argentiero, A., Solimando, A.G., Vincenzi, B., Tonini, G. and Santini, D., 2020. Erratum: Liquid biopsy and tumor heterogeneity in metastatic solid tumors: The potentiality of blood samples (J Exp Clin Cancer Res. (2020) 39 (95) DOI: 10.1186/s13046-020-01601-2). *Journal of Experimental and Clinical Cancer Research*, 39(1), pp.1–13.

Salvatorelli, L., Calabrese, G., Parenti, R., Vecchio, G.M., Puzzo, L., Caltabiano, R., Musumeci, G. and Magro, G., 2020. Immunohistochemical expression of Wilms' tumor 1 protein in human tissues: From ontogenesis to neoplastic tissues. *Applied Sciences (Switzerland)*, 10(1).

Sánchez Vega, J.F., Murillo Bacilio, M. del R., Vintimilla Condoy, A.S., Palta González, A.M., Crespo Astudillo, J.A. and Mora-Bravo, F.G., 2018. Predictive equation of metastasis in patients with malignant ovarian epithelial tumors with the Ca-125 marker. *BMC Cancer*, 18(1), pp.1–5.

Sato, S. and Itamochi, H., 2014. Neoadjuvant chemotherapy in advanced ovarian cancer: Latest

results and place in therapy. *Therapeutic Advances in Medical Oncology*, 6(6), pp.293–304.

Schneck, H., Gierke, B., Uppenkamp, F., Behrens, B., Niederacher, D., Stoecklein, N.H., Templin, M.F., Pawlak, M., Fehm, T. and Neubauer, H., 2015. EpCAM-independent enrichment of circulating tumor cells in metastatic breast cancer. *PLoS ONE*, [online] 10(12), pp.1–23. Available at: <http://dx.doi.org/10.1371/journal.pone.0144535>.

Scholler, N. and Urban, N., 2007. CA125 in Ovarian Cancer. *Biomarkers in Medicine*, 4(1), pp.513–523.

Shi, L.F., Wu, Y. and Li, C.Y., 2016. Hormone therapy and risk of ovarian cancer in postmenopausal women: A systematic review and meta-analysis. *Menopause*, 23(4), pp.417–424.

Sidney, L.E., Branch, M.J., Dunphy, S.E., Dua, H.S. and Hopkinson, A., 2014. Concise review: Evidence for CD34 as a common marker for diverse progenitors. *Stem Cells*, 32(6), pp.1380–1389.

Sin, D.D., Man, S.F.P., McWilliams, A. and Lam, S., 2008. Surfactant protein D and bronchial dysplasia in smokers at high risk of lung cancer. *Chest*, [online] 134(3), pp.582–588. Available at: <http://dx.doi.org/10.1378/chest.08-0600>.

Siravegna, G., Mussolin, B., Venesio, T., Marsoni, S., Seoane, J., Dive, C., Papadopoulos, N., Kopetz, S., Corcoran, R.B., Siu, L.L. and Bardelli, A., 2019. How liquid biopsies can change clinical practice in oncology. *Annals of Oncology*, 30(10), pp.1580–1590.

Sorensen, G.L., 2018. Surfactant protein D in respiratory and non-respiratory diseases. *Frontiers in Medicine*, 5(FEB).

Steffensen, K.D., Madsen, C.V., Andersen, R.F., Waldstrøm, M., Adimi, P. and Jakobsen, A., 2014. Prognostic importance of cell-free DNA in chemotherapy resistant ovarian cancer treated with bevacizumab. *European Journal of Cancer*, 50(15), pp.2611–2618.

Stimpfl, M., Schmid, B.C., Schiebel, I., Tong, D., Leodolter, S., Obermair, A. and Zeillinger, R., 1999. Expression of mucins and cytokeratins in ovarian cancer cell lines. *Cancer Letters*, 145(1–2), pp.133–141.

Strotman, L.N., Millner, L.M., Valdes, R. and Linder, M.W., 2016. Liquid Biopsies in Oncology and the Current Regulatory Landscape. *Molecular Diagnosis and Therapy*, 20(5), pp.429–436.

Sturgeon, C.M., Duffy, M.J. and Walker, G., 2011. The National Institute for Health and Clinical Excellence (NICE) guidelines for early detection of ovarian cancer: The pivotal role of the clinical laboratory. *Annals of Clinical Biochemistry*, 48(4), pp.295–299.

Sueblinvong, T. and Carney, M.E., 2009. Current understanding of risk factors for ovarian cancer.

Current Treatment Options in Oncology, 10(1–2), pp.67–81.

Sung, H.K., Ma, S.H., Choi, J.Y., Hwang, Y., Ahn, C., Kim, B.G., Kim, Y.M., Kim, J.W., Kang, S., Kim, J., Kim, T.J., Yoo, K.Y., Kang, D. and Park, S., 2016. The effect of breastfeeding duration and parity on the risk of epithelial ovarian cancer: A systematic review and meta-analysis. *Journal of Preventive Medicine and Public Health*, 49(6), pp.349–366.

Swann, J.B. and Smyth, M.J., 2007. Immune surveillance of tumours. *Journal of Clinical Investigation*, 117, pp.1137–1146.

Takahashi, Y., Shirai, K., Ijiri, Y., Morita, E., Yoshida, T., Iwanaga, S. and Yanagida, M., 2020. Integrated system for detection and molecular characterization of circulating tumor cells. *PLoS ONE*, [online] 15(8 August), pp.1–13. Available at: <http://dx.doi.org/10.1371/journal.pone.0237506>.

Tanos, R. and Thierry, A.R., 2018. Clinical relevance of liquid biopsy for cancer screening. *Translational Cancer Research*, 7(6), pp.S105–S129.

Telleria, C.M., 2013. Repopulation of Ovarian Cancer Cells after Chemotherapy. *Cancer Growth and Metastasis*, 6, p.CGM.S11333.

Thakur, G., Prakash, G., Murthy, V., Sable, N., Menon, S., Alrokayan, S.H., Khan, H.A., Murugaiah, V., Bakshi, G., Kishore, U. and Madan, T., 2019. Human SP-D Acts as an Innate Immune Surveillance Molecule Against Androgen-Responsive and Androgen-Resistant Prostate Cancer Cells. *Frontiers in Oncology*, 9(July), pp.1–15.

Thiery, J.P., 2002. Epithelial-mesenchymal transitions in tumor progression. *Nature Reviews Cancer*, 2(6), pp.442–454.

Tkach, M. and Théry, C., 2016. Communication by Extracellular Vesicles: Where We Are and Where We Need to Go. *Cell*, 164(6), pp.1226–1232.

Tortora, G. and Derrickson, B., 2005. *Principles of Anatomy and Physiology*.

Trindade, F., Tellechea, Ó., Torrelo, A., Requena, L. and Colmenero, I., 2011. Wilms tumor 1 expression in vascular neoplasms and vascular malformations. *American Journal of Dermatopathology*, 33(6), pp.569–572.

Vajjhala, P.R., Macmillan, E., Gonda, T. and Little, M., 2003. The Wilms' tumour suppressor protein, WT1, undergoes CRM1-independent nucleocytoplasmic shuttlingy. *FEBS Letters*, 554(1–2), pp.143–148.

Vermes, I., Haanen, C. and Reutelingsperger, C., 2000. Flow cytometry of apoptotic cell death.

Journal of Immunological Methods, 243(1–2), pp.167–190.

Vieira, F., Kung, J.W. and Bhatti, F., 2017. Structure, genetics and function of the pulmonary associated surfactant proteins A and D: The extra-pulmonary role of these C type lectins. *Annals of Anatomy*, 211, pp.184–201.

Volcic, M., Karl, S., Baumann, B., Salles, D., Daniel, P., Fulda, S. and Wiesmüller, L., 2012. NF-κB regulates DNA double-strand break repair in conjunction with BRCA1-CtIP complexes. *Nucleic Acids Research*, 40(1), pp.181–195.

Wan, J.C.M., Massie, C., Garcia-Corbacho, J., Mouliere, F., Brenton, J.D., Caldas, C., Pacey, S., Baird, R. and Rosenfeld, N., 2017. Liquid biopsies come of age: Towards implementation of circulating tumour DNA. *Nature Reviews Cancer*, [online] 17(4), pp.223–238. Available at: <http://dx.doi.org/10.1038/nrc.2017.7>.

Wang, C., Liang, Z., Liu, X., Zhang, Q. and Li, S., 2016. The association between endometriosis, tubal ligation, hysterectomy and epithelial ovarian cancer: Meta-analyses. *International Journal of Environmental Research and Public Health*, 13(11).

Wang, J., Huang, X., Xie, J., Han, Y., Huang, Y. and Zhang, H., 2021. Exosomal analysis: Advances in biosensor technology. *Clinica Chimica Acta*, 518(March), pp.142–150.

Wang, S., Wang, K. and Zheng, C., 2013. Interspecies heterokaryon assay to characterize the nucleocytoplasmic shuttling of herpesviral proteins. *Methods in Molecular Biology*, 1064, pp.131–140.

de Wit, S., van Dalum, G. and Terstappen, L.W.M.M., 2014. Detection of Circulating Tumor Cells. *Scientifica*, 2014, pp.1–11.

Wong, K.H.K., Tessier, S.N., Miyamoto, D.T., Miller, K.L., Bookstaver, L.D., Carey, T.R., Stannard, C.J., Thapar, V., Tai, E.C., Vo, K.D., Emmons, E.S., Pleskow, H.M., Sandlin, R.D., Sequist, L. V., Ting, D.T., Haber, D.A., Maheswaran, S., Stott, S.L. and Toner, M., 2017. Whole blood stabilization for the microfluidic isolation and molecular characterization of circulating tumor cells. *Nature Communications*, [online] 8(1), pp.1–10. Available at: <http://dx.doi.org/10.1038/s41467-017-01705-y>.

Yamanouchi, K., Ohta, T., Liu, Z., Oji, Y., Sugiyama, H., Shridhar, V., Matsumura, S., Takahashi, T., Takahashi, K. and Kurachi, H., 2014. The Wilms' tumor gene WT1 −17AA/−KTS splice variant increases tumorigenic activity through up-regulation of vascular endothelial growth factor in an in vivo ovarian cancer model. *Translational Oncology*, [online] 7(5), pp.580–589. Available at: <http://dx.doi.org/10.1016/j.tranon.2014.07.008>.

Yang, L., Han, Y., Saurez Saiz, F. and Minden, M.D., 2007. A tumor suppressor and oncogene: The WT1 story. *Leukemia*, 21(5), pp.868–876.

Yoshihara, K., Tajima, A., Komata, D., Yamamoto, T., Kodama, S., Fujiwara, H., Suzuki, M., Onishi, Y., Hatae, M., Sueyoshi, K., Fujiwara, H., Kudo, Y., Inoue, I. and Tanaka, K., 2009. Gene expression profiling of advanced-stage serous ovarian cancers distinguishes novel subclasses and implicates ZEB2 in tumor progression and prognosis. *Cancer science*, [online] 100(8), pp.1421–8. Available at: <http://www.ncbi.nlm.nih.gov/pubmed/19486012>.

Zavridou, M., Mastoraki, S., Strati, A., Koutsodontis, G., Klinakis, A., Psyrri, A. and Lianidou, E., 2020. Direct comparison of size-dependent versus EpCAM-dependent CTC enrichment at the gene expression and DNA methylation level in head and neck squamous cell carcinoma. *Scientific Reports*, 10(1), pp.1–9.

Zhang, Q., Shan, F., Li, Z., Gao, J., Li, Y., Shen, L., Ji, J. and Lu, M., 2018. A prospective study on the changes and clinical significance of pre-operative and post-operative circulating tumor cells in resectable gastric cancer. *Journal of Translational Medicine*, [online] 16(1), pp.1–12. Available at: <https://doi.org/10.1186/s12967-018-1544-1>.

Zheng, G., Yu, H., Kanerva, A., Forsti, A., Sundquist, K. and Hemminki, K., 2018. Familial risks of ovarian cancer by age at diagnosis, proband type and histology. *PLoS ONE*, 13(10), pp.1–10.

Zheng, H.C., Sun, J.M., Wei, Z.L., Yang, X.F., Zhang, Y.C. and Xin, Y., 2003. Expression of Fas ligand and Caspase-3 contributes to formation of immune escape in gastric cancer. *World Journal of Gastroenterology*, 9(7), pp.1415–1420.

Zuba-Surma, E.K., Kucia, M., Abdel-Latif, A., Lillard, J.W. and Ratajczak, M.Z., 2007. The ImageStream system: A key step to a new era in imaging. *Folia Histochemica et Cytobiologica*, 45(4), pp.279–290.

Zurawski, V.R., Orjaseter, H., Andersen, A. and Jellum, E., 1988. Elevated serum CA 125 levels prior to diagnosis of ovarian neoplasia: Relevance for early detection of ovarian cancer. *International Journal of Cancer*, 42(5), pp.677–680.